Titre: Title:	3D Numerical Evaluation of Consolidation of Tailings Co-Disposed with Waste Rocks in Open Pits
Auteur: Author:	Ngoc Dung Nguyen
Date:	2022
Type:	Mémoire ou thèse / Dissertation or Thesis
Référence: Citation:	Nguyen, N. D. (2022). 3D Numerical Evaluation of Consolidation of Tailings Co-Disposed with Waste Rocks in Open Pits [Thèse de doctorat, Polytechnique Montréal]. PolyPublie. https://publications.polymtl.ca/10564/

URL de PolyPublie: PolyPublie URL:	https://publications.polymtl.ca/10564/
Directeurs de recherche: Advisors:	Thomas Pabst
Programme: Program:	Génie minéral

POLYTECHNIQUE MONTRÉAL

affiliée à l'Université de Montréal

3D numerical evaluation of consolidation of tailings co-disposed with waste rocks in open pits

NGOC DUNG NGUYEN

Département des génies civil, géologique et des mines

Thèse présentée en vue de l'obtention du diplôme de *Philosophiae Doctor*

Génie minéral

Septembre 2022

POLYTECHNIQUE MONTRÉAL

affiliée à l'Université de Montréal

Cette thèse intitulée:

3D numerical evaluation of consolidation of tailings co-disposed with waste rocks in open pits

présentée par **Ngoc Dung NGUYEN**

en vue de l'obtention du diplôme de *Philosophiae Doctor*

a été dûment acceptée par le jury d'examen constitué de:

Li LI, président

Thomas PABST, membre et directeur de recherche

Samuel YNIESTA, member

Nicholas BEIER, membre externe

DEDICATION

To my beloved family

ACKNOWLEDGEMENTS

It has been a truly challenging period for me, yet I thought I have been very lucky, and I would have not reached where I am today without priceless help and support from various sources, specifically:

First and foremost, I would like to gratefully thank my supervisor, Professor Thomas Pabst. What still left in my mind are his invaluable advice, continuous support, and especially his patience which is something that any graduate student would expect from his/her supervisor. My scientific skills have been notably improved under his guidance and constant discussion. Finally, I also had a chance to come back to Vietnam and contribute to serve as a bridge for the cooperation between Hanoi University of Mining and Geology and Polytechnique Montreal under his persistent encouragement and financial support from his project provided by the Ministère des Relations internationals et de la Francophonie.

I also would like to express my great gratitude to Dr. Huy Tran, Dr. Kazim, Dr. Nghia Tran, Dr. Abtin and Itasca technical support team for their precious instruction and advice to correct and improve the quality of my numerical works with FLAC3D. Dr. Carlos A Contreras and Dr. Karim Essayad are also thanked for their discussion on the use of Itasca software to do coupled analysis and on the performance of the column test respectively. I also would like to thank Noura EI-Harrak, Patrick Bernèche and Samuel Chénier for their support in performing my laboratory tests. Dr. Hai Minh, Dr. Hoang Tung are also thanked for their support in analyze my laboratory results.

Many thanks are extended to my fellow students in IRME and Vietnamese friends both in Vietnam and in Montreal, my colleague at Hanoi University of Mining and Geology that I cannot list them out here. This is a really tough journey and longer than I thought. I just want to let you know that it has been lucky for me to meet and talk to you all who were always willing to listen to my difficulties and share my story (and Vietnamese coffee) not only in doing research but also in many other daily life's aspects. Each of you for sure will be an unforgettable memory whenever I think about my time at RIME. My life in Montreal was also much more enjoyable being around with you.

I would like to take this opportunity to express my gratitude to financial support from Fonds de recherche du Québec - Nature et Technologies (FRQNT), and our industrial partners of the Research Institute on Mines and the Environment (RIME UQAT-Polytechnique).

Finally, words cannot express how grateful I am to my beloved parents and parents in law who have always loved and supported me unconditionally. My sister, my brother-in-law, my nephew, and my niece – Bi and Cún for supporting me spiritually and I know you always have been there to support me through ups and downs. Especially, a new family member was born during this period who is my son – Minh Nhật - Milky. I just want to let you know that you are the biggest incentive whenever I was feeling down, and motivation to finish my studies and to be with you as soon as I can! I also cannot express how grateful I am to my wife as she has raised our son without me being around during this difficult period. (Từ ngữ không thể diễn tả hết sự biết ơn của con dành cho các bố, các mẹ, những người luôn luôn yêu thương và sẵn sàng giúp đỡ con vô điều kiện. Em cũng xin cảm ơn chị Nhíp, anh Vượng, cậu cám ơn cháu Bi và cháu Cún vì sự giúp đỡ về mặt tinh thần và đã luôn ở bên em và cậu trong những lúc khó khăn nhất. Đặc biệt, một thành viên mới của gia đình đã ra đời trong quãng thời gian này, đó là con Minh Nhật – Sữa. Papa chỉ muốn con biết rằng con luôn là động lực lớn nhất mỗi khi papa gặp khó khăn để có thể sớm hoàn thành công việc và sớm quay trở về bên con. Sau cùng, xin cám ơn vợ vì đã thay mặt anh chăm sóc con khi anh không thể ở bên cạnh 2 mẹ con trong giai đoạn hết sức khó khăn này).

RÉSUMÉ

Les résidus et les stériles sont les deux principaux déchets miniers résultant des activités minières. Une gestion et une valorisation appropriées de ces déchets miniers sont nécessaires pour éviter les dommages environnementaux et les défaillances géotechniques ayant des conséquences importantes pour les activités minières et l'environnement environnant. Les problèmes environnementaux peuvent inclure le drainage minier acide ou le drainage neutre contaminé, tandis que des défaillances géotechniques peuvent se produire avec une liquéfaction dynamique ou statique, ce qui peut entraîner des conséquences catastrophiques en aval.

Une technique de gestion des déchets miniers est le stockage en fosse qui présente de nombreux avantages par rapport aux infrastructures d'entreposage (TSF) en surface. Cette technique permet d'isoler physiquement les résidus à l'aide du milieu environnant et réduire les coûts de maintenance à long terme. Une enveloppe perméable, composée de matériaux grossiers ou d'une paroi rocheuse naturelle poreuse et installée le long du périmètre de la fosse, peut en outre contribuer à contrôler les contaminations potentielles par lessivage des résidus. Le principe fondamental de cette technique est que l'enveloppe perméable est plus perméable que les résidus et que l'eau souterraine s'écoule donc autour de la masse de résidus au lieu de la traverser. Des inclusions de stériles (WRI) ont également été proposées pour accélérer la consolidation des résidus et donc améliorer à la fois la stabilité dynamique des TSF de surface du sol et le taux de consolidation des résidus et ces effets ont été prouvés numériquement et expérimentalement. Les WRI peuvent également renforcer les parcs à résidus, empêcher le déplacement excessif des parcs à résidus pendant et après les événements sismiques. L'enveloppe perméable pourrait également contribuer à améliorer le taux de consolidation des résidus en fonctionnant de la même manière que le WRI dans les ISR. L'application de stériles sous forme d'enveloppe perméable (drain latéral) et d'inclusions (drain central) pour former de multiples voies de drainage dans la fosse pourrait favoriser davantage les avantages mentionnés ci-dessus. Les applications de cette nouvelle approche de gestion des déchets miniers peuvent également rencontrer plusieurs défis et inconnus qui peuvent limiter son application. Par exemple, les inconnus sur les évolutions non linéaires des propriétés de consolidation des résidus en pulpe (les travaux antérieurs considèrent généralement une conductivité hydraulique et une rigidité constante des résidus), les gains ou pertes nets de volume des résidus, et les effets des contraintes pratiques lorsque la méthode de co-disposition est appliqué

dans la fosse reste difficile. L'objectif principal de cette étude était donc d'étudier numériquement les comportements de consolidation des résidus co-disposés avec plusieurs voies de drainage composées de stériles dans une fosse. Plus précisément, une approche visant à modifier les propriétés des matériaux devait d'abord être développée et validée. Il était également très important d'étudier les influences du WRI sur les consolidations des résidus et les gains/pertes nets de volume en utilisant l'approche proposée. Enfin, les effets des contraintes pratiques sur l'application de la technique de co-disposition en fosse devaient également être examinés.

Une approche pour modifier les paramètres de Mohr Coulomb a d'abord été proposée et intégrée dans FLAC3D pour simuler explicitement la non-linéarité des propriétés des résidus, des simulations numériques couplées hydromécaniques ont ensuite été réalisées pour relever ces défis lorsque la technique de co-disposition a été réalisée dans une ISR simplifiée. Et dans une fosse à échelle réelle. Les résultats ont montré que l'approche développée pouvait représenter raisonnablement bien l'évolution non linéaire des propriétés des résidus lors du processus de remplissage. Les résultats ont également montré que l'estimation utilisant une rigidité et une conductivité hydraulique constantes pouvait entraîner une consolidation significativement différente en termes d'ampleur et de vitesse par rapport à celles obtenues à partir de modèles avec des propriétés mises à jour. Les modèles Kozeny-Carman et Kozeny-Carman Modified ont également permis une estimation satisfaisante du taux de consolidation des résidus, du moins pour les études préliminaires. Les modifications simples des codes numériques via FISH en FLAC3D proposées dans cette thèse pourraient donc améliorer significativement la prédiction de la consolidation des résidus à court terme sur la base d'une approche qui peut modéliser le comportement représentatif des résidus et contribuer à une meilleure planification des schémas de déposition à la fois en TSF conventionnels et dans des fosses à ciel ouvert.

Après une validation réussie, l'effet du WRI sur les comportements de consolidation de divers types de résidus déversés dans une ISR simplifiée a été étudié à l'aide de l'approche proposée. Les différences potentielles entre l'estimation de la consolidation basée sur les propriétés constantes et mises à jour lors de l'application du WRI ont ensuite été examinées. Les effets du rapport volumique entre les résidus et le WRI sur les gains ou les pertes de volume des résidus, les influences du taux de remplissage et du schéma de remplissage ont également été étudiés. Les résultats ont indiqué que le WRI pourrait augmenter le taux de dissipation des résidus d'environ

3,3 fois selon la distance au WRI. La zone d'influence du WRI sur le taux de consolidation des résidus était différente pour chaque type de résidus. Les simulations utilisant des propriétés mises à jour ont montré des différences significatives par rapport aux modèles avec des valeurs constantes en termes d'ampleur et de vitesse de tassement. La présence de WRI peut réduire le volume disponible pour le stockage des résidus dans l'ISR et le changement volumétrique net résultant du tassement des résidus en cas de WRI avec ou sans pourrait être calculé explicitement. Des équations prédisant l'évolution des gains/pertes de volume en fonction des ratios de volume des résidus et du WRI ont ainsi été proposées. Les influences du WRI étaient plus importantes avec l'augmentation du taux de remplissage et l'hypothèse d'un remplissage instantané avait un effet négligeable sur le taux de consolidation des résidus.

Après des résultats encourageants obtenus à partir de simulations des essais de colonne et de co-disposition dans les ISR conventionnels, l'approche proposée a été extrapolée pour réaliser une série de modèles numériques 3D ouplés afin d'examiner quantitativement l'évolution de la consolidation des résidus sous l'influence des stériles co-disposés avec des résidus dans une fosse à ciel ouvert à l'échelle du terrain. Différents scénarios de déposition ont été étudiés, dont la présence d'une enveloppe perméable uniquement et l'ajout de WRI comme inclusion centrale. L'influence des aspects opérationnels et pratiques tels que le taux de remplissage des résidus, les angles de pente de la fosse, les propriétés hydrogéotechniques des stériles et des résidus et la morphologie de la fosse ont été étudiées. Les résultats ont indiqué qu'une enveloppe perméable pourrait favoriser la dissipation de l'excès de pression interstitielle (PWP) et accélérer la consolidation des résidus. La zone d'influence de l'enveloppe perméable était relativement limitée et environ 2 fois la hauteur des résidus. L'utilisation d'un WRI combiné à une enveloppe perméable pourrait donc être géotechniquement bénéfique pour les fosses larges (c'est-à-dire lorsque le rayon de la fosse était supérieur à deux fois sa profondeur). Les angles de pente, le taux de remplissage et la morphologie de la fosse ont quelque peu affecté le taux de consolidation des résidus, mais leur effet était relativement limité et avait tendance à diminuer avec la distance aux voies de drainage. Enfin, la co-disposition des résidus et des stériles semble particulièrement pertinente pour les résidus fins à faible conductivité hydraulique.

L'application de plusieurs voies de drainage composées d'une enveloppe perméable lors du stockage en fosse avec la combinaison de drains WRI et de drainage de fond semble être bénéfique

à la fois en termes d'aspects environnementaux et géotechniques. Ces résultats pourraient être utiles aux praticiens et contribuer à proposer un co-disposition efficace dans les mines à ciel ouvert.

ABSTRACT

Tailings and waste rocks are the two main mine wastes resulting from mining activities. Proper management and reclamation of these mine wastes is required to avoid environmental damages and geotechnical failures with significant consequences for mining activities and surrounding environment. Environmental issues might include acid mine drainage or contaminated neutral drainage, while geotechnical failures might occur with either dynamic or static liquefaction, which may bring about catastrophic downstream consequences

A mine waste management technique is in-pit disposal which has many advantages relative to the surface TSFs. It can contribute to physically isolate tailings with the surrounding environment and reduce the long-term maintenance costs. An engineered permeable envelope, which is composed of coarse materials or porous natural rock wall and installed along the perimeter of the pit, can further contribute to control potential leaching contaminations from tailings. The fundamental principle of this technique is that permeable envelope is more permeable than tailings and the groundwater therefore flows around the tailings mass instead of flowing through it. Waste rocks inclusions (WRIs) were also proposed to accelerate tailings consolidation and therefore improve both dynamic stability of the ground surface TSFs and consolidation rate of tailings and these effects have been proved numerical and experimental. WRIs can also reinforce tailings impoundment, prevent excessive displacement of tailings impoundments during and after seismic events. The permeable envelope could also contribute to enhance consolidation rate of tailings by functioning in a similar way as WRI in the TSFs. The application of waste rocks in the form of permeable envelope (side drain) and inclusions (central drain) to form multiple drainage paths in the pit might further promote the above-mentioned benefits. Applications of this novel mine waste management approach may also encounter several challenges and unknowns that can limit its application. For instance, unknowns on the non-linear evolutions of consolidation properties of slurry tailings (previous works usually consider constant hydraulic conductivity and stiffness of tailings), the net volume gains or losses of tailings, geotechnical benefits of the permeable envelope on the tailings consolidation, and the effects of practical constraints when co-disposal method is applied in the pit remains challenging. The main objective of this study was therefore to numerically investigate the consolidation behaviour of tailings co-disposed with multiple drainage paths composed of wastes rocks in a pit. Specifically, an approach to modify material properties

needed to be first developed and validated. It was also very important to investigate the influences of WRI on the tailings consolidations and the net volume gains/losses using the proposed approach. Finally, the effects of practical constraints on the application of co-disposal technique in the pit also needed to be examined.

An approach to modify Mohr Coulomb parameters was first proposed and integrated in FLAC3D to explicitly simulate the non-linearity of tailings properties, coupled hydro-mechanical numerical simulations were then carried out to address these challenges when co-disposal technique was performed in a simplified TSF and in a real scale pit. Results showed that the developed approach could capture reasonably well the non-linear evolution of tailings properties under filling process. Results also showed that estimation using constant stiffness and hydraulic conductivity could results in a consolidation that was significantly different in terms of both magnitude and rate in comparison with those obtained from models with updated properties. Kozeny-Carman and Kozeny-Carman Modified models also resulted in a satisfactory estimation of consolidation rate of tailings, at least, for preliminary studies. The simple modifications to the numerical codes via FISH in FLAC3D proposed in this thesis could therefore significantly improve the prediction of tailings consolidation in the short term based on an approach that can model the representative tailings behaviour and contribute to a better planning of discharging schemes both in conventional TSFs and in open pits.

After successfully validating, the effect of WRI on consolidation behaviour of various types of tailings discharged in a simplified TSF was investigated using the proposed approach. Potential differences between consolidation estimation based on constant and updated properties when applying WRI were subsequently examined. Effects of volume ratio between tailings and WRI on the volume gains or losses of tailings, influences of the filling rate and filling scheme were also investigated. Results indicated that WRI could increase the rate of dissipation of tailings by around 3.3 times depending on the distance to the WRI. The zone of influence of WRI on tailings consolidation rate was different for each type of tailings. Simulations using updated properties showed significant differences compared to models with constant values in terms of both the magnitude and the rate of settlement. The presence of WRI can reduce volume available for the storage of tailings in TSF and the net volumetric change resulting from tailings settlement in case of with or without WRI could be calculated explicitly. Equations predicting the evolution of

volume gains/losses based on the volume ratios of tailings and WRI were accordingly proposed. The influences of WRI were more significant with the increase in the filling rate and the assumption of instantaneous filling had a negligible effect on the tailings consolidation rate.

After encouraging results obtained from simulations of the column tests and co-dispose in the conventional TSFs, the proposed approach was extrapolated to perform a series of 3D coupled numerical models to quantitatively examine the evolution of tailings consolidation under the influences of waste rocks co-disposed with tailings in a field-scale open pit. Various disposal scenarios were investigated, including the presence of a permeable envelop only and the addition of WRI as a central inclusion. The influence of operational and practical aspects such as the tailings filling rate, pit slope angles, waste rock and tailings hydro-geotechnical properties, and pit morphology were investigated. Results indicated that a permeable envelope could promote the dissipation of excess pore water pressure (PWP) and accelerate tailings consolidation. The influence zone of the permeable envelope was relatively limited and around 2 times the tailings height. Using a WRI combined with a permeable envelope could therefore be geotechnically beneficial for wide pits (i.e., when the radius of the pit was larger than twice its depth). Slope angles, filling rate and pit morphology somewhat affected tailings consolidation rate, but their effect was relatively limited and tended to decrease with the distance to the drainage paths. Finally, co-disposal of tailings and waste rocks seems particularly relevant for fine tailings with low hydraulic conductivity.

The application of multiple drainage paths composed of permeable envelope during in-pit disposal with the combination of WRI and bottom drainage drains appears to be beneficial both in terms of environmental and geotechnical aspects. These results could be useful for practitioners and contribute to propose efficient co-disposal in surface mines.

TABLE OF CONTENTS

LIST OF TABLES

LIST OF FIGURES

LIST OF SYMBOLS AND ABBREVIATIONS

Symbols

A	Ranges from 0.29 to 0.51
B	The Bulk modulus
C	Factor of shape and tortuosity
C_H	Material coefficient
C_G	A constant (= 0.1)
C_U	Coefficient of uniformity of tailings
C_v	Coefficient of consolidation (cm^2/s)
C_c	Compression index
C_r	Recompression index
CM	Canadian Malartic
D_{10}	Diameter corresponding to 10% passing (mm)
D_{50}	Diameter corresponding to 50% passing (mm)
D_{60}	Diameter corresponding to 60% passing (mm)
D_e	Equivalent diameter of the soil cylinder (m)
DV	The differences of volume change
D_R	Relative density of solids
E	The Young's modulus
$F(n_e)$	Drain spacing factor
G_s	Specific gravity
G	The stiffness modulus
H	Maximum drainage distance (m)

H_0	Initial thickness of soil layer
L_L	Liquid limit (%)
P	Pulp density (%)
ΔP	Applied force (kN)
P_L	Plastic index (%)
S	Specific surface of material (m^2/kg)
R_{t90}	Ratio of t_{90} between models with and without WRI
T_v	Time factor
U	Degree of consolidation (%)
$\overline{U_f}$	Average degree of consolidation under combination of vertical and horizontal drainage
$\overline{U_h}$	Average degree of consolidation due to radial drainage
$\overline{U_v}$	Average degree of consolidation due to vertical drainage
V_t	Volume change of model with tailings only (m^3)
V_w	Volume change of model with WRI (m^3)
Z	Position factor
a_v	Coefficient of compressibility
c'	Drained cohesion (kPa)
c'	Undrained cohesion (kPa)
C_h	Horizontal coefficient of consolidation (m^2/s)
e	Void ratio
f_f	Function of the fluid properties ($m^{-1}s^{-1}$)
f_v	Function of the void space

g	Gravitational acceleration (m/s^2)
$g(e)$	Finite-strain coefficient of consolidation
k_{sat}	Saturated hydraulic conductivities (m/s)
k_h	Horizontal saturated hydraulic conductivities (m/s)
k_v	Vertical saturated hydraulic conductivities (m/s)
m_v	Coefficient of volume change
n	Porosity
q	Specific flow (m/s)
r	Radial distance of the considered point (m)
r_w	Equivalent radius (m)
s	Settlement (m)
t	Time (s)
t_{50}	Times corresponding to a vertical degree of consolidation of 50% (s)
t_{90}	Times corresponding to a vertical degree of consolidation of 90% (s)
u_0	Initial excess pore water pressure (kPa)
i	Hydraulic gradient
v	Fluid velocity (m/s)
w_{opt}	The optimum water content (%)
x	Tortuosity factor (=2)
ε_v	Vertical compression of tailings
ϕ'	Drained friction angle (º)
ϕ	Undrained friction angle (º)

$\lambda(e)$	Linearization constant
γ_s	Dry unit weight (kN/m^3)
γ_w	Unit weight of water (kN/m^3)
μ_w	Dynamic viscosity of water (Pa.s)
μ	Coefficient of friction
ρ_w	Water density (kg/m^3)
ρ_{dmax}	Maximum dry density (kg/m^3)
σ_v'	Effective stress (kPa)
σ_{cor}	Corrected axial compression stress (kPa)
u_w	water pressure (kPa)

Abbreviations

AMD	Acid mine drainage
CND	Contaminated neutral drainage
DTMF	Deilmann tailings management facility
KC	Kozeny-Carman
KCM	Kozeny-Carman modified
MC	Mohr Coulomb
MCC	Modified Cam-Clay
PSD	Particles size distribution
PWP	Porewater pressure
PVDs	Prefabricated vertical drains
RLITMF	Rabbit Lake in-pit tailings management
TSFs	Tailings storage facilities
WRIs	Waste rocks inclusions

LIST OF APPENDICES

CHAPTER 1 INTRODUCTION

1.1 Statement of problem

Mining operations and related exploitation activities often generate large quantities of solid wastes, including coarse waste rocks and mine tailings (Vick, 1990; FSCONSOL, 1999; Bussière & Guittonny, 2020). These mine wastes can be partly returned underground as backfilled materials but are often disposed of on the surface. Tailings are commonly transported hydraulically to tailings storage facilities (TSFs) surrounded by retaining structures built with earth materials or mine wastes (Blight, 2010), while waste rocks are often stored in piles (Aubertin, 2013; MEND, 2015).

Improper management and reclamation of these storage facilities can result in geo-environmental and geotechnical issues with significant consequences for mining activities as well as the surrounding environment (Aubertin et al., 2016; Bussière & Guittonny, 2020; Rana et al., 2021). Environmental issues often result from mine wastes containing sulfide minerals, which can oxidize and generate acid mine drainage (AMD) or contaminated neutral drainage (CND) (Nordstrom et al., 2015; Bussière & Guittonny, 2020). Tailings are also susceptible to both dynamic and static liquefaction due to their high-water content, large porosity and low strength characteristics (James & Aubertin, 2009; James et al., 2013; Morgenstern et al., 2016), causing geotechnical instabilities (Azam & Li, 2010; Rana et al., 2021). These failures of TSFs may result in catastrophic downstream consequences, including significant environmental destruction, detrimental infrastructure damages, and sometimes loss of lives (Azam & Li, 2010; Robertson et al., 2019). Waste rocks inclusions (WRIs) were proposed by Aubertin et al. (2002) to enhance tailings consolidation rate and therefore improve both dynamic stability of TSFs and consolidation rate of tailings (Aubertin et al., 2016). Numerical and experimental studies have shown that WRIs can create preferential drainage paths for water movement since the hydraulic conductivity of waste rock is significantly greater than that of tailings (James, 2009; Bolduc & Aubertin, 2014). WRIs can also contribute to mechanically reinforce tailings impoundment, prevent excess deformation of tailings impoundments during and after seismic solicitations and thus improve the overall static and dynamic stability of retaining structures (James et al., 2013; Ferdosi et al., 2015b; Zafarani et al., 2020).

Another promising mine waste management technique that has received more interest in recent years is in-pit disposal (MEND, 2015). In-pit disposal has indeed many advantages compared to surface TSFs. It can, for example, reduce metal leaching (MEND, 2015), contribute to physically isolating tailings and stabilizing pit walls and reducing the long-term maintenance and management costs (Cameron & Dave, 2015). An engineered permeable envelope, installed along the walls of the pit, can further contribute to controlling potential leaching contamination and preventing interaction between groundwater and mobile contaminants from tailings (MEND, 2015; Rousseau & Pabst, 2022). The concept of such a pervious surround relies on the principle that it is more permeable than tailings and therefore contributes to direct the groundwater flow around the tailings instead of flowing through it. Permeable envelope could be either an engineered porous or porous natural rock wall surrounding the pit (Rousseau & Pabst, 2022). The technique is usually combined with engineered tailings and bottom drainage to enhance the efficiency of the technique (Cameron & Dave, 2015). Rousseau and Pabst (2022) showed that internal inclusions and drainage paths can also help control contamination. The permeable envelope could also contribute to accelerate consolidation of tailings by functioning in a similar way as WRI because of its higher hydraulic conductivity compared to that of tailings, yet these effects have not been adequately addressed in literature. Tailings and waste rock co-disposal (in the form of multiple drainage paths with permeable envelope combined with WRI) in a pit could therefore contribute to improve the overall geotechnical and geochemical instabilities.

Applications of this novel mine waste management approach also faces several challenges and unknowns that has somewhat limited its application so far. Previous works usually consider constant values of hydraulic conductivity and stiffness of tailings (Bolduc & Aubertin, 2014; Boudrias, 2018). However, the consolidation properties of slurry tailings were proven to be non-linear during the filling process (i.e., hydraulic conductivity would decrease, and the stiffness would increase as void ratio decreases) (Gibson et al., 1967; Carrier et al., 1983; Townsend & McVay, 1990). The conventional consolidation theory with the assumption of constant consolidation properties might thus not be applicable to the estimation of tailings consolidation behaviour. Numerical models, thus, should integrate non-linear changes of stiffness and hydraulic conductivity resulting from changes in the void ratio of tailings. These parameters could be either measured in the laboratory or estimated using predictive models. Secondly, the storage capacity of pits is also limited, and the volume ratio of tailings and waste rocks needs to be carefully considered when both tailings and waste rocks (used

for inclusions and/or permeable envelope) are co-disposed (Jahanbakhshzadeh et al., 2019) as the objective of this technique could be to reduce the size of TSFs or to remove any needs of waste rock piles on the surface. There could also be a volume gain because of faster consolidation of tailings (i.e., application of WRI can help to increase volume of tailings that could be stored because of a faster consolidation rate of tailings in the presence of WRI). Filling rate, tailings and waste rocks hydro-mechanical properties could significantly influence the performance of the permeable envelope, yet the effects of these factors were not clearly indicated in the literatures. Permeable envelope, WRIs and complex geometry of pits might result in 3-D effects. Finally, the effects of the depth of the pit, the slope angles of rock walls on the performance of the permeable envelope concept should be carefully studied before the technique is applied to real pits.

1.2 Objectives

The principal objective of this research was therefore to numerically evaluate the geotechnical benefit on the acceleration of the consolidation rate of tailings co-disposed with multiple drainage paths composed of wastes rocks (i.e., either in the form of permeable envelope or/and WRIs) in a pit.

Several sub-objectives were completed to reach the main objective:

- To develop and validate a numerical approach that can consider the variation with time and at various position of the stiffness and hydraulic conductivity of tailings under sequential filling to better represent the real behaviour of tailings,
- To determine the volume gains or losses of tailings because of the presence of WRI and the effect of the ratio of volume between tailings and WRI on the volume gains or losses of tailings based on practical operation aspects, and
- To determine potential effects of various practical constraints on the evolution of dissipation of PWP with the use of drainage paths composed of waste rocks materials co-disposed with tailings in pits (i.e., depth of the pit, overall pit wall slope angles, filling rate, mine waste hydraulic properties and pit morphology).

1.3 Research hypothesis

The study was performed with the hypothesis that in-pit co-disposal of waste rocks and tailings can contribute to accelerating the consolidation of tailings, and thus enhancing the storage capacity in open pits and reducing the long-term deformation of tailings.

1.4 Originality and contributions

In this research, a numerical procedure along with a numerical code using the FISH language of FLAC3D has been proposed to take into account the non-linear evolutions of properties of hard rock mine tailings with the presence of drainage paths (in the form of permeable envelope and WRI) in open pits. The numerical results demonstrate, for the first time, the geotechnical benefits of a permeable envelope and WRI co-disposed with tailings in open pits. The numerical approach in this study can also cover the 3-D effects resulting from the complex geometry of the drainage paths and the open pit to investigate the consolidation behaviour of tailings with the application of the co-disposal technique. It also shed more light on the effects of various predictive functions on the prediction of tailings hydraulic conductivity under sequential loading. Quantitative estimation on the discrepancies between models using constant and updated tailings properties was also derived for the cases where co-disposal technique was applied. This study also examined the consolidation behaviour of various types of tailings when co-disposal technique was applied. Finally, the study quantitatively evaluated the evolution of tailings consolidation (mostly on the evolution of excess PWP) in a field-scale open pit with the application of permeable envelope under various permeable conditions (i.e., central drainage with the combination with WRI and bottom drainage with the installation of a bottom drain layer).

The procedure of numerical simulation along with the FISH code presented in this research can therefore be applied by researchers and practitioners to alternate tailings properties and investigate the non-linear behaviour of tailings consolidation. Estimation of the volume gains or losses of tailings can help practitioners to prepare a better disposal plan regarding the volume of WRI and tailings that can be placed in a pit (i.e., the reduction of volume available for the storage of tailings because of the presence of WRI, and the additional height of the TSFs that the mine needs to build to compensate for the presence of WRI). Reclamation activities can also be better planned based on the evolution of

excess PWP of tailings with the application of the co-disposal technique. For instance, the numerical approach can help to estimate the starting time for the reclamation activities and/or estimate the post-settlement of tailings (if any) that might have influence on the performance of the covering system. Finally, results in this research can also be used for the validation purpose of other research (if any) working on the same topic of co-disposal of tailings and drainage paths in the pit.

1.5 Content of the thesis

Chapter 1 presents a brief introduction and problematic statement of the thesis, the objectives, and the organization of the thesis.

Chapter 2 presents the state of the art and practice of literature related to the investigated topic, which include conventional mine waste management techniques, integrated mine waste management, geotechnical properties of mine tailings and waste rocks, consolidation theory applied for slurry tailings, acceleration of consolidation of tailings using drainage pathways, and numerical tools available for the simulation of tailings consolidation.

Chapter 3 presents the methodology used to reach the research objectives of this thesis.

Chapter 4 (Article 1) presents an approach to update Mohr Coulomb parameters to integrate the evolution of hydraulic conductivity and stiffness of tailings materials with the reduction of the void ratio. The model was validated by comparing simulation results with measurements from laboratory column tests. A parametric study was also performed to assess the performance of various predictive functions to estimate hydraulic conductivity for field applications. Finally, the developed approach was applied to a simplified model of tailings impoundment filled sequentially.

Chapter 5 (Article 2) presents a fully coupled fluid-mechanical analysis to assess the evolution of consolidation of four types of tailings in the presence of WRI for a simplified impoundment. The effects of WRI and volume ratio of tailings over WRI on the net volume gains or losses was investigated.

Chapter 6 (Article 3) presents a series of 3D coupled models conducted to examine the behaviour of tailings co-disposed with waste rocks in a pit. Various disposal scenarios were also investigated, including the presence of a permeable envelope and the addition of WRI through the pit in the form of a central inclusion. An extensive parametric analysis on the influence of operational and practical

constraints such as the depth of the pit, pit wall slope angles, filling rate, mine waste hydraulic properties and pit morphology were also investigated.

A general discussion and summary of this research are presented in Chapter 7.

Conclusions and recommendations are finally presented in Chapter 8.

CHAPTER 2 LITERATURE REVIEW

2.1 Conventional mine waste management

Valuable ores and minerals are extracted from underground or open pit mines and concentrated gravimetrically or chemically at the concentrator (Vick, 1990). Mining operations and related activities generate large quantities of solid wastes, including coarse waste rocks and fine-grained tailings (Vick, 1990; Aubertin, 2018; Bussière & Guittonny, 2020), which are usually disposed of in surface storage facilities (i.e., impoundments for tailings and piles for waste rocks).

2.1.1 Tailings management

2.1.1.1 Geotechnical properties of tailings

The range and values of these properties that are commonly encountered are presented in table 2.1. The coefficient of uniformity of tailings C_U (= D_{60}/ D_{10}) typically varies between 2 and 30 (Bussière, 2007). Specific gravity, G_s, of mine tailings is usually significantly higher compared to those for naturally occurring soils, ranging from 2.6 to 3.3 (and more) depending on metal and sulfide contents (Wijewickreme et al., 2005). Hard rock mine tailings are typically non-plastic or of very low plasticity with a typical plastic limit smaller than 15% and a liquid limit below 40% (Wijewickreme et al., 2005; Bussière, 2007). Void ratio of hard rock tailings ranges from 0.5 to 1.7 in TSF, while their dry unit weight is generally comprised between 14 and 18 kN/m^3 (Qiu & Sego, 2001).

The coefficient of consolidation, C_v, is usually comprised between 10^{-1} and 10^{-4} cm^2/s (Qiu & Sego, 2001). Compression index, C_c, and recompression index, C_r, of hard rock tailings are typically between 0.05 and 0.54 and between 0.03 and 0.01, respectively (Hu et al., 2017). These values are relatively similar to those obtained from natural silts (Holtz & Kovacs, 1981). Tailings are generally non-cohesive material with a drained friction angle ϕ' around 35^o (Bussière, 2007).

Saturated hydraulic conductivity of both remoulded and undisturbed tailings is typically between 10^{-9} m/s and 10^{-4} m/s (Bussière, 2007). The ratio of horizontal and vertical saturated hydraulic conductivity, k_H/k_v, varies from 2 to 10 (Chapuis, 2012), and can exceed 100 in some cases when the extensive inter-layering of finer and coarser materials occurs during deposition (Vick, 1990).

Mechanical properties of tailings can vary widely depending on the properties of the parent rocks, the physical and chemical processing of mineral extraction and the deposition method (Blight, 2010). Tailings deposited hydraulically from pipes are also subjected to segregation as coarser particles typically settle closer to the outlets of the slurry pipes forming beaches, while finer material can travel further (Vick, 1990; Bussière, 2007). Mine tailings have low relative densities after deposition but tend to consolidate under the effect of self-weight and the pressure from subsequently adding layers. This leads to the evolution of tailings properties and in particular the void ratio, hydraulic conductivity and stiffness of tailings (Bussière, 2007). However, most of the conventional estimation of tailings consolidation only consider constant properties of tailings. As a result, these can lead to, for example, overestimation or underestimation of the evolution of excess PWP, which is very important for the management of the discharge plan for the tailings. Properties of tailings in TSF can therefore be heterogeneous depending of the deposition method, age, distance to the dams and deposit height (James, 2009).

Table 2-1: Typical geotechnical properties of hard rock mine tailings.

Parameter	Symbol	Value(s)/range(s)	References
Diameter corresponding to 10% passing	D_{10} (mm)	0.001 – 0.016	(Bussière, 2007)
Diameter corresponding to 60% passing	D_{60} (mm)	0.01 – 0.15	(Bussière, 2007)
Coefficient of uniformity	C_u (D_{60}/ D_{10})	2.15 – 30	(Bussière, 2007) (Qiu & Sego, 2001)
Specific gravity	G_s	2.6 – 3.23	(Bussière, 2007) (Wickland & Wilson, 2005)
Solid content	P (%)	30 – 85	(Bussière, 2007) (Vick, 1990)
Plasticity	P_L	<15%	(Bussière, 2007)

			(Wickland & Wilson, 2005)
	L_L	<40%	(Bussière, 2007) (Wickland & Wilson, 2005)
Void ratio	e	0.5 - 1.7	(Qiu & Sego, 2001)
Dry unit weight	γ_s (kN/m^3)	14 – 18	(Qiu & Sego, 2001)
Consolidation	C_v (cm^2/s)	10^{-4} - 10^{-1}	(Bussière, 2007) (Qiu & Sego, 2001)
	C_c	0.05 – 0.54	(Bussière, 2007) (Qiu & Sego, 2001)
	C_r	0.03 – 0.01 (0.05C_c to 0.2C_c)	(Bussière, 2007) (Qiu & Sego, 2001)
Saturated hydraulic conductivity	k_{sat} (m/s)	1.0x10^{-9} - 1.0x10^{-4}	(Bussière, 2007) (Aubertin et al., 1996)
Anisotropy of hydraulic conductivity	$r_k = k_h/k_v$	2 - 10	(Chapuis, 2012)
Cohesion	c' (drained) (kPa) c (undrained) (kPa)	0 0 – 100	(Hu et al., 2017) (Li et al., 2018)
Friction angle	ϕ' (drained) (º) ϕ (undrained) (º)	30 – 42 14 - 25	(Bussière, 2007) (Hu et al., 2017)

2.1.1.2 Ground surface tailings managements

Tailings are typically hydraulically transported and disposed of as a slurry in TSFs surrounded by impoundments. Slurry tailings usually have a solid content between 25% and 45% and are characterized by a low shear strength and are prone to both dynamic and static liquefaction (James & Aubertin, 2009; James et al., 2013; Morgenstern et al., 2016).

Tailings impoundments are typically built with earth materials or mine wastes (Blight, 2010) and raised along with the filling of tailings in the TSF. Dykes are usually designed and constructed according to either upstream, downstream or centreline configuration (Blight, 2010). Upstream method is the most economical method, where each new embankment is raised toward the impounded tailings and where part of the new dyke rests on the tailings materials. With the downstream method, tailings are deposited behind the dykes which are constructed and supported on top of the downstream slope of the previous stage. Centreline method represents a compromise between upstream and downstream designs where tailings are discharged behind the dykes and the embankment crest is raised vertically and resting on both tailings and existing embankment (Vick, 1990).

In practice, particle segregation often occurs during tailings discharge and fine tailings tend to settle further from the discharge points while coarser materials tend to settle closer to the discharge points thus forming beaches (Vick, 1990). Such segregation can contribute to the development of interbedded layers of tailings of various grain sizes also contribute to drain the water table close to the dam, which is rather positive (James, 2009). The use of conventional ground surface TSFs might be associated with the risk of failures because the high excess PWP might be encountered during the discharge process of slurry tailings (Rana et al., 2021). Also, there might be a risk of acid mine drainage released from these tailings materials (Aubertin et al., 2016).

2.1.2 Waste rock management

2.1.2.1 Geotechnical properties of waste rocks

Waste rocks properties depend on the characteristic of parent rocks, including its hardness, brittleness, distribution and frequencies of discontinuity systems and the excavation methods (James, 2009; Aubertin, 2013). In situ hydro-geotechnical properties of waste rock (i.e., porosity, volumetric

water content, hydraulic conductivity) usually present significant spatial variability in piles, depending on the degrees of compaction and segregation (Molson et al., 2005; Lahmira et al., 2017).

Coefficient of uniformity, C_U, of waste rock is typically greater than 20 because of the presence of both large blocks (which diameter can exceed a meter) and fine particles (Lahmira et al., 2017). Porosity is usually between 0.3 and 0.5, and can vary with time because of the settlement, crushing following haul-truck traffic and fine particle migration (McLemore et al., 2009; Peregoedova, 2012). Variation of porosity can, in turn, influence waste rocks hydraulic conductivity and shear strength (Aubertin, 2013). Dry density measured in piles usually ranges from 1500 to 2500 kN/m^3 (McLemore et al., 2009).

Saturated hydraulic conductivity of waste rock depends on the grain size distribution, especially the finer fraction, and the porosity, and is usually comprised between 10^{-3} and 10^{-5} m/s (Molson et al., 2005). In situ hydraulic conductivity of waste rocks can vary significantly throughout piles because of the layered structure caused by waste rock segregation during dumping (Molson et al., 2005; Aubertin, 2013; Maknoon, 2016).

The stiffness modulus, G, of waste rocks can reach 50 MPa and their Young's modulus is often greater than 100 MPa (Maknoon, 2016). Internal friction angle φ' can be between 21° and 62°, with most common values comprised between 34^0 and 45^0 (McLemore et al., 2009; Aubertin, 2013). Internal friction angle can be influenced by the mineralogy, grain size distribution, shape and roughness of particles, and stress levels (McLemore et al., 2009). The effective cohesion, c', of dry or saturated waste rock is usually zero (Fala et al., 2005).

Table 2-2*:* Typical geotechnical properties of hard rock mines waste rocks.

Parameter	Symbol	Value(s)/range(s)	References
Diameter corresponding to 10% passing	D_{10} (mm)	0.008 – 6	(Lahmira et al., 2017) (McLemore et al., 2009)
Diameter corresponding to 50% passing	D_{50} (mm)	0.3 – 60	(Lahmira et al., 2017) (McLemore et al., 2009)
Diameter corresponding to 60% passing	D_{60} (mm)	1 – 80	(Lahmira et al., 2017) (McLemore et al., 2009)
Coefficient of uniformity	C_u (D_{60}/ D_{10})	20 – 100	(Lahmira et al., 2017) (McLemore et al., 2009)
Porosity	n	0.3 – 0.5	(McLemore et al., 2009)
Dry density	ρ_d (kN/m^3)	1500 – 2500	(McLemore et al., 2009)
Specific gravity	G_s	2.1 – 3.7	(James, 2009)
Stiffness	G (MPa)	<50	(Maknoon, 2016)
	E (MPa)	<100	(Maknoon, 2016)
Saturated hydraulic conductivity	k_{sat} (m/s)	1.0x10^{-3} - 1.0x10^{-5}	(Maknoon, 2016) (Aubertin, 2013)
Cohesion	c' (drained) (kPa)	0	(Fala et al., 2005)
Friction angle	ϕ' (drained) (º)	21 – 62	(McLemore et al., 2009) (Aubertin, 2013)

2.1.2.2 Constructions of waste rock piles

Waste rocks are often disposed of in piles (Aubertin, 2013; MEND, 2015) which can sometimes exceed 300 m in height and occupy up to 500 million m^3. Construction methods of waste rock piles are based on practical and economic considerations (Aubertin, 2013) and three main techniques are typically used (Fala et al., 2005; Aubertin, 2013; Maknoon, 2016):

- End dumping involves dumping waste rocks on the side slope from the crest of the pile. This method generates significant segregation with finer particles remaining close to the deposition point while coarser particles tend to move towards the toe (Aubertin, 2013).
- In the push dumping method, the truck loads are dumped on the surface of the pile and pushed along the slope by dozers. Particle segregation is somewhat lower compared to the end dumping approach.
- The third construction method is free-dumping. Waste rocks are deposited in small heaps on the pile surface and spread by dozers and graders. The degree of segregation is the lowest among other techniques (Hawley & Cunning, 2017). The method is usually applied at the early stages of the construction and then replaced by the end- or push dumping methods.

Each construction method brings various levels of compaction and segregation that, in turn, influence the movement of water and air within the waste rock piles (Fala et al., 2005; Molson et al., 2005; Aubertin, 2013; Maknoon, 2016). Sub-horizontal layers are often observed during the construction of waste rock piles because of a wide range of particle size of the waste rock materials (Aubertin, 2013; Lahmira et al., 2017). Cobbles and coarse particles particularly tend to accumulate at the toe of the piles, which can locally increase water and air flow. Surface and slopes of the waste rock pile can be inclined to favour surface runoff, lateral diversion, and reduce infiltration to the centre of the pile (Aubertin, 2013; Dubuc et al., 2017; Martin, 2017). The construction of waste rock piles usually requires a large ground surface area. The failure of those waste rock piles and AMD released from those structures might occur in some areas where improper management of these mine waste might be encountered (Aubertin, 2013).

2.1.3 Challenges in mine waste management

The management and reclamation of mine waste storage facilities raise geo-environmental and geotechnical challenges for the mining industry (Aubertin et al., 2016; Bussière & Guittonny, 2020; Rana et al., 2021). Environmental issues usually originate from mine wastes containing sulfide minerals that can oxidize and generate acid mine drainage (AMD) or contaminated neutral drainage (CND) (Nordstrom et al., 2015; Wilson et al., 2018). Contaminated mine drainage remains one of the most critical environmental challenges for the mining industry (Bussière & Guittonny, 2020). AMD is typically characterized by low pHs and high concentrations of metals and sulfates generated when these metals are exposed to the atmospheric conditions (Amos et al., 2015; Nordstrom et al., 2015). CND is characterized by metal contamination at near neutral pHs (Lindsay et al., 2015) and is often generated by sulfide minerals which oxidize without producing acid or in presence of buffering minerals (Bussière & Guittonny, 2020).

The main objective of reclamation is to limit the availability of either oxygen or water to prevent oxidation reactions and contaminated drainage generation at the source (Bussière, 2007; Aubertin et al., 2016). For example, cover systems constructed using materials with low saturated hydraulic conductivity can contribute to limit the infiltration of water (Aubertin, 2018). Water covers can act as oxygen barrier and limit oxygen diffusion to the reactive mine wastes (Awoh et al., 2014). A mono layer cover coupled with an elevated water table can contribute to control water balance on site and maintain mine wastes saturated, thus limiting their oxidation (Dobchuk et al., 2013; Pabst et al., 2017). Reclamation design must be adapted to site conditions and carefully planned before the beginning of the production (Bussière & Guittonny, 2020)

Geotechnical stability of tailings storage facilities (TSFs) is another major challenge for the industry and the society (Rana et al., 2021). Over 18,400 tailings dams are reported worldwide, and their height and storage capacity tend to increase over the years (Azam & Li, 2010). Caren tailings dams in central Chile, for instance, was designed with a maximum height of 108 m, and Bahuerachi tailings dam in Mexico has a designed maximum height of 100 m with a capacity of 200 million m^3 (Azam & Li, 2010; Hu et al., 2017). However, fine-grained tailings from hard rock mines are typically characterized by high water contents, large porosity and low strength, and are therefore highly susceptible to instabilities (Vick, 1990; Blight, 2010). Nearly eighty major failure events were

recorded over the past three decades and failure rate of tailings dams is around 1.2% which is more than two orders of magnitude higher than for conventional water retention dams (Azam & Li, 2010). Among these events, approximately 90% of failures occurred in active mines (Azam & Li, 2010). Failures of TSFs is usually followed by fast-moving flow of tailings that can result in catastrophic downstream consequences, including significant environmental damages, severe infrastructure damages, and sometimes casualties (Santamarina et al., 2019). The cumulative outflow volume released from tailings dam failures tend to increase with the multiplication of large operations, and the number of casualties also steadily increases (e. g., 1985 Stava in Italy with 268 deaths and 2019 Brumadinho failures in Brazil with 272 deaths) (Santamarina et al., 2019; Rana et al., 2021).

Main causes to tailings dams failure include slope and foundation instability, surface erosion, internal erosion, overtopping, seismic/static tailings liquefaction, and decantation damage (Azam & Li, 2010). Inadequate drainage systems have been among the most frequent triggers for tailings dams failures since 1996 (Rana et al., 2021). Indeed, tailings consolidation is a time-dependent process and until excess pore water pressures (PWP) are completely drained, tailings remain susceptible to strain-softening and liquefaction (Rana et al., 2021). For example, drainage issues were identified as a major cause to liquefaction (and ultimately failure) in the two recent major tailings dam failures, i.e., Samarco (2015) and Brumadinho (2019) in Brazil (Morgenstern et al., 2016; Robertson et al., 2019). More specifically, insufficient internal drainage system in Brumadinho dam led to an increase of the water level downstream of the dyke slopes, thus generating a portion of loose and weak tailings close to the dam crest which may have contributed to trigger undrained flow liquefaction in the tailings impoundment (Robertson et al., 2019). New management approaches are therefore required to address the increase of tailings production and reduce risks of catastrophic instabilities failures.

2.2 Integrated mine waste management

Innovative integrated mine waste managements techniques include dewatering (Bolduc & Aubertin, 2014; Bhuiyan et al., 2015; Mbemba & Aubertin, 2021a), valorization and reuse of mine wastes in cover systems (Pabst et al., 2018; Larochelle et al., 2019) or in road construction (Hao & Pabst, 2022), or waste mixing (Wickland et al., 2006; Aubertin, 2013; Ferdosi et al., 2015b). Other integrated mine waste management approaches (such as waste rock inclusions and in-pit disposal) aim to improve the stability of TSFs or open pit and will be discussed in more details in the following.

2.2.1 Co-disposal of tailing and waste rocks in tailings impoundments

Progressive deposition of slurry tailings in TSFs can lead to the build-up of excess pore water pressure (PWP) that has been linked to various geotechnical instabilities issues, including failure of tailings impoundments and static/dynamic liquefaction of tailings (Aubertin et al., 2002; Morgenstern et al., 2016; Aubertin, 2018; Mbemba & Aubertin, 2021b; Rana et al., 2021). The use of waste rocks inclusions (WRIs) in TSFs was therefore proposed by Aubertin et al. (2002) to accelerate tailings consolidation by creating preferential drainage paths for water (James, 2009; Bolduc & Aubertin, 2014). WRIs can also reinforce mechanically tailings impoundment thus enhancing both static and dynamic stability of the retaining structures (James, 2009). The technique consists in placing a layer of coarse waste rock at the bottom and on the sides of a tailings impoundment, together with a series of vertical inclusions within the tailings (figure 2-1). These waste rock structures separate the tailings impoundments into compartments and act as vertical drain columns (Aubertin et al., 2002). In practice, WRI are being used at the Canadian Malartic mine site located in Quebec (figure 2-2).

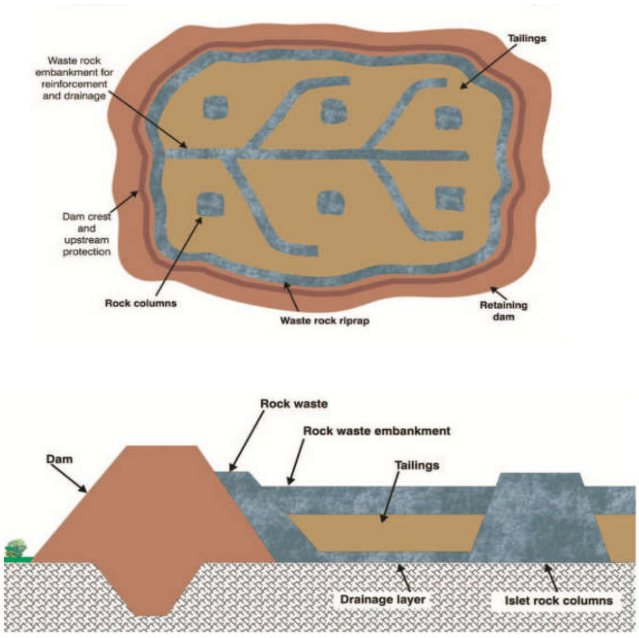

Figure 2-1: Waste rock inclusion within tailings storage facilities (modified after Bussière *(*2007*)*). Coarse waste rocks are placed at the bottom and the side of the TSFs and vertical inclusions are constructed within the TSFs to divide TSFs into compartments and create vertical drainage pathways, thus enhancing both dynamic stability and tailings consolidation rate.

Figure 2-2: Malartic mine tailings impoundment with WRIs (Quebec, Canada). WRIs (shown with red dashed lines) are around 12 m wide and divide the impoundment into several compartments (IRME, 2019).

2.2.1.1 The use of WRIs to improve dynamic stability of the TSFs

WRIs are able to reduce the deformation because of the provided reinforcement and could thus improve the overall strength and stability of TSF (James et al., 2013; Ferdosi et al., 2015b; Jahanbakhshzadeh et al., 2019; Zafarani et al., 2020). For example, the effect of WRI in mitigating liquefaction of mine tailings was numerically evaluated using FLAC code (Itasca Int., 2021) and UBC Sand constitutive model by James (2009). Numerical results have shown that WRIs can efficiently decrease displacements in impoundments by increasing the stiffness of the tailings mass. Similarly, results obtained from Ferdosi et al. (2015b) revealed that displacement of reinforced impoundment decreased by around 10 times compared to those for conventional impoundment (figure 2-3). WRIs can also contribute to prevent excess deformation of tailings under post-seismic influences (Contreras et al., 2020). In general, downstream slope deformation tends to decrease with the increase of inclusion width and with the increase in inclusion spacing (Ferdosi et al., 2015b).

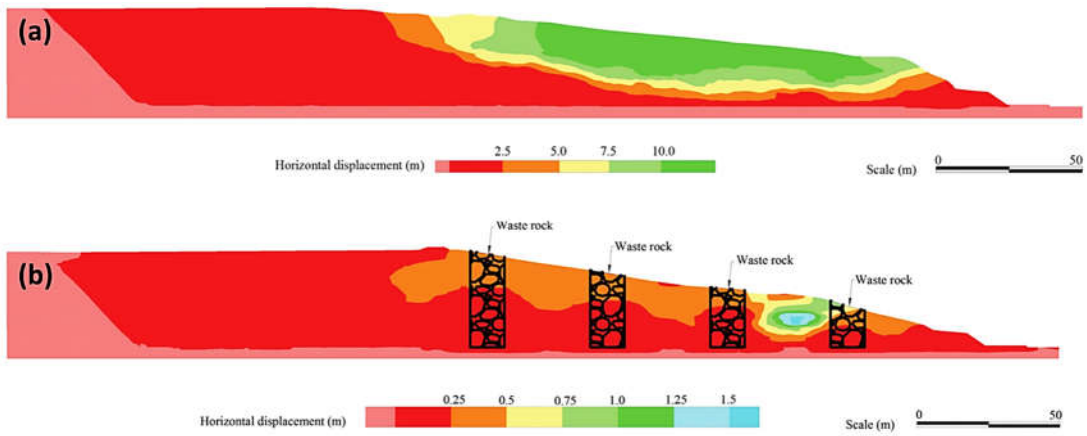

Figure 2-3: Simulated horizontal displacement of a tailings impoundment with and without WRIs from E3-sag earthquake record (M_w = 7.0 and d = 30 km). WRIs can significantly reduce displacement of tailings under cyclic loading generated by an earthquake by about 10 times (modified after (Ferdosi et al., 2015b)).

2.2.1.2 The use of WRIs to accelerate tailings consolidation rate

In addition to their global reinforcing effect, WRIs also divide the tailing impoundment into several compartments, and can therefore act as drainage channels to enhance excess PWP dissipation rate. Various studies have been carried out both numerically and experimentally to evaluate the consolidation and pore-water pressure dissipation of tailings under the impact of WRIs (Bolduc, 2012; Bolduc & Aubertin, 2014; Boudrias, 2018; Essayad et al., 2018; Mbemba & Aubertin, 2021b, 2021a).

Tailings closer to the WRI drain faster and WRI's radius of influence is usually around twice the thickness of the tailings deposited. The higher the hydraulic conductivity of the tailings, the quicker the dissipation of excess PWP (Bolduc & Aubertin, 2014). However, tailings hydraulic conductivity did not significantly influence the magnitude of the initial excess PWP nor the final settlement of tailings (Bolduc & Aubertin, 2014). Similarly, a greater compression index (C_c) would result in a larger settlement and a longer period to fully dissipate excess PWP. Filling rate, waste rock Young's modulus and the shape or geometry of inclusions did not have a significant effect on the consolidation rate (Bolduc & Aubertin, 2014).

Consolidation evolution of saturated and unsaturated tailings in instrumented columns subjected to progressive loading was simulated (i.e., hydraulic conductivity in Modified Cam clay and elastic perfectly plastic models and stiffness modulus in elastic perfectly plastic models were updated at each loading step). Results from models with unsaturated tailings were in good agreement with measured settlements, yet the rate of dissipation of excess PWP was overestimated compared to experiments (Boudrias, 2018). Full-scale model of a tailings impoundment with and without WRI were then simulated and compared (Boudrias, 2018). Simulated vertical displacement was smaller close to the WRI which was attributed to the significantly higher rigidity of the WRI compared to that of the tailings.

Experimental study on the effect of WRI

The consolidation rate and magnitude of tailings in the presence of WRI also were experimentally evaluated using physical laboratory tests (Mbemba & Aubertin, 2021a, 2021b). Experimental tests were composed of tailings placed in large columns (one layer or multilayer deposition of slurry tailings), with a vertical drainage path installed in the centre of the column and made of waste rocks

(figure 2-4). Results revealed that the presence of a central drainage pathway favoured the horizontal movement of water within the tailings, and thus enhanced their consolidation. The dissipation rate of excess PWP also increased with the increase of the WRI diameter (Mbemba & Aubertin, 2021a).

Another physical test conducted in the laboratory consisted of a rigid box which was divided into two compartments and filled with waste rocks and tailings respectively using a metal mesh to evaluate the consolidation behaviour of tailings under the impact of WRI (Mbemba & Aubertin, 2021a). Results indicated that WRI can promote horizontal water movement, and thus, accelerate consolidation of tailings, which is identical to those obtained in Mbemba and Aubertin (2021b). The consolidation test without geotextile at the tailings-waste rocks interface experienced a bit higher settlement compared to that for the test with geotextile used. This was attributed to the possible migration of fine tailings and these displaced tailings seemed not to affect the time to finish consolidation of tailings (Mbemba & Aubertin, 2021a). Another physical experiment was also conducted by Essayad et al. (2018) to investigate possible movement of tailings towards WRI and results also indicated that clogging at the interface between tailings and WRI was negligible.

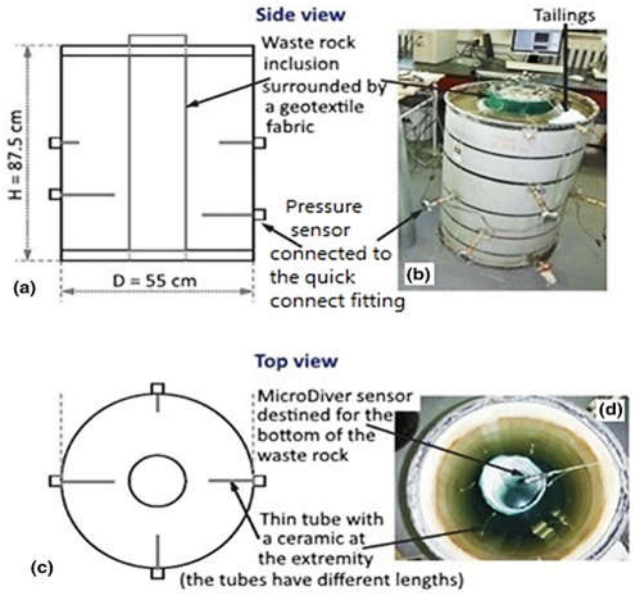

Figure 2-4: Configuration of column tests with centred WRI column (modified after Mbemba and Aubertin (2021b)).

2.2.2 In-pit disposal of mine wastes

2.2.2.1 Advantages and limitations of in-pit disposal

The increase of mineral demand and production and the degree in the average ore grade during the last decades has led to an increase of the volume of tailings produced, and therefore of the risks of major failures events in surface TSFs. Practitioners were therefore encouraged to find alternative approaches for tailings disposal. Tailings can for example be backfilled in underground spaces or in mined-out pits. Underground mine backfill, either in the form of hydraulic fill or paste backfill, can contribute to reduce stope instability and the area required for surface disposal (Aubertin et al., 2003; Fahey et al., 2010; Jahanbakhshzadeh et al., 2017). In-pit disposal is another alternative for surface mines which can contribute to reduce metal leaching and to physically isolate contaminants (MEND, 2015). Backfilling can also stabilize pit walls, eliminate potential solids release, and reduce the long-term management and maintenance of retaining structures compared to conventional surface disposal (Cameron & Dave, 2015; MEND, 2015). The costs for pit backfilling is potentially lower compared to the construction and management of surface TSF (Cameron & Dave, 2015). In-pit disposal could also improve the site aesthetics after closure (Guerin et al., 2006). Once backfilled, the pit can be reclaimed using engineered cover systems to prevent further contaminated mine drainage generation and integrated into the surrounding landscape, thus reducing the footprint of mining activities (Mudd et al., 2011). In practice, all types of mine wastes can be suitable for disposal in open pits, including waste rock, tailings, treatment sludge and contaminated soils and materials. Four main concepts are generally considered for the disposal of mine waste in open pits: dry disposal, wet disposal, chemically and physically stabilization, and engineered pit containment among which wet disposal is preferred because of its simplicity to perform (MEND, 2015).

In-pit tailings disposal is widely used in Australia, mostly for gold and uranium mines (Mudd et al., 2011). The first major project where mined-out pit was used for slurry tailings storage was the Ranger uranium project which started operations in 1996. Tailings were initially planned to be disposed of in a surface TSF, but major public concern was raised regarding potential contamination of the surrounding environment. In-pit tailings deposition was therefore proposed as an alternative to conventional TSF to improve tailings long-term management (Mudd et al., 2011). In-pit disposal of tailings approach was also applied for K1SE pit in Marymia gold mine and Criterion pit in Bulong

Nickel mine (McDonald & Lane, 2010). Tailings from Marymia mine were considered hazardous and were thus disposed sub-aerially in K1SE pit. Reclamation was conducted after tailings fully consolidated and the pit was successfully integrated to become part of the local natural landscape (McDonald & Lane, 2010). A total of 14.5 m of slurry tailings were also deposited in Nickel mine pit in 2002 (McDonald & Lane, 2010). Solid content of the tailings was around 20%, which caused large deformations during consolidation. Closure and reclamation were conducted after consolidation was almost finished (McDonald & Lane, 2010). In-pit tailings management in these two mine sites was reported to have been rather cost-effective compared to conventional surface TSFs, and provided various environmental benefits, including an increase of tailings physical stability and a reduction of the raw-water requirements (MEND, 2015).

However, in-pit disposal also presents some constraints which can limit its application, including safety and hydrological aspects together with site-specific conditions (MEND, 2015; Rousseau & Pabst, 2022). For example, potential migration of contaminants to the surrounding fractured rock mass and groundwater must be evaluated and controlled (Davies, 2002; Moïse & Thomas, 2018). Other constraints include resource sterilization, operational complexities especially regarding mine waste transport and deposition in the pit. Pit disposal can only start after all of the activities in the pit are completed, and thus additional temporary surface disposal areas are required (Bhuiyan et al., 2015). Also, surface pillar stability and infiltration can be problematic if production continues underground during deposition (MEND, 2015).

2.2.2.2 Principles and implementation of the permeable envelope concept

The idea of an engineered pervious envelope surrounding the tailings mass was first proposed in 1984 by Cameco Corporation, Saskatchewan (MEND, 2015). The objective of the permeable envelope is to control potential environmental contamination by directing the groundwater around the tailings mass instead of flowing through it thus limiting the interactions between local groundwater and potential contaminants (process pore water or reactive minerals) (Cameron & Dave, 2015). This can be done by installing a highly permeable envelope compared to tailings around the pit and local groundwater would, therefore, flow around the tailings mass instead of flowing through them (figure 2-5).

The pervious surround was constructed with a gradational increase in grain size as in the Rabbit Lake in-pit tailings management (RLITMF) (i.e., a fine sand filter at the tailings surfaces, and a crushed rock layer at the outermost zone of the envelope which might be constructed by waste rocks from the adjacent mining activities). The pervious envelope was continuously constructed as tailings was filled in the pit (MEND, 2015). The permeable envelope could also be porous natural rock surround as in the case of JEB pit in the McClean Lake uranium mine facilities (i.e., JEB tailing pit required the tailings placed in a pit need to have hydraulic conductivity at least ten times lower than the surrounding host rocks) (MEND, 2015). A partial engineered pervious surround was also applied at the Deilmann tailings management facility (DTMF) (Khaled, 2012). Bottom drain system was constructed at the lower portions of the pit to enhance consolidation of the tailings and increase the density of the tailings (Cameron & Dave, 2015). The same concept with the implementation of bottom drainage and partial pervious surround was also applied for the uranium Langer Heinrich mine in the Republic of Namibia (Cameron & Dave, 2015). The drainage materials were made from coarse-grained waste rocks resulting from mining activities on sites which were highly permeable compared to the placed tailings mass (i.e., the hydraulic conductivity contrast of the under-drainage system, pervious and tailings materials was around 6 orders of magnitude) to prevent water from flowing through the tailings body (Cameron & Dave, 2015). Apart from environmental benefits, pervious envelope can also contribute to accelerate consolidation of tailings in the pit which is similar to the effect of WRI in the tailings impoundment, yet these effects have not been mentioned nor quantitatively evaluate in literatures.

The combination of permeable envelope and WRI in the pit would be used for the first time as multiple drainage paths in the pit. The combination would possibly further promote the benefits of those two techniques. Unknowns related to the performances of both permeable envelope and WRI, and their influences on the consolidations behaviour of tailings, however, remains challenging.

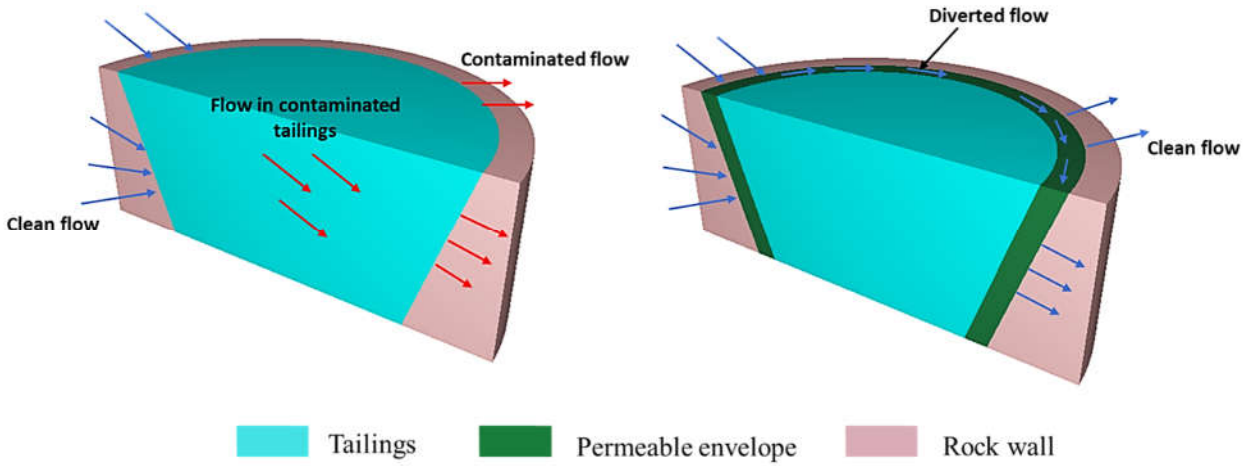

Figure 2-5: Conceptualized structure of water movement in and around the pit (a) without the installation of the pervious surround and (b) with the presence of the pervious surround. Regional groundwater flows around the tailings following the more permeable envelope rather than through the contaminated tailings.

2.2.2.3 Critical concerns in integrated mine waste management in-pit

In-pit tailings disposal, despite numerous advantages compared to surface TSF, is also facing several challenges and unknowns that could somewhat limit its application. Preventing environmental contamination is particularly critical, and tailings hydraulic conductivity therefore needs to be decreased to isolate them and enhance the performance of the permeable envelope. Reclamation construction also requires that tailings settlement is completed to avoid long-term deformation of cover systems (and thus deterioration or even performance loss). Finally, pit storage capacity also needs to be explicitly estimated when both tailings and waste rocks are co-disposed.

A successful in-pit disposal implementation thus requires to properly capture the evolution of tailings consolidation and excess PWP dissipation. Such evaluation requires to combine experimental characterization of waste materials and numerical simulations of consolidation behaviour. Numerical models must also integrate non-linear changes of stiffness and hydraulic conductivity resulting from changes in the void ratio of tailings to precisely estimate volume changes with time. Several factors can influence the effectiveness of the technique such as tailings filling rate, tailings and waste rocks hydro-mechanical properties, layer thicknesses, overall pit wall angles, and WRIs design should be

considered. The applicability and advantages of tailings and waste rock co-disposal also needs to be thoroughly proven and optimized before it can be implemented in the field. A solid understanding of tailings consolidation characteristic is therefore required to predict the rate and magnitude of short- and long-term settlement of tailings disposed of in the pit. The objective of the following sections is thus to review geotechnical properties of mine tailings and waste rocks, consolidation theories applied to slurry tailings, application of vertical drainage path to accelerate tailings consolidation and numerical tools available to simulate non-linear tailings consolidation. Understanding of water movement and predictive functions to estimate hydraulic conductivity of tailings was critical to have a proper prediction of consolidation process of tailings.

2.3 Movement of water in mine wastes

2.3.1 Water flow in saturated zone

The hydraulic head is defined as the amount of energy stored per unit mass of fluid. The Bernoulli's equation describes the components of the hydraulic head of fluid under simplified conditions (i.e., for an incompressible non-viscous fluid and a laminar, non-turbulent flow) (Holtz & Kovacs, 1981):

$$h(x,y,z) = z + \frac{u_w}{\rho_w g} + \frac{v^2}{2g} \tag{2.1}$$

Where u_w: water pressure (kPa); ρ_w: water density (kg/m^3); g: gravitational acceleration (m/s^2) and v: fluid velocity (m/s).

The movement of water in saturated medium can be described by Darcy's law with the assumption of saturated medium, incompressible fluid and laminar flow (Holtz & Kovacs, 1981):

$$q = -k_{sat} i \tag{2.2}$$

Where q: specific flow, frequently called Darcy's velocity (m/s); k_{sat}: saturated hydraulic conductivity (m/s); i: hydraulic gradient, i.e., the variation of hydraulic head, h, over a certain distance, ∂z, which is derived in one-dimension as:

$$i = \frac{\partial h}{\partial z} \tag{2.3}$$

2.3.2 Predictive models of saturated hydraulic conductivity

The saturated hydraulic conductivity, k_{sat}, of a soil could be measured in the laboratory by either hydraulic conductivity test in a rigid wall (ASTM D2434), or from flexible wall (ASTM D5084). Measuring hydraulic conductivity of soils can, however, be time-consuming especially when it has to be performed for various void ratios, various predictive models have been therefore proposed to estimate the saturated hydraulic conductivity of porous materials based on their geotechnical properties (Mbonimpa et al., 2002; Chapuis & Aubertin, 2003; Chapuis, 2004).

One of the most commonly used predictive functions is Hazen (Mbonimpa et al., 2002):

$$k = C_H (D_{10})^2 (cm/s) \tag{2.4}$$

Where C_H: a material coefficient; and D_{10}: the diameter corresponding to 10% passing on the cumulative particle-size distribution curve.

The model was developed for loose sands and gravels with $C_u < 5$ and 0.1 mm $\leq D_{10} \leq$ 3 mm (Chapuis, 2004). When D_{10} is smaller than 0.1 mm (i.e., silty materials), Hazen coefficient can vary significantly (Mbonimpa et al., 2002). The model proposed by Hazen is therefore not always precise to determine tailings hydraulic conductivity (Mbonimpa et al., 2002).

Kozeny-Carman model determines the hydraulic conductivity as a function of the void ratio, e, the specific surface S (m^2/kg of solids), and a factor C which represents the shape and tortuosity of flow channels (Chapuis & Aubertin, 2003):

$$k = C \frac{g}{\mu_w \rho_w} \frac{e^3}{S^2 D_R^2 (1+e)} \tag{2.5}$$

Where S: specific surface of material (m^2/kg); g: gravitational constant ($m^{-3}kg^{-1}s^{-2}$); e: void ratio; μ_w: the dynamic viscosity of water ($\mu_w \approx 10^{-3}$ Pa.s at 20 ^{0}C); ρ_w: density of water (ρ_w = 998 kg/m^3 at 20 ^{0}C); D_R: relative density of solids (or specific gravity G_s).

KC model was also presented in another form by Chapuis and Aubertin (2003) based on the concept of the equivalent diameter derived from the specific surface area of the solid grains, S_m:

$$\log(k) = A + \log\left[\frac{e^3}{S_m^2 D_R^2 (1+e)}\right] \tag{2.6}$$

Where k unit is in m/s; A range from 0.29 to 0.51 for a C value between 0.2 and 0.5 as indicated by Carman (1939).

Hydraulic conductivity of tailings predicted by KC model are usually slightly overestimated because of the particles angularity, the creation of new fines during compaction and possible chemical reactions occurring during hydraulic conductivity tests (Chapuis & Aubertin, 2003). Chapuis and Aubertin (2003), therefore, proposed a modified and more precise equation for the prediction of tailings hydraulic conductivity:

$$log\left[\frac{k}{1\ m/s}\right] = 1.5\left\{0.5 + log\left[\frac{e^3}{S_m^2 D_R^2 (1+e)}\right]\right\} + 2 \tag{2.7}$$

Kozeny-Carman Modified (KCM) model (Mbonimpa et al., 2002)

Mbonimpa et al. (2002) proposed some modifications to the Kozeny-Carman function to include the properties of porous space, void ratio and the grain surface characteristics:

$$k = f_f f_v f_s \tag{2.8}$$

With:

$$f_f = \frac{\gamma_w}{\mu_w}$$

$$f_v = \frac{e^{(3+x)}}{(1+e)}$$

$$f_s = C_U^{1/3} D_{10}^2$$

Hence:

$$k_G = C_G \frac{\gamma_w}{\mu_w} \frac{e^{(3+x)}}{(1+e)} C_U^{1/3} D_{10}^2 \quad (2.9)$$

Where f_f: function of the fluid properties in the general hydraulic conductivity model ($m^{-1}s^{-1}$); f_v: function of the void space in the general hydraulic conductivity model [-]; f_s: function of the solid grain surface in the general hydraulic conductivity model (m^2); C_G: a constant (C_G = 0.1); γ_w: unit weight of water (γ_w = 9.81 kN/m^3); x: tortuosity factor (x =2); C_U: the uniformity coefficient ($C_U = D_{60} / D_{10}$).

Hydraulic conductivity estimated using Kozeny-Carman Modified (KCM) model usually differs by up to one or two orders of magnitude from Kozeny-Carman (KC) because of the difference in the determination of the specific surface of particles, especially when the proportion of fine particles is significant (Peregoedova et al., 2013).

Predictive equations presented above were proposed based on the effective diameter D_{10}. However, when the materials contain large-size blocks, such as waste rocks, predictive equations can lead to some uncertainties in the estimation of the hydraulic conductivity (Peregoedova et al., 2013). Consequently, other predictive models have been developed based on D_{50} to consider the effect of coarse particles more precisely on the hydraulic conductivity.

Taylor (1948)

$$k_{sat} = C_1 \frac{\gamma_w}{\mu_w} \frac{e^3}{(1+e)} D_{50}^{1.5} \quad (2.10)$$

Where D_{50}: diameter of grains corresponding to 50% passing on the grain size curve (cm); C_1: a constant identified from experimental results.

Shepherd (1989)

$$k_{sat} \left(\frac{cm}{s}\right) = 3.53 \times 10^{-4} \times [100 D_{50}^{1.5}] \quad (2.11)$$

Model of Taylor predictive equations usually provides fairly accurate estimation (within a factor of 3) of waste rocks hydraulic conductivity (Peregoedova, 2012).

Hydraulic conductivity of materials would play a key role on the rate of dissipation of PWP, and hence on the rate of consolidation of materials.

2.4 Consolidation of tailings

2.4.1 Consolidation phases

Consolidation of soft fine-grained materials in general, and of mine tailings in particular, and which have a high initial water content and void ratio, is driven by gravitational body forces (i.e., buoyant weight of solids) with or without external load (Carrier et al., 1983; Ito & Azam, 2013; Ahmed & Siddiqua, 2014; Qi et al., 2017). An overlaying water layer is typically formed during the consolidation process as excess pore water drains upwards, leading to an increase of the effective stress (Lee & Sills, 1981; Bartholomeeusen et al., 2002; Ito & Azam, 2013).

Sedimentation of tailings soft deposits can be divided into three successive (and partially overlapping) stages: flocculation, settling/sedimentation, and consolidation (Imai, 1981; Bonin et al., 2014; Agapito & Bareither, 2018; Pu et al., 2018). During flocculation, the solid content of the mixture is very low, and solid particles are still far away from each other. Particle segregation is expected to occur during this phase (Jeeravipoolvarn, 2010). Then, sedimentation of particles takes places, accompanied with the reduction of porosity and the progressive increase of solid contents. Soil particles, nevertheless, are still in an effective-stress-free state. In the last stage, tailings undergo consolidation which could be induced by either or a combination of gravitational force (i.e., self-weight consolidation) or external surcharge loading (e.g., loads due to the sequential filling of tailings). During consolidation, effective stress will build up with the dissipation of pore water pressure, and there is a clear interface between the settling solids and the supernatant water, and this boundary tends to move downwards while consolidation occurs. Settling and consolidation phenomenon usually take place simultaneously and it can be difficult to differentiate them (Imai, 1981). There is a transition zone between settling and consolidation behaviour when effective stress is partially developed (Somogyi, 1980; Imai, 1981; Schiffman et al., 1988; Tan et al., 1990). Primary and secondary consolidation are usually observed from typical deformation curves. Primary consolidation relates to the settlement of tailings layer because of the dissipation of excess pore water pressure. Primary consolidation ceases when the hydrostatic pressure reaches an equilibrium (i.e.,

when the excess pore-water pressure has entirely dissipated) (Imai, 1981; Schiffman et al., 1988; Bonin et al., 2014). Secondary consolidation refers to the consolidation that follows primary consolidation when excess pore water pressure has reached zero and is typically related to a reorganization of tailings particles. The secondary consolidation rate depends on the viscous resistance of the soil structure, while primary consolidation is controlled by Darcy's law. Secondary consolidation can be significant for soft clay and organic soils (Mittchell & Soga, 2005), but more rarely for hard rock mine tailings.

2.4.2 Consolidation of tailings under applied loading

When tailings are subjected to external loads, pore water in the voids is squeezed out, leading to the volumetric strain of the solid medium. During this process, the loading is transferred from pore water to tailings particles, and the process terminates once excess pore water pressure totally dissipates. Degree of consolidation U at a given time can be expressed as (Taylor, 1948):

$$U\ (\%) = \left(1 - \frac{\Delta u}{u_0}\right)\ x\ 100\% \tag{2.12}$$

Where Δu: excess pore water pressure (kPa), and u_0: initial excess pore water pressure (kPa).

As Δu decreases, the degree of consolidation *U* increases. When excess pore pressure becomes zero, the pore pressure equals hydrostatic pressure. The dissipation of water in the voids is accompanied by the settlement of the tailings and the reduction of voids (assuming that the fluid is incompressible (Holtz & Kovacs, 1981):

$$s = \frac{\Delta e}{1 + e_0} H_0 \tag{2.13}$$

Where *s*: settlement (m), e_0: initial void ratio (-), and H_0: initial thickness of soil layer (m).

Consolidation of tailings might be studied in the laboratory using conventional odometer tests (ASTM D2435/D2435M − 11) which give the relationship between void ratio and the effective stress σ_v' (kPa).

The coefficient of compressibility a_v is calculated from oedometer test results as (Holtz & Kovacs, 1981):

$$a_v = \frac{-\Delta e}{\Delta \sigma_v'} \tag{2.14}$$

When the results are expressed as a function of the volumetric strain, the slope of the compression curve is called the coefficient of volume change, m_v, and:

$$m_v = \frac{-\Delta \varepsilon_v}{\Delta \sigma_v'} = \frac{a_v}{1 + e_0} \tag{2.15}$$

Where ε_v: vertical compression of tailings.

Results can also be presented in terms of void ratio versus the logarithm of effective stress, in which case the slope of the virgin compression curve is defined as the compression index, C_c, (Holtz & Kovacs, 1981):

$$C_c = \frac{-de}{dlog\sigma_v'} = \frac{\Delta e}{log\frac{\sigma_2'}{\sigma_1'}} \tag{2.16}$$

Terzaghi's 1D consolidation theory

Terzaghi's theory describes 1D soil consolidation with the assumption of a linear relationship between stress and strain. The basic governing equation of Terzaghi's theory represents equilibrium condition, stress-strain relationship and continuity equation, and can be expressed in the following form (Holtz & Kovacs, 1981):

$$C_v \frac{\partial^2 u}{\partial z^2} = -\frac{\partial \sigma_v'}{\partial t} \tag{2.17}$$

Where C_v: vertical coefficient of consolidation (m^2/s); u: excess pore pressure (kPa); t is time (s).

C_v is assumed to be constant in this theory and represents the material properties that govern the consolidation process as expressed in the following equation (Holtz & Kovacs, 1981):

$$C_v = \frac{(1+e_0)k_v}{\gamma_w a_v} = \frac{k_v}{\gamma_w m_v} \tag{2.18}$$

C_v can be obtained experimentally using odometer test with step loading. The methods of Casagrande (1938) and Taylor (1948) are commonly used to determine graphically the relationships between displacement and time (Holtz & Kovacs, 1981):

- Method of Casagrande (1938)

$$C_v = \frac{0.197H^2}{t_{50}} \tag{2.19}$$

- Method of Taylor (1948)

$$C_v = \frac{0.848H^2}{t_{90}} \tag{2.20}$$

In equations 2.19 and 2.20, H is the maximum drainage distance (m); and t_{50} and t_{90} are the times corresponding to a vertical degree of consolidation of 50% and 90% respectively. For radial consolidation with horizontal flow, equation 2.18 becomes (Holtz & Kovacs, 1981):

$$C_h = \frac{k_h}{\gamma_w m_v} \tag{2.21}$$

Where C_h: horizontal coefficient of consolidation (m^2/s); k_h: horizontal hydraulic conductivity of soil (m/s). The horizontal coefficient of consolidation is usually 2 to 5 times greater than the vertical coefficient of consolidation (Atkinson & Eldred, 1981; Bergado et al., 1993). Equation 2.17 can be modified by expressing the vertical effective stress by total stress and pore water pressure as:

$$C_v \frac{\partial^2 u}{\partial z^2} = \frac{\partial u}{\partial t} - \frac{\partial \sigma_v}{\partial t} \tag{2.22}$$

The solution of Terzaghi's equation for different boundary conditions allows to express excess pore water pressure u as a function of time factor T_v and position factor Z (= z/H) (Mittchell & Soga, 2005; Das, 2010):

$$u_v = \sum_{m=0}^{\infty} \frac{2u_0}{M}\left(\sin\frac{MZ}{H}\right)e^{-M^2T_v} \tag{2.23}$$

This value equals the thickness of the compressible layer in case of one single drainage and is half of the layer thickness in case of double drainage system. In equation 2.23:

$$\mathrm{M} = \frac{\pi}{2}(2m+1) \tag{2.24}$$

Where *m*: an integer.

Time factor T_v relates to the coefficient of consolidation C_v by equation:

$$T_v = \frac{c_v t}{H^2} \tag{2.25}$$

Where *t* is the time necessary to obtain the degree of consolidation corresponding to the time factor at the interested point.

Terzaghi's theory has been successfully applied in many geotechnical problems in practice (Holtz & Kovacs, 1981). The principal assumptions of Terzaghi's theory include: the soil is fully saturated, soil particles and water are incompressible, Darcy's law is valid, and finally consolidation properties of the materials are constant. However, some differences can be observed between measured and calculated settlement of slurry materials (such as tailings or dredged soils), which can be attributed to Terzaghi's theory physical assumptions (Gibson et al., 1981; Schiffman, 1982; Fox, 1999; Morris, 2002; Bolduc & Aubertin, 2014). For example, equation 2-18 considers that hydraulic conductivity and coefficient of compressibility are constant, while in practice they vary with the void ratio (Schiffman, 1982; Cargill, 1984; Morris, 2002). Also, equation 2.17 neglects self-weight consolidation behaviour which can be significant for tailings. For all these reasons, the large strain theory was proposed (Somogyi, 1980; Lee & Sills, 1981; Schiffman, 1982; Morris, 2002). Finally, the Terzaghi's theory is valid only for vertical consolidation, and horizontal water movement and settlement of materials are thus neglected. This might cause some uncertainties in the estimation of tailings settlement where 3D effect of tailings consolidations is significant (i.e., tailings disposed in an open pit).

2.4.3 Large strain consolidation theory for mine tailings

A general form of one-dimensional non-linear finite strain consolidation for saturated soil (including tailings) layers was proposed by Gibson et al. (1967) to overcome the limitations of Terzaghi's small strain theory. Gibson's equation can accommodate large strain evolution and variations in hydraulic conductivity and soil stiffness during the consolidation process. Finite strain consolidation theory is, therefore, more representative of tailings behaviour in field conditions (Schiffman, 1982; Bartholomeeusen et al., 2002; Fahey et al., 2010).

The first general form of one-dimensional non-linear finite strain consolidation for saturated thick soil layers was proposed by Gibson, et al. (1967):

$$\left(\frac{\gamma_s}{\gamma_w}-1\right)\frac{d}{de}\left[\frac{k(e)}{1+e}\right]\frac{\partial e}{\partial z}+\frac{\partial}{\partial z}\left[\frac{k(e)}{\gamma_w(1+e)}\frac{d[\sigma'(e)]}{de}\frac{\partial e}{\partial z}\right]=-\frac{\partial e}{\partial t} \tag{2.26}$$

Where *e*: void ratio; γ_s and γ_w: solid and water unit weights respectively; *k(e)*: the hydraulic (Townsend & McVay, 1990)conductivity expressed as a function of the void ratio (m/s); σ': effective stress (kPa).

Gibson et al. (1981) also derived finite-strain coefficient of consolidation *g(e)* as follows:

$$g(e)=-\frac{k(e)}{\gamma_w(1+e)}\frac{\partial\sigma'}{\partial e} \tag{2.27}$$

The finite-strain coefficient of consolidation $g(e)$ can also be related to the conventional coefficient of consolidation C_v as follows (Gibson et al., 1981):

$$g(e)=\frac{C_v}{(1+e)^2} \tag{2.28}$$

A linearization constant $\lambda(e)$ was also proposed by Gibson, 1981:

$$\lambda(e)=-\frac{d}{de}\left(\frac{de}{d\sigma'}\right) \tag{2.29}$$

Equation 2.26 can then be analytically solved with the assumption of constant *g(e)* and $\lambda(e)$:

$$\frac{\partial^2 e}{\partial z^2} + \lambda(\gamma_s - \gamma_w)\frac{\partial e}{\partial z} = \frac{1}{g}\frac{\partial e}{\partial t} \tag{2.30}$$

In practice, neither void ratio – effective stress nor hydraulic conductivity – effective stress relationships are linear, and only coefficient of consolidation $g(e)$ can be assumed constant only for a limited range of σ' and *e*. Several attempts to use the average and constant values of $\lambda(e)$ and *g(e)* usually resulted in poor estimations (Lee & Sills, 1981; Morris, 2002).

Koppula (1970) adjusted the original equation of Gibson et al. (1967) by considering the excess pore-water pressure *u* as dependent variable:

$$\frac{\partial}{\partial z}\left[-\frac{k}{\gamma_w(1+e)}\frac{\partial u}{\partial z}\right] + \frac{de}{d\sigma'}\frac{\partial \sigma'}{\partial t} = 0 \tag{2.31}$$

Somogyi (1980) then proposed to define the time variation of effective stress as:

$$\frac{\partial \sigma'}{\partial t} = \left[(G_s - 1)\gamma_w \frac{d(\Delta Z)}{dt}\right] - \frac{\partial u}{\partial t} \tag{2.32}$$

Where ΔZ represents an additional volume of solid particles in a continuous accretion (e.g., during tailings deposition). Equation 2.26 can therefore be rewritten in terms of excess pore water pressure *u* (Somogyi (1980):

$$\frac{\partial}{\partial z}\left[\frac{k(e)}{\gamma_w(1+e)}\right]\frac{\partial u}{\partial z} + \frac{k(e)}{\gamma_w(1+e)}\frac{\partial^2 u}{\partial z^2} + \frac{de}{d\sigma'}\frac{\partial u}{\partial t} - \frac{de}{d\sigma'}\left[(G_s - 1)\gamma_w \frac{d(\Delta Z)}{dt}\right] = 0 \tag{2.33}$$

Equation 2.26 and 2.33 where the dependent variables are either the void ratio or the excess PWP are usually the ones used to describe slurry tailings consolidation (Jeeravipoolvarn et al., 2008).

2.4.4 Constitutive relationships for the estimation of slurry tailings consolidation

Appropriate constitutive relations are necessary to precisely estimate the evolution of compressibility and hydraulic conductivity of tailings as void ratio changes during consolidation. These relations are typically highly non-linear for slurry tailings and can significantly change over low values of pressured applied (Somogyi, 1980; Schiffman, 1982).

Various mathematical functions representing the relationship between effective stress and void ratio have been proposed (table 2.3), including power function (Somogyi, 1980), extended power function (Liu & Znidarčić, 1991), logarithmic function (Bartholomeeusen et al., 2002), and Weibull function (Jeeravipoolvarn et al., 2008). Each function has its own advantages and limitations. For example, the extended power function proposed by Liu and Znidarčić (1991) can define the void ratio at zero effective stress, while power function cannot. Also, Weibull function is particularly practical to capture the pre-consolidation behaviour of oil sand tailings under loadings (Jeeravipoolvarn et al., 2008). Best practice usually consists in determining these functions (and in particular parameters *A, B, C, D, E* and *F* in table 2-3) using experimental tests (Jeeravipoolvarn, 2010).

Table 2-3: Void ratio and effective stress relationship

Equations	**Functions**	**Authors**
$e = A\sigma' B$	Power function	Somogyi (1980)
$e = A(\sigma' + B)^C$ $e = A{\sigma'}^B + M$	Extended power function	Liu and Znidarčić (1991) Agapito (2015)
$e = A\ ln\sigma' + B$ $e = C\ \ln(k) + D$	Logarithmic function	(Bartholomeeusen et al., 2002)
$e = \mathrm{A} - \mathrm{Bexp}[-\mathrm{E}.{\sigma'}^{\mathrm{F}}]$	Weibull function	Jeeravipoolvarn et al. (2008)

Laboratory experiments include various types of consolidation test (sometimes coupled with hydraulic conductivity measurements) including step loading test, constant rate loading, constant rate deformation, continuous loading test, seepage induced test and centrifuge test (Ahmed & Siddiqua, 2014). These tests should preferably cover the range of void ratio, hydraulic conductivity and effective stress that tailings are expected to experience in practice (Jeeravipoolvarn et al., 2008)

Hydraulic conductivity can be expressed as a power function of void ratio as proposed by Somogyi (1980):

$$k = Ce^D \tag{2.34}$$

For mine tailings, the following empirical equation was suggested by Carrier et al. (1983):

$$k = E\frac{e^F}{1+e} \tag{2.35}$$

Where k = hydraulic conductivity of materials (m/s); and C, E, F = fitting parameters.

It is noted that KC and KCM models can also be used to relate void ratio with hydraulic conductivity and predict values of hydraulic conductivity for mine tailings as described in section 2.4.4.

2.5 Mohr Coulomb model

Mohr-Coulomb model has been widely applied to solve various geotechnical problems because of its simple input parameters required. The relationship between stress and strain in the Mohr-Coulomb model was linear up to the yielding point. Once material reaches the yielding state, the relation between the stress and the strain is perfectly plastic (i.e., the strain continues to increase without any change in the stress applied) (figure 2-6). The ratio between stress and strain within the elastic deformation regime was called elastic Young's modulus (figure 2-6) (Holtz & Kovacs, 1981).

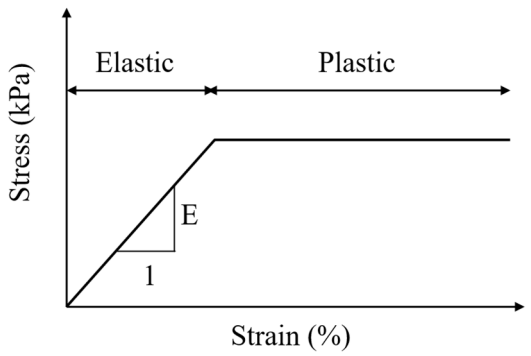

Figure 2-6: Stress-strain relation in Mohr-Coulomb model.

The general incremental elastic law in terms of the generalized stress and strain increments can be expressed as follows (Itasca, 2021):

$$\Delta\sigma_1 = \alpha_1\Delta\epsilon_1 + \alpha_2(\Delta\epsilon_2 + \Delta\epsilon_3) \tag{2.36}$$

$$\Delta\sigma_2 = \alpha_1 \Delta\epsilon_2 + \alpha_2(\Delta\epsilon_1 + \Delta\epsilon_3) \quad (2.37)$$

$$\Delta\sigma_3 = \alpha_1 \Delta\epsilon_3 + \alpha_2(\Delta\epsilon_1 + \Delta\epsilon_2) \quad (2.38)$$

Where α_1 and α_2: material constant defined as the shear modulus, *G*, and bulk modulus, *K*, as:

$$\alpha_1 = K + \frac{4}{3}G \quad (2.39)$$

$$\alpha_2 = K - \frac{2}{3}G \quad (2.40)$$

Mohr-Coulomb model requires following properties that need to be assigned in the numerical model: elastic bulk modulus, cohesion, dilation angle, internal friction angle, Poisson's ratio, elastic shear modulus or Young's modulus (Only either bulk modulus and shear modulus or Young's modulus is required to define the elasticity. When the latter was chosen, Young's modulus needs to be input in advance of the Poisson's ratio) (Itasca, 2021).

The elastic-perfectly plastic Mohr-Coulomb model was used in literature to simulate tailings consolidation behaviour with the presence of WRI (Jaouhar et al., 2013; Boudrias, 2018) and it was also commonly used for the estimation of compressibility behaviour of mining backfill (Wang et al., 2021a). This model was utilized by Boudrias (2018) without updating properties of tailings (or they were updated at the beginning of each loading steps) and Zhou et al. (2019) (with continuous update of tailings properties) to investigate the consolidation of tailings, and results obtained shown a reasonable agreement with literature and laboratory experiment results. It is, however, noticed that the Mohr-Coulomb model cannot capture the plastic volumetric strain developed under isotropic compression (Wang et al., 2021a).

2.6 Acceleration of consolidation using drainage paths

Primary consolidation of tailings (and soft fine-grained materials in general) can take a very long time because of their low hydraulic conductivity and their large initial water content. This delay before reaching equilibrium significantly affect the construction and maintenance of tailings

impoundments. Drainage systems have therefore been proposed and successfully applied to accelerate consolidation (Casagrande & Poulos, 1969; Fredlund & Hasan, 1979; Qin et al., 2010; Shan et al., 2014). Their objective is to shorten the length of the drainage path (i.e., promoting the horizontal movement of water toward the drain materials - radial consolidation, instead of vertical movement only in case where no drain materials were presented) (Bergado et al., 2002; Indraratna et al., 2012; Liu & Rowe, 2015). Vertical drains pathways are often used, for example, in clay where horizontal hydraulic conductivity is usually significantly greater than the vertical hydraulic conductivity (Atkinson & Eldred, 1981). A direct advantage of the vertical drains is that shear strength builds up faster as consolidation progresses (Bergado et al., 1993; Indraratna et al., 2005), therefore increasing the overall stability of the material. The use of WRI as drainage pathways in tailings impoundments is a direct application of the technique to TSF (section 2.2.1).

2.6.1 Various techniques on consolidation acceleration of soft materials

Preloading/surcharge is among the most popular techniques used to improve soft ground condition and consists in applying a temporary loading (usually compacted earth materials) upon compressible subsoil (often before permanent construction load is applied). Stresses applied by preloading must exceed pre-consolidation pressure to be efficient. The technique can be applied alone or in combination with vertical drains (Bergado et al., 1993; Indraratna, 2015; Liu & Rowe, 2015; Lu et al., 2015).

Stone or gravel columns can also promote consolidation of soft soils and reduce total and differential settlements. Stone columns can provide a drainage path and dissipate excess pore-water pressure. A transfer of stress from soft materials to the stone column is also usually observed because of their higher stiffness (Barksdale, 1987; Guetif et al., 2007; Basack et al., 2018), which can in turn contribute to reduce the vertical stress applied on the subsoil and diminish the excess pore water pressure (Han & Ye, 2002). Hydraulic conductivity of stone columns can sometimes decrease because of clogging by fine particles (Han & Ye, 2002; Basack et al., 2015; Basack et al., 2018). WRI has been implemented in TSFs applying a similar principle as stone columns to enhance tailings consolidation (also see section 2.2.1). The arching effect occurring during the application of stone column was also observed with WRI in tailings settlement (James & Aubertin, 2009; Li & Aubertin, 2009b; Boudrias, 2018; Lévesque, 2019). The distribution of decrease of settlement of tailings

because of the arching effect was not quantitatively indicated in the literature as this can somewhat influence the estimation of tailings volume that can be stored in the TSFs. Tailings particle migration has no significant effect on WRI hydraulic conductivity in TSFs (Essayad et al., 2018; Mbemba & Aubertin, 2021b).

Prefabricated vertical drains (PVDs) are widely used to improve soft cohesive soils (Holtz, 1987). PVDs consist of a porous synthetic material surrounding a plastic core which objective is to favour water movement, while preventing the migration of soil particles and limiting the clogging of the core drain.

2.6.2 Consolidation theory with combination of vertical and radial drainage

Consolidation equation with vertical and radial drainage effects was proposed as a combination of the separate solutions for vertical drainage and radial drainage (Carrillo, 1942; Barron, 1948). The degree of consolidation $\overline{U_f}$ at any time can be expressed as (Carrillo, 1942):

$$\overline{U_f} = \overline{U_h} + \overline{U_v} - \overline{U_h}\,\overline{U_v} = 1 - (1 - \overline{U_v})(1 - \overline{U_h}) \tag{2.41}$$

Where $\overline{U_f}$: average degree of consolidation under combination of vertical and horizontal drainage, $\overline{U_h}$ and $\overline{U_v}$: average degree of consolidation due to radial and vertical drainage respectively.

- Radial consolidation theory: Barron's model (1948)

Barron (1948) theory extended one-dimensional vertical flow theory of Terzaghi to a radial flow problem. This solution is based on two types of soil consolidations that are free strain consolidation and equal strain consolidation (Barron, 1948). Various assumptions were made in the Barron's theory:

- All the additional loads applied are initially carried by excess pore pressure. In other words, the considered materials are saturated.
- Darcy's law is valid.
- All compressive strains within the soil mass are vertical, and no shear stress exists.
- The horizontal sections remain horizontal during consolidation.

- The influence zone of each well is cylinder.
- The top of the layer is freely draining, but the bottom is impervious.
- The hydraulic conductivity of the vertical drains is considered infinite compared to that of the surrounding materials.

A governing partial differential equation for the one-dimensional compression with vertical and radical flow is given by Barron (1948) as follows:

$$c_v \frac{\partial^2 u_r}{\partial z^2} + c_h \left(\frac{\partial^2 u_r}{\partial r^2} + \frac{1}{r} \frac{\partial u_r}{\partial r} \right) = \frac{\partial u_r}{\partial t} \tag{2.42}$$

With c_h: radial coefficient of consolidation ($c_h = k_h / \gamma_w m_v$) (m^2/s), t: time elapsed after the application of loading (s), u_r: pore-water pressure depending on time t (kPa), the depth z and the radial distance r of the considered point from the centre of the drained material cylinder. For the single radial drain, equation 2.42 becomes:

$$c_h \left(\frac{\partial^2 u_r}{\partial r^2} + \frac{1}{r} \frac{\partial u_r}{\partial r} \right) = \frac{\partial u_r}{\partial t} \tag{2.43}$$

Pore-water pressure at the radial distance r:

$$u_h = \frac{4u}{D_e^2 F(n_e)} \left[r_e^2 ln \left(\frac{r}{r_w} \right) - \frac{r^2 - r_w^2}{2} \right] \tag{2.44}$$

Average degree of consolidation $\overline{U_h}$ because of radial drainage:

$$\overline{U_h} = 1 - exp \left[\frac{-8T_h}{F(n_e)} \right] \tag{2.45}$$

With drain spacing factor $F(n_e)$ and the spacing ratio n_e:

$$F(n_e) = \frac{n_e^2}{n_e^2 - 1} \ln(n_e) - \frac{3n_e^2 - 1}{4n_e^2} \tag{2.46}$$

With: $n_e = D_e / D_w = r_e / r_w$

The conventional radial consolidation proposed by Barron (1948) considers m_v and k_h as constant values for prefabricated vertical drains, and therefore they do not change with the change of void ratio e. This might not be representative for mine tailings under loadings as hydraulic conductivity and stiffness of tailings usually change with the settlement of tailings (Somogyi, 1980; Townsend & McVay, 1990; Fourie et al., 2022).

Radial and vertical drainage was decoupled in the approach of Barron (1948), and a closed-form solution for the degree of consolidation was not derived from this study. Hansbo et al. (1981) proposed a simple closed-form solution of the degree of consolidation for the case of equal strain. The overall solution was calculated as the product of vertical and radial drainage solutions (Leo, 2004). Solutions of Barron (1948) and Hansbo et al. (1981), however, only dealt with instantaneous loads which is usually not the case in practice. The effect of both vertical and radial drainage in a coupled fashion under a progressive loading condition with the effect of well resistance and smeared zone was considered by Leo (2004). Results indicated that incremental loading could lead to a slower degree of consolidation of soils compared to that of progressive filling. Tailings was usually considered to be instantaneously placed in TSFs, while it was usually filled in TSFs progressively with the presence of WRI (Bolduc & Aubertin, 2014). The effect of the assumption of instantaneous filling on the consolidation of tailings thus needs to be further investigated.

2.6.3 Spatial distribution of effected zones around vertical drains

2.6.3.1 Smear zone of a representative unit cells

The consolidation behaviour of compressible soil layer around a vertical drain is usually represented by an axisymmetric unit cell (Barron, 1948; Yoshikuni & Nakanodo, 1974; Hansbo, 1981). A single vertical drain is assumed to be surrounded by a ring of soft material, itself composed of two zones: the smear zone of disturbed tailings created during the installation of the vertical drain and the undisturbed tailings. The equivalent radius r_w [L] in case band-shaped drain with width a and thickness b was used can be calculated as follows (Hansbo et al., 1981):

$$r_w = (a + b)/\pi \tag{2.47}$$

Installation of vertical drains can cause disturbance in the vicinity of the drains (Hansbo, 1981; Walker & Indraratna, 2007; Lu et al., 2015). Smeared zone can induce diminution of the horizontal hydraulic conductivity of soils within the disturbed zone and a linear decrease of the radial hydraulic conductivity is generally representative of the smear effect caused by the installation of drains (figure 2-7) (Hansbo et al., 1981; Leo, 2004; Lu et al., 2015). Regarding the application of WRI, this effect might be negligible as tailings and WRI are usually raised at the same time in practice (section 2.2.1). Vertical drain hydraulic conductivity can decrease with time because of the movement of fine soil particles towards the drainage wells (Casagrande & Poulos, 1969; Hansbo et al., 1981; Barksdale, 1987; Han & Ye, 2002). The discharge/drainage capacity can then become limited, and the consolidation rate could be reduced. This phenomenon is commonly called “well resistance”. Well resistance was, however, experimentally demonstrated to be insignificant for WRI (Essayad et al., 2018; Mbemba & Aubertin, 2021b).

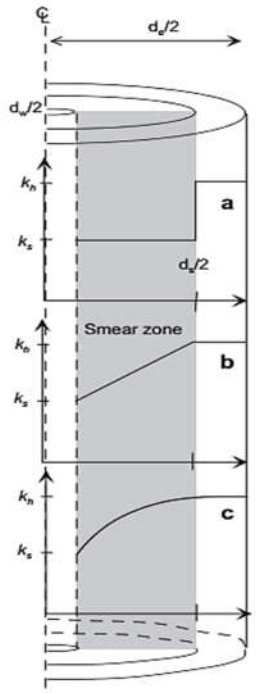

Figure 2-7: Patterns of various zones of radial hydraulic conductivity changes around vertical drains (modified after Indraratna et al. (2012)).

2.6.3.2 Radius of influence of stone columns and WRI

Granular columns are typically installed in square or triangular patterns in practice. The influence zone around the drains can be represented by a cylindrical zone. The time required to reach a certain degree of consolidation depends on the equivalent diameter of the soil cylinder, D_e (Rixner et al., 1986). The value of influencing zone *De* will depend upon the distance between drain well, *S,* and the configuration of the well distribution:

For a square pattern:

$$D_e = 1.13\,S\ (r_e = 0.565\,S) \tag{2.48}$$

For a triangular pattern:

$$D_e = 1.05\,S\ (r_e = 0.525\,S) \tag{2.49}$$

The triangular configuration is usually more efficient in practice since the drains are closer, although installation of vertical drains following a square configuration can be more practical (Han, 2015). Also, the diameter ratios of gravel columns, which is the ratio between the diameter of the influencing area and the diameter of the gravel columns, is usually smaller than that of sand drains or prefabricated vertical drains (Han & Ye, 2002).

The stiffness of the column material is much higher than the surrounding soils in practice usually from 10 to 20 or sometimes higher), which can lead to the stress concentration at the interface between rigid columns and soils, reducing the vertical stress in the soil adjust to the columns (Han & Ye, 2002; Han, 2015). The stress concentration phenomenon could also be encountered in co-disposal of tailings and WRI under external loading, reducing the vertical stress applied on tailings and consequently their settlement (figure 2-8). Stone columns are usually constructed in a group, while the WRIs are considered as single granular columns. The effect of WRI on the settlement of tailings might, thus, be different compared to the group of columns during the filling process, yet quantitative studies on this effect are still limited.

Numerical study on the effect of WRI on the tailing consolidation rate to quantify the extent of the influence zone of inclusions using SIGMA/W was also conducted by Bolduc and Aubertin (2014);

Boudrias (2018). The dissipation of excess PWP was much faster near the WRIs compared to the further distance, and the zone of influence of WRIs on the dissipation of the excess PWP could extend to a distance of around 2 times the thickness of the tailings (Bolduc & Aubertin, 2014; Boudrias, 2018) (figure 2-9). More details on the influences of WRIs on the consolidation behaviour of tailings disposed in TSFs and effects of some influencing factors (i.e., tailings properties, filling rate) can be seen in 2.2.1. Tailings consolidation can be either estimated by closed-form solutions or serval numerical tools can be used to predict these behaviours in practice.

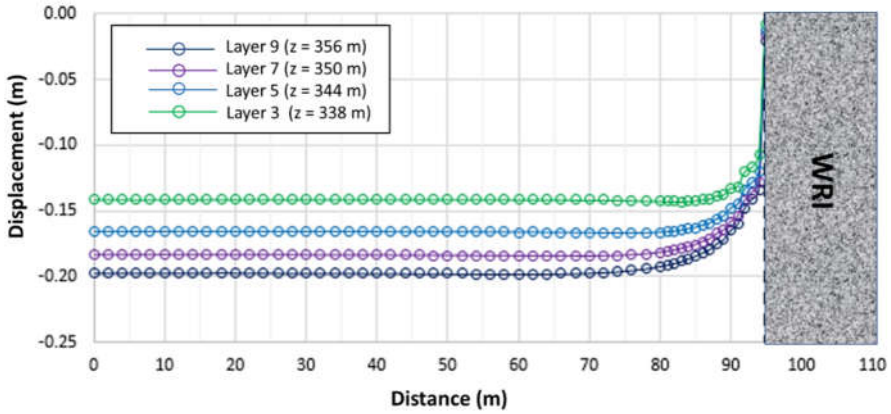

Figure 2-8: Distribution of settlement of tailings under the presence of a single WRI. Settlement was smaller at the location of WRI due to the stress concentration at the interface of the two materials (modified after Boudrias (2018)). Settlements of tailings were smaller for distance to the WRI smaller than 5 m and almost zero at the boundary of tailings and WRI.

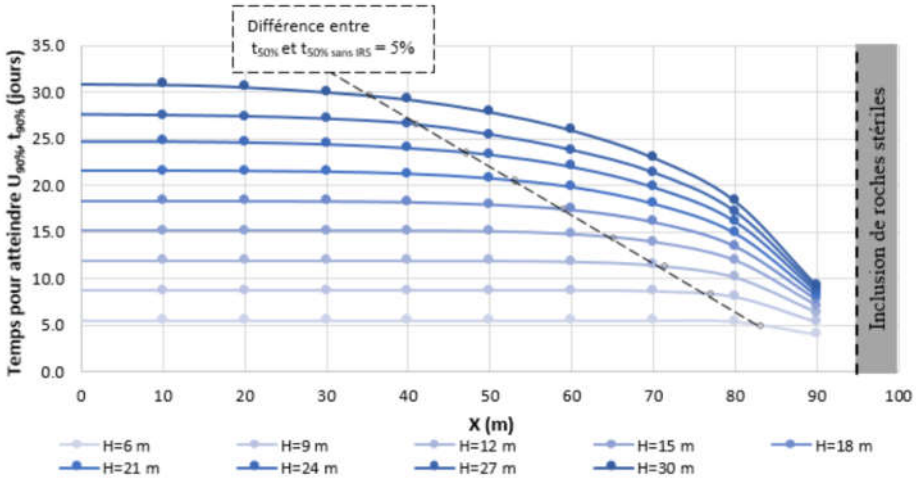

Figure 2-9: Influence zone of WRI on the rate of consolidation of tailings (modified after Boudrias (2018)). The zone increased as the thickness of tailings increased and can be estimated as around 2 times the thickness of tailings, reaching around 60 m after the thickness of tailings was 30 m.

2.7 Numerical tools available for the simulation of tailings consolidation

Various numerical tools have been developed to describe and predict consolidation of tailings (Yao & Znidarcic, 1997; Fredlund et al., 2009; McDonald & Lane, 2010; Bolduc & Aubertin, 2014; Agapito, 2015; Zhou et al., 2019). These computer programs are often used in mining practice for the analysis of 1D-, 2D- and 3D analysis of TSF. However, these programs use different spatial coordinate systems, dependent variables (void ratio versus pore water pressure), solving techniques (e.g., implicit or explicit, finite difference or finite element) which can lead to different results (Jeeravipoolvarn, 2010). The advantages and limitations of each of the computational programs must therefore be carefully considered before choosing to proceed with one or the other codes.

A summary of software available described in the aforementioned section with the constitutive relations that can be simulated, and the multi-dimensionality of each software is presented (table 2-4). From the table, it can be seen that FLAC/FLAC3D can simulate any type of constitutive relations in either 2D or 3D analysis, which offer various benefits when it comes to model the real consolidation behaviour of tailings and when complex boundary conditions might be encountered in practice. Brief description on the advantages and limitations of each software was presented. It is

noted that apart from these above-mentioned software, there are also a few more software that can be used to estimate consolidation of materials, such as Plaxis 3D, Settle3, and Abaqus. User-defined models are also available in these software, which can also enhance the flexibility of the tools to solve the complex issues. However, only software that is commonly used to estimate the tailings consolidation was mentioned in this reviewing section.

Table 2-4: Summary of software that has been used for the simulation of tailings consolidation

Software	**Constitutive relations**	**Dimensionality**	**References**
CONDES	Extended power function	1D, pseudo-3D	(Yao & Znidarcic, 1997)
FSConsol	Extended power function	1D, pseudo-3D	(FSCONSOL, 1999)
SVOffice	Power/extended power function Weibull function	2D, 3D	(Bentley, 2021)
Plaxis	Constant values	2D	(Bentley, 2021)
SIGMA/W	Constant values	2D	(Bentley, 2021)
FLAC/FLAC3D	Power/extended power function Weibull function	2D, 3D	(Itasca, 2021)

2.7.1 CONDES

CONDES is a 1-D large strain consolidation program that was first developed at the university of Colorado by Yao and Znidarcic (1997). The program employed the one-dimension consolidation equation proposed by Gibson et al. (1967) as the governing equation for the model. Regarding the $e - \sigma'$ relationship, CONDES applies the extended power function, while it utilizes the power function for the *k*-*e* relationship (Liu & Znidarčić, 1991).

CONDES was later updated by Coffin (2010) to develop a three-dimensional consolidation model. Updated program simulates a three-dimensional consolidation in a storage facility by repeatedly

using the one-dimensional consolidation analysis (Priestley, 2011; Robert, 2012). The models used a geometrical discretization scheme with volume of the storage facility is replaced by several concentric cylinders. However, the discretization scheme of the facility volume still results in a two-dimensional consolidation problem and these two-dimensional columns will then need to be transformed into one-dimensional columns (Robert, 2012). This quasi-multidimensional analysis, thus, does not cover the lateral deformation and horizontal fluxes in the model (Priestley, 2011). The code was also not capable of simulating lateral drainage such as a permeable envelope (Bhuiyan et al., 2015).

2.7.2 FSConsol

FSConsol (GWP Geo Software, Edmonton, Alberta, Canada) was also based on the finite strain consolidation theory of Gibson et al. (1967). The program used the extended power for the compressibility relationship, while a power law function was used to correlate hydraulic conductivity with void ratio.

$$e = A\sigma'^{B} + M \tag{2.50}$$

Full-scale models of a copper mine TSF were simulated with FSConsol and compared with measurements (Agapito, 2015). Results suggested that 1-D consolidation analysis performed by FSConsol could provide a reliable prediction of tailings heights and the storage capacity of the TSF (Agapito, 2015). FSConsol provides two different filling schemes where either instantaneous filling of tailings (i.e., consolidation only occurred after the complement of filling) or gradual filling of tailings (i.e., consolidation can occur during the placement of tailings) c be simulated. FSConsol also allowed to perform analysis with various types of tailings in multiple layers, while CONDES only allow analysis of a certain type of tailings. This program could also be used to solve 3D problems in a pseudo-3D analysis manner via a geometrical discretization procedure somewhat similar to that of CONDES (Agapito, 2015).

2.7.3 Plaxis

The finite element modelling program Plaxis was used by McDonald and Lane (2010) to model two-dimensional in-pit deposition of Gold and Nickel tailings. The Modified Cam-clay formulation for

the modelling was used by McDonald and Lane (2010). Such model can only solve the problem with the assumption of constant values of hydraulic conductivity and linearization of compressibility relationship (Jeeravipoolvarn, 2010). In this case, numerical simulations predicted post-filling settlement of tailings lasting approximately one year, while in practice, measurements in the field showed that consolidation lasted around 3 years. The faster prediction of the rate of consolidation could be attributed to the use of a fixed value of hydraulic conductivity, while this value actually decreases as consolidation of tailings progresses. The magnitude of post-settlement predicted for the gold tailings was around 7.1 m which was twice the measured value, while the difference between predicted and measured values for Nickel tailings was around 10% (McDonald & Lane, 2010).

2.7.4 SVOffice

SVOffice was developed by SoilVision in 2009 (now Bentley, 2021), and is a finite element package that can model the large consolidation of tailings in a multiple-dimensional system when tailings were stored in minded out pit (Fredlund et al., 2009). The governing equations used by the software is different from the large strain formulation proposed by Gibson et al. (1967) and based upon a rigorous general continuum solid mechanics formulation rather than a void ratio-based formulation (Priestley, 2011; Fredlund et al., 2015). In this software, 3D seepage, stresses and deformations analysis are all coupled and included in the computation process. SVOffice can estimate the horizontal deformation and flow of the material during the analysis, which is not feasible in the previous software. SVOffice can implement power and extended power functions, logarithmic and Weibull functions. Limitations on the simulation of interaction between tailings and the pit wall were also noticed (Priestley, 2011) implying that models do not necessarily reflect the real interaction between tailings and pit wall in practice (Priestley, 2011).

2.7.5 SIGMA/W

The finite element code SIGMA/W (Bentley Inc., 2021) was used to evaluate the influence of WRI on tailings consolidation. Hydraulic conductivity and stiffness of tailings were either constant (Bolduc & Aubertin, 2014; Lévesque, 2019) or updated discretely at each filling stage (Boudrias, 2018). Numerical study using SIGMA/W on the effect of WRI on the tailing consolidation rate as well as influence factors on the performance of WRI at the field-scale was conducted by Bolduc and

Aubertin (2014) and Boudrias (2018), and simulated results were discussed in section 2.2.1. Lévesque (2019) studied consolidation behaviour of tailings in a pit co-disposed with WRI, permeable envelope and bottom drainage. Tailings was assigned modified Cam-Clay model in these simulations. The properties of tailings in these models were, however, constant due to the limitation of the software in modelling continuous update of tailings properties.

2.7.6 FLAC/FLAC3D

2.7.6.1 The use of FLAC/FLAC3D for tailings consolidation estimation

FLAC and FLAC 3D (Fast Lagrangian Analysis of Continua) use the explicit finite difference method to perform coupled analyses of solid/fluid interactions in both two and three dimensions (Itasca, 2021). FLAC traditionally used to evaluate dynamic behaviour of tailings stored in TSFs (James & Aubertin, 2009; Contreras et al., 2020; Zafarani et al., 2020) or the interaction between cemented tailings backfilled with the underground mining structure (Shahsavari & Grabinsky, 2014; Yang et al., 2017; Wang et al., 2021b). FLAC/FLAC3D can also be used to model continuous change of hydraulic conductivity and compressibility of tailings materials throughout the filling process by utilizing the built-in FISH code functions (Zhou et al., 2019; Itasca, 2021). Description on how to perform coupled model and simulate continuous evolution of tailings properties in FLAC3D will be discussed in chapter 4 later.

A fully coupled FLAC3D code was implemented by Shahsavari and Grabinsky (2014) to validate the numerical and analytical solutions by modelling the same problem studied by Gibson (1958). The effect of non-zero PWP condition due to the presence of a water layer on top of the cemented paste backfilled in underground mine was then studied. The consolidation properties of tailings were, however, set fixed in this study. Zhou et al. (2019) first validated the capability of FLAC to consider non-linear evolution of tailings stiffness and hydraulic conductivity by modelling consolidation of waste clay tailings under several disposal scenarios summarized in Townsend and McVay (1990). Results on the model of consolidation of copper tailings disposed in a tailings impoundment with the presence of wick drain systems, in which updated values of hydraulic conductivity and stiffness of tailings were considered, was able to correctly simulate the horizontal movement of waters in tailings towards the wick drain system, side wall and bottom (which were assigned as permeable boundary

conditions). The configurations of these WRIs, however, lead to the necessity of considering 3D effect. Thus, a similar approach implemented in 3D models considering updated values of tailings properties with the presence of permeable envelope and/or WRIs in an open pit (or TSFs) will be presented in chapter 3.

Consolidation analysis was performed in FLAC3D in a similar manner to that of solving dynamic problem using explicit scheme, in which the equation of motion was solved (Itasca, 2021). This scheme might be computationally expensive for the consolidation problem, as it would make the time step of the analysis become quite small (Itasca, 2021). Also, the presence of 2 materials with contrastive hydraulic conductivity (i.e., WRI and tailings) would even make the analysis more computational expensive (Itasca, 2021). Finally, skilled modellers are usually required to perform complex analysis in FLAC3D. It was also noted that Biot's consolidation theory was utilized in FLAC3D to estimate the consolidation of the material.

2.7.6.2 Biot's consolidation theory

The one-dimensional Terzaghi's consolidation theory was generalized to the three-dimensional and for more general materials, such as porous rock, by Biot (1941). The following assumptions were made in the Biot's theory:

- The material is isotropic.
- The reversibility of stress-strain relations is encountered in the final equilibrium conditions.
- Stress-strain relations are linear.
- Strains are small.
- The water is incompressible and might contain air bubbles.
- Movement of water flow follows Darcy's law.

Basic stress-strain relations in the Biot's theory are presented as follows:

$$G\nabla^2 u + \frac{G}{1-2\nu}\frac{\partial \varepsilon}{\partial x} - \alpha\frac{\partial \sigma}{\partial x} = 0 \tag{2.51}$$

$$G\nabla^2 v + \frac{G}{1-2\nu}\frac{\partial \varepsilon}{\partial y} - \alpha\frac{\partial \sigma}{\partial y} = 0 \tag{2.52}$$

$$G\nabla^2 w + \frac{G}{1-2\nu}\frac{\partial \varepsilon}{\partial z} - \alpha\frac{\partial \sigma}{\partial z} = 0 \tag{2.53}$$

$$\nabla^2 = \frac{\partial^2}{\partial x^2} + \frac{\partial^2}{\partial y^2} + \frac{\partial^2}{\partial z^2} \tag{2.54}$$

Where G: shear modulus; ν: Poisson's ratio; *u, v, w*: displacement in x, y and z directions respectively; ε: volumetric strain; α: Biot coefficient.

Biot coefficient, α, used to relate the change in pore pressure and total applied pressure for various porous medium (i.e., soil, rock and concrete) as follows:

$$\sigma' = \sigma - \alpha u \tag{2.55}$$

Biot (1941) firstly proposed the equation to calculate the value of α:

$$\alpha = \frac{2(1+v)G}{3(1-2v)H} \tag{2.56}$$

Where H: a physical constant depending on the considered materials. It is noted that α is equal to 1 for the conventional Terzaghi's theory.

2.7.6.3 Coupled hydro-mechanical analysis in FLAC/FLAC3D

FLAC3D is capable of performing coupled analysis to simulate solid/fluid interaction of the medium in three dimensions. The analysis of flow modelling could be done in a coupled or parallel manner with the mechanical modelling (Itasca, 2021). Coupled analysis can be performed in an incremental format in FLAC3D, which follows the quasi-static Biot's theory. During the coupled analysis, the changes in the PWP due to fluid flow together with volumetric strain increments from mechanical loops are evaluated in the hydraulic loops. These changes in PWP are then passed to the mechanical loops to update effective stresses in mechanical loops. These changes in effective stress are then used to calculate the failure (if any) and the change in volumetric strain increments. The coupled process

is implemented alternately in FLAC3D to update change in PWP and volumetric strain. The constitutive law that represents the relation between stress, strain and fluid pressure used in FLAC3D is as follows (Itasca, 2021):

$$\frac{1}{M}\frac{\partial p}{\partial t}+\frac{n}{s}\frac{\partial s}{\partial t}=\frac{1}{s}\frac{\partial \zeta}{\partial t}-\alpha\frac{\partial \varepsilon}{\partial t} \tag{2.57}$$

Where M: Biot modulus (N/m^2); p: fluid pressure; n: porosity; s: degree of saturation; α: Biot coefficient; ζ: variation of fluid content; ε: mechanical volumetric strain.

2.7.7 Critical challenges on simulation approaches for the co-disposal of tailings and WRI in a pit

Some studies might use SIGMA/W to estimate consolidation of tailings with the presence of WRI using only constant properties (Jaouhar et al., 2013; Bolduc & Aubertin, 2014) or they can be updated at each loading steps (Boudrias, 2018). However, the continuous update of tailings properties was recommended in these studies. Various software programs have also been developed to simulate non-linear consolidation behaviour of slurry tailings with continuous updated properties, in either 1-D, 2-D or 3-D as mentioned previously. Common practice for TSF design is usually to perform 1-D simulations using Gibson consolidation theory (Priestley, 2011; Agapito & Bareither, 2018) which can produce good results when impoundments have small depths relative to their width and length, and when the fluid flow direction is essentially vertical (Fredlund et al., 2015). In these cases, one-dimensional assumption is deemed suitable and lateral stress and deformation might be ignored in analysis. For multidimensional problems such as tailings filled in minded out pit, pseudo-3D models may be suitable (e.g., CONDES and FSConsol), yet these models often require site-specific calibration (Zhou et al., 2019). Zhou et al. (2019) utilized FLAC to evaluate consolidation behaviour of tailings with the presence of wick drain systems that can also continuously update tailings properties. However, this was also only 2D analysis.

Conditions may be different for in-pit disposal, which usually exhibits complex site geometry and drainage conditions, including the presence of permeable regions around the pits (fractured rock, permeable envelope). In these cases, a more complex multi-dimensional flow should be considered, or 1-D or pseudo-3D analysis could miss the principal effect of lateral flow and strains on the solution

(Coffin, 2010; Fredlund et al., 2015). Thus, an advanced 3D model that is capable of considering complex geometry, multiple flow directions and continuous update of tailings properties at the same time is required. FLAC3D with its flexibility and capability was thus chosen to investigate how tailings interact with multiple drainage paths co-disposed in an open pit.

2.8 Final remarks on the integrated mine waste management using co-disposal in pit technique

Tailings storage in a pit with the installation of permeable envelope made of coarse waste rocks and/or combined with WRI inclusions as central drainage paths can offer not only environmental benefits but also geotechnical advancement (i.e., no failure of TSFs and enhancement of consolidation of tailings). The acceleration effect of consolidation rate of permeable envelope can be beneficial to the reclamation activities as well. This technique, however, also faces several unknowns that could somewhat limit its application. Non-linear evolutions of tailings need to be properly captured to better reflect the real behaviour of tailings. Volume gains or losses (change in the volume that is available for the storage of tailings because of the presence of WRI) of tailings also need to be explicitly estimated based on practical operation aspects for a better management of the filling plan. Finally, potential influencing factors that include depth of the pit, overall pit slope angles, filling rate, mine waste hydraulic properties and the morphology of the pit need also to be thoroughly investigated. All of these factors require a comprehensive numerical tool to adequately solve and take them into the consideration for the analysis.

CHAPTER 3 METHODOLOGY

The project consisted of two main parts: laboratory tests to characterize hydro-geotechnical properties of tailings and numerical simulations to simulate tailings consolidation behaviour under various conditions (from column tests at the laboratory scale to the full-scale open pit). Laboratory testing included characterization of tailings samples and consolidation tests in columns. The results of the characterization tests were used as input data to validate (and calibrate if necessary) advanced 3D numerical models and analyze the geotechnical behaviour of tailings and waste rock in the pit. The operational constraints, such as volumes of wastes produced or various disposal scenarios, were integrated in the analyses to assess realistic disposal solutions and their effects on the consolidation behaviour of tailings. WRI was also proposed to be used in pit to optimize the consolidation of tailings. The numerical simulations were carried out with FLAC3D (version 7.0; Itasca).

3.1 Characterization of mine tailings in the laboratory

3.1.1 Investigated mine sites, tailings sampling, transport and preparation

Tailings were sampled at Canadian Malartic (CM). This gold mine is in Abitibi, Quebec province, around 20 km west of Val d'Or. Canadian Malartic is one of the largest gold mines in operation in Canada (James et al., 2013). The mine started production in 2011, and the mineral plant processes an average of 55,000 tons of ore per day. Mining activities produce around 125,000 tons of waste rock and 55,000 dry tons of tailings per day. 3 barrels of tailings at an initial water content of around 64% were sampled at the concentrators by the mining partner during summer 2019 and transported to the RIME laboratory at Polytechnique Montreal.

The project started with the characterization of the grain size distribution, compressibility, specific gravity, and hydraulic conductivity of the tailings. Tailings were first homogenized. To do so, they were mixed with water in buckets using a mixer until a homogenous slurry was obtained, and then filled back in a large barrel, where they were homogenized again using a mixer.

3.1.2 Basic geotechnical properties of tailings

The grain size curves of tailings are determined according to ASTM Standard No. D422-63 (2016) *"Standard Test Method for Particle Size Analysis of Soils"*. The test included sieving for the particles remaining on the sieve 200, and hydrometer analysis for the particles passing through the sieve 200. After being homogenized, three samples (one sample per one bucket) were tested. From the grain size curves, values of D_{10}, D_{60}, and the coefficient of uniformity – C_U (D_{60}/D_{10}) could be determined. The results were then used to classify tailings materials based on The Unified Soil Classification System (USCS, ASTM D2478-17, 2017).

The average value of D_{10} (the diameter corresponding to 10% passing in the particle-size distribution curve) was 0.0041 mm, the average D_{60} (the diameter corresponding to 60% passing in the particle-size distribution curve) was 0.04 mm, leading to the average coefficient of uniformity C_u ($C_u = D_{60} / D_{10}$) being around 9.8, the average percentage of particles smaller than 75 µm and 2 µm in diameter are 77% and 7% respectively (figure 3-1 and table 3-1). These materials were thus slightly coarser than the same tailings obtained by Bolduc (2012) and Essayad (2015), yet these values in the typical range for hard rock mine tailings (Bussière, 2007). These mine tailings were classified as low plasticity silts (ML) according to the Unified Soil Classification System (ASTM D2487-17, 2017).

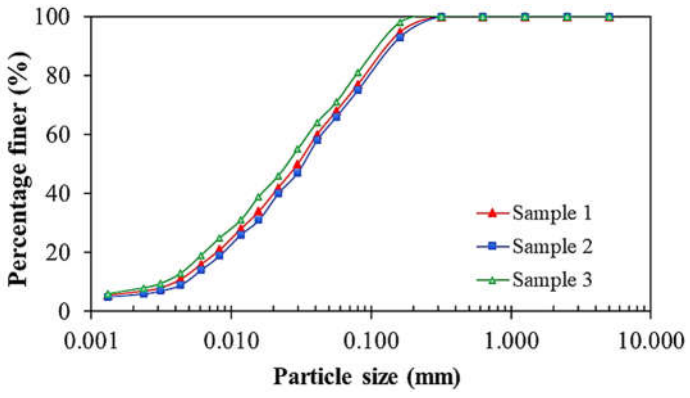

Figure 3-1: Particle size distribution of Malartic tailings used in this project.

Table 3-1: Particle size characteristic of tailings samples.

	D_{10} (mm)	**D_{60} (mm)**	**C_u**	**d < 75 µm**	**d < 2 µm**
Sample 1	0.004	0.04	10	77%	6.5%
Sample 2	0.0044	0.041	9.3	75%	6%
Sample 3	0.004	0.04	10	78%	7%
Average	0.0041	0.04	9.8	76.7%	6.5%

The specific gravity of tailings was measured using a pycnometer conforming to ASTM Standard No. D854-14 (2016). 3 tests were performed, and the average value of the specific gravity was estimated. The average specific gravity G_s was around 2.61 in the range for Quebec gold tailings (Bussière, 2007) (table 3-2). However, this value was lower than that of similar tailings materials which was around 2.75 (Bolduc, 2012), 2.76 (Essayad, 2015) and 2.71 (Boudrias, 2018). Thus, the value of specific gravity was assigned 2.75 in this study.

Table 3-2: Specific gravity G_s of tailings samples.

	Min	**Max**	**Average**
Sample 1	2.61	2.59	2.60
Sample 2	2.61	2.63	2.62
Sample 3	2.61	2.62	2.62
Average			2.61

Compaction test was also conducted with tailings samples based on the Modified Proctor Test Standard (ASTM D1557-12) to evaluate the relationship between the water content, w, and the dry density, ρ_d, of the tailings. The optimum water content, w_{opt}, the maximum dry density, ρ_{dmax}, were determined from these tests. 2 samples of tailings were tested.

The optimum moisture content $W_{opt,}$ obtained from the modified proctor test was around 13% and maximum dry density, γ_{dmax}, was around 1820 kg/m^3 (figure 3-2). These were quite similar to those obtained by Boudrias (2018). W_{opt} was lower than those measured by Bolduc (2012) (15.6%), and the material in this study was somewhat denser at the optimum water content compared to those obtained by Bolduc (2012) (1720 kg/m^3). The measured properties were similar to previous studies on hard rock mines tailings (Qiu & Sego, 2001; Bussière, 2007)

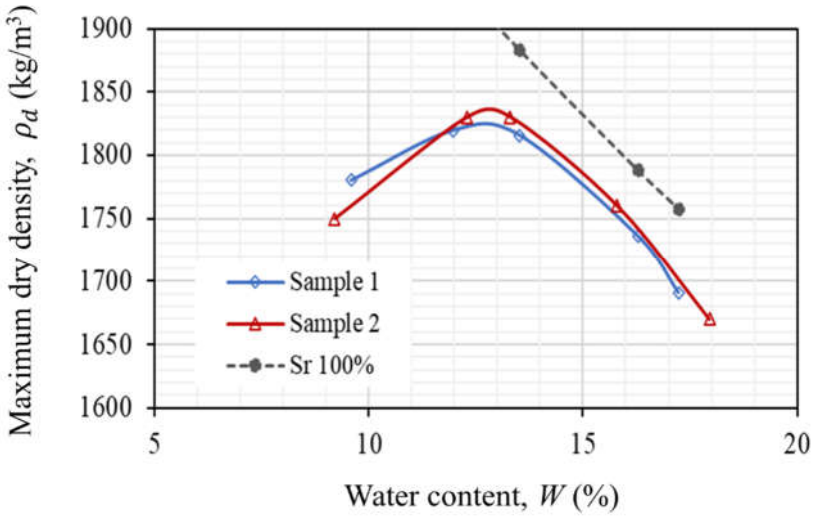

Figure 3-2: Modified proctor test on the studied tailings materials.

3.1.3 Column test

Two consolidation tests (S1 and S2) were carried out in rigid columns following the protocol proposed by Essayad and Aubertin (2021). Columns were 50 cm high with 10 cm internal diameter (figure 3-1). Around 30 cm of tailings were placed in the columns as slurry and subjected to incremental loadings. Samples were prepared with a solid content of around 74%, which is typical of slurry tailings in hard rock mines (Blight, 2010), but slightly greater than that at CM mine (Essayad, 2015). This solid content aimed to prevent segregation of slurry tailings materials (Essayad, 2015; Boudrias, 2018). The tailings column was left for 24 hours after being poured into the column to eliminate the influences of sedimentation. Loadings were applied at the surface of the specimen to

simulate accretion of tailings layers. Excess PWP were monitored continuously using three pore water pressure sensors in each column (Trustability, accuracy: ±0.20%) and installed 3.5 cm, 15 cm and 23.5 cm from the base of the column. A T50 LVDT (Novotechnic) was placed on top of each column to measure the displacement at the surface of the tailings. Maximum excess PWP measured during the tests was up to 40% smaller than the loading applied at each step which was explained by the influence of side friction between tailings and instrumented columns wall. The effect of friction between column wall and tailings was therefore corrected for both column tests using the procedure proposed by Essayad and Aubertin (2021). Particularly, analytical solutions proposed by Aubertin et al. (2003) and Li and Aubertin (2009c) were used here to assess the influence of the wall friction on the measured consolidation properties. These equations were first proposed to evaluate the effect of stress state in backfilled openings, taking into consideration rock wall friction. In general, the shear stress, τ [kPa], of the interface between the 2 materials can be calculated based on the Mohr-Coulomb criteria as (Holtz & Kovacs, 1981):

$$\tau = \sigma_h' \, \mu \tag{3.1}$$

Where σ_h': horizontal stress [kPa]; and μ $(= \tan\delta)$ is called the coefficient of friction; δ: friction angle [°]. Equation (3.1) can be further expressed as:

$$\tau = K_0 \frac{\Delta P}{A} \, \mu \tag{3.2}$$

Where A $(= \pi r^2)$: the area of the sample (with radius *r* and height *h*) [m^2]; ΔP: applied force [kN], K_0: coefficient of earth pressure at rest.

The shearing force *S* [kN], which is generated by the wall friction, is calculated as:

$$\mathrm{S} = \tau \, (2\pi \mathrm{rh}) \tag{3.3}$$

From equations 3.2 and 3.3, we have:

$$\mathrm{S} = K_0 \frac{2\mathrm{h}}{r} \Delta P \mu \tag{3.4}$$

Equation (3.4) can be re-written as:

$$S = \mu' \text{ x } \Delta P \tag{3.5}$$

Where μ' is called correction coefficient, expressed as follows:

$$\mu' = K_0 \frac{2h}{r} \mu \tag{3.6}$$

It can be calculated as (Essayad & Aubertin, 2021):

$$\mu' = 1 - \frac{\Delta u}{\Delta \sigma} \tag{3.7}$$

The corrected axial compression stress at the top of the sample can then be calculated as:

$$\sigma_{cor} = \frac{(\Delta P - S)}{A} \tag{3.8}$$

Equation 3.7 was used in this study to consider the effect of friction between column wall and tailings. Detailed values of loads at each step, coefficient of friction and corrected values for column S1 and S2 are presented in the Tables 3-3 and 3-4 respectively. Next loading step was applied once PWP had reached hydrostatic equilibrium (i.e., after around 3 to 4 hours). The maximum loading applied to the tailings in this study was around 200 kPa (corresponding to an overburden of 20 m of tailings). The maximum load was chosen following the loading capacity limitation of the loading system of the column test.

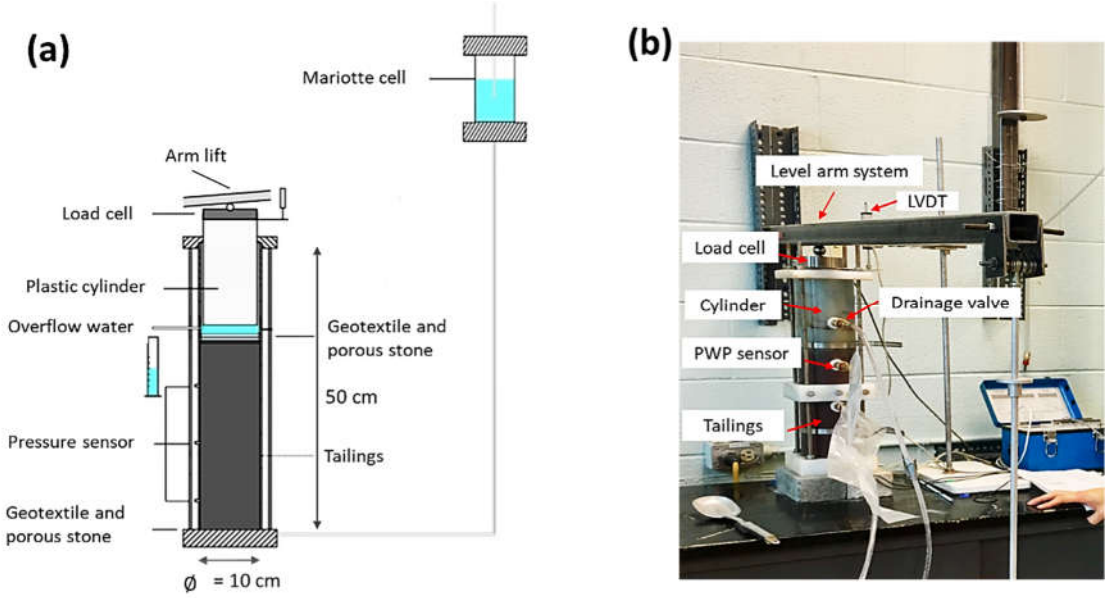

Figure 3-3: Instrumented column test setup used to measure saturated tailings compressibility. A lever arm was used to apply increasing loading and a PVC cylinder transmitted the vertical compression loading to the tailings surface. LVDT and PWP sensors (placed at different elevations) (modified after Lévesque (2019)).

Saturated hydraulic conductivity was measured at the end of each loading stage for column S1 using constant head test inspired by ASTM D5856 (2015). A constant hydraulic head was applied at the base of the column using a Mariotte cell (figure 3-3). The outflow was measured at the upper drainage valve in the column to estimate the saturated hydraulic conductivity (Lévesque, 2019). For practical reasons, the hydraulic conductivity was measured by imposing an upward flow, contrary to what is recommended by standards ASTM D5856 (2015), and results could, therefore, have been slightly underestimated (i.e., this can contribute to increase the degree of saturation of tailings, yet gravitational force can affect the movement of the water flow). The difference was, however, deemed negligible (Lévesque, 2019). Detailed results in terms of evolution of excess PWP and displacement of these column tests are presented and discussed in chapter 4.

Table 3-3: Loads applied at each step for column S1 and corrected values because of the effects of frictions

Loading steps	**Stress (kPa)**	**Change in Vertical stress ΔP/A (kPa)**	μ'	**Shearing stress S/A (kPa)**	**$\text{Stress}_{\text{corr}}$ (kPa)**	**Duration (hours)**
1	3.2	3.2	0	0	3.2	9
2	26.4	23.2	0.1	0.2	26.3	5
3	64.0	37.6	0.22	8.4	55.5	5
4	101.4	37.4	0.33	12.5	80.4	8
5	138.6	37.2	0.58	21.7	95.9	5
6	174.6	36.0	0.44	15.7	116.2	5
7	248.5	73.9	0.69	51	139.1	13
8	322.5	74.0	0.74	55	158.1	5
9	397.2	74.4	0.72	54	178.8	5
10	472.4	75.1	0.74	55.4	198.5	5

Table 3-4: Loads applied at each step for column S2 and corrected values because of the effects of frictions

Loading steps	Stress (kPa)	Change in Vertical stress ΔP/A (kPa)	μ'	Shearing stress S/A (kPa)	$\text{Stress}_{\text{corr}}$ (kPa)	Duration (hours)
1	3.2	3.2	0	0	3.2	7
2	26.5	23.3	0.18	4.1	22.6	5
3	63.6	37.1	0.23	8.5	51.2	5
4	100.6	36.9	0.46	16.9	71.2	5
5	139.2	38.6	0.58	22.4	87.4	15
6	174.2	35.0	0.57	20.1	102.3	5
7	248.8	74.6	0.68	50.7	126.1	5
8	321.9	73.2	0.71	51.9	147.4	5
9	397.2	75.3	0.78	58.8	163.9	5
10	471.7	74.4	0.77	57.6	180.7	6

3.2 Numerical study

3.2.1 General description of numerical purposes and the numbers of simulations

Numerical studies were carried out using FLAC3D (Itasca., Inc, 2021). FLAC3D can simulate tailings' consolidation behaviour by coupled analysis (Shahsavari & Grabinsky, 2015), and it is suitable to represent the 3D geometry of open pit mines. FLAC3D can also model the continuous change of hydraulic conductivity and compressibility of tailings throughout the filling process. General descriptions of numerical approaches in this project corresponding are presented hereafter.

Coupled fluid-mechanical simulations using FLAC3D (Itasca Int., 2021) were performed in chapter 4 to develop and validate an approach to modify Mohr Coulomb parameters using laboratory column test results. A parametric analysis to investigate the effect of various estimation methods of the hydraulic conductivity was also performed. Models were run to investigate the potential effects of

the assumption of constant properties (stiffness and hydraulic conductivity) of tailings. Values of Young's modulus and hydraulic conductivity in models P1-5, P1-6, P1-8 and P1-9 were chosen based on the maximum and intermediate values for tailings obtained from column test (see section 4.3.1, 4.3.3 and figure 4-5) for more details. It is noted that the value of hydraulic conductivity, k [m^2/(Pa/sec)] used in FLAC3D are not the same as typical value, k_h [m/s], used in geotechnical engineering (i.e., $k = \frac{k_h}{\rho_w g}$, with g being the gravitational acceleration). The value of bulk modulus of water was reduced to $5x10^4$ kPa in this study. The potential effect of this reduced bulk modulus of water can be seen in Appendix D. Finally, models simulating a simplified tailings impoundment inspired by a real case study to scale up the developed approach were carried out. There was a total of 15 models that were simulated. Brief description on the type of models, properties and specific features for simulations are presented in table 3-5.

Table 3-5: List of models simulating column test and general descriptions of models in chapter 4.

Model	**Properties**		**Specific features**
	Stiffness	**Hydraulic conductivity**	
P1-1	Updated	Updated	Simulation of column S1
P1-2	Updated	Updated	Simulation of column S2
P1-3	Updated	Updated	Simulation column S2 Hydraulic conductivity was updated based on KC model
P1-4	Updated	Updated	Simulation column S2 Hydraulic conductivity was updated based on KCM model
P1-5	Fixed	Fixed	Simulation column S1 k = 2 x 10^{-7} m/s and E = 2500 kPa
P1-6	Fixed	Fixed	Simulation column S2 k = 2 x 10^{-7} m/s and E = 2500 kPa

P1-7	Updated	Updated	Upscaling model
P1-8	Updated	Fixed	Upscaling model E = 1800 kPa
P1-9	Updated	Fixed	Upscaling model E = 4500 kPa
P1-10	Updated	Updated	Upscaling model Young modulus was only updated at the beginning of each loading step
P1-11	Fixed	Updated	Upscaling model K_{sat} = 3.5x10^{-7} m/s
P1-12	Fixed	Updated	Upscaling model K_{sat} = 1.7x10^{-7} m/s
P1-13	Fixed	Updated	Upscaling model K_{sat} = 1.2x10^{-7} m/s
P1-14	Updated	Updated	Upscaling model Models were run Hydraulic conductivity was updated based on KCM model
P1-15	Updated	Updated	Upscaling model Hydraulic conductivity was updated based on KC model

The objective of the chapter 5 was to investigate numerically the influences of WRI on various types of tailings progressively filled in a simplified TSF considering the continuous changes of consolidation properties. 4 types of tailings were used in this study (A, B, C and D), in which A and B were gold mine tailings from mine sites in Quebec, C was the uranium tailings from Saskatchewan and D was the bauxite tailing from a mine site in the US. Models were then carried out to investigate potential differences on the settlement evolutions of models using fixed and updated properties when WRI was applied. Effects of volume ratio between tailings and WRI on the volume gains or losses

of tailings in the impoundment were examined. Parametric analysis on the effects of the filling rate of the tailings, the assumption of instantaneous filling in simulations compared to the progressive filling scheme in practice was also investigated. A total of 67 models were run in this paper and their general descriptions are presented in table 3-6.

Table 3-6: List of models simulating tailings co-disposed with WRI in a simplified TSF and their general descriptions in chapter 5.

Model	**Properties**		**WRI**	**Specific features**
	Stiffness	**Hydraulic conductivity**		
P2-1 to P2-4	Updated	Updated	Yes	Simulation of tailings co-disposed with WRI for tailings A, B, C and D
P2-5 to P8	Updated	Updated	No	Simulation of tailings only for tailings A, B, C and D for comparison purposes
P2-9 to P2-16	Fixed	Fixed	Yes	Running 8 models with the presence of WRI with constant hydraulic conductivity to find an equivalent value of hydraulic conductivity that resulted in a similar result with a model using updated properties for tailings A. Young's modulus was the same in this model and equal to 5000 kPa
P2-17 to P2-24	Fixed	Fixed	No	Running 8 models with tailings only using the same values of constant hydraulic conductivity and stiffness for tailings A in the models P2-9 to P2-16

P2-25 to P2-29	Fixed	Fixed	Yes	Running 5 models with the presence of WRI with constant hydraulic conductivity to find an equivalent value of hydraulic conductivity that resulted in a similar result with a model using updated properties for tailings B. Young's modulus was the same in these models and equal to 4000 kPa
P2-30 to P2-34	Fixed	Fixed	No	Running 5 models with tailings only using the same values of constant hydraulic conductivity and stiffness for tailings B in the models P2-25 to P2-29
P2-35 to P2-40	Fixed	Fixed	Yes	Running 6 models with the presence of WRI with constant hydraulic conductivity to find an equivalent value of hydraulic conductivity that resulted in a similar result with a model using updated properties for tailings C. Young's modulus was the same in these models and equal to 2500 kPa
P2-41 to P2-45	Fixed	Fixed	No	Running 6 models with tailings only using the same values of constant hydraulic conductivity and stiffness for tailings C in the models P2-35 to P2-40
P2-46 to P2-47	Updated	Updated	Yes	2 models with filling rate increased to 6 and 9 m/year respectively for tailings A
P2-48 to P2-49	Updated	Updated	No	2 models with filling rate increased to 6 and 9 m/year respectively for tailings A

P2-50 to P2-53	Updated	Updated	Yes	4 models with thickness of WRI increased to 10, 12, 18 and 24 m respectively for tailings A to evaluate effect of volume ratio of tailings and WRI
P2-54 to P2-57	Updated	Updated	Yes	4 models with thickness of WRI increased to 10, 12, 18 and 24 m respectively for tailings B to evaluate effect of volume ratio of tailings and WRI
P2-58 to P2-61	Updated	Updated	Yes	4 models with thickness of WRI increased to 10, 12, 18 and 24 m respectively for tailings C to evaluate effect of volume ratio of tailings and WRI
P2-62 to P2-63	Updated	Updated	Yes	2 models with 2 different filling schemes for tailings A (2 x 1.5 m per year and 3 x 1 m per year instead of an instantaneously adding (i.e., layer of 1.5 m per 6 months and layer of 1 m per 4 months, respectively)
P2-64 to P2-67	Fixed	Fixed	Yes	4 models with several values of Young's modulus for tailings A to study the effect of WRI on the settlement of tailings

Models in chapter 6 were performed to quantitatively examine the influences of a permeable envelope on the tailings consolidation in an open pit. Models with various co-disposal scenarios were subsequently performed. The slope angle was 51° which corresponded to the optimum slope angle of the pit whose height was smaller than 100 m (Utili et al., 2022). The depth of the pit was 60 m, which was smaller than the common depth of the pit (Blight, 2010), yet this depth was chosen to reduce the computation time. An extensive parametric analysis was conducted to examine various operational

constraints that can affect the performance of co-disposal technique on the tailings consolidation and the application of this concept for other types of tailings. A total of 19 models were run in this paper and their general descriptions are presented in table 3-7.

Table 3-7: List of models simulating tailings co-disposed with WRI in a simplified TSF and their general descriptions in chapter 6.

Model	**Permeable Envelope**	**WRI**	**Bottom drainage**	**Heights (m)**	**Slope angles (°)**	**Specific description**
P3-1	No	No	No	60	51	
P3-2	Yes	No	No	60	51	
P3-3	Yes	No	Yes	60	51	
P3-4	No	Yes	No	60	51	
P3-5	Yes	Yes	Yes	60	51	
P3-6	Yes	Yes	Yes	80	51	To test the depth of the pit
P3-7	Yes	No	No	60	60	To test the influences of slopes angles
P3-8	Yes	No	No	60	70	To test the influences of slopes angles
P3-7	No	No	No	60	60	Model with tailings only
P3-8	No	No	No	60	70	Model with tailings only
P3-9 to P3-10	Yes	No	No	60	51	Filling rate was changed to 7.5 and 10m/year respectively
P3-11 to P3-12	No	No	No	60	51	Filling rate was changed to 7.5 and 10m/year respectively

						(model with tailings only)
P3-13 to P3-15	Yes	No	No	60	51	Hydraulic conductivity of permeable evelope was changed
P3-16 to P3-17	No	No	No	30	56	Models with sharped and curvy corner to evaluate morphology effect of the pit
P3-18 to P3-19	Yes	No	No	30	56	Models with sharped and curvy corner to evaluate morphology effect of the pit

Description on the choice of mesh size, boundary condition and convergence criteria are presented in the following sections.

3.2.2 Conceptualized models

Models were run to simulate column tests under sequential loadings (chapter 4), tailings progressively filled in a simplified TSF (chapter 5), and tailings disposed in a mine-scale open pit with the presence of permeable envelope under various disposal scenarios (chapter 6). The time step in a hydro-mechanical coupled simulation was usually very small that can make the simulation become computationally expensive (Itasca, 2021). The mesh size of each model was, thus, chosen to achieve the compromise between the level of precision and a reasonable computational time derived from a mesh sensitivity analysis (see Appendix B). Also, hydraulic conductivity of coarse waste rock materials was also reduced to increase the time step in models where there were two types of materials with contrastive hydraulic conductivity existing (i.e., tailings and waste rocks) (see section 6.4.4). Preliminary calculations were usually done (on the choice of mesh size and hydraulic conductivity of waste rocks) to ensure that those factors had negligible effect on the results obtained. Node elements in models were hexahedrons, and the domains were composed of various built-in blocks in FLAC3D (figure 3-4).

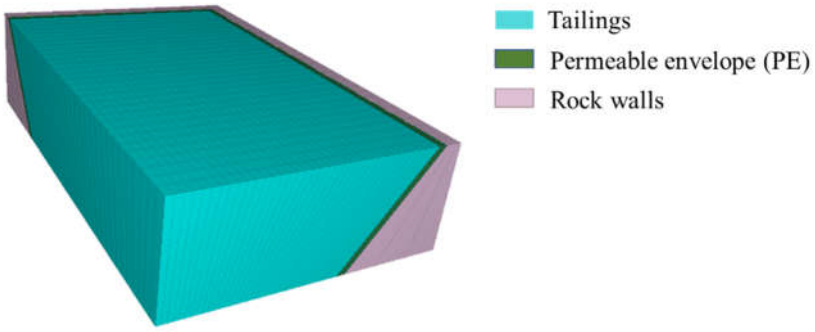

Figure 3-4: Simulated domain of tailings co-disposed with permeable envelope in an open pit.

Regarding the boundary conditions (BC), two types of boundary conditions were used in this study, which was hydraulic and mechanical boundary conditions. Hydraulic boundary conditions included permeable and/or impermeable condition, while mechanical boundary conditions included fixed and/or free boundary conditions. Water tables were considered at the surface of tailings layers and a permeable surface (table 3-8).

The convergence criteria for nodes in these models for the undrained condition was based on the ratio of the current mechanical force ratio to the target force ratio of the node, which was set equal to 1 (Itasca, 2021). The duration of models widely varied and depended on the size of each model and the number of materials in each model. Simulations in chapter 4 usually took around 7 hours to run, 2 days for each model in chapter 5 and around 2 weeks for each model in chapter 6.

Table 3-8: Hydraulic and mechanical boundary conditions for models in this study

	Bottom		Side		Top	
	Hydraulic BC	**Mechanical BC**	**Hydraulic BC**	**Mechanical BC**	**Hydraulic BC**	**Mechanical BC**
Column tests	Impermeable	Fixed all directions	Impermeable	Fixed horizontally	Permeable	Free
TSFs	Impermeable	Fixed all directions	Impermeable	Fixed horizontally	Permeable	Free
Open pit	Impermeable	Fixed all directions	Impermeable	Fixed horizontally	Permeable	Free

3.2.3 Updating of tailings properties

Linear elastic-perfectly plastic Mohr-Coulomb model was modified in this study to consider the continuous variation of stiffness and hydraulic conductivity of tailings during consolidation. Equations 3-9 and 3-10 were used to simulate the non-linear relations between the stiffness and the hydraulic conductivity with the void ratio. Void ratio was calculated from displacements measured during the test, and a relation between void ratio and effective stress was established (figure 3-5a):

$$e = A\sigma'^{\mathrm{B}} \tag{3.9}$$

Hydraulic conductivity decreased as void ratio decreased. A power law function of hydraulic conductivity was fitted on the experimental results of column tests (figure 3-5b):

$$k = Ce^{D} \tag{3.10}$$

Young's modulus was also calculated at each loading step based on Poisson's ratio and volumetric compressibility coefficient as (Holtz & Kovacs, 1981):

$$E = \frac{(1+\nu)(1-2\nu)}{(1-\nu)m_v} \tag{3.11}$$

Where ν: Poisson's ratio ($\nu = \frac{1-sin\theta'}{2-1-sin\theta'}$); m_v: coefficient of volumetric compressibility (kPa^{-1}) which can be estimated as:

$$m_v = \frac{-\Delta\varepsilon_v}{\Delta\sigma_v'} = \frac{a_v}{1+e_0} \tag{3.12}$$

Where a_v: coefficient of compressibility (kPa^{-1}), in which:

$$a_v = \frac{-\Delta e}{\Delta\sigma_v'} \tag{3.13}$$

Tailings stiffness increased during each loading step. The relation between Young's modulus and effective stress was then derived and fitted using the following power law function (figure 3-5c):

$$E = F\ x\ \sigma'^{G} \tag{3.14}$$

The extrapolation of the power function tended to lead to very small (and unrealistic) stiffnesses at small effective stresses (i.e., < 0.1 kPa), a minimum value of the Young's modulus E = 180 kPa (which corresponded to the Young's modulus of tailings at the first loading stage obtained from column tests) was assigned in the models to prevent excessive displacements during the first loading step.

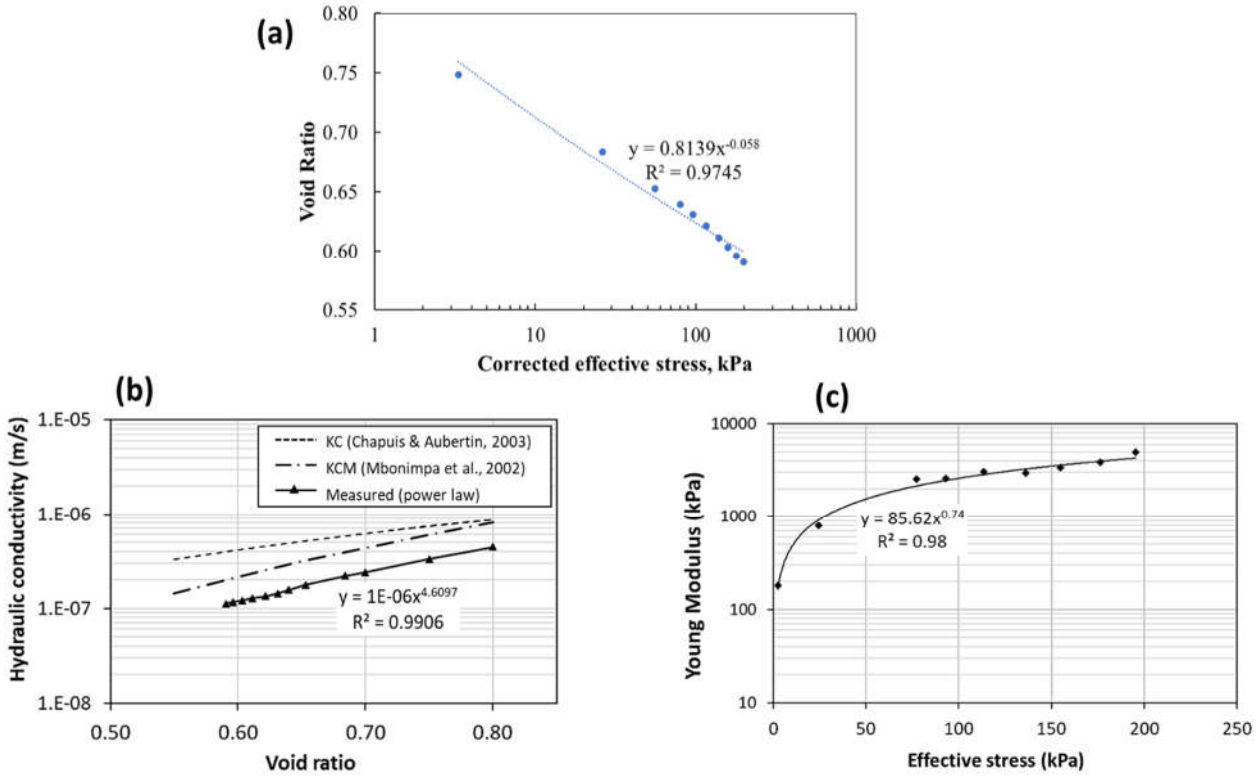

Figure 3-5: Constitutive relations obtained from column test S1 for (a) void ratio – effective stress, (b) hydraulic conductivity – void ratio, and (c) Young's modulus and effective stress.

3.2.4 Numerical scheme

The numerical scheme to simulate consolidation of tailings and integrate the continuous update of tailings properties into the model is presented in figure 3-6. The geometry of the domain was first created, and the boundary conditions were assigned. Then the input parameter for the fluid phase (porosity, fluid bulk modulus, fluid tension, hydraulic conductivity, and degree of saturation) and solid phase (dry density, friction angle, cohesion, bulk modulus, and shear modulus) were assigned for the models. At first, flow is prevented (fluid loops off and mechanical loops on) and the model is stepped to equilibrium to establish the initial undrained conditions. When the model was converged, drainage was then allowed by setting the pore pressure to zero at the top of the column and turn on both fluid and mechanical loops in the model. Equations 3-9, 3-10, 3-14 were introduced in the simulations via FISH coding language in FLAC3D to automatically update the hydraulic conductivity

and stiffness values. Particularly, during the analysis, the value of the void ratio was updated at every iteration based on the value of effective stress, and this new value of void ratio was then used to conduct an automatic update of hydraulic conductivity and stiffness in FLAC3D. It is however noted that the value of the void ratio used in this model was not necessarily the same as those derived from the volumetric strain of the simple. More discussion on this can be seen in section 7.2. Subsequently, updated values of hydraulic conductivity and Young's modulus were assigned for the materials in the new iterations. Finally, from updated Young's modulus, the values of shear and bulk modulus were updated and assigned to the material. Simple codes to input necessary parameters for the models and to demonstrate how to modify the hydraulic conductivity and stiffness of tailings using FISH are presented in Appendix C. The PWP, displacement, hydraulic conductivity and Young's modulus can be monitored during the modelling process.

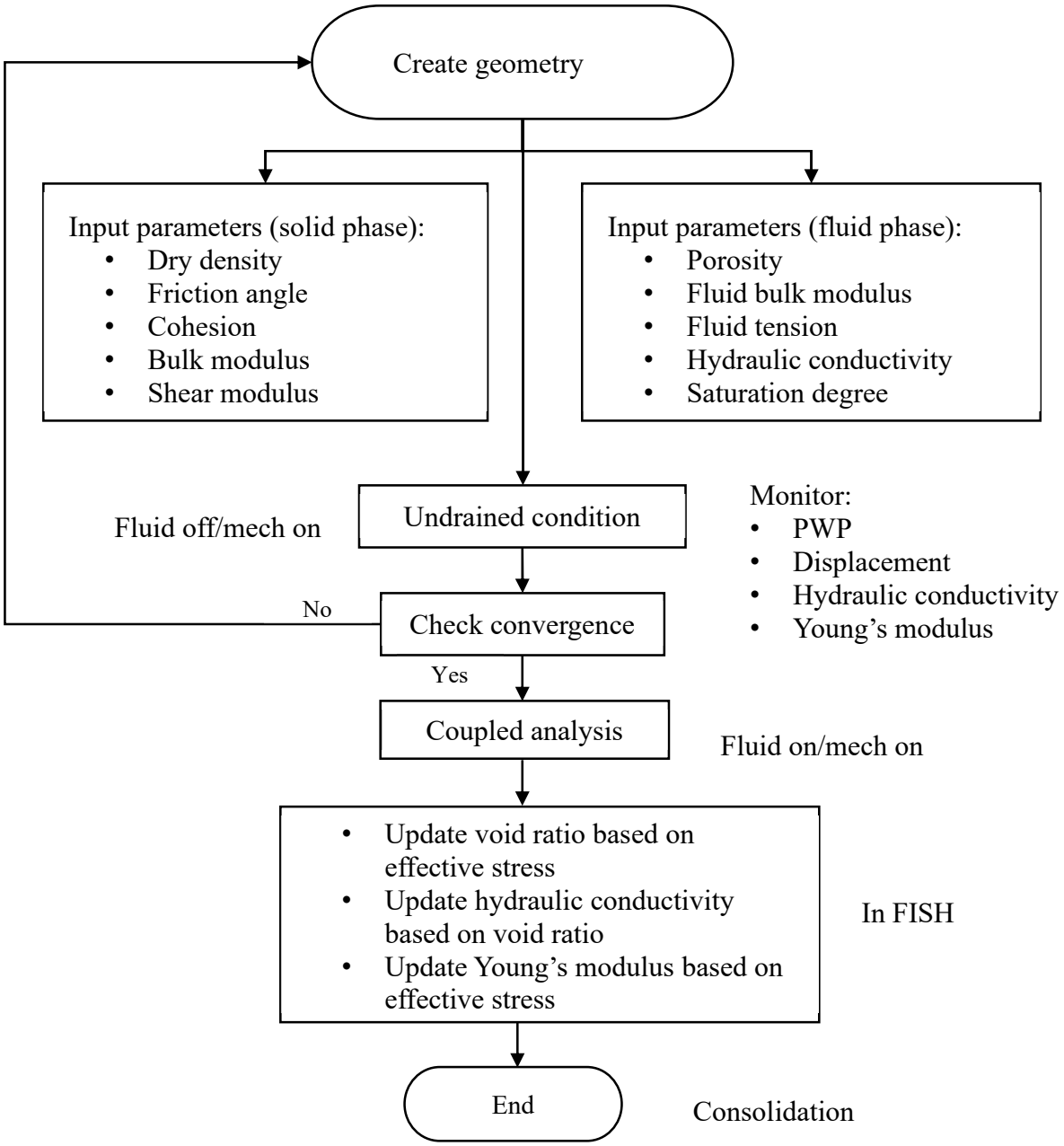

Figure 3-6: Flowchart of numerical scheme to simulate consolidation of tailings considering continuous update of tailings properties

CHAPTER 4 ARTICLE 1: NUMERICAL STUDY OF SLURRY TAILINGS CONSOLIDATION CONSIDERING CONTINUOUS UPDATE OF MATERIAL PROPERTIES

Ngoc Dung Nguyen, Thomas Pabst

Article submitted to International journal of Mining Science and Technology in August 2022

ABSTRACT

Slurry tailings demonstrate a highly non-linear evolution of stiffness and hydraulic conductivity during consolidation and explicitly modelling the non-linearity of tailings properties can contribute to improve the prediction of tailings consolidation for the estimation of storage capacity of tailings storage facilities (TSFs) as well as their static and dynamic stability. In this study, an approach to update Mohr Coulomb parameters was proposed and embedded in a finite difference code to represent real evolution of material properties under sequential loadings. This model can simulate the continuous evolution of hydraulic conductivity and stiffness of tailings materials with the reduction of the void ratio. The model was then validated using laboratory column tests. A parametric study was also carried out to assess the performance of various predictive functions to estimate hydraulic conductivity for field applications. Finally, the developed approach was applied to a simplified model of tailings impoundment filled sequentially. Results from models with continuous update of stiffness and hydraulic conductivity were compared to those of models with fixed values to investigate the potential changes in the estimation of the magnitude and the rate of settlement of slurry tailings. Results from this study indicates that the approach developed was able to capture fairly well the non-linearity properties of tailings during consolidation. Results also showed that models using fixed stiffness and hydraulic conductivity could induce a magnitude and rate of consolidation that was much less/higher compared to those obtained from models with updated values. Predictive models such as Kozeny-Carman and Kozeny-Carman Modified models also gave a satisfactory estimation of tailings behaviour, at least, for preliminary studies. The simple modifications to the numerical codes

proposed in this paper could therefore significantly improve the numerical simulation of tailings behaviour in the short term and contribute to a better planning of filling schemes.

Keyword: Slurry tailings, consolidation, updated properties, predictive equation, coupled numerical simulation.

4.1 Introduction

Hard rock mine tailings generated during mining operations are typically deposited as slurry in TSFs and consolidate with time (Townsend & McVay, 1990). Consolidation of mine tailings in TSFs can take a very long time because of their initially high water content and their relatively low hydraulic conductivity (Bussière, 2007; Jeeravipoolvarn, 2010; Agapito & Bareither, 2018). Consequently, tailings mechanical properties remain low, which can induce geotechnical instabilities, including dam failure and dynamic and/or static liquefaction (Azam & Li, 2010; Rana et al., 2021; Fourie et al., 2022). Several factors can influence tailings consolidation such as their hydraulic conductivity and the presence of drainage pathways, e.g., wick drains (Zhou et al., 2019), waste rock inclusions (Bolduc & Aubertin, 2014) or drainage layer at the bottom of TSFs (Lévesque, 2019).

Conventional estimation of consolidation of geomaterials is usually based on Terzaghi's consolidation theory with the principal assumption that hydraulic conductivity and the coefficient of compressibility are constant. However, those parameters of slurry materials such as tailings or dredged soils vary with time and void ratio, and assuming constant hydraulic conductivity and compressibility is often not representative of their actual behaviour (Somogyi, 1980; Schiffman, 1982; Morris, 2002). A general form of one-dimensional non-linear finite strain consolidation for saturated thick soil layers was therefore proposed by Gibson et al. (1967) to overcome the limitations of the small strain theory. Gibson's equation can accommodate large strain evolution and variations in hydraulic conductivity and soil stiffness during consolidation. Finite strain consolidation theory is, therefore, more representative of tailings behaviour in field conditions (Schiffman, 1982; Bartholomeeusen et al., 2002; Fahey et al., 2010).

Research that quantitatively compared differences in tailings settlement of models with the assumption of non-linear and constant properties of tailings is, however, still limited. For example, McDonald and Lane (2010) studied the consolidation of gold tailings disposed in a pit assuming a

constant hydraulic conductivity. In this case, numerical simulations predicted that post-filling settlement of tailings would last approximately one year, while measurements in the field showed that consolidation lasted around 3 years in practice. Considering changes in stiffness and hydraulic conductivity of tailings with time seems, therefore, necessary to improve the understanding of short-term behaviour of tailings. Carrier et al. (1983) also demonstrated the impact of consolidation estimation with constant properties compared to that with non-linear properties. However, this research was carried out with clay-like tailings, and there was no presence of drainage paths in these studies.

Various mathematical functions representing compressibility evolution have been proposed, including power function (Somogyi, 1980), extended power function (Liu & Znidarčić, 1991) and Weibull function (Jeeravipoolvarn, 2010). The power function is often used for its simplicity and good representativeness (Townsend & McVay, 1990; Agapito & Bareither, 2018; Zhou et al., 2019):

$$e = A\sigma'^{\mathrm{B}} \tag{4.1}$$

Where e is the void ratio (-), and A and B are empirical adjustment parameters.

A power function is also commonly used to estimate the variation of hydraulic conductivity as a function of the void ratio (Somogyi, 1980; Coffin, 2010; Fredlund et al., 2015):

$$k = Ce^{D} \tag{4.2}$$

where k is the hydraulic conductivity (m/s), and C and D are empirical adjustment parameters.

Numerical models are then usually performed for upscaling laboratory results to field conditions with various numerical tools being developed to investigate the settlement of mine tailings. For instance, the finite element modelling program Plaxis (Bentley System Int., 2021) was employed by McDonald and Lane (2010) to model consolidation of Gold and Nickel tailings in a pit, while Bolduc and Aubertin (2014) and Boudrias (2018) investigated the influence of WRIs on the consolidation evolution of tailings using SIGMA/W (Bentley System Int., 2021). These studies were carried out with the assumption that either the tailings properties were constant (McDonald & Lane, 2010) or it was updated after the addition of each new tailings layer (Boudrias, 2018). Using continuously updated values of hydraulic conductivity and stiffness in future works was recommended in these

studies, which indicated that assumptions of constant properties could have important effects in tailings management. The explicit finite volume code FLAC/FLAC3D (Itasca Int., 2021) is another effective code frequently used to simulate non-linear consolidation of tailings materials (Zhou et al., 2019). Zhou et al. (2019) first validated the capability of FLAC to consider non-linear evolution of tailings stiffness and hydraulic conductivity by modelling consolidation of clay tailings under several disposition scenarios using continuously updated values of hydraulic conductivity and stiffness. However, these were only 2D analysis. Models with 3D analysis might be required in cases where the complexity of TSFs geometry and drainage boundary/configurations are encountered (Fredlund et al., 2015).

The objective of this research was, therefore, to perform a series of coupled fluid-mechanical simulations using FLAC3D (Itasca Int., 2021) to evaluate the potential differences between models using constant and updated values and the performances of various predictive models of hydraulic conductivity. An approach to modify Mohr Coulomb parameters was first developed and validated using laboratory column test results. A parametric analysis evaluating the effect of various estimation methods of the hydraulic conductivity on PWP dissipation rate was also performed. Finally, the model was evaluated at a large scale by simulating a simplified tailings impoundment inspired by a real case study.

4.2 Material properties and methodology

4.2.1 Tailings sampling and characterization

Studied tailings materials were sampled from the concentrator of an active gold mine site in Quebec and transported to the laboratory at Polytechnique Montreal for characterization. Tailings particles size distribution (PSD) was determined using ASTM D7928 (2017) for particles finer than 75 μm and ASTM D6913M (2017) for coarser particles. The values of D_{10} (the diameter corresponding to 10% passing in the particle-size distribution curve) was 0.004 mm, D_{60} (the diameter corresponding to 60% passing in the particle-size distribution curve) was 0.04 mm, and the coefficient of uniformity C_u ($C_u = D_{60} / D_{10}$) was 10. These hard rock mine tailings were classified as low plasticity silts (ML) according to the Unified Soil Classification System (ASTM D2487-17, 2017). The specific gravity $G_s = 2.71$ was determined according to ASTM D854 (2016). This value was lower than that of similar

tailings materials which was around 2.75 (Bolduc, 2012), 2.76 (Essayad, 2015) and 2.71 (Boudrias, 2018). Thus, the value of specific gravity was assigned 2.75 in this study. Modified proctor test was performed according to ASTM D1557 (2015) which indicated an optimum moisture content $W_{opt,}$ = 13% and a maximum dry density, γ_{dmax}, = 1830 kg/m^3. The measured properties were similar to previous studies on hard rock mines tailings (Qiu & Sego, 2001; Bussière, 2007).

4.2.2 Consolidation tests

Two consolidation tests (S1 and S2) were carried out in rigid columns following the protocol proposed by Essayad and Aubertin (2021). Columns were 50 cm high with 10 cm internal diameter (figure 4-1). Around 30 cm of tailings were placed in the columns as slurry and compressed under incremental loadings. Samples were prepared with a solid content of around 74%, which is higher than that of typical hard rock mine tailings (Bussière, 2007). This solid content aimed to prevent segregation of tailings materials (Essayad, 2015; Boudrias, 2018). Excess PWP were monitored continuously using three pore water pressure sensors (Trustability, accuracy: ±0.20%) installed 3.5 cm, 15 cm and 23.5 cm from the base of the column. A LVDT was placed on top of each column to measure the displacement at the surface of the tailings. Maximum excess PWP measured during the tests was up to 40% smaller than the loading applied at each step which was explained by the influence of side friction between tailings and instrumented columns wall (figure 4-1). The effect of friction between column wall and tailings was therefore corrected for both column tests at each loading step using the procedure proposed by Essayad and Aubertin (2021). Corrected values were used and presented in the following (figure 4-2). Loads in column S2 were smaller than those in column S1, which could be attributed to the fact that correction of effective stress in 2 columns was different (i.e., friction was different in 2 columns) and the measurement of hydraulic conductivity was only performed for column S1 (which might alter the stress state in the column). Next loading step was applied when PWP reached the hydrostatic value (i.e., after around 3 to 4 hours). The maximum loading applied to the tailings in this study was around 200 kPa (corresponding to an overburden of around 25 m) but larger values could be applied as well to reflect higher values of loading that might be encountered in the field.

Saturated hydraulic conductivity was measured at the end of each loading stage for column S1 using constant head test inspired by ASTM D5856 (2015). A constant hydraulic head was applied at the

base of the column using a Mariotte cell (figure 4-2). The outflow was measured at the upper drainage valve in the column to estimate the saturated hydraulic conductivity (Lévesque, 2019). For practical reasons, the hydraulic conductivity was measured by imposing an upward flow, contrary to what is recommended by standards ASTM D5856 (2015), and results could, therefore, have been slightly underestimated. The difference was, however, deemed negligible (Lévesque, 2019).

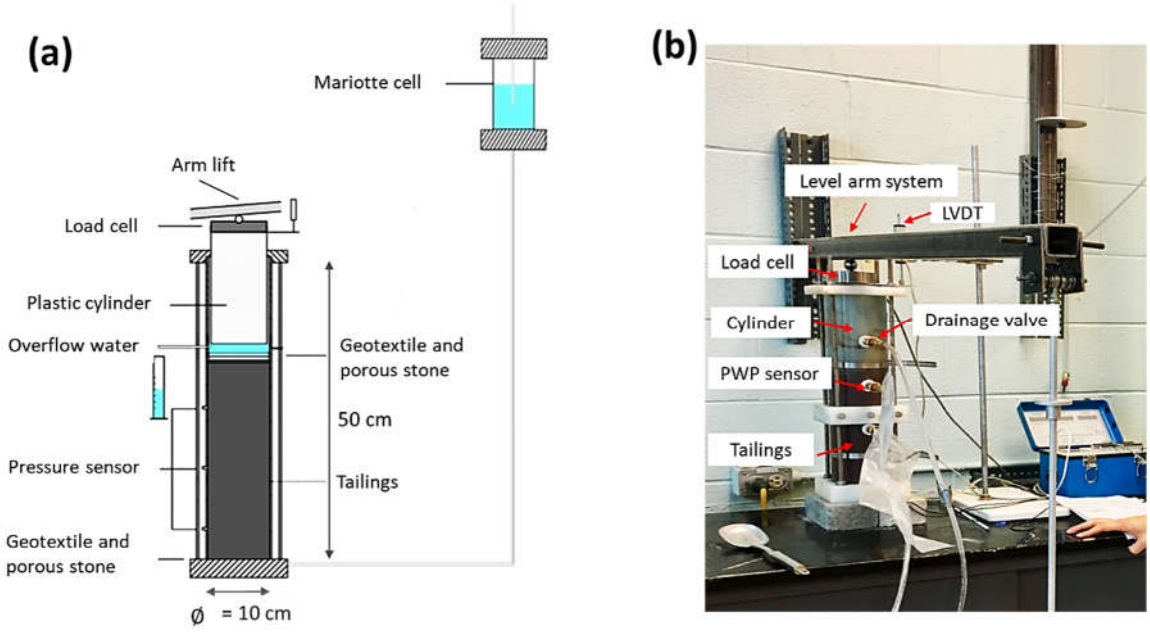

Figure 4-1: Instrumented column test setup used to measure saturated tailings compressibility. A lever arm was used to apply increasing loading and a PVC cylinder transmitted the vertical compression loading to the tailings surface. LVDT and PWP sensors (placed at different elevations) were connected to a data logger (modified after Lévesque (2019) and Nguyen and Pabst (2020)).

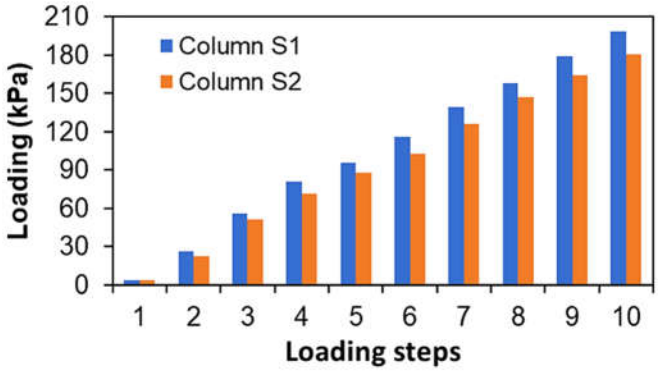

Figure 4-2: Loading applied at various steps in column test S1 and S2. Values of loading was corrected for friction (see text for details).

4.2.3 Numerical simulations

4.2.3.1 Conceptual model

Column tests S1 and S2 were simulated in FLAC3D (Itasca Int., 2021) by a cylinder with a radius of 10 cm and a height of 30 cm. The mesh was vertically divided into 15 zones (mesh size was selected to reduce calculation time while not affecting the precision of the results) (see Appendix B). PWP at tailings surface was fixed at zero to simulate the water table position and allow an upward free drainage condition. The bottom boundary was considered impervious similarly to laboratory conditions. Displacement at the bottom boundary was fixed as zero in all three directions and only vertical displacement was allowed along the side boundaries of the models. Loading was simulated at the surface of the model in 10 stages.

4.2.3.2 Hydraulic conductivity and stiffness update

Properties of elastic-perfectly plastic Mohr-Coulomb model was modified in this study to consider the continuous variation of stiffness and hydraulic conductivity of tailings during consolidation. Equations 4-1 and 4-2 were used to simulate the non-linear relations between the stiffness and the hydraulic conductivity with the void ratio.

Void ratio was calculated from displacements measured during the test, and a relation between void ratio and effective stress was established (figure 4-3a) (R^2 = 0.97):

$$e = 0.814\ x\ \sigma'^{-0.058}$$

Hydraulic conductivity decreased as void ratio decreased. For example, hydraulic conductivity at the end of cycle 3 was around 2 times smaller compared to that at the end of cycle 2 (figure 4-3b). A power law function of hydraulic conductivity was fitted on the experimental results (R^2 = 0.99):

$$k = 1.24\ x\ 10^{-6}\ \ e^{4.61}$$

Young modulus was also calculated at each loading step based on Poisson's ratio and volumetric compressibility coefficient (Holtz & Kovacs, 1981). Tailings stiffness increased during each loading step and was for example almost three times greater at the end of cycle 2 compared to cycle 1 (figure 4-3c). The relation between Young's modulus and effective stress was then derived and fitted using the following power law function (R^2 = 0.95):

$$E = 85.6\ x\ \sigma^{0.74}$$

The extrapolation of the power function tended to lead to very small (and unrealistic) stiffnesses at small effective stresses (i.e., < 0.1 kPa), a minimum value of the Young's modulus E = 180 kPa was assigned in the models to prevent excessive displacements during the first loading step (this value corresponded to the Young's modulus of tailings at the first loading stage obtained from column tests). Equations were introduced in the simulations via FISH coding language in FLAC3D to automatically update the hydraulic conductivity and stiffness values at each iteration. Equations were validated by simulating column tests S1 and S2. Column models were adjusted to simulate accurately the initial height and values of loadings applied, but all the other parameters (i.e., density, Poisson's ratio and internal friction angle, and stiffness and hydraulic conductivity functions) were identical in both models.

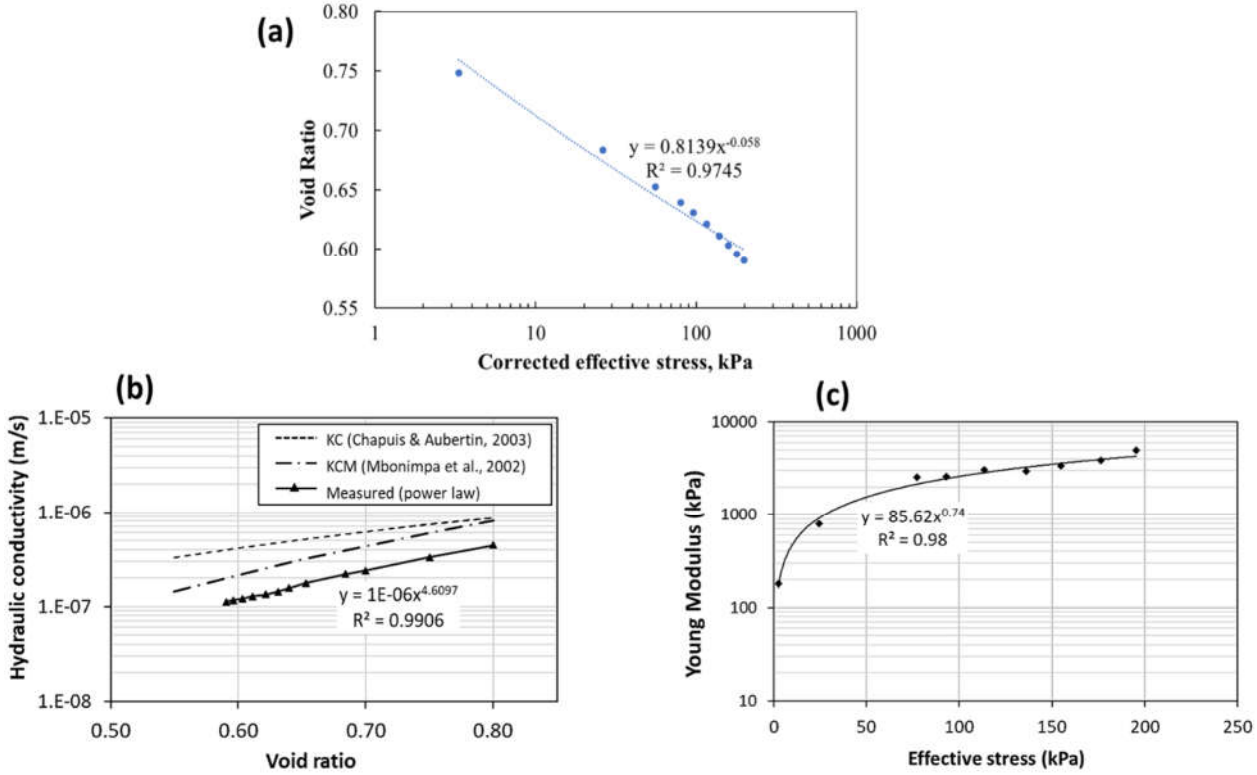

Figure 4-3: Evolutions of (a) void ratio as a function of effective stress, (b) hydraulic conductivity as a function of the void ratio for and (c) Young's modulus as a function of effective stress for column test S1. Measurements (points) and fitted power law functions (solid lines) are shown. Experimental hydraulic conductivities are compared with KC (Chapuis & Aubertin, 2003) and KCM (Mbonimpa et al., 2002) predictive models. It is noted that these functions were derived from results for column S1 and was considered identical for column S2 as the same materials were used for these 2 column tests.

4.2.3.3 Predictive functions of hydraulic conductivity

In practice, measuring hydraulic conductivity can be time-consuming, especially if the measurements need to be repeated for several void ratios (Mbonimpa et al., 2002; Babaoglu & Simms, 2020). Various predictive functions have, therefore, been proposed to estimate hydraulic conductivity from more common and easy-to-obtain parameters, such as the particle size distribution curve or limit of plasticity (Mbonimpa et al., 2002). Mbonimpa et al. (2002) have proposed a predictive function that is specifically dedicated to hard rock mine tailings. This KCM function is the extensions of the

Kozeny–Carman equation which considers the tortuosity of the porous medium, the pore size distribution and the solid grain surface characteristics. KCM model can be expressed as follows (Mbonimpa et al., 2002):

$$k_G = C_G \frac{\gamma_w}{\mu_w} \frac{e^{3+x}}{1+e} C_U^{1/3} D_{10}^2 \tag{4.3}$$

Where k_G is in cm/s, C_G = 0.1, x = 2, γ_w is the unit weight of water (kN/m^3), μ_w is the dynamic viscosity and is expressed in Pa.s, C_U is the coefficient of uniformity (-) and d_{10} is the particle diameter that corresponds to 10% passing on the cumulative grain-size curve (cm).

Chapuis and Aubertin (2003) also adapted Kozeny–Carman (KC) to estimate the hydraulic conductivity of tailings based on the concept of the equivalent diameter derived from the specific surface area of the solid grains, S_m. Tailings hydraulic conductivity estimation based on KC model can be written (Chapuis and Aubertin, 2003):

$$k = 10^{\left[0.5 + \log\left(\frac{e^3}{D_R^2 S^2 (1+e)}\right)\right]} \tag{4.4}$$

Where D_R is the specific weight of material ($D_R = \rho_s/\rho_w$)(-).

Simulations using various prediction methods of hydraulic conductivity (i.e., power function, KC and KCM) were performed, and dissipation rate of PWP and evolution of the settlement of tailings were compared with measurements. Similar models were also carried out for large-scale models (see below).

4.2.3.4 Upscaling models

To evaluate the aforementioned approach under more realistic conditions, column test results were scaled up to simulate tailings consolidation behaviour in a typical tailings storage facility with a sequential filling. In practice, tailings deposition rate (i.e., the thickness of tailings layers per unit of time) widely varies depending on the production rate, TSF size and operational conditions at each mine site. For example, filling rate for the tailings impoundments in Malartic mine, Canada, is usually assumed to be around 3 m per year (Bolduc & Aubertin, 2014), while the thickness of tailings disposed per year at the Rabbit Lake mine, Canada, was comprised between 2 m and 14 m (MEND,

2015). In this study, a filling rate of 12 m per year was chosen as the base case, corresponding to the deposition of a 2-m thick layer every two months for a total of 6 layers. A pseudo 3-D 12 m high model was simulated, with a 0.5-m zone size mesh. Bottom boundary was fixed, and no displacements were allowed, while the side boundaries were only allowed to move vertically. The base of the model was considered impervious simulating, for example, an impermeable bottom liner, and the water table was maintained at the surface of the model (as observed on slurry TSF). Tailings properties were the same as those in column test simulations (see above). A friction angle of 38 degrees was applied and tailings were considered cohesionless (Boudrias, 2018). Initial porosity of tailings was 0.437 (similarly to that in the columns), and a value of 0.28 (calculated based on friction angle as $\nu = \frac{1-sin\theta'}{2-1-sin\theta'}$) was used for Poisson's ratio.

4.3 Results

4.3.1 Column test simulations

Column test results showed that largest measured settlements occurred during the first few loading steps and the total measured settlements in columns S1 and S2 were around 3.15 and 3.44 cm respectively, corresponding to around 10% of strain, at the final loading steps (figure 4-4a and 4-4b). The total simulated settlement in column S1 was 3.28 cm (4% greater than the measured value), and around 3.29 cm for column S2 (i.e., 4% lower than measured values) (figure 4-4a and 4-4b). The largest measured settlements occurred at the end of the 2nd loading step, with around 1 cm displacement for both columns (figure 4-4c and 4-4d). Settlements then tended to decrease as loadings increased and the tailings became stiffer. For example, measured settlement in column S1 was 0.52 cm during the 3rd cycle, and 0.1 cm during the last loading step (figure 4-4c). Simulated settlements showed a good agreement with measurements for all loading cycles and for both columns (figure 4-4c and 4-4d). The difference between measured and simulated settlements was relatively small and usually below 15%. Maximum difference of around 33% (at the end of the 8th cycles) and 24% (at the end of the 3rd cycle) was observed in column S1 and S2, respectively (figure 4-4c and 4-4d). These good agreements between the simulations and the measurements showed the advantages of the developed approach that can simulate the evolution of stiffness of tailings.

Model with constant values of stiffness, E = 2500 kPa, corresponding to the intermediate value was also performed for both columns to evaluate the differences of tailings behaviour between constant and updated properties used in column tests. Simulated displacements using a constant stiffness were significantly smaller compared to measured values (figure 4-4c and 4-4d). For example, simulated settlements at the end of the 2nd and 3rd cycles in column S1 and S2 were around 5 and 3 times lower than measurements, respectively. The total simulated settlement in column S1 and S2 with constant stiffness was around 1.85 and 1.73 cm respectively, which was approximately half of measured values. Results, therefore, confirm that using a constant value for tailings stiffness may induce significant discrepancies compared to real tailings behaviour.

For each loading step, the excess PWP first increased to values corresponding to the loading applied and then gradually decreased towards the hydrostatic pressure within usually around 1 hour for both measured and simulated values (figure 4-5a). The trend of evolution of simulated PWP in the middle of the columns agreed relatively well with measured values (figure 4-5a). For column S1, simulated t_{50} and t_{90} were generally greater than measured values. During the 3rd cycle, for example, around 10 minutes were required to dissipate 50% of excess PWP in column S1, but around double (i.e., 21 minutes) in the simulation, while simulated t_{90} was around 8 minutes higher than measured value during the 6th cycle (figure 4-5a). The largest difference between measured and simulated of t_{50} was at the end of the 2nd cycle, with simulated t_{50} being 2.6 times longer than measured value, while that of t_{90} was around 41% at the end of the 7th cycle (figure 4-5b and 4-5c). These indicated that the models predicted relatively well the long-term dissipation of excess PWP compared to the short-term evolutions. Difference between measured t_{90} and those of models with constant hydraulic conductivity (k = 2.0 x 10^{-7} m/s) was around 40% and a maximum of 63% at the end of cycle 9 (figure 4-5a). Similar trends were also observed for other cycles and for the column S2. Despite these limited differences, simulations were deemed acceptable considering usual uncertainties in displacement and hydraulic conductivity measurements.

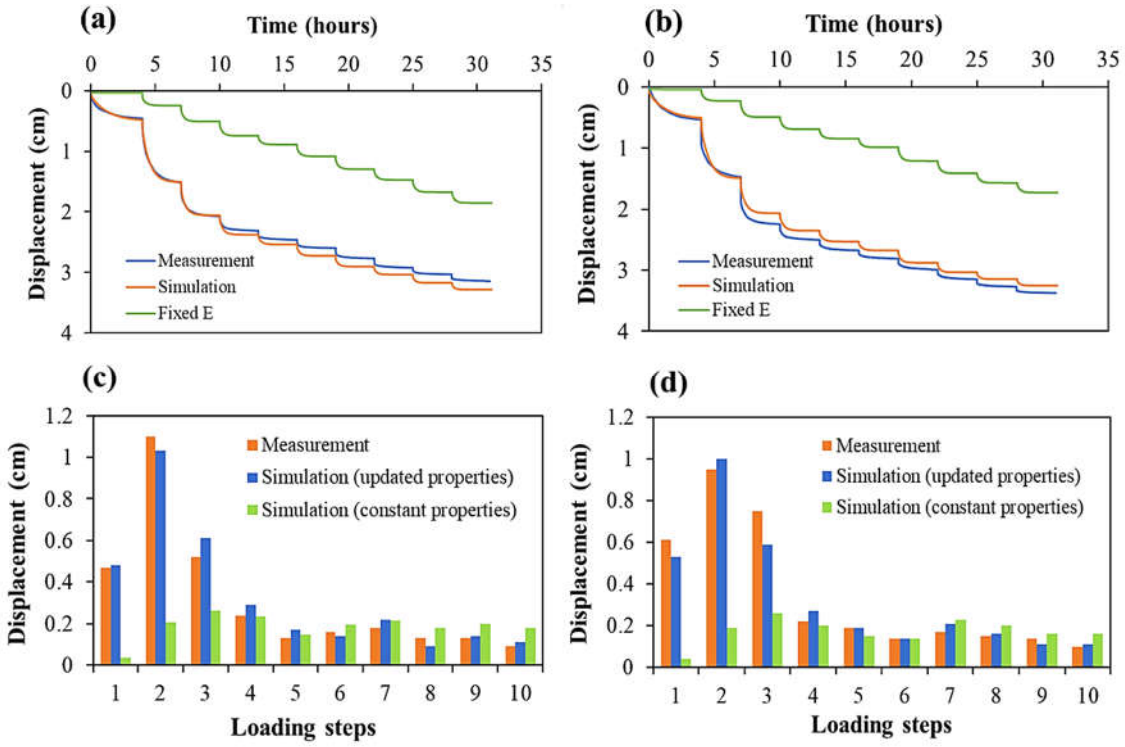

Figure 4-4: Comparison of evolutions of simulated settlement with updated properties and measured settlement for the whole loading cycles for (a) column S1, (b) column S2, and comparison of simulated (with updated and constant properties) settlements and measured settlement at each loading step for (c) column S1 and (d) column S2. Constant values of hydraulic conductivity (2.0 x 10^{-7} m/s) and stiffness (2500 kPa) corresponding to the intermediate values were assigned for tailings.

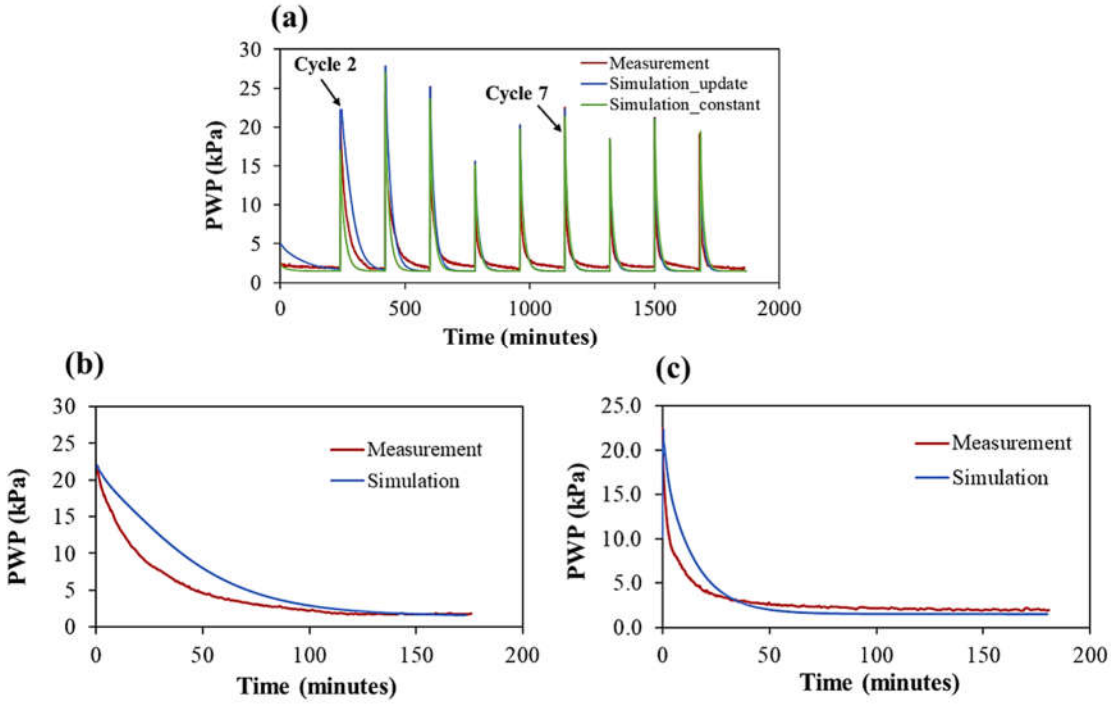

Figure 4-5: Evolution of measured and simulated PWP in column S1 for (a) all cycles, (b) the 2nd cycle and (c) the 7th cycle.

Simulated evolutions of hydraulic conductivity and stiffness in column S1 were in a good agreement with measured values at each loading step (figure 4-6). In general, the difference between measured and simulated hydraulic conductivity was less than 10%. Saturated hydraulic conductivity exhibited significant decrease after the first few layers and the changes of this parameter became lower as loads increased. Saturated hydraulic conductivity decreased, for example, by almost half after the 2nd loading was applied, while it changed only less than 10% after the application of the last few layers (figure 4-6a). Similar trends were observed for measured and simulated Young's modulus. A maximum difference of around 700 kPa (i.e., 20%) was observed at the last cycle, but in general the difference between measured and simulated stiffnesses did not exceed 8% (figure 4-6b). Most of the changes in simulated hydraulic conductivity and stiffness occurred during the first 30 minutes after the load was applied.

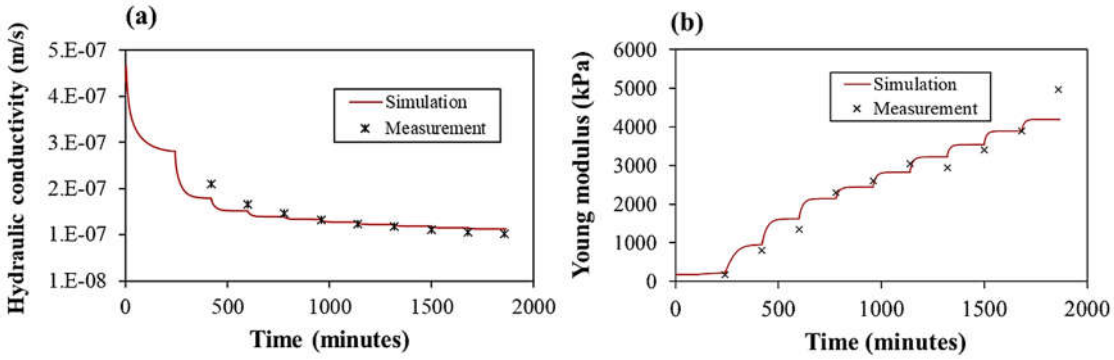

Figure 4-6: Evolution of (a) tailings hydraulic conductivity and (b) Young modulus in column S1 during column tests.

4.3.2 Prediction of hydraulic conductivity function

In this study, the variation of hydraulic conductivity with the void ratio was evaluated by conducting hydraulic conductivity test at the end of each loading cycle and then fitted using a power law. Such tests are, however, time consuming and somewhat complex to carry out, and using predictive models could therefore offer some advantages. Predictive models KCM and KC (figure 4-7) were used here to estimate the hydraulic conductivity as a function of the void ratio of the studied tailings and compared with laboratory measurements. Simulations using KCM and KC methods exhibited a faster dissipation rate of excess PWP compared to measured values. For example, around 20 minutes were required to dissipate 90% of excess PWP during the 3rd cycle with KC model, and 37 minutes with KCM, while measured t_{90} was around 61 minutes (figure 4-7a). A good agreement between results from KCM and KC models was observed at the beginning of the dissipation process (i.e., the difference of t_{50} between simulated and measured values was less than 20%). Similar trends were observed for the rate of settlements for all cycles (figure 4-7b). Results, therefore, indicated that the hydraulic conductivity prediction using KCM, and KC models can provide acceptable results, at least, during the beginning of the dissipation process and can be used for a primary design stage. However, they tended to overestimate the dissipation rate of PWP for long-term (t_{90} values) and measuring hydraulic conductivity is therefore recommended to improve the precision of the simulations. This might also be predictable when comparison was made for evolution of hydraulic conductivity using KC, KCM and measured values (see figure 4-3)

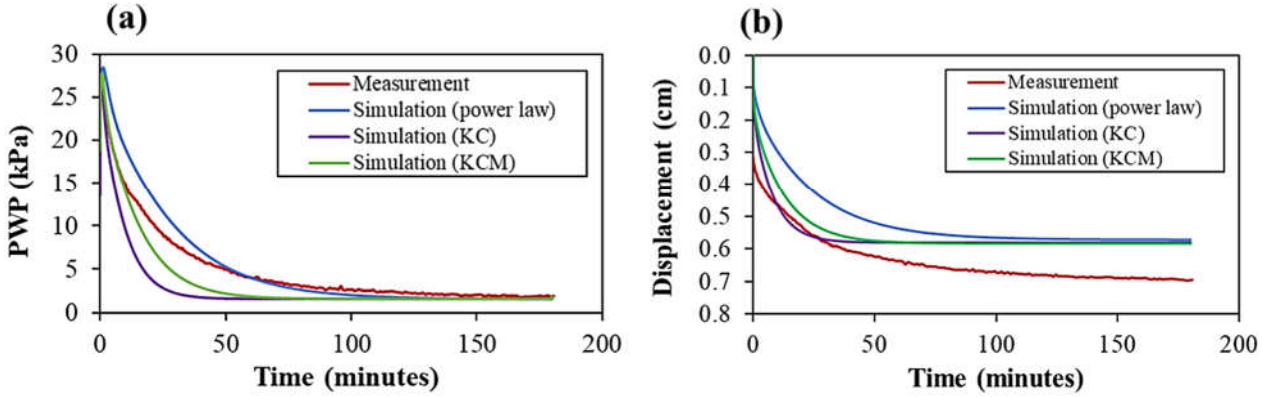

Figure 4-7: Evolution of (a) excess PWP and (b) settlement with time during the 3rd loading step of column S2 for various estimation methods of hydraulic conductivity.

4.3.3 Large scale implications

Large scale field models were simulated to evaluate the implications of using continuous updated hydraulic conductivity and stiffness to investigate tailings consolidation behaviour. For model with continuously updated hydraulic conductivity, hydraulic conductivity decreased by around 2.5 times from 3.5×10^{-7} m/s at the beginning of filling process to 1.4×10^{-7} m/s after the filling of the last layer with a significant decrease occurring during the first 2 steps (figure 4-8a). On the contrary, Young's modulus increased tenfold during filling, reaching around 2500 kPa at the end of the filling process for model where Young's modulus was updated (figure 4-8b). Model with updated stiffness and hydraulic conductivity was then compared with simulations using a fixed value of Young's modulus or hydraulic conductivity (as frequently assumed in many literatures; see introduction).

Simulations were performed with fixed values of hydraulic conductivity (k_{sat} = 3.5×10^{-7}, 1.7×10^{-7} and 1.4×10^{-7} m/s, corresponding to the maximum, intermediate and minimum values, respectively; stiffness was updated). PWP first instantaneously increased by 40 kPa with the addition of each new 2-m thick tailings layer and subsequently dissipated until it reached hydrostatic conditions (figure 4-9a). The same trend was observed for all models but the rates of excess PWP dissipation were different for models with updated or fixed values of hydraulic conductivity (figure 4-9). After the 2nd layer was filled, the model with maximum value of hydraulic conductivity observed the fastest rate of PWP dissipation t_{90} at the base of the tailings mass, around 4 days, which was nearly haft of that

for a model with updated hydraulic conductivity (figure 4-9b). Around 10.2 days were required to dissipate 90% of PWP when minimum hydraulic conductivity was assigned. t_{90} of model with updated and intermediate hydraulic conductivity was essentially the same, which was around 7.8 days (figure 4-9b). After the addition of the sixth layer, the hydraulic conductivity of tailings at the bottom of the model was small and close to its minimum value. Indeed, t_{90} for both models with minimum hydraulic conductivity and updated hydraulic conductivity were close and around 35 days (figure 4-9c). t_{90} for model with maximum hydraulic conductivity was around 13.8 days, which was nearly 2.5 times faster compared to model with updated conductivity (figure 4-9c). As the evolution of PWP is critical for the computation of tailings consolidation rate, stability analysis and mine closure design in practice, a comprehensive method that can cover the evolution of hydraulic conductivity of tailings during the filling process could, therefore, contribute to improve the accuracy level of such analysis.

Models with values of E = 1800 and 4500 kPa corresponding, respectively, to the intermediate and maximum values of Young's modulus derived from tailings properties in column test were then performed (hydraulic conductivity was updated) (figure 4-8b). Another method to estimate consolidation of tailings also consists in updating Young's modulus at the beginning of each loading step (corresponding to each new addition of a tailings layer) as mentioned previously. A model was therefore simulated where Young's modulus was assigned a constant value at the beginning of each loading step was also performed (i.e., 180, 270, 890, 1390, 1800 and 2230 kPa corresponding to the loading step from 1 to 6). Results showed that tailings settlements during sequential filling simulated with constant stiffness could lead to significant differences compared to those obtained with updated values. Model with maximum stiffness resulted in a settlement that was 5 times lower than that of a model with updated stiffness, while settlement of model with stiffness being updated at the beginning of each filling step was around 2.5 times higher than that of model with continuous update stiffness (figure 4-10a). Specifically, total settlement of the first layer for model with continuously updated properties was around 15.7 cm, while those for model with maximum and intermediate values of Young's modulus were around 3.5 and 8.5 cm, respectively (figure 4-10a). Total settlement of model with Young's modulus being updated at the beginning of each filling stage was around 39 cm (figure 4-10a).

Also, the largest settlement of the first layer in updated stiffness model occurred after the filling of the first two layers and then decreased as loading increased, while those of models with constant

stiffness were relatively identical throughout the filling process (figure 4-10b). For example, the largest settlement of the first layer for the former was around 4.1 cm after the adding of the second layer, while that for model with maximum and intermediate stiffness was somewhat constant at around 0.7 and 1.6 cm for almost all loading steps (figure 4-10b). Settlement of the first layer in model with updated stiffness was up to 3 times higher than those of model with intermediate stiffness (after the adding of the second layer) and up to 3 times lower than those of models with stiffness updated at each step (after the filling of the 5th layer) (figure 4-10b). This indicates that using a certain value of stiffness of tailings material could lead to a significant difference in settlement results compared to the model with updated stiffness following changes in loads applied. The implication of model with continuously updated values could, therefore, favour better estimation of settlement of tailings and subsequently the volume of tailings that can be disposed in the containment in practice.

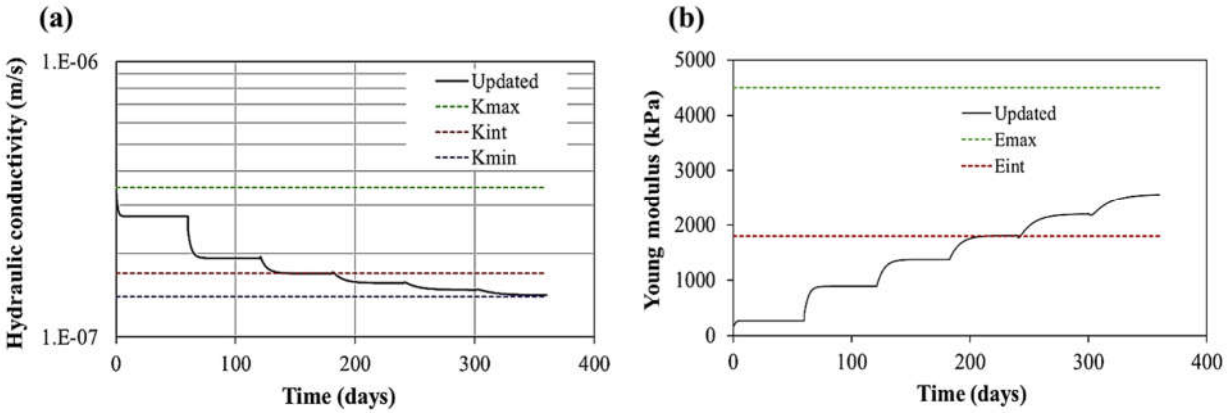

Figure 4-8: Evolutions of (a) hydraulic conductivity and (b) Young modulus of tailings at the middle of the first layer with time for models with updated and fixed properties.

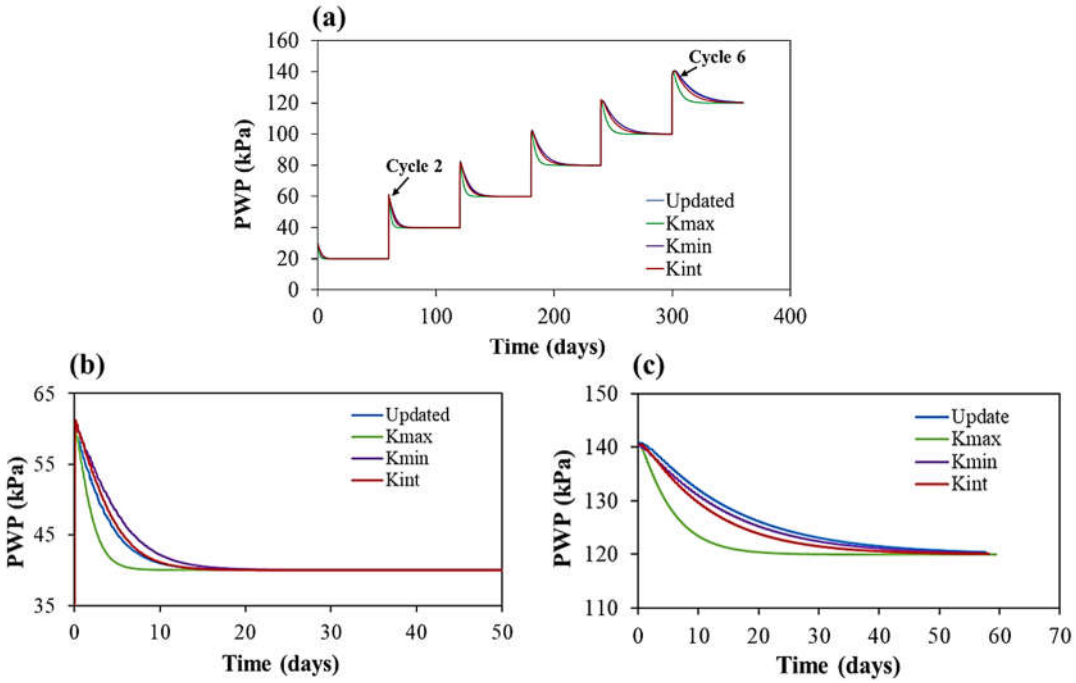

Figure 4-9: Evolution of excess PWP at the base of the model (a) for the case of 2 m thick tailings layer, (b) after adding the 2nd layer and (c) after adding the 6th layer for models where hydraulic conductivity was updated or fixed values were assigned.

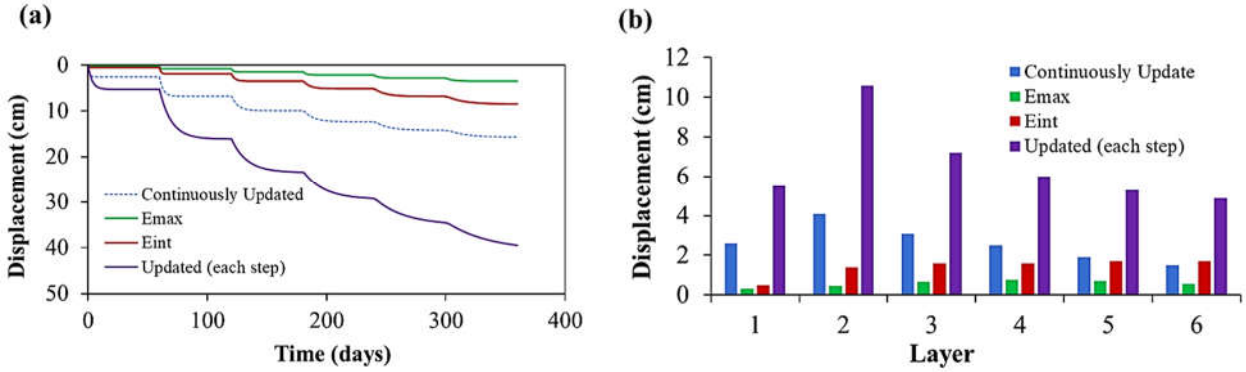

Figure 4-10: Comparison of (a) evolution of the settlement of the first layer with time after filling of other layers in case of models with updated hydraulic conductivity and stiffness and models with fixed value of stiffness and (b) settlement of layer 1 resulting from the placement of other successive layers for these models.

Combining with the results on the evolutions of hydraulic conductivity and stiffness in column tests in section 4.3.1 (small scale), using a certain value for these parameters to estimate the consolidation of tailings might lead to some uncertainties in practice. Using a fixed value of hydraulic conductivity, the difference in the dissipation rate of excess PWP obtained can reach up to 2.5 times compared to the models with updated values. Using a fixed value of Young's modulus could also lead to the settlement results that are much less/higher than those obtained from models using updated value of stiffness (i.e., up to 5 times).

The effect of various estimation methods for hydraulic conductivity was also evaluated in the case of large-scale study. The evolution of excess PWP at the middle of the first layer after adding the 3rd layer was fastest in the model with KC function, with t_{90} being around 7 days, while that of model with KCM function was around 11 days. The dissipation rate induced by power law was lowest, with t_{90} being around 18 days (figure 4-11a). The similar trend was also observed on the rate of consolidation at the point located in the middle of the first layer (figure 4-11b).

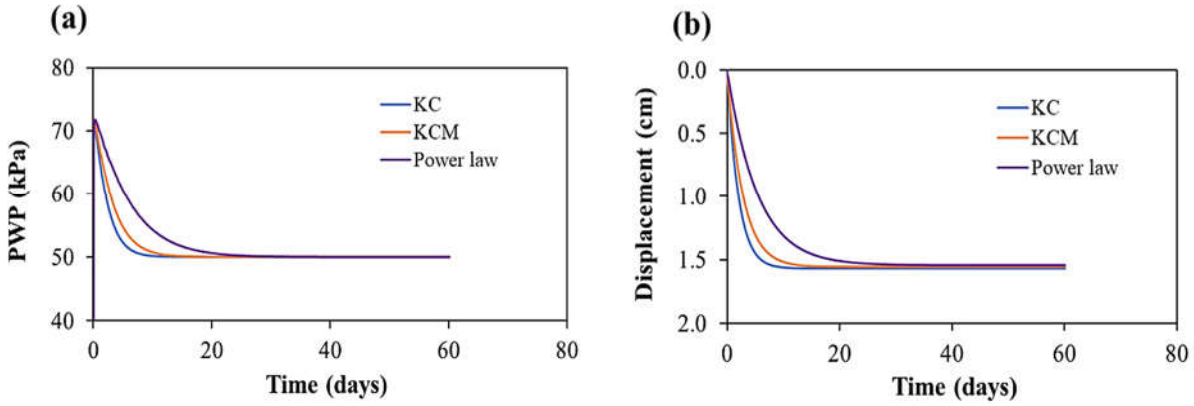

Figure 4-11: Evolution of (a) excess PWP and (b) settlement as a function of time at the middle of layer 1 after adding of layer 3 for various estimation methods of hydraulic conductivity.

4.4 Discussion

More loading stages might be added at the beginning of the column test at low pressures where most of the non-linear behaviour of tailings occur (Babaoglu & Simms, 2020; Nguyen & Pabst, 2020) to better capture the evolution of tailings at low values of load applied, which might be important in

case the test is performed for the fine tailings (Fourie et al., 2022). Only one measurement of hydraulic conductivity and 2 column tests were performed in this study, additional column tests and measurements of hydraulic conductivity could also be performed to improve the precision of constitutive models of stiffness and hydraulic conductivity of tailings, which can be subsequently used as the input for the models of tailings consolidation. For predictive functions, although both KCM and KC models can be used to estimate hydraulic conductivity of tailings at the primary design stage, care must be taken regarding the estimation of surface area while using KC model to improve the precision of the prediction (Chapuis & Aubertin, 2003).

There might be occurrence of desaturation and desiccation at the top of tailings layers, which was observed quite commonly in the real TSFs. These can alter the rate of consolidation at these locations as well (Mbemba & Aubertin, 2021b), these aspects were not considered in this study. The approach developed in this study also makes it possible to take these effects into account. Specifically, work can be performed on this phenomenon by introducing some negative PWP at the top of the tailings in column test (Essayad & Aubertin, 2021) to obtain relations for the evolution of tailings properties, which, in turn, can be numerically assigned to comprehensively simulate settlement behaviour of tailings.

The research outputs can then be compared with field measurement data to confirm the capability of the extrapolation of this study to investigate the consolidation behaviour of tailings deposited in real TSFs. It could also help to perform research in which some materials with much higher hydraulic conductivity to enhance the rate of consolidation of tailings are presented (i.e., wick drains and waste rock inclusions). A large-scale implication has been performed in this study, these are, however, simplified model, and the geometry of TSFs could also have influences on the rate of consolidation. By using FLAC3D, some factors related to the geometry effect, configuration of drainage system or boundary conditions could also be performed. These are all included in an on-going project in the group.

Being able to consider continuous change of saturated tailings properties can help to capture the evolution of excess PWP more precisely. This is crucial for the practical short-term design of TSFs, where it is necessary to calculate the filling rate of tailings to prevent the build-up of excess PWP, reducing the risk of TSFs failure (Rana et al., 2021; Fourie et al., 2022). The output results can also

help to facilitate the estimation of volume of tailings that can be placed in TSFs, which is beneficial to the mine waste management operation in practice.

4.5 Conclusion

This paper investigated the non-linear consolidation properties of saturated mine tailings under compression in a column test and a simplified large-scale model. A comprehensive study has been carried out to first propose an approach to consider the non-linear behaviour of tailings based on experimental results from column tests and integrate them in FLAC3D. The capability of the modified model was then successfully validated by modelling the column tests of saturated tailings. Later, the effect of several predictive functions for *k-e* relation (KCM and KC) which was based on sound physical concepts were applied for tailings in the parametric study. Finally, studies on column tests and large-scale models demonstrated the effect of using a fixed value for stiffness and hydraulic conductivity on the magnitude of the settlement and the dissipation rate of PWP. From this study, the following conclusions can be drawn as follows:

These results show that the modified constitutive model is capable of simulating the non-linear behaviour of tailings during the consolidation process with an acceptable accuracy. Total simulated settlement was 3.15 and 3.44 cm for column S1 and S2 respectively, which was fairly close to the measured values. Maximum difference between measured and simulated settlement during staged loading could reach up to 33%, while that for the rate of excess PWP was around 40%, yet these differences were deemed reasonable considering uncertainty in the displacement and hydraulic conductivity measurements in the tests. The difference between simulation and measurement was less than 10% for hydraulic conductivity values and 20% for stiffness values. Using constant properties (assigned in this study) in column test can lead to a total settlement being around 2 times lower than measured values.

Direct measurement of hydraulic conductivity integrated in column tests is deemed to capture the evolution of hydraulic conductivity of tailings. In the meantime, results from this study indicated that other estimation methods on hydraulic conductivity of saturated tailings (KCM and KC) could also be used to predict the hydraulic conductivity of tailings, at least, for the preliminary design stage. In the parametric study, KCM model capture fairly well the evolution of excess PWP, while KC model tended to give a much faster dissipation rate. KCM model can, thus, be used in case the measurement

of hydraulic conductivity of tailing is not available in the lab, while a good estimation of surface area can increase the reliability of KC model.

For up-scaling model where tailings properties were updated, hydraulic conductivity decreased by around 2.5 times during the filling process with a significant decrease occurring during the first 2 steps. Young's modulus, on the other hand, increased by ten times during filling, which indicated a highly non-linear change of the stiffness of tailings.

The rate of excess PWP of tailings using a constant hydraulic conductivity could be 2.5 times faster compared to the model with updated hydraulic conductivity. The use of a constant value of stiffness could induce significant differences in the estimation of the settlement of tailings (i.e., up to 5 times of difference), while the settlement of models with stiffness being updated at the beginning of each filling step was around 2.5 times higher than that of model with continuously updated stiffness. These indicated that the use of updated values is more suitable when computing tailings consolidation behaviour.

Results achieved from this study can prove the advantages of models with continuously updated values of stiffness and hydraulic conductivity of tailings, which, in turn, can facilitate the understand of short-term behaviour of tailings and the improved calculation of storage capacity of TSFs. Further work can also be carried out to scale up and study consolidation of tailings disposed of in an open pit.

4.6 Acknowledgement

The authors are thankful to the financial support from NSERC, FRQNT and the partners of the Research Institute on Mines and the Environment (RIME UQAT - Polytechnique; http://rime-irme.ca/en). The authors also gratefully acknowledge Dr. Huy Tran, Dr. Kazim, Itasca technical support team, and Dr. Jahanbakhshzadeh (Polytechnique Montreal) for their valuable support and comments to improve the code in this study.

4.7 References

Agapito, L. A., & Bareither, C. A. (2018). Application of a one-dimensional large-strain consolidation model to a full-scale tailings storage facility. *Minerals Engineering, 119*, 38-48. https://doi.org/https://doi.org/10.1016/j.mineng.2018.01.013

ASTM D2487-17. (2017). *Standard practice for classification of soils for engineering purposes (Unified Soil Classification System)* (ASTM International.

ASTM D5856. (2015). *Standard test method for measurement of hydraulic conductivity of porous material using a rigid-wall, compaction-mold permeameter: West Conshohocken Philadelphia* (ASTM International.

ASTM D6913/D6913M − 17. (2017). *Standard Test Methods for Particle-Size Distribution (Gradation) of Soils Using Sieve Analysis* (ASTM International.

ASTM D7928 − 17. (2017). *Standard Test Method for Particle-Size Distribution (Gradation) of Fine-Grained Soils Using the Sedimentation (Hydrometer) Analysis* (ASTM International.

Azam, S., & Li, Q. (2010). Tailings Dam Failures: A Review of the Last One Hundred Years. *Geotechnical news, 28*, 50-53. https://ksmproject.com/wp-content/uploads/2017/08/Tailings-Dam-Failures-Last-100-years-Azam2010.pdf

Babaoglu, Y., & Simms, P. (2020). Improving Hydraulic Conductivity Estimation for Soft Clayey Soils, Sediments, or Tailings Using Predictors Measured at High-Void Ratio. *146*(10). https://doi.org/doi:10.1061/(ASCE)GT.1943-5606.0002344

Bartholomeeusen, G., Sills, G. C., Znidarčić, D., Kesteren, W. V., Merckelbach, L. M., Pyke, R., . . . Chan, D. (2002). Sidere: numerical prediction of large-strain consolidation. *Géotechnique, 52*(9), 639-648. https://doi.org/10.1680/geot.2002.52.9.639

Bolduc, F., & Aubertin, M. (2014). Numerical investigation of the influence of waste rock inclusions on tailings consolidation. *Canadian Geotechnical Journal, 51*(9), 1021-1032. https://doi.org/10.1139/cgj-2013-0137

Boudrias, G. (2018). *Évaluation numérique et expérimentale du drainage et de la consolidation de résidus miniers à proximité d'une inclusion de roches stériles* [Mémoire de maîtrise, École Polytechnique de Montréal].

Bussière, B. (2007). Colloquium 2004: Hydrogeotechnical properties of hard rock tailings from metal mines and emerging geoenvironmental disposal approaches. *Canadian Geotechnical Journal, 44*(9), 1019-1052. https://doi.org/10.1139/t07-040

Chapuis, R. P., & Aubertin, M. (2003). On the use of the Kozeny - Carman equation to predict the hydraulic conductivity of soils. *Canadian Geotechnical Journal, 40*(3), 616-628. https://doi.org/10.1139/t03-013

Coffin, J. (2010). *A 3D Model for Slurry Storage Facilities. Boulder, Colorado* [Ph.D., University of Colorado].

Essayad, K., & Aubertin, M. (2021). Consolidation of hard rock tailings under positive and negative pore-water pressures: testing procedures and experimental results. *58*(1), 49-65. https://doi.org/10.1139/cgj-2019-0594

Fahey, M., Helinski, M., & Fourie, A. (2010). Consolidation in accreting sediments: Gibson's solution applied to backfilling of mine stopes. *Géotechnique, 60*(11), 877-882. https://doi.org/10.1680/geot.9.P.078

Fourie, A., Ramon, V., Annika, B., Luis Alberto, T.-C., & Dobroslav, Z. (2022). *Geotechnics of mine tailings: a 2022 State of the Art.* the 20th ICSMGE-State of the Art and Invited Lectures, Sydney, Australia.

Fredlund, M., Donaldson, M., & Chaudhary, K. (2015). *Pseudo 3-D deposition and large-strain consolidation modeling of tailings deep deposits.* Tailings and Mine Waste, Vancouver, BC.

Gibson, R. E., England, G. L., & Hussey, M. J. L. (1967). The Theory of One-Dimensional Consolidation of Saturated Clays. *Géotechnique, 17*(3), 261-273. https://doi.org/10.1680/geot.1967.17.3.261

Holtz, R. D., & Kovacs, W. D. (1981). *An Introduction to Geotechnical Engineering*. Englewood NJ: Prentice-Hall, Inc.

Jeeravipoolvarn, S. (2010). *Geotechnical Behavior of In-Line Thickened Oil Sands Tailings* [Ph.D., University of Alberta].

Lévesque, R. (2019). *Consolidation des résidus miniers dans les fosses en présence d'inclusions de roches stériles* [Mémoire de maîtrise, Ecole Polytechnic Montreal].

Liu, J. C., & Znidarčić, D. (1991). Modeling One Dimensional Compression Characteristics of Soils. *Journal of Geotechnical Engineering, 117*(1), 162-169. https://doi.org/10.1061/(ASCE)0733-9410(1991)117:1(162)

Mbemba, F., & Aubertin, M. (2021). Physical Model Testing and Analysis of Hard Rock Tailings Consolidation Considering the Effect of a Drainage Inclusion. *Geotechnical and Geological Engineering, 39*(4), 2777-2798. https://doi.org/10.1007/s10706-020-01656-0

Mbonimpa, M., Aubertin, M., Chapuis, R. P., & Bussière, B. (2002). Practical pedotransfer functions for estimating the saturated hydraulic conductivity. *Geotechnical & Geological Engineering, 20*(3), 235-259. journal article. https://doi.org/10.1023/a:1016046214724

McDonald, L., & Lane, J. C. (2010). *Consolidation of in-Pit tailings.* Mine Waste 2010, Perth, Australia (pp. 49-62).

MEND. (2015). MEND Report 2.36.1 In-Pit Disposal of Reactive Mine Wastes: Approaches, Update and Case Study Results.

Morris, P. H. (2002). Analytical Solutions of Linear Finite-Strain One-Dimensional Consolidation. *Journal of Geotechnical and Geoenvironmental Engineering, 128*(4), 319-326. https://doi.org/doi:10.1061/(ASCE)1090-0241(2002)128:4(319)

Nguyen, D., & Pabst, T. (2020). *Comparative experimental study of consolidation properties of hard rock mine tailings.* 73rd Canadian Geotechnical Conference (GeoVirtual 2020), Online.

Qiu, Y. J., & Sego, D. C. (2001). Laboratory properties of mine tailings. *Canadian Geotechnical Journal, 38,*, 183-190. https://doi.org/https://doi.org/10.7939/R3WW7704C

Rana, N. M., Ghahramani, N., Evans, S. G., McDougall, S., Small, A., & Take, W. A. (2021). Catastrophic mass flows resulting from tailings impoundment failures. *Engineering Geology, 292*, 106262. https://doi.org/https://doi.org/10.1016/j.enggeo.2021.106262

Schiffman, R. L. (1982). The consolidation of soft marine sediments. *Geo-Marine Letters, 2*(3-4), 199-203. https://doi.org/10.1007/bf02462763

Somogyi, F. (1980). *Large Strain Consolidation of Fine Grained Slurries.* Presentation at the Canadian Society for Civil Engineering, Winnipeg, Manitoba.

Townsend, & McVay. (1990). SOA: Large Strain Consolidation Predictions. *Journal of Geotechnical Engineering, 116*(2), 222-243. https://doi.org/doi:10.1061/(ASCE)0733-9410(1990)116:2(222)

Zhou, Amodio A, & N., B. (2019). *Informed mine closure by multi-dimensional modelling of tailings deposition and consolidation.* Mine Closure 2019, Perth, Australia.

CHAPTER 5 ARTICLE 2: CONSOLIDATION BEHAVIOUR OF VARIOUS TYPES OF SLURRY TAILINGS WITH WASTE ROCK INCLUSIONS: A NUMERICAL STUDY

Ngoc Dung Nguyen, Thomas Pabst

Article submitted to the Journal of Environmental Earth Sciences in August 2022

ABSTRACT

The co-disposition of mine tailings and waste rock in tailings storage facilities (TSFs) could contribute to increase the rate of consolidation of tailings, reduce time to reach static and dynamic stability, and decrease long-term settlement of tailings. Non-linear change of tailings properties during the filling process and interaction between tailings and waste rock inclusion (WRI) are a critical aspect to mechanical analysis but can, however, be complicated to simulate. The question of net volume gains or losses of tailings was also raised. In this study, fully coupled fluid-mechanical analysis which considered continuous variation of hydraulic conductivity and stiffness of tailings were performed to assess the evolution of consolidation of various types of tailings in the presence of WRI. Secondly, the effects of WRI and volume ratio of tailings over WRI on the net volume gains or losses was investigated. Finally, the effect of several practical aspects such as filling rates, and instantaneous filling assumption on the consolidation of tailings were also considered. Results from this study indicated that WRI could increase by 3.3 times the rate of consolidation of tailings. The zone of influence of WRI on tailings consolidation rate varied for each type of tailings. Using updated properties showed significant differences compared to models with constant values. The application of WRI can reduce volume available for the storage of tailings in TSF and net volumetric change due to consolidation of the tailings with or without WRI could be estimated explicitly. Equations predicting evolution of volume gains/losses with the changes in the volume ratios of tailings and WRI were accordingly proposed. The effect of WRI was more pronounced with the increase of the filling

rate. Finally, the assumption of instantaneous filling seemed to have little effect on the simulated rate of consolidation.

Keyword: Slurry tailings, waste rock inclusions, consolidation, comparative study, volume gains or loss, filling rate, FLAC3D

5.1 Introduction

Tailings generated from mining activities are typically deposited hydraulically (i.e., as a slurry) in tailings storage facilities. Consolidation of mine tailings can take a very long time because of their initially high-water content and their relatively low hydraulic conductivity (Vick, 1990; Blight, 2010). Progressive deposition of slurry tailings in TSFs might lead to the build-up of excess pore water pressure (PWP) that has been linked to various geotechnical instabilities issues, including failure of tailings impoundments and static/dynamic liquefaction of tailings (Azam & Li, 2010; Morgenstern et al., 2016; Robertson et al., 2019). A novel approach of tailings and waste rocks co-disposal was developed for surface tailings storage facilities that could contribute to accelerate tailings consolidation. In this method, waste rocks are placed as linear inclusions within the tailings and raised at the same time (figure 5-1). This technique can contribute to accelerate the dissipation rate of excess PWP generated during the continuous accretion of tailings (and thus speed up the consolidation of tailings) by promoting horizontal movement of pore water (Bolduc & Aubertin, 2014). WRI can also provide other advantages such as reducing the size of waste rock piles (i.e., WRI could contribute to completely remove the necessity to build a waste rock piles for underground mines) (Aubertin, 2013, 2018; Mbemba & Aubertin, 2021a). The strength and stiffness of tailings can consequently be improved more quickly. The increase in the consolidation rate and magnitude of tailings in the presence of WRI were experimentally evaluated using physical laboratory tests (Mbemba & Aubertin, 2021a, 2021b), while consolidation behaviour of tailings in the vicinity of WRIs was also numerically investigated at the large scale (Jaouhar et al., 2013; Bolduc & Aubertin, 2014; Boudrias, 2018). WRIs can also help to provide mechanical reinforcement to the tailings impoundment enhancing both static and dynamic stability of the retaining structures (James, 2009; Pépin et al., 2012; Ferdosi et al., 2015a). Effect of WRI configuration was evaluated by changing various values of width of the inclusions and center-to-center spacing between these inclusions (Ferdosi et al., 2015b). In general, results indicated that downstream slope deformation tended to

decrease with the increase of the number of inclusions and to increase with the increase of spacing between inclusions (Ferdosi et al., 2015b).

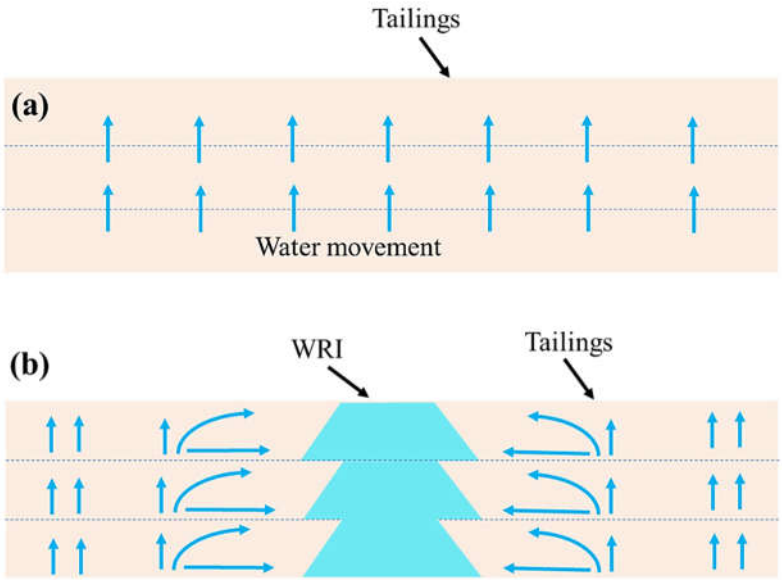

Figure 5-1: Conceptual configuration of a simple WRIs system in a tailings impoundment with (a) only tailings and water can only move upward and (b) tailings co-disposed with WRI and water can move either vertically or horizontally due to the presence of WRI, reducing the length of the drainage pathway (modified after James (2009)).

Critical concerns when studying consolidation of tailings with WRI include capturing properly the evolution of tailings consolidation characteristics and the acceleration of dissipation of excess PWP in tailings. A balance should also be found between maximizing the quantities of tailings deposited and ensuring a good performance of WRI by reducing the distance between them. WRI design optimization, thus, requires considering net volume gains or losses due to the addition of waste rocks within the tailings and thus volume available for the storage of tailings afterwards (Bolduc & Aubertin, 2014; Mbemba & Aubertin, 2021a). Several factors can pose uncertainties to the efficiency of this technique, including the filling rate and hydro-mechanical properties of tailings and waste rocks (Bolduc & Aubertin, 2014). Finally, comparative research on the behaviour of different types of tailings applying co-disposal technique can accordingly contribute further to the application of this

technique to management operations of various types of tailings and somewhat improve optimization of co-disposal technique as a function of tailings properties.

The objective of this paper was, therefore, to evaluate numerically the effects of WRI on consolidation behaviours of various types of tailings sequentially filled in a simplified TSF and considering the evolution of consolidation properties. Potential differences of models with constant and updated properties when WRI was applied were subsequently investigated. Effects of volume ratio between tailings and WRI on the volume gains or losses of tailings in the impoundment were studied. Influences of the filling rate on the consolidation rate of tailings were examined. Finally, influences of the assumption of instantaneous filling in simulations (i.e., no consolidation of tailings occurs during the filling process) compared to the progressive filling scheme in practice (i.e., consolidation occurs during the filling process) was studied. Limitations of the models were also discussed in this study.

5.2 Methodology

Many multidimensional codes have been developed to investigate the settlement of slurry tailings under sequential filling (Liu & Znidarčić, 1991; Fredlund et al., 2015) and the explicit finite volume code FLAC3D (Itasca Int., 2021) is one of the most frequently used to simulate multidimensional and non-linear consolidation of tailings materials. For example, Shahsavari and Grabinsky (2015) used FLAC3D to investigate the effect of non-zero boundary condition on the consolidation of the cemented paste backfill layers, while Zhou et al. (2019) simulated mine tailings consolidation in an impoundment with the presence of wick drain systems. Nguyen and Pabst (2022b) also studied consolidation of tailings in column tests covering continuous update of stiffness and hydraulic conductivity of tailings using FLAC3D. In this study, a series of simulations were performed using FLAC3D to model tailings placed sequentially in a simplified TSF with WRI. Common practice for TSFs design usually considers 1-D geometries (Fredlund et al., 2015). 1-D models are fast and particularly suited for cases where impoundments have small depths compared to the width and the length of the retaining structures. In these cases, the fluid flow direction and the consolidation are essentially vertically-oriented (Priestley, 2011; Fredlund et al., 2015). However, such assumption may not be applicable when highly permeable regions and horizontal drainage systems (such as WRIs

or wick drains) are installed in TSFs. In these cases, a 2-D or 3-D analysis is required to capture the principal effect of lateral flow and strain (Coffin, 2010; Fredlund et al., 2015).

5.2.1 Conceptual models

A 100 × 5 m section was modelled to simulate the consolidation of tailings in the TSF and the effect of the WRI (Figure 5-2). The dimensions of the model were chosen to reduce the mesh size and computation time, yet remaining representative of field conditions (see Appendix B). This width of the TSF was assumed to be far enough from the dams so they would not affect simulated settlements. The influences of the volume ratio between tailings and WRI on the calculated results were also investigated. The simulated WRI represented a simple central inclusion whose crest width was around 12 m. WRI geometry was simplified as parallelepiped instead of the typical successive trapezes usually constructed on real mine sites. This assumption has shown no influence on the results but reduces numerical instabilities (Bolduc & Aubertin, 2014). Saturated tailings were filled into the TSF in successive 10 layers over a period of 10 years. Each layer was 3 m thick for a total height of 30 m. Tailings deposition was assumed instantaneous (i.e., a new 3 m thick layer was added every year at once and left to consolidate before a new layer was added one year later). Four types of tailings were modelled in this study (see below). WRI was raised sequentially at the same rate as tailings (similarly to field conditions).

Displacements at the bottom of the TSF were fixed in all directions, and an impervious bottom was considered. Side boundaries of the models were allowed to move vertically only and also considered impervious (i.e., axis of symmetry). Zero PWP was assigned at the surface of the model to simulate groundwater table and to allow upward movement of water in the tailings. The deposition of a new layer of tailings induced the generation of excess PWP, followed by the dissipation of PWP (towards the surface and the WRI) and the consolidation of the materials. A parametric analysis was also conducted to evaluate the impact of filling rate and effect of the filling scheme.

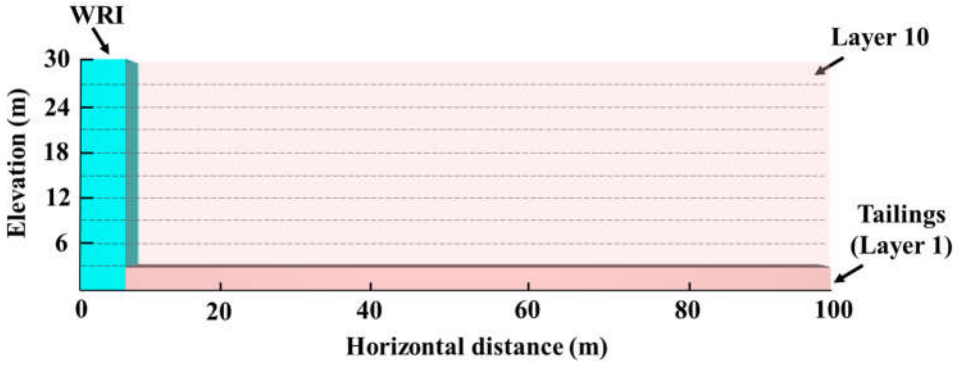

Figure 5-2: Conceptual model with sequential filling of tailings (94 m wide) in 10 layers and the inclusion of granular waste rocks (6m wide) (dash lines represented the interfaces between tailings layers).

5.2.2 Material properties

Four different tailings were considered in this study: 2 types of gold mine tailings (tailings A and B), uranium mine tailings (tailings C) and bauxite mine tailings (tailings D). Tailings properties (i.e., unit weight, relative density, friction angle, and relations of void ratio – effective stress and hydraulic conductivity – void ratio) of tailings A were obtained from experiments by authors, while those for other mine tailings were obtained from literature (Somogyi, 1976; Bhuiyan et al., 2015; Lévesque, 2019). Unit weight was highest for tailings A (e.g., around 19.5 kN/m^3), while that for tailings B, C, D was around 18.7, 13.0 and 17.5 kN/m^3 respectively. Specific gravity of those materials was 2.75, 2.82, 2.70 and 3.27 respectively (the relative high value of tailings D was attributed to the presence of iron). These corresponded to dry density of 1.55, 1.39, 0.46 and 0.98 respectively (Das, 2010), which indicated high initial void ratios of uranium and bauxite tailings relative to those of gold tailings. Friction angles were assigned as 38°, 36°, 30° and 39° for those tailings respectively. All four tailings were cohesionless as mine tailings usually are (tailings D was clay-like material, yet there is no data on the cohesion of the materials, yet cohesion was assumed to have negligible on the consolidation of the tailings materials) (Blight, 2010). The relations between void ratio and effective stress, hydraulic conductivity and void ratio, and Young's modulus and effective stress were derived from column test for tailings A, B and C. There were some differences in terms of dimensions of

samples and load applied in the tests for tailings C: the dimension of the columns used was around 10 x 10 cm, and tailings were undergone incremental loads (from 1 to 8 kPa) while those for tests on tailings A and B might reach around 300 kPa (Bhuiyan et al., 2015; Lévesque, 2019; Nguyen & Pabst, 2020). Details on how to derive these relations from compression column tests can be seen in Essayad (2015) and Lévesque (2019). Those relations were obtained from conventional consolidation tests in conjunction with hydraulic conductivity measurements for tailings D (Somogyi, 1976).

Table 5-1: Properties and constitutive relations of various types of tailings used in the simulations.

Properties	**A**	**B** (Lévesque, 2019)	**C** (Bhuiyan et al., 2015)	**D** (Somogyi, 1976)
Unit weight (kN/m^3)	19.5	18.7	13.0	17.5
Specific gravity	2.75	2.82	2.70	3.27
Dry density (10^3kg/m^3)	1.55	1.39	0.46	1.13
Friction angle (degree)	38	36	30	39
Cohesion (kPa)	0	0	0	10
Poisson's ratio	0.28	0.28	0.33	0.27
e-σ' relation	$0.81\sigma'^{-0.06}$	$1.01\sigma'^{-0.06}$	$3.94\sigma'^{-0.10}$	$2.31\sigma'^{-0.10}$
k-*e* relation	$1.2x10^{-6}e^{4.6}$	$2.0x10^{-7}e^{3.7}$	$1.2x10^{-9}e^{4}$	$6x10^{-10}e^{5.3}$
E-σ' relation	$85.6\sigma'^{0.74}$	$35.0\sigma'^{0.91}$	$4.0\sigma'^{1.9}$	$15.9\sigma'^{0.94}$

The same waste rocks were considered for WRI in all models. WRI were assigned a linear elastic constitutive model with a high Young's modulus to represent the very high stiffness of the material (i.e., E = 500 MPa) and a Poisson's ratio of 0.277 (Bolduc & Aubertin, 2014). WRIs were assigned a hydraulic conductivity of 3 x 10^{-6} m/s (around 20 times higher than that of tailings) to facilitate the horizontal drainage of water in tailings. In practice, the hydraulic conductivity of WRI might be greater but a smaller value was chosen to reduce computational time. This is because the presence of the two materials with contrastive permeabilities in the model can significantly increase the computational time of the model (Itasca, 2021).

5.2.3 Constitutive models and update of tailings properties

Tailings properties vary with time as their void ratio decreases and the assumptions of constant properties might not be representative of the actual and non-linear behaviour of slurry materials (Somogyi, 1980; Schiffman, 1982; Townsend & McVay, 1990; Morris, 2002). Several studies have shown discrepancies between tailings consolidation simulated with assumption of constant properties and field observations. For instance, simulated consolidation rates were around 3 times faster than observation in the case of gold tailings disposed in pits (McDonald & Lane, 2010). Other examples shown that simulated consolidation magnitude of tailings columns with models using a constant stiffness could be 2 times lower than those measured from experimental tests (Nguyen & Pabst, 2022b). Various mathematical functions representing the relations effective stress - void ratio and void ratio - hydraulic conductivity for slurry tailings have been proposed. These include power function (Somogyi, 1980), extended power function (Liu & Znidarčić, 1991), logarithmic function (Bartholomeeusen et al., 2002), Weibull function and modified Kozeny–Carman equation (Mbonimpa et al., 2002; Chapuis & Aubertin, 2003). Among these, the power function is often used for its simplicity and good representativeness (Priestley, 2011; Agapito & Bareither, 2018), and was chosen in the present study to represent variation of tailings hydraulic conductivity with void ratio (table 5-1). From hydraulic conductivity relations (table 5-1), tailings A and B exhibited a reduction of around 2.5 times after the first 3 loading before continuing to decrease slightly for the next loading steps (Lévesque, 2019; Nguyen & Pabst, 2022b), while those for tailings C and D decreased by around 3 and 4 times (Somogyi, 1976; Bhuiyan et al., 2015). Young's modulus of those tailings remained relatively small at low levels of loads and non-linearly increased with the increased of

applied loads, and values of tailings A and B were usually somewhat double that of tailings D (table 5-1).

Linear elastic-perfectly plastic Mohr-Coulomb model was used to simulate tailings. The non-linear relations between e-σ', k-e and Young's modulus and effective stress of the four types of tailings followed an approach applied in FLAC3D to modify these properties and were based on relations from table 5-1. During the analysis, the value of the void ratio was updated at every iteration based on the value of effective stress, and this new value of void ratio was then used to conduct an automatic update of hydraulic conductivity and stiffness in FLAC3D. The validity and precision of continuous update of tailings properties in FLAC were presented by Zhou et al. (2019) and Nguyen and Pabst (2022b). This approach was compared with simulations using a constant saturated hydraulic conductivity.

5.3 Results

5.3.1 Effect of WRI on the dissipation of excess PWP

Simulation results indicated that WRI significantly contributed to the horizontal dissipation of PWP and therefore to the acceleration of consolidation. For example, the PWP iso-contours immediately after the addition of the 7th layer for tailings A (i.e., t = 7 years) were curved close the WRI, indicating a higher dissipation rate of PWP (figure 5-3). In other words, the dissipation of PWP close to the WRI could occur both vertically (to the surface of the TSF) and horizontally (to the WRI). Also, PWP always reached hydrostatic equilibrium at the end of each consolidation period (even for the cases without inclusions), therefore suggesting that no excess PWP remained before adding new tailings layers. Similar trends were observed for tailings B and C. The presence of WRI also contributed to accelerate tailings consolidations of tailings D, but excess PWP did not completely dissipate during the considered period and their effect was more limited compared to those for other tailings. For example, the maximum degree of consolidation, U, after the addition of the 4th layer was around 93% at 2 m from the WRI, while that reached only around 80% at 6 m from the WRI and excess PWP thus cannot fully dissipate. Such limited effect can be attributed to the relatively low hydraulic conductivity of these tailings (Newson et al., 2006; Matt, 2015; Zhang et al., 2021). Results therefore indicated that WRI effectiveness is strongly affected by the tailings' hydraulic conductivity and that

WRI for clay-like tailings might be significant in terms of improvement of the overall strength of the impoundment (Ferdosi et al., 2015b) rather than improvement of consolidation rate of tailings.

Simulations results showed that the effect of WRI on consolidation decreased rapidly with the distance from WRI (figure 5-4). For example, after the deposition of the 5th layer the degree of consolidation (at the base of the TSF, i.e., z = 0 m) for tailings A reached 95% in 13 days at 2 m from the inclusion, 34 days 14 m from the inclusion and 43 days 29 m from the inclusion (value for the case without inclusion was 45 days) (figure 5-4a). Consequently, the rate of dissipation of excess PWP was increased by over three times, but only in the direct vicinity of the inclusion. The decrease in the effect of WRI on the consolidation rate with the increase of the distance for tailings B, C, and D were also demonstrated for points at 6 m and 29 m after the placement of the 5th layer (figure 5-4b, 5-4c, 5-4d). Accordingly, the radius of influence of the WRI was estimated as the location where time t_{90} for the cases with and without WRIs were less than 5% different. For example, the radius of influence for tailings A was around 54 m when the tailings thickness was 30 m, 44 m for the thickness of 24 m and 34 m for the thickness of 18 m. The ratio between WRI's radius of influence and the thickness of tailings could be then estimated for each type of tailings (e.g., equal around 1,8 for the tailings A) (figure 5-5). This ratio for tailings B and C were around 1.8 and 2.6 at the end of the filling process (i.e., the 10th layer) respectively (figure 5-5). The WRI's zone of influence for tailings D could not be estimated from t_{90} values as excess PWP did not fully dissipate, and this value was thus estimated as the distance where the differences of U between models with and without WRI were smaller than 5%. The radius of influence in that case was around 3.4 times the thickness of tailings (figure 5-5). Boudrias (2018) estimated this value being around 2 times the tailings thickness.

The radius of influence was different for each type of tailings, but they all exhibited a similar trend, that is a rapid and strong decrease after the filling of the first four layers before becoming relatively stable (figure 5-5). The ratio between WRI's radius of influence and the thickness of tailings after the placement of the 2nd layer was around 4 for tailings A and B, 8 and 10 for tailings C and D, respectively, before decreasing to somewhat stable values when the tailings thickness was higher than 12 m (i.e., after the placement of the 4th layer) (figure 5-5). The decrease of the radius of influence during the deposition of the first few layers can be attributed to the decrease of the hydraulic conductivity of the tailings under the applied loading and the decrease of void ratio under tailings

settlement. These decreases in hydraulic conductivity of tailings can lead to the change in the hydraulic gradient and therefore possibly in the radius of influence (Hansbo et al., 1981; Indraratna et al., 2012; Han, 2015; Mbemba & Aubertin, 2021a). Models using different constant permeabilities of tailings were performed to check the influences of hydraulic gradient on the radius of influence of WRI. Results, however, showed a limited effect of the hydraulic gradient on the WRI's radius of influence. A similar trend was also observed by Bolduc and Aubertin (2014).

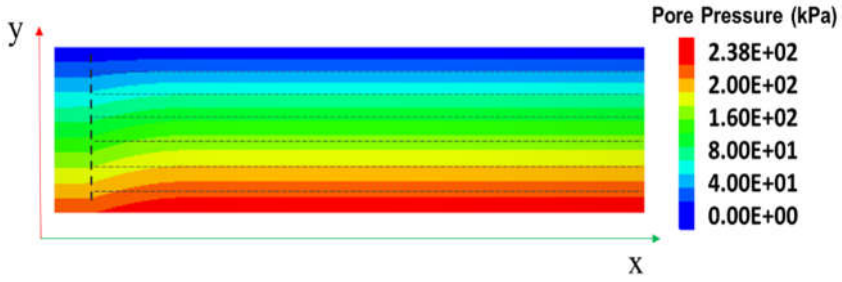

Figure 5-3: Distribution of PWP right after the placement of the 7th layer for tailings A (the vertical dashed line indicates the boundary between WRI and tailings, and the horizontal dashed line shows tailings layers).

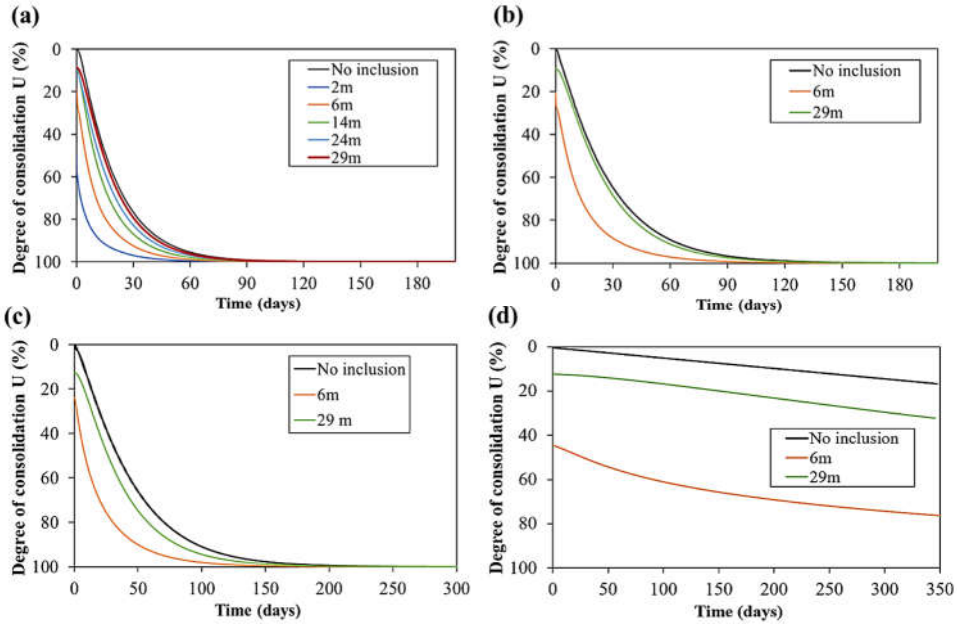

Figure 5-4: Degree of consolidation *U* (%) at various locations at the base of TSF after the deposition of the 5th layer for (a) tailings A, (b) tailings B, (c) tailings C and (d) tailings D.

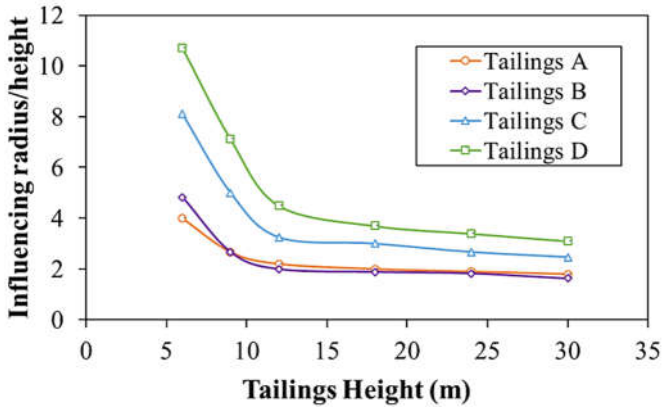

Figure 5-5: Ratio of radius of influence of WRI over the tailings thickness for various types of tailings. The influence radius was different for each type of tailings and varied during the filling process: it exhibited a significant decrease after the placement of the first few layers before tending to a relatively constant value after the thickness reached around 12 m.

Simulations also indicated using updated hydraulic conductivity values (changing with void ratio during consolidation) or constant values had a strong influence on the results. For example, the time required to reach 90% consolidation (or t_{90}) for tailings A 65 m from the inclusion after the placement of the 10th layer was 130 days for model with updated properties, 41 days with k_{sat} = 3.5 x 10^{-7} m/s, and 162 days with k_{sat} = 1.0 x 10^{-7} m/s (figure 5-6). Using updated properties, however, requires to measure hydraulic conductivity in the laboratory for various void ratios to fit a descriptive model (Bhuiyan et al., 2015; Nguyen & Pabst, 2022b), and to input the hydraulic conductivity functions in the code, which is not always convenient. In practice, using a constant value k_{sat} = 1.3 x 10^{-7} m/s yielded somewhat similar results in terms of consolidation rate which corresponded to a void ratio of 0.62 (figure 5-6). The equivalent hydraulic conductivity for tailings B and C was 1.2 x 10^{-7} and 1.1 x 10^{-7} m/s, corresponding to the void ratio of 0.87 and 3.09 respectively.

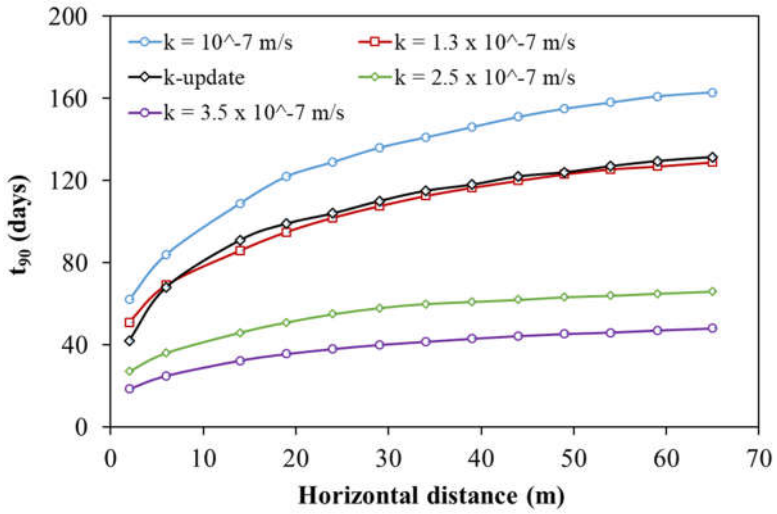

Figure 5-6: Comparison of t_{90} at the base of the TSF (tailings A) after the placement of the 10th layer as a function of the horizontal distance from the WRI and for various estimations of the hydraulic conductivity. A value of 1.3 x 10^{-7} m/s generated somewhat similar results to those obtained with the model using updated hydraulic conductivity, while a value of 3.5 x 10^{-7} m/s could yield results 3 times lower than those for models with updated hydraulic conductivity.

5.3.2 Tailings settlement

Settlements occurred as pore pressures dissipated and varied depending on tailings properties, time and distance to the WRI. For example, the total settlement of the tailings body at the end of the placement process (t = 10 years) for tailings A was around 1.67 m, around 1.65, 0.5 and 1.94 m for tailings B, C and D, respectively. The increase in displacements of layer 1 reduced with the increase of tailings thickness, which indicated that the stiffness of the materials increased under staged filling. For example, displacements in layer 1 for tailings A one year after the filling of the 3rd layer increased by around 47% but only 5 % after the placement of the 10th layer (figure 5-7). Similar trends were observed for the other tailings with the increase of displacement after the filling of the last layer was generally less than 5%. Models thus represented very well the change in the stiffness of the materials. Settlement of tailings tended to be smaller close to the WRI, which was attributed to the difference in the strength and stiffness between WRI and the tailings. Loads from the filling of tailings were, thus, partially transferred to the WRI. This depends on the modulus ratio of the WRI and surrounding tailings (Van Eekelen et al., 2013; Han, 2015) and the interface elements used in the models (Li & Aubertin, 2009b). The volume change of tailings due to the presence of WRI can then be estimated based on the settlement evolution of tailings.

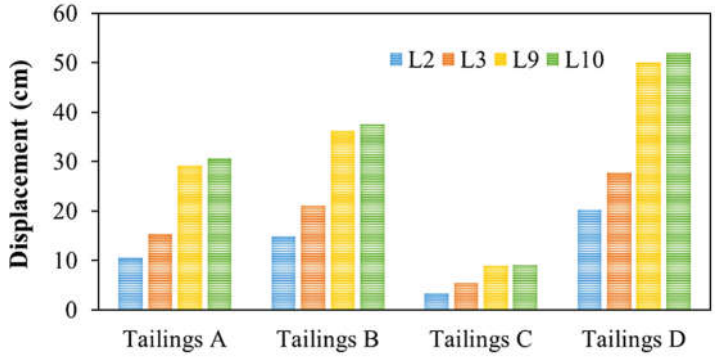

Figure 5-7: Displacements of the first layer 1 year after the addition of the 2nd, 3rd, 9th and 10th layer (noted as L2, L3, L9 and L10) for 4 types of tailings.

5.4 Results analysis

5.4.1 Volume change of tailings with the presence of WRI

The amount of volumetric compression of the tailings body resulting from the settlement of tailings (i.e., equal to the average settlement of the tailings body times the area of the TSF, which was automatically calculated using a FISH function) was estimated. Simulated results indicated that volume change always increased with time as more tailings were disposed (figure 5-8a). For example, volume change after the placement of the 2nd layer for tailings A without WRI was around 62 m^3 and increased to around 132 m^3 after the placement of the 10th layer. The changes in the slope of the curves also indicated a slower rate of volume change as tailings height increased (figure 5-8a). Tailings C had the smallest volume change (around only 40 m^3) among simulated tailings, which was explained by the smallest settlement of this type of tailings (session 3.2).

The presence of WRI can increase the consolidation rate of tailings, but they also occupy some space in the TSF. In practice, results have shown that most of the simulated tailings were fully consolidated after around 6 months. Using WRI therefore did not have a significant influence on the volume gain, but rather contributed to decrease the space available for tailings deposition. In other words, the volume of tailings that could be deposited in the TSF with the presence of WRI was always smaller than the case without WRI for all types of tailings (figure 5-8a). For example, the volume change of tailings A without WRI after the placement of the 10th layer was around 132 m^3/per 5 linear meters, i.e., around 14% more than that of model with WRI (113 m^3/ per 5 linear meters) (figure 5-8a). The difference of volume change (*DV*) between models with and without WRI was estimated as:

$$\frac{(V_t - V_w)}{V_t} * 100\%$$

Where V_t: the volume change of model with tailings only (m^3); V_w: the volume change of model with WRI (m^3).

DV tended to become relatively constant after the deposition of the first fifth layers (figure 5-8b). For instance, *DV* of tailings A decreased from 25% after the placement of the 2nd layer to 16% after the filling of the 5th layer, while that of tailings C exhibited a reduction of nearly 17% (figure 5-8b). *DV* for tailings C and D tended to be greater than those of tailings A and B. For example, *DV* for gold

tailings after the filling of the last layers were around 15%, while that for tailings C were somewhat higher, at around 20% (figure 5-8b). These differences could be explained by the difference in the stiffness evolution during compression of other types of tailings.

The additional height of the TSF required to dispose the same amount of tailings with WRI presence as without WRI can be accordingly estimated. This height can be estimated as the sum of volume occupied by WRI and total differences of volume change of tailings body between models with and without WRI divided by the area of the TSF (table 5-2). These heights were around 2.22, 2.17, 2.06 and 2.45 m for tailings A, B, C and D, respectively. In other words, the increase of thickness of the TSF was less than 8% total thickness of tailings (table 5-2). This was very meaningful for practitioners to briefly calculate the additional height of TSFs required when applying co-disposal technique (at least at the primary design stage).

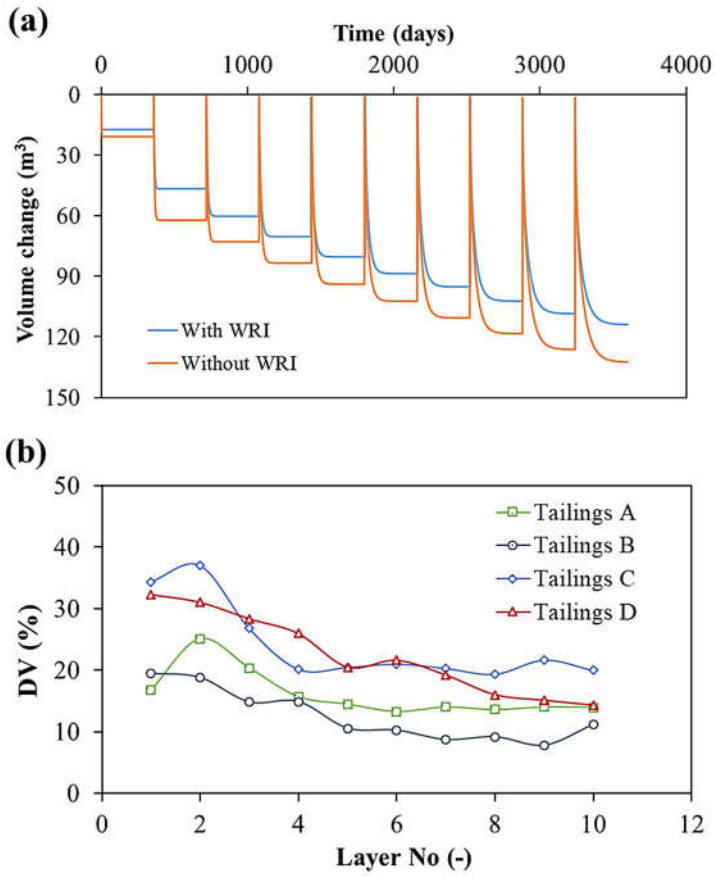

Figure 5-8: (a) Evolutions of average volume changes as a function of time resulting from tailings settlement for models with and without WRI for tailings A and (b) differences of volume change (expressed in percentage) between models with and without WRI for various types of tailings.

Table 5-2: Additional height required because of the presence of WRI in the TSF for various types of tailings

	Volume occupied by WRI (m^3)	Total volume loss* (m^3)	TSF area (m^2)	Additional height (m)
Tailings A	900	143	470	2.22
Tailings B	900	119	470	2.17
Tailings C	900	69	470	2.06
Tailings D	900	251	470	2.45

* Equal total differences of volume change resulting from tailings settlement between models with and without WRI

The ratio between volume of tailings and WRI disposed in this study was around 15.7. In practice, this ratio could widely change depending on the practical considerations of each mine sites. For example, this could depend on the primary goal of mine waste management of each mine site. Some might prioritize the volume of WRI that can be disposed to eliminate the need for the construction of waste rock piles. Coarse waste rocks might, indeed, contain sulfide minerals that can oxidize and generate acid mine drainage, and the placement of waste rock as inclusions inside the TSF could therefore efficiently contribute to prevent potential AMD generation (Jahanbakhshzadeh et al., 2019; Bussière & Guittonny, 2020). The volumes of tailings and waste rock produced by mining activities can also vary widely in practice depending on the ore body characteristic and production technique (Blight, 2010). The ratio of tailings and waste rocks volume was thus changed by changing the width of WRI in the model (i.e., from 6 m to 10, 12, 18 and 24 m corresponding to the volume ratio of 15.7, 9.0, 7.3, 4.6 and 3.2, respectively) to estimate the volume loss as a function of the quantity of waste rocks used in the TSF as inclusions. In general, the more volume of WRI placed in the pit, the less space dedicated for tailings that can be stored in the TSF (figure 5-9). For example, the *DV* values of tailings A for model with WRI width of 24 m was around 30 % which was nearly 2 times higher than

that of the model with WRI width of 6 m. The same trend was recorded for tailings B and C (figure 5-9). The trend of tailings A and B was somewhat similar to each other, while *DV* for tailings C seemed to be higher than those of tailings A and B. Accordingly, equations presenting the evolution of *DV* with the changes in the volume ratio of tailings and WRI were derived as: $DV = 49.6\frac{V_{tailings}}{V_{WRI}}^{-0.48}$ ($R^2 = 0.97$) for tailings A, $DV = 55.6\frac{V_{tailings}}{V_{WRI}}^{-0.58}$ for tailings B ($R^2 = 0.99$) and $DV = 56.8\frac{V_{tailings}}{V_{WRI}}^{-0.39}$ ($R^2 = 0.980$) for tailings C. These results can, thus, provide practitioners with a brief estimation (at least for the primary design stage) the potential volume of tailings that might be loss due to the presence of WRI for various volume ratios.

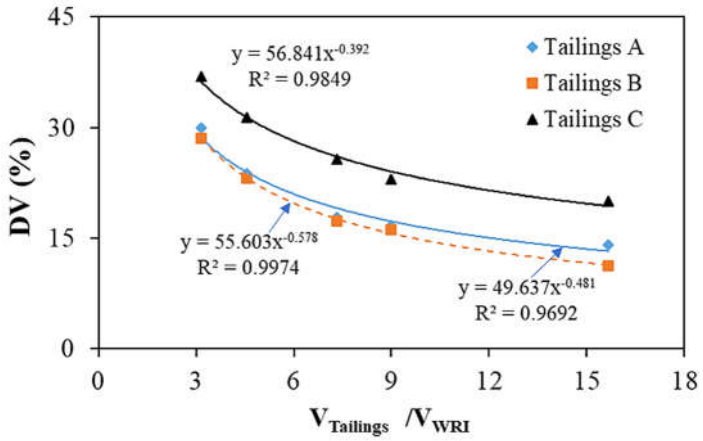

Figure 5-9: Evolution of DV with the ratio of volume of tailings and WRI in the TSF. Calculations assumed that the displacement at the boundary interface is zero and the width of the tailings part was large enough to reduce the effect of TSF sides.

5.4.2 Effect of the filling rate

TSF depth and deposition rates vary with mine size, production rate and type of operations (surface or underground) (Blight, 2010; MEND, 2015). Filling rate for TSF at Malartic mine is, for example, around 3 m per year (Boudrias, 2018), and between 2 m and 14 m per year at Rabbit Lake mine (MEND, 2015). Additional simulations corresponding to 6 and 9 m/year filling rate were therefore

carried out for tailings A to evaluate effects of tailings thickness on the evolution of tailings consolidation with the presence of WRI. Filling rate seemed to have a negligible effect on the volume change between the cases with and without WRI, which remained around 14% at the end of the filling process for all models regardless of layer thickness (figure 5-10a).

A ratio $R_{t90,}$ i.e., the ratio of t_{90} between models with and without WRI, was introduced to represent the effect of filling rate on the consolidation rate of tailings (figure 5-10b). The effect of WRI on the consolidation rate was increased for greater filling rates, which indicated that the use of WRI would be more beneficial with higher filling rate in practice. R_{t90} at 10 m from the WRI after the deposition of the 6th layer was 1.45, 1.70 and 1.83 for the 3-m, 6-m and 9-m thick models respectively (figure 5-10b). The ratio also increased with the number of tailings layers. This ratio was, for example, around 1.46 and 1.54 for the 6-m thick model after the placement of the 2nd and 4th layer (figure 5-10b).

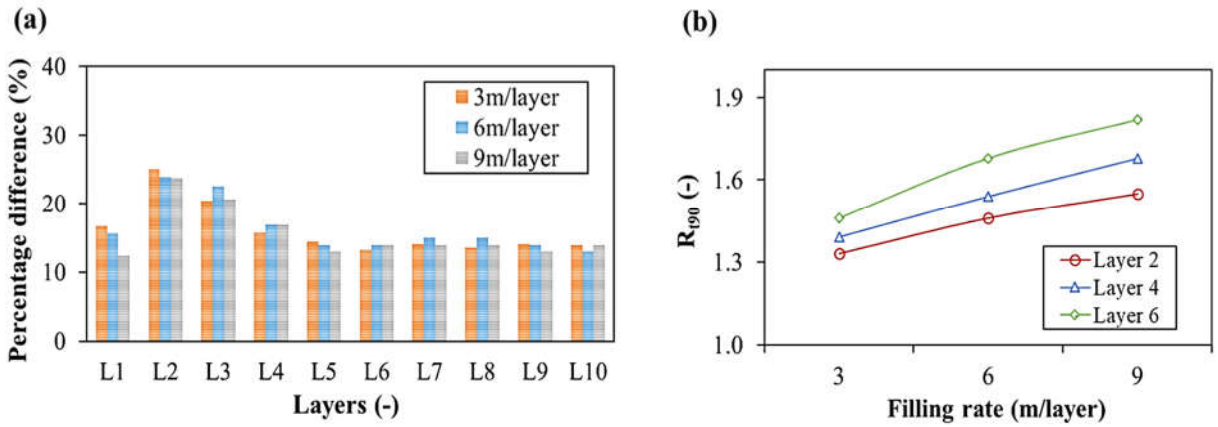

Figure 5-10: (a) DV values for models with various filling rates and (b) R_{t90} values for the point located at 10 m from WRI at the TSF base after the placement of the 2nd, 4th and 6th layer for models of 3-m, 6-m and 9-m thick layers for tailings A.

Models with 3 m/year but with different filling scheme instead of an instantaneously adding (i.e., layer of 1.5 m per 6 months and layer of 1 m per 4 months, respectively) were performed for tailings A to evaluate the potential effect of the assumption of an instantaneous filling scheme on the rate of

consolidation of tailings. Simulated results indicated that the effect of instantaneous filling on the rate of consolidation of tailings was insignificant. It took essentially the same amount of time with such filling intervals to dissipate 90% of excess PWP (see Appendix E). The same trend was also observed by Boudrias (2018).

5.5 Discussions

WRI can contribute to accelerate the rate of consolidation of tailing but also reduces the volume available for tailings storage at the same time. The geometry of the TSF in this study and the configuration of the WRIs were simplified, and the results can be applied for the relatively simple geometry TSFs. This paper only dealt with one row of inclusion, while there might be several orthogonal inclusions (not only parallel inclusions) installed for the typical design of WRIs in TSFs (Aubertin et al., 2016). Other simulations on the more complex geometries of the TSFs and various permeable conditions (i.e., only central WRI was considered in this study) can be further performed to evaluate their influences on the evolution of tailings consolidation.

The models carried out with various types of tailings highlighted the importance of the constitutive relations describing the changes in the consolidation properties of tailings, which are unique for each type of tailings. For example, the relations for the tailings C were derived from large strain consolidation tests with pressure up to 8 kPa (Bhuiyan et al., 2015). In practice, the loads resulting from the filling of tailings might be significantly higher, and the change in the hydraulic conductivity and stiffness of tailings might become less non-linear when the applied loadings increase. Tests covering the actual range of pressures that are expected in the field are therefore recommended to improve the accuracy of constitutive relations.

Models with several values of constant Young's modulus of tailings were performed for tailings A to test the effect of stiffness differences on the influence of WRI on the settlement of tailings materials. In general, the higher the stiffness of tailings, the smaller zone of influence of WRI. Also, tailings settlement simulated close to the WRI may be affected by the interface element used in this numerical study. The interface elements introduced in the simulations might not necessarily represent the real contact between WRI and tailings in practice. It is recommended that stiffness and frictions angles of the contact interface between these two materials should be estimated to improve the

precision of the calculation. Despite these boundary effects, general behaviours are expected to remain similar (Li & Aubertin, 2009b; Yang, 2016). Finally, field-scale investigations would be required to validate or calibrate the numerical results and the upscaling of the approach in this study.

5.6 Conclusion

An investigation on the effect of a drainage system composed of WRI on the consolidation behaviour of several types of tailings in a simple TSF were numerically performed using FLAC3D. Simulations were conducted considering continuously updating properties of tailings under sequential filling. Several practical considerations related to the operational aspects that could have effect on the settlement of tailings were also evaluated. Results including excess PWP dissipation rate and magnitude of consolidation were compared, bringing the following conclusions:

WRI had a significant effect on the acceleration of PWP dissipation and thus on tailings consolidation rate. The effect of WRI depended on the distance and the thickness of the tailings. PWP always reached the hydrostatic value at the end of each filling stage for tailings A, B and C, while excess PWP in tailings D were not fully dissipated after one year because of their relatively low hydraulic conductivity.

Significant differences (up to 3 times) were observed when using a model with updated properties or with constant properties. Equivalent constant values of hydraulic conductivity were derived for these types of tailings, which can bring about an acceptable tolerance of t_{90} compared to the model with updated properties, reducing the computational efforts and the necessity of laboratory tests on non-linear evolution of tailings' properties. These values, however, aimed to provide practitioners with a recommended value for the same materials under the same loading and boundary conditions. Other types of tailings with other loading/boundary conditions would require performing the simulation with the proposed approach again.

The zone of influence of WRI was different for each type of tailings, decreasing significantly during the filling of the first few layers before remaining relatively constant after the thickness of tailings reached 12 m. The zone of influence was usually a function of the thickness of the tailings, around 1.8 times tailings thickness for tailings A and B, 2.6 for tailings C and 3.4 for tailings D respectively. Settlement of tailings C was smallest, while largest value was observed for the tailings D. Changes

in the tailings settlement was less pronounced after the placement of few last layers which demonstrated very well the increases in the stiffness of the materials during the consolidation process.

The volume change due to the settlement of tailings of model with only tailings was always greater than that of model with WRI for all types of tailing. In other words, the use of WRI decreased the volume available for the storage of tailings in the TSF, despite the acceleration of their consolidation. Additional height required when applying WRI was less than 8% of the total thickness of tailings. *DV* for tailings A, B and D after the filling of the last layers were around 15%, while that for tailings C was around 20%.

Space available for tailings to be stored in the TSF was lower with the increase of volume of WRI placed in the TSF, and formulations estimating evolution of *DV* with the changes in the volume ratio of tailings and WRI were proposed. Increase of the filling rate led to a more pronounced influence of WRI on the consolidation rate of tailings but had a negligible effect on the *DV* values. Finally, 3D effects because of complex drainage paths and permeable conditions are being investigated in an on-going project in the group.

5.7 Acknowledgements

The authors are thankful to the financial support from NSERC, FRQNT and partners of Research Institute on Mines and the Environment (RIME UQAT - Polytechnique; http://rime-irme.ca/en). The authors also gratefully acknowledge Dr. Huy Tran, Dr. Kazim and Itasca technical support team for their valuable support and comments to improve the code in this study.

5.8 References

Agapito, L. A., & Bareither, C. A. (2018). Application of a one-dimensional large-strain consolidation model to a full-scale tailings storage facility. *Minerals Engineering, 119*, 38-48. https://doi.org/https://doi.org/10.1016/j.mineng.2018.01.013

Aubertin, M. (2013). *Waste rock disposal to improve the geotechnical and geochemical stability of piles.* 23rd World Mining Congress, Montreal, Canada.

Aubertin, M. (2018). *Waste rock inclusions in tailings impoundment: analysis (and design) based on the Canadian Malartic Mine.* Mines and the environment, Rouyn Noranda, Quebec, Canada.

Aubertin, M., Bussière, B., Pabst, T., James, M., & Mbonimpa, M. (2016). *Review of reclamation techniques for acid generating mine wastes upon closure of disposal sites.* Geo-Chicago 2016, Chicago, Illinois, USA. https://doi.org/10.1061/9780784480137.034

Azam, S., & Li, Q. (2010). Tailings Dam Failures: A Review of the Last One Hundred Years. *Geotechnical news, 28*, 50-53. https://ksmproject.com/wp-content/uploads/2017/08/Tailings-Dam-Failures-Last-100-years-Azam2010.pdf

Bartholomeeusen, G., Sills, G. C., Znidarčić, D., Kesteren, W. V., Merckelbach, L. M., Pyke, R., . . . Chan, D. (2002). Sidere: numerical prediction of large-strain consolidation. *Géotechnique, 52*(9), 639-648. https://doi.org/10.1680/geot.2002.52.9.639

Bhuiyan, I., Azam, S., & Landine, P. (2015). Consolidation Behavior of a Uranium Tailings Storage Facility in Saskatchewan. *Journal of Hazardous, Toxic, and Radioactive Waste, 19*(4), 040150051-040150057. https://doi.org/doi:10.1061/(ASCE)HZ.2153-5515.0000281

Blight, G. E. (2010). *Geotechnical engineering for mine waste storage facilities*. CRC Press.

Bolduc, F., & Aubertin, M. (2014). Numerical investigation of the influence of waste rock inclusions on tailings consolidation. *Canadian Geotechnical Journal, 51*(9), 1021-1032. https://doi.org/10.1139/cgj-2013-0137

Boudrias, G. (2018). *Évaluation numérique et expérimentale du drainage et de la consolidation de résidus miniers à proximité d'une inclusion de roches stériles* [Mémoire de maîtrise, École Polytechnique de Montréal].

Bussière, B., & Guittonny, M. (2020). *Hard Rock Mine Reclamation From Prediction to Management of Acid Mine Drainage*. CRC Press.

Chapuis, R. P., & Aubertin, M. (2003). On the use of the Kozeny - Carman equation to predict the hydraulic conductivity of soils. *Canadian Geotechnical Journal, 40*(3), 616-628. https://doi.org/10.1139/t03-013

Coffin, J. (2010). *A 3D Model for Slurry Storage Facilities. Boulder, Colorado* [Ph.D., University of Colorado].

Das, B. (2010). *Principles of Geotechnical engineering*. Cengage Learning.

Essayad, K. (2015). *Développement de protocoles expérimentaux pour caractériser la consolidation de résidus miniers saturés et non saturés à partir d'essais de compression en colonne* [Mémoire de maîtrise, École Polytechnique de Montréal].

Ferdosi, B., James, M., & Aubertin, M. (2015a). Effect of waste rock inclusions on the seismic stability of an upstream raised tailings impoundment: a numerical investigation. *Canadian Geotechnical Journal, 52*(12), 1930-1944. https://doi.org/10.1139/cgj-2014-0447

Ferdosi, B., James, M., & Aubertin, M. (2015b). Investigation of the Effect of Waste Rock Inclusions Configuration on the Seismic Performance of a Tailings Impoundment. *Geotechnical and Geological Engineering, 33*(6), 1519-1537. https://doi.org/10.1007/s10706-015-9919-z

Fredlund, M., Donaldson, M., & Chaudhary, K. (2015). *Pseudo 3-D deposition and large-strain consolidation modeling of tailings deep deposits.* Tailings and Mine Waste, Vancouver, BC.

Han, J. (2015). *Principles and Practice of Ground Improvement*. Wiley.

Hansbo, S., Jamiolkowski, M., & Kok, L. (1981). Consolidation by vertical drains. *Géotechnique, 31*(1), 45-66. https://doi.org/10.1680/geot.1981.31.1.45

Indraratna, B., Rujikiatkamjorn, C., Balasubramaniam, A. S., & McIntosh, G. (2012). Soft ground improvement via vertical drains and vacuum assisted preloading. *Geotextiles and Geomembranes, 30*, 16-23. https://doi.org/https://doi.org/10.1016/j.geotexmem.2011.01.004

Itasca. (2021). *FLAC3D 7.0 (Fast Lagrangian Analysis of Continua in 3 Dimensions) User Manual*. Itasca Consulting Group, Inc.

Jahanbakhshzadeh, A., Aubertin, M., Yniesta, S., & Zafarani, A. (2019). *On the seismic response of tailings dikes constructed with the upstream and center-line methods.* 72nd Canadian Geotechnical Conference (GEO 2019), St. John's, Canada.

James, M. (2009). *The use of waste rock inclusions to control the effects of liquefaction in tailings impoundments* [Ph.D. , École Polytechnique de Montréal].

Jaouhar, E. M., Aubertin, M., & James, M. (2013). *The effect of tailings properties on their consolidation near waste rock inclusions.* 66th Canadian Geotechnical Conference (GeoMontréal 2013), Montréal, Canada.

Lévesque, R. (2019). *Consolidation des résidus miniers dans les fosses en présence d'inclusions de roches stériles* [Mémoire de maîtrise, Ecole Polytechnic Montreal].

Li, L., & Aubertin, M. (2009). Numerical Investigation of the Stress State in Inclined Backfilled Stopes. *International Journal of Geomechanics, 9*(2), 52-62. https://doi.org/doi:10.1061/(ASCE)1532-3641(2009)9:2(52)

Liu, J. C., & Znidarčić, D. (1991). Modeling One Dimensional Compression Characteristics of Soils. *Journal of Geotechnical Engineering, 117*(1), 162-169. https://doi.org/10.1061/(ASCE)0733-9410(1991)117:1(162)

Matt, G. (2015). *Geotechnical Characterization of Bauxite Residue* [Ph.D., The University of Texas at Austin].

Mbemba, F., & Aubertin, M. (2021a). Physical and numerical modelling of drainage and consolidation of tailings near a vertical waste rock inclusion. *Canadian Geotechnical Journal, 0*(0), 1-14. https://doi.org/10.1139/cgj-2020-0372

Mbemba, F., & Aubertin, M. (2021b). Physical Model Testing and Analysis of Hard Rock Tailings Consolidation Considering the Effect of a Drainage Inclusion. *Geotechnical and Geological Engineering, 39*(4), 2777-2798. https://doi.org/10.1007/s10706-020-01656-0

Mbonimpa, M., Aubertin, M., Chapuis, R. P., & Bussière, B. (2002). Practical pedotransfer functions for estimating the saturated hydraulic conductivity. *Geotechnical & Geological Engineering, 20*(3), 235-259. journal article. https://doi.org/10.1023/a:1016046214724

McDonald, L., & Lane, J. C. (2010). *Consolidation of in-Pit tailings.* Mine Waste 2010, Perth, Australia (pp. 49-62).

MEND. (2015). MEND Report 2.36.1 In-Pit Disposal of Reactive Mine Wastes: Approaches, Update and Case Study Results.

Morgenstern, N., Vick, S., Viotti, C., & Watts, B. (2016). *Report on the Immediate Causes of the Failure of the Fundão Dam. Fundão Tailings Dam Review Panel*.

Morris, P. H. (2002). Analytical Solutions of Linear Finite-Strain One-Dimensional Consolidation. *Journal of Geotechnical and Geoenvironmental Engineering, 128*(4), 319-326. https://doi.org/doi:10.1061/(ASCE)1090-0241(2002)128:4(319)

Newson, T., Dyer, T., Adam, C., & Sharp, S. (2006). Effect of Structure on the Geotechnical Properties of Bauxite Residue. *Journal of Geotechnical and Geoenvironmental Engineering, 132*(2), 143-151. https://doi.org/doi:10.1061/(ASCE)1090-0241(2006)132:2(143)

Nguyen, D., & Pabst, T. (2020). *Comparative experimental study of consolidation properties of hard rock mine tailings.* 73rd Canadian Geotechnical Conference (GeoVirtual 2020), Online.

Nguyen, D., & Pabst, T. (2022). Numerical study of slurry tailings consolidation considering continuous update of material properties. *International Journal of Mining Science and Technology (Under reviewed)*.

Pépin, N., Aubertin, M., & James, M. (2012). Seismic table investigation of the effect of inclusions on the cyclic behaviour of tailings. *Canadian Geotechnical Journal, 49*(4), 416-426. https://doi.org/10.1139/t2012-009

Priestley, D. (2011). *Modeling multidimensional large strain consolidation of tailings* [Master, University of British Columbia].

Robertson, P. K., Lucas de Melo, David J. Williams, & Wilson., G. W. (2019). *Report of the Expert Panel on the Technical Causes of the Failure of Feijão Dam I.*

Schiffman, R. L. (1982). The consolidation of soft marine sediments. *Geo-Marine Letters, 2*(3-4), 199-203. https://doi.org/10.1007/bf02462763

Shahsavari, M., & Grabinsky, M. (2015). *Mine backfill porewater pressure dissipation: numerical predictions and field measurements.* 68th Canadian Geotechnical Conference (GeoQuébec 2015), Québec, Canada.

Somogyi, F. (1976). *Dewatering And Drainage Of Red Mud Tailings* [Ph.D., University of Michigan].

Somogyi, F. (1980). *Large Strain Consolidation of Fine Grained Slurries.* Presentation at the Canadian Society for Civil Engineering, Winnipeg, Manitoba.

Townsend, & McVay. (1990). SOA: Large Strain Consolidation Predictions. *Journal of Geotechnical Engineering, 116*(2), 222-243. https://doi.org/doi:10.1061/(ASCE)0733-9410(1990)116:2(222)

Van Eekelen, S. J. M., Bezuijen, A., & van Tol, A. F. (2013). An analytical model for arching in piled embankments. *Geotextiles and Geomembranes, 39*, 78-102. https://doi.org/https://doi.org/10.1016/j.geotexmem.2013.07.005

Vick, S. G. (1990). *Planning, Design and Analysis of Tailings Dams*. BiTech Publishers Ltd.

Yang, P. (2016). *Investigation of the geomechanical behavior of mine backfill and its interaction with rock walls and barricades* [Ph.D., École Polytechnique de Montréal].

Zhang, J., Yao, Z., Wang, K., Wang, F., Jiang, H., Liang, M., . . . Airey, G. (2021). Sustainable utilization of bauxite residue (Red Mud) as a road material in pavements: A critical review. *Construction and Building Materials, 270*, 121419. https://doi.org/https://doi.org/10.1016/j.conbuildmat.2020.121419

Zhou, Amodio A, & N., B. (2019). *Informed mine closure by multi-dimensional modelling of tailings deposition and consolidation.* Mine Closure 2019, Perth, Australia.

CHAPTER 6 ARTICLE 3: ACCELERATION OF CONSOLIDATION OF TAILINGS IN A PIT USING WASTE ROCKS CO-DISPOSAL

Ngoc Dung Nguyen, Thomas Pabst

Article submitted to the Bulletin of Engineering Geology and the Environment in August 2022

ABSTRACT

The co-disposition of tailings and waste rocks as a permeable envelope or waste rock inclusions (WRI) in an open pit can be beneficial for mine waste management and contribute to prevent transport of contaminants from tailings to the local groundwater. These drainage paths could also affect the tailings consolidation behaviour and contribute to the acceleration of the tailings settlement rate and should therefore be considered to optimize in-pit disposal. Coupled numerical models were run to examine the evolution of tailings consolidation under the influences of co-disposed waste rocks. Various disposal scenarios were investigated, including the presence of a permeable envelop only and the addition of WRI as a central inclusion. The influences of operational and practical aspects such as the tailings filling rate, pit slope angles, waste rock and tailings hydro-geotechnical properties, and pit morphology were investigated. Results indicated that a permeable envelope could promote the dissipation of excess pore water pressure (PWP) and accelerate tailings consolidation. The influence zone of the permeable envelope was relatively limited and around 2 times the tailings height. Using a WRI combined with a permeable envelope could therefore be geotechnically beneficial for wide pits whose radius was larger than twice of its depth. Slope angles, filling rate and pit morphology somewhat affected tailings consolidation rate, but their effect was relatively limited and decreased with the increase in the distance to the drainage paths. Finally, co-disposal of tailings and waste rocks seems relevant for fine tailings with low hydraulic conductivity.

Keywords: co-disposal, permeable envelopes, waste rocks, consolidations, pit slopes, pit morphology

6.1 Introduction

The continuously increasing demand for natural resources and minerals has induced a significant increase of the volume of tailings produced by mining operations , therefore also increasing the risks for major failures events of surface tailings storage facilities (TSFs), and encouraging practitioners to find alternative approaches for tailings disposal (Vick, 1990; Blight, 2010). Innovative integrated mine waste managements techniques include tailings dewatering (Bolduc & Aubertin, 2014; Bhuiyan et al., 2015; Abdulnabi et al., 2022), valorization and reuse of mine waste in cover systems (Pabst et al., 2018; Larochelle et al., 2019), or tailings and waste rocks mixing (Wickland et al., 2006; Aubertin, 2013). Tailings can also be backfilled either in underground stopes (Li & Aubertin, 2009a; Cui & Fall, 2016) or disposed in open pits (Cameron & Dave, 2015). Underground backfilling can contribute to the reduction of mineral dilution (Blight, 2010), improve stability of the operations by providing secondary support (Li & Aubertin, 2009a; Yang, 2016), reduce exposure of tailings to oxygen (and therefore reduce risks for acid mine drainage generation) (Benzaazoua et al., 2004), and reduce the area required for surface disposal (Fahey et al., 2010; Jahanbakhshzadeh et al., 2019). In-pit disposal is also considered an alternative deposition approach for surface mines, and presents many advantages both in terms of environmental, physical and social aspects (McDonald & Lane, 2010; Aubertin, 2013; Bhuiyan et al., 2015; Cameron & Dave, 2015). For example, pit backfill can contribute to stabilize pit walls and reduce long-term management and maintenance costs compared to conventional surface disposal sites (Cameron & Dave, 2015; MEND, 2015). Once backfilled, the pit can also be reclaimed using engineered cover systems to prevent contaminated mine drainage generation and facilitate its integration into the surrounding landscape (McDonald & Lane, 2010). Also, in pit disposal reduces the risk of dam failure (MEND, 2015). However, in-pit disposal is also facing several challenges and unknowns that somewhat limit its applications. For example, preventing environmental contamination can be complex when there is a direct contact between groundwater and backfilled wastes, especially because pit walls are usually strongly disturbed by blasting during operations and therefore become relatively permeable (Cameron & Dave, 2015; Rousseau, 2021). Reclamation construction also requires that tailings settlement to be completed to avoid long-term differential deformation of cover systems (and thus a decrease or even loss of performance (McDonald & Lane, 2010).

The concept of an engineered pervious envelope surrounding the tailings mass was first proposed to control potential environmental contamination by directing the groundwater around the tailings (instead of flowing through them), thus limiting the interactions between groundwater and potential contaminants (e.g., processed pore water or reactive minerals) (MEND, 2015). This can be achieved by placing a more permeable material compared to tailings around the perimeter and at the bottom of the pit (Bhuiyan et al., 2015). The pervious surround is often made of sand or coarse materials (Cameron & Dave, 2015) but using non acid-generating waste rock can be a more advantageous solution. Indeed, waste rocks have adequate properties, and their valorization on site contributes to decrease the volumes of waste rock to be disposed of on the surface (thus also reducing costs and risks) (Jahanbakhshzadeh et al., 2019; Lévesque, 2019). The permeable envelope concept could also contribute to accelerate tailings consolidations which might offer further benefits such as the reduction of long-term displacements, a better control of deposition, and the possibility to undertake progressive reclamation (McDonald & Lane, 2010; Lévesque, 2019). Drainage pathways inside the backfilled pit could also contribute to further improve the behaviour of a permeable envelope. For example, waste rock inclusions (WRI) were initially developed for surface TSFs, where they can promote dissipation of excess pore water pressure (PWP), accelerate tailings consolidations and improve static and dynamic stability of tailings dams (Aubertin, 2013; Ferdosi et al., 2015b). WRI were also shown beneficial to increase the performance of a permeable envelope if they are built across the pit and in the direction of the regional flow (Rousseau, 2021). The application of permeable envelope, potentially coupled with WRI, might therefore facilitate the long-term management of mine wastes in pits.

These benefits remain, however, theoretical as the technique has never been used for that purpose in the field. The advantages and potential limitations of tailings co-disposal with permeable envelope and/or WRI thus need to be evaluated in more details before it can be implemented into practice. Several factors influencing the effectiveness of the technique also need to be considered, including the overall slope angles of the pit, variable tailings filling rate (the width of a pit increasing with its elevation, the filling rate will thus decrease during backfilling, assuming a constant production), tailings and waste rocks hydro-mechanical properties, WRI design, and the morphology of the pit. The objective of this research was, therefore, to quantitatively evaluate the effects of a permeable envelope and various co-disposal scenarios on the evolution of tailings consolidation in an open pit

using 3-D simulations carried out with the code FLAC3D (Itasca, 2021). Results in terms of PWP evolution and degree of consolidation were compared to give recommendations to optimize the approach.

6.2 Methodology

6.2.1 Conceptual models

A 320 m wide × 620 m long × 60 m deep pit, inspired by a real pit in Quebec, Canada, was considered and simulated using FLAC3D (Itasca, 2021). The pit usually exhibits somewhat circular corners in practice which was simplified as an orthogonal geometry in these models (i.e., parallelepipedal pit). The effect of this assumption would be discussed later. Considering the symmetry axes, only one fourth of the pit was modelled to reduce computational time without decreasing mesh size nor simulation precision (i.e., around 39 000 zones instead of almost 160 000 zones for a full pit model) (figure 6-1). The domains were discretized using a hexahedral mesh resulting from the built-in blocks in the software. The angle of the pit wall was 51°, which was slightly smaller than usual slopes in practice (Utili et al., 2022), but this value also aimed to increase the mesh size of the simulated domain. The pit wall is usually constructed with several benches, yet the influences of these benches would be neglected in the case a permeable envelope was constructed, and these benches therefore were not simulated in the models.

Various disposal scenarios were simulated (table 6-1 and figure 6-1). Case 1 was the base case scenario, considering the regular deposition of 5 m thick saturated tailings in 12 layers over 12 years for a total height of 60 m. Each layer was deposited instantly, i.e., 5 m at once every year. This was corresponding to a production rate of about 1.3 million m^3 of tailings per year, which is somewhat similar to the rate from a mine with a high production rate (Blight, 2010). The second case simulated the situation where tailings were co-disposed with an 8-m wide permeable envelope made of coarse waste rock and placed progressively as the tailings were deposited. In the third case, a bottom drainage layer made of coarse waste rocks 5 m thick was added to the permeable envelope, thus representing the typical design of the method in practice. In the fourth case, a WRI alone was considered, placed in the centre of the pit. The WRI has the thickness of 16 m with the same height as the tailings, and there was no interface element used between WRI, permeable envelope and

tailings. For simplicity, WRI was represented as parallelepipeds instead of the typical trapezes usually constructed in practice. This assumption had, however, no influence on the results and could actually contribute to reduce numerical instabilities (Bolduc & Aubertin, 2014).

Cases combining the permeable envelope, the bottom drainage and the WRI were performed with the tailing thickness of 60 m, 65 m, 70 m, 75 m, and 80 m corresponding to the case 5, 6, 7, 8 and 9 respectively. Rock wall and bottom drain were constructed first, while permeable envelope and WRI were constructed and raised at the same time with tailings. Comparision between deposition scenarios was conducted in terms of tailings consolidation rate, in particular along section A-A' (in the middle of the pit at y = 160 m) and section B-B' (in the middle of the pit at x = 80m) (figure 6-1).

Regarding the parametric analysis, the effects of benches would be negligible when the permeable envelope was constructed, but the overall slopes of the pit wall might affect the consolidation of tailings because of the changes in the length to the drainage paths (figure 6-1). The overall slope angles of the pit with the depth smaller than 100 m can reach up to 70° (Utili et al., 2022), simulations with slopes of the rock walls being 60° and 70° corresponding to cases 10 and 11 respectively were, thus, performed to examine the effect of slope angles on the tailings consolidation when applying permeable envelope concept. Simulations where layer thickness of the first two layers was 7.5 and 10 m respectively (thickness of other following layers were still 5 m) were also carried out (i.e., cases 12 and 13 respectively). These rates were chosen to investigate the potential effects of changes in the filling rate due to change in the pit surface on the evolution of consolidation of tailings.

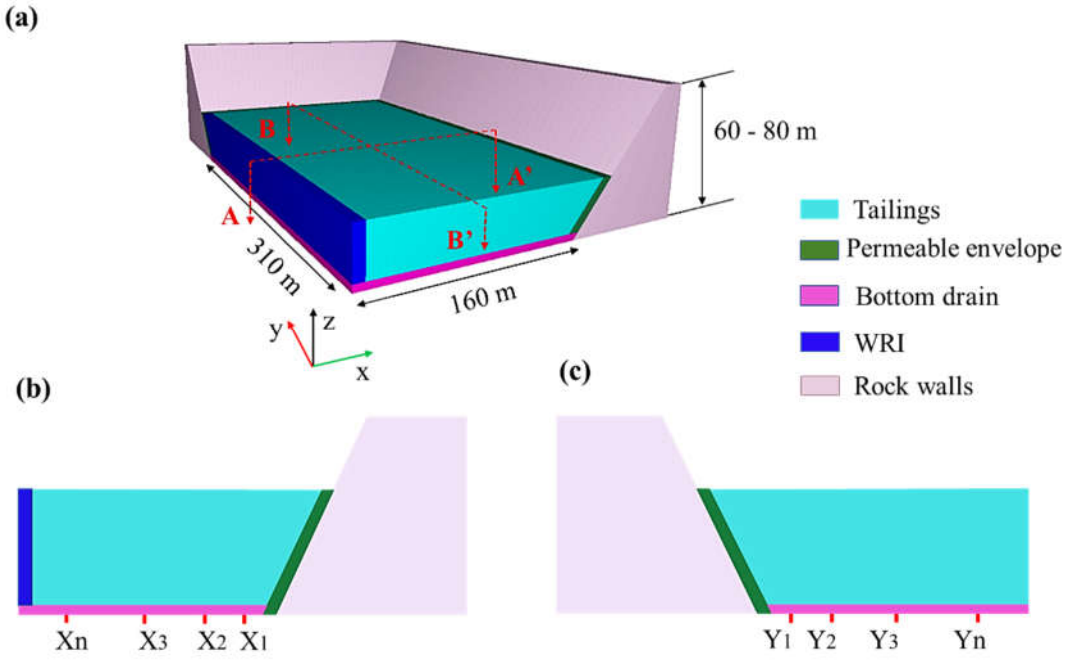

Figure 6-1: General view of (a) one fourth of the pit; (b) and (c) cross section A-A’ and B-B' respectively with monitoring points at various distances from the drainage paths.

Table 6-1: Simulated disposition scenarios to investigate the effect of various co-disposal approaches.

	Permeable Envelope	WRI	Bottom drainage	Tailings thickness (m)	Pit slope angle (°)	Thickness of the first 2 layers (m)
Case 1	No	No	No	60	51	5
Case 2	Yes	No	No	60	51	5
Case 3	No	Yes	No	60	51	5
Case 4	Yes	No	Yes	60	51	5
Case 5	Yes	Yes	Yes	60	51	5
Case 6	Yes	Yes	Yes	65	51	5
Case 7	Yes	Yes	Yes	70	51	5
Case 8	Yes	Yes	Yes	75	51	5
Case 9	Yes	Yes	Yes	80	51	5
Case 10	Yes	No	No	60	60	5
Case 11	Yes	No	No	60	70	5
Case 12	Yes	No	No	60	51	7.5
Case 13	Yes	No	No	60	51	10

6.2.2 Material properties

The gold mine tailings simulated in this study were sampled from Malartic mine site, an open pit gold mine located in Quebec Province, and classified as low plasticity silts (ML) (ASTM D2487-17, 2017) (Nguyen & Pabst, 2022b). Malartic tailings were characterized in the laboratory (table 6-2). Value of D_{60} (the diameter corresponding to 60% passing in the particle-size distribution curve) was around 0.04 mm, and the value of D_{10} (the diameter corresponding to 10% passing in the particle-size distribution curve) was around 0.0035 mm, leading to a coefficient of uniformity C_u ($C_u = D_{60} / D_{10}$) around 11.5 (figure 6-2). Tailings dry density was 1.55 tone/m^3. A friction angle of 38° was measured using triaxial test and tailings were considered cohesionless (Boudrias, 2018). Initial porosity of tailings was 0.437, and Poisson's ratio (estimated from internal friction angle) was 0.28.

Initial stiffness and hydraulic conductivity were estimated as 2.2 x 10^{-7} m/s and this value was typical for hard rock mine tailings (Bussière, 2007). However, stiffness and hydraulic conductivity of slurry tailings vary as their void ratio decreases and assuming constant properties in the simulations might not be representative of their actual non-linear behaviour (Somogyi, 1980; Schiffman, 1982; Townsend & McVay, 1990; Morris, 2002). Various mathematical formulas relating void ratio with effective stress and hydraulic conductivity with void ratio have been proposed for slurry tailings (Priestley, 2011; Agapito & Bareither, 2018; Nguyen & Pabst, 2022b). In this study, the power function was chosen for its simplicity and good representativeness (Nguyen and Pabst, 2022b).

Linear elastic-perfectly plastic Mohr-Coulomb model (MC) was first assigned for tailings. Stiffness and hydraulic conductivity of tailings in Mohr-Coulomb model were modified based on non-linear relations between e-σ', k-e and Young modulus - effective stress obtained from compression column tests on the same tailings materials (Nguyen and Pabst (2022b)). Void ratio was updated based on effective stress following the equation of $e = 0.814\ x\ \sigma'^{-0.058}$, while the relation of hydraulic conductivity and void ratio was expressed as $k = 1.24\ x\ 10^{-6}\ e^{4.61}$. Finally, Young modulus was updated based on the following equation $E = 85.6\ x\ \sigma'^{0.74}$. During the simulations, void ratio was updated every iteration based on the value of effective stress, followed by an automatic update of hydraulic conductivity and stiffness. These modifications on the Mohr–Coulomb constitutive model's properties were executed via FISH in FLAC3D (Nguyen & Pabst, 2022b).

The permeable envelope and WRI were assumed to be made of the same coarse waste rock and to have homogenous and similar properties in all the models. Waste rock materials were simulated using a simple linear elastic constitutive model with a high Young modulus to represent a very stiff material (E = 500 MPa) and a Poisson's ratio of 0.277 (Bolduc & Aubertin, 2014). Waste rocks were assigned a hydraulic conductivity of 2 x 10^{-6} m/s (i.e., around 20 times greater than that of tailings). This value is significantly lower than the usual hydraulic conductivity of waste rocks which commonly ranges from 10^{-5} to 10^{-3} m/s (James, 2009; Boudrias, 2018), but was chosen to reduce computational time. Indeed, a domain consisting of 2 types of materials with contrastive permeabilities in a model would significantly reduce the time step of the model (Itasca, 2021). A limited parametric analysis was also conducted to evaluate the effect of reducing waste rocks' hydraulic conductivity (see below).

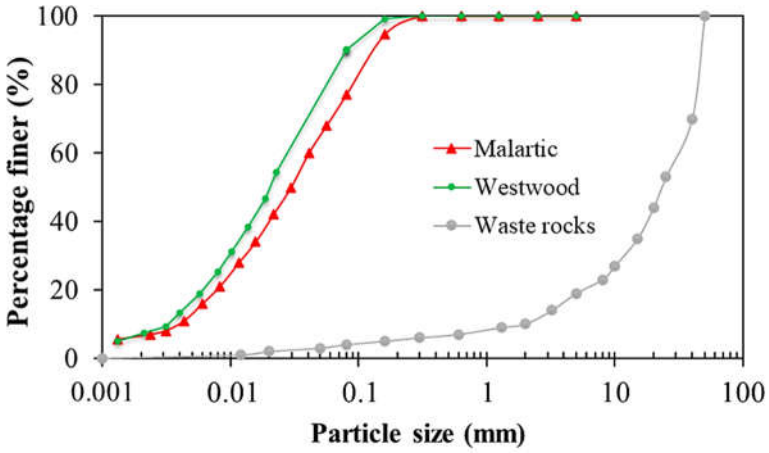

Figure 6-2: Particle size distribution for Malartic (Nguyen & Pabst, 2022b) and Westwood (Lévesque, 2019) gold tailings, and waste rocks (Essayad et al., 2018) used in this study.

Table 6-2: Properties of tailings and WRI used in the numerical models.

Properties	**Malartic Tailings** (Boudrias, 2018)	**Westwood Tailings** (Lévesque, 2019)	**WRI** (Boudrias, 2018)
Constitutive model	MC	MC	MC
Unit weight (kN/m^3)	19.5	18.7	-
Specific gravity	2.75	2.82	-
Dry density (10^3kg/m^3)	1.55	1.39	-
Friction angle (degree)	38	36	-
Cohesion (kPa)	0	0	-
Poisson's ratio	0.28	0.28	0.277
Young's modulus (MPa)	$85.6\sigma'^{0.74}$	$35.0\sigma'^{0.91}$	500
Hydraulic conductivity (m/s)	$1.2\ x\ 10^{-6}e^{4.6}$	$2.0\ x\ 10^{-7}e^{3.7}$	2 x 10^{-6}

6.2.3 Boundary and initial conditions

Displacement at the bottom of the pit was fixed at zero in all directions, and side boundaries of the models were fixed horizontally. Rock was considered relatively impermeable (see above) so bottom and side boundaries were assumed impervious. Local groundwater flowed around the pit and assumed to have no interaction with tailings, and thus was expected not to have much impact on the results. Zero PWP was assigned at the surface of tailings to represent the groundwater table therefore

allowing upward movement of water from the tailings. The undrained condition with the generation of excess PWP development was first generated, followed by a dissipation of PWP and consolidation of the materials (Itasca, 2021). The convergence criteria for a node (i.e, the ratio of the current mechanical force ratio to the target force ratio of the node) is set to 1 (Itasca, 2021).

6.3 Results

6.3.1 Effect of permeable envelope on tailings consolidation performance

Case 1 and case 2 models were first compared to evaluate the effect of the permeable envelope on the consolidation rate of tailings. One year after the placement of the 12th layer (i.e., t = 12 years), tailings at the bottom of the pit (z = 0 m) had not achieved full dissipation in the case with tailings only (case 1), with a degree of consolidation not exceeding around 80% (figure 3a). In other words, the depth of the pit was so important that excess PWP did not have the time to dissipate to the surface of the tailings as it can usually be observed in simulations of TSFs (Jaouhar et al., 2013; Boudrias, 2018; Lévesque, 2019). Such situation would be unfavourable for reclamation of the pit as post-settlement could continue to occur after the construction of the cover system (McDonald & Lane, 2010). The use of a permeable envelope, however, contributed to increase the degree of consolidation of tailings (figure 6-3a). For example, consolidation at z = 0 m and at a horizontal distance of 2, 12, and 32 m along the cross section A-A' were around 98%, 95% and 90% respectively after 12 years. The degree of consolidation at X = 52 m was, however, smaller and around 84%, but it was still greater than the case without permeable envelope (= 80%). Similar results were observed throughout the entire pit and at all times. A permeable envelope could therefore increase significantly the degree of consolidation of tailings, but this effect tended to decrease further away from the envelope or closer to the tailings surface. 3D effect of the permeable envelope at the corner of the pit on the acceleration of the tailings consolidation would also be discussed in detailed in the discussion session later.

Not only did the permeable envelope contributed to increase the degree of consolidation, it also accelerated the time required to dissipate excess PWP. For example, time to achieve 90% of consolidation, often noted t_{90}, at 2 and 12 m from the permeable envelope at the base of the pit (z = 0 m) 1 year after the placement of the fifth layer (i.e., t = 5 years) was around 42 and 70 days, respectively, that was 66 and 38 days faster than in the case with tailings only (figure 6-3b). The

difference of t_{90} between the cases with and without a permeable envelope 52 m from the permeable envelope was, however, much less significant, and less than 5%. The zone of influence of the permeable envelope (i.e., the zone where the permeable envelope reduce t_{90} by at least 5%) was around 2 times the height of tailings filled (figure 6-3b) which was somewhat similar to that of a WRI in surface TSFs (Bolduc & Aubertin, 2014). Similar results were obtained along section B-B' (figure 6-3c). For example, the permeable envelope in the horizontal direction contributed to accelerate the dissipation of PWP after the placement of the 10^{th} layer (i.e., 184 days and 15 days faster at 2 and 90 m respectively from the horizontal permeable envelope compared to those in case 1). This positive effect, however, became negligible at a distance of 102 m from the permeable envelope (figure 6-3c).

The zone of influence of the permeable envelope after the placement of 60 m of tailings was therefore around 120 m and thus could not cover the entire width of the pit (i.e., which was around 160 m at its base). A combination of a permeable envelope with other drainage pathways (i.e., WRI and bottom drainage) were thus investigated.

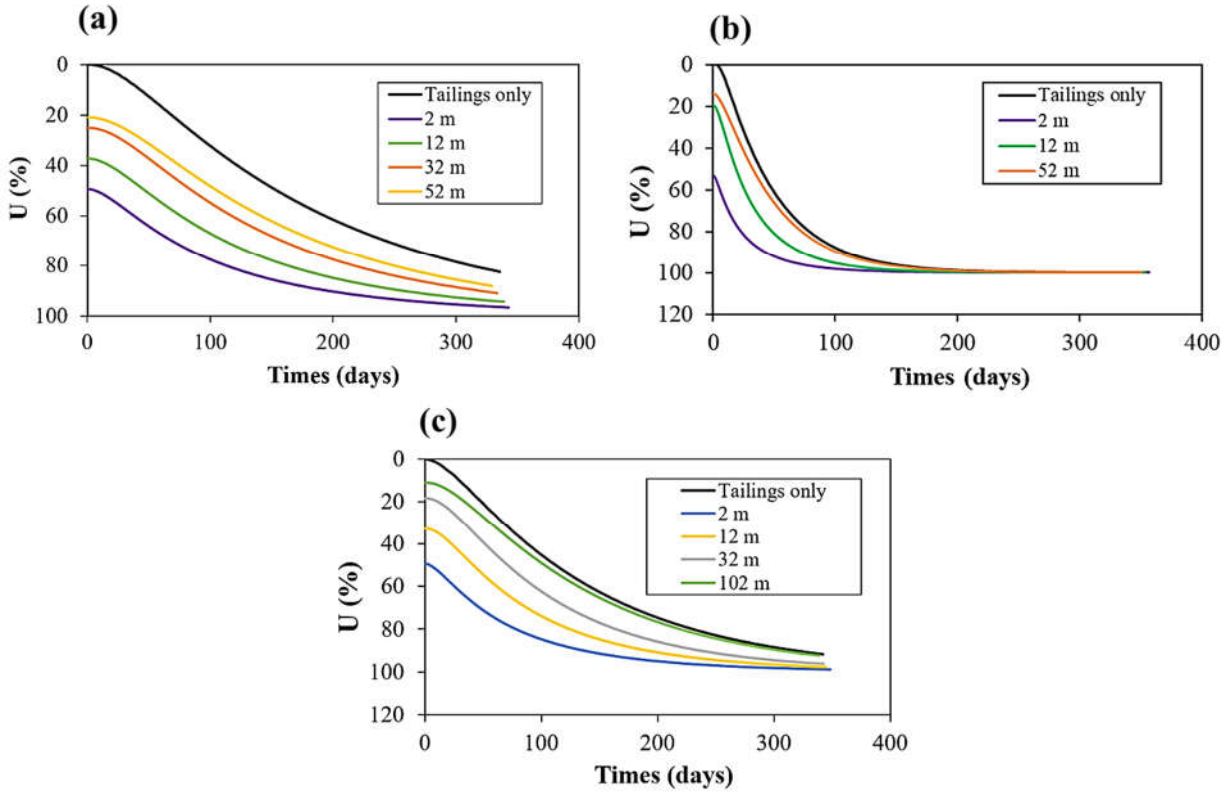

Figure 6-3: Degree of consolidation in the tailings with a permeable envelope (case 2) at various horizontal distances from the permeable envelope in the longitudinal direction (see figure 6-1) at the bottom of the pit along section A-A' (a) after the addition of the 12th layer, (b) after the placement of the 5th layer and (c) at various distances from the permeable envelope in the horizontal direction along section B-B' after the addition of the 10th layer. Results with tailings only (case 1) are also presented for comparison.

6.3.2 Tailings consolidation under various drainage paths

The use of a WRI alone has a similar effect to a permeable envelope and can also contribute to enhance tailings consolidation rate in the pit (case 3). All the results presented hereafter were simulated along section A-A' but similar results were obtained elsewhere in the model. t_{90} in the middle of the 1st layer (z = 2.5 m) after the placement of the 10th layer (i.e., t = 10 years) with only WRI ranged from around 133 days (X = 2 m) to 340 days (X = 110 m) (figure 6-4a), which was

significantly faster than in the case with tailings only (case 1), and somewhat similar to the case with a permeable envelope (case 2) (figure 6-4a). However, t_{90} 4 m from the permeable envelope was somewhat greater than 4 m from the WRI (i.e., 178 days compared to 133 days), which can be attributed to the difference in terms of geometry of these drainage paths (i.e., inclined envelope compared to the vertical WRI). However, these differences remained limited and usually did not exceed 40 days (25%).

In practice, a permeable envelope is usually combined with a bottom drainage which can contribute to accelerate even more the dissipation of excess PWP and particularly in the bottom half of the pit (case 4). For example, t_{90} in the middle of the 1st layer (i.e., z = 7.5 m, that is 2.5 m above the bottom drain which was 5 m thick) was around 280 days at horizontal position from 4 to 40 m, which is up to 60 days faster compared to the case with only permeable envelope (figure 6-4a). This effect tended to decrease higher up and farther way from the bottom drain, where t_{90} then became similar to the case with permeable envelope only (see more discussion below).

Finally, the combination of a permeable envelope, a WRI and a bottom drainage was investigated (case 5). This configuration was the most efficient in terms of acceleration of excess PWP (figure 6-4). For example, t_{90} of tailings at the middle of the first layer (z = 7.5 m) was 215 days at X = 90 m, which was around 100 days faster than the case with only permeable (case 2), and 135 days faster than the case with no drainage pathway at all (figure 6-4a). The use of various drainage pathways, separately or together, however, depends on site-specific operational aspects which would be discussed later.

From the vertical profile of the degree of consolidation, U, at X = 80 m along section A-A' for model with only tailings, U was significantly lower compared to that of a model with drainage paths (i.e., 60% compared to around 87%, respectively in the middle of the first layer) 1 year after the placement of 80 m of tailings (i.e., case 9, see section 6.4.1 as well) (figure 6-4b). These differences tended, however, to decrease closer to the tailings surface and were smaller than 5% at z = 60 m). Despite the presence of the bottom drainage paths, the degree of consolidation, U, tended to decrease between z = 5 to 30 m (e.g., the lowest degree of consolidation was around 85% at z = 20 m), and then increased as distances to the surface decreased (figure 6-4b). This therefore indicated that there was

an effect of the depth of the pit in the case of using bottom drain (i.e., distance to the drainage path in practice).

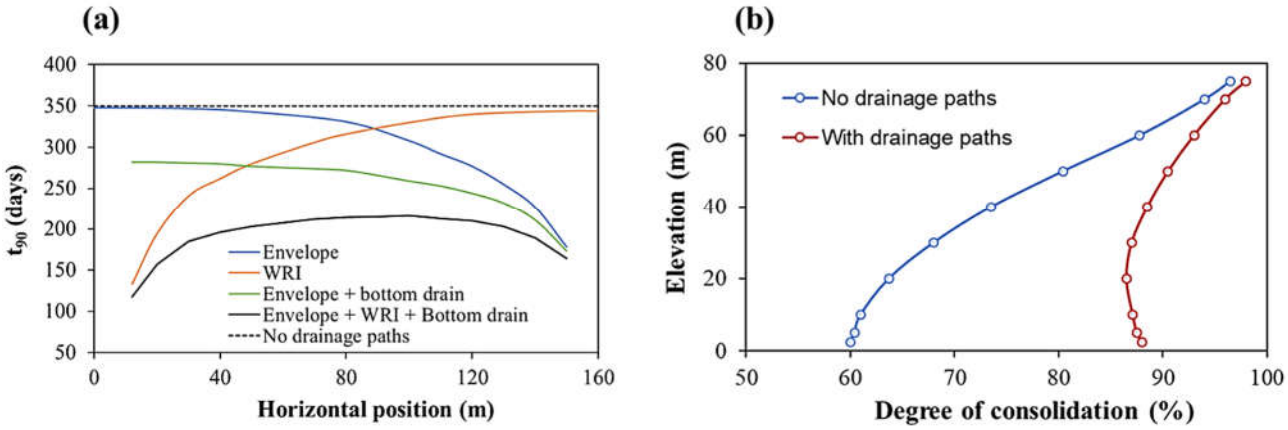

Figure 6-4: Time t_{90} along the section A-A' in the middle of the 1st layer (z = 2.5 m or 7.5 m for case without or with bottom drain respectively) 1 year after the placement of the 10th layer (t = 10 years) for various co-disposal scenario (also see table 1). The combined effect of the permeable envelope, WRI and bottom drainage contributed to significantly increase excess PWP dissipation rate, and (b) vertical evolutions of degree of consolidation at X = 80 m (section A-A') with drainage paths (case 9) 1 year after the placement of 80 m of tailings.

6.4 Parametric analysis

Based on the results presented above, co-disposal of tailings with waste rock (either in the form of permeable envelope, WRI and/or bottom drain) contributed to significantly accelerate the dissipation of excess PWP, and thus contributed to the reduction of both post-settlement after closure and contact of tailings with local groundwater. Practical constraints that could potentially affect the effectiveness of this technique include the depth of the pit, the change of filling rate, the pit slope angles, the WRI hydraulic properties, the pit morphology, and the tailings properties.

6.4.1 Effect of the pit depth

The disposal scenario with the combination of permeable envelope, WRI and bottom drain at the same time produced the most effective performance in terms of consolidation rate enhancement, at

least for the tested conditions. Results also shown, however, that the performance of the technique was strongly dependent on the distance to the drainage paths. The effect of pit depth, and tailings thickness, were therefore investigated.

Simulations showed that if the tailings thickness was greater than 80 m, there were some locations at the middle of the pit where excess PWP in tailings might not fully dissipate after one year of filling (i.e., before the addition of the next layer; figure 6-5). For example, the maximum t_{90} in the middle of the 1st layer (i.e., 2.5 m above the bottom drain) was around 260 days at X = 100 m after the placement of 60 m of tailings, around 310 days after the placement of 70 m of tailings, and above one year after the placement of 80 m of tailings (degree of consolidation was around 87% after one year) (figure 6-5).

From the above results when tailings thickness reached 80 m, some delay in tailings consolidation at the middle positions in the pit can be expected. One solution might be to install additional WRI so that the distance between the tailings and the nearest drainage path never exceed twice their thickness. Such solution would, however, significantly reduce the volume of tailings that can be stored in the pit (also see discussion below).

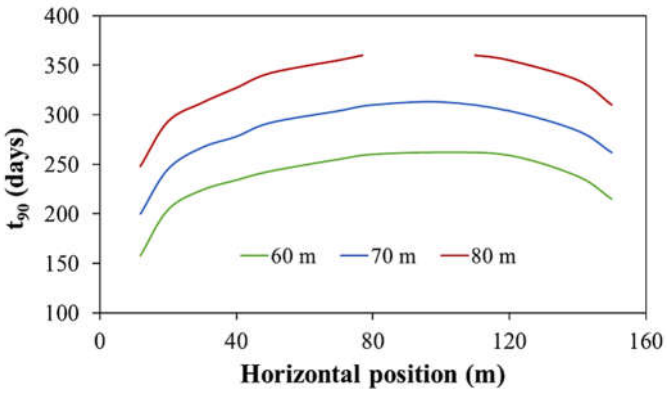

Figure 6-5: Time t_{90} along section A-A' 2.5 m above the bottom drain (z = 7.5 m) 1 year after the placement of the 12th, 14th and 16th layers (i.e., corresponding to a tailings thickness of 60, 70 and 80 m, respectively) in models with the combination of permeable envelope, WRI and bottom drain. Excess PWP was not able to fully dissipate in one year when the tailings thickness was greater than 80 m from horizontal positions of X = 80 m to X = 100 m (the line was cut off at these positions).

6.4.2 Effect of pit wall slope angle

The pit wall slope usually depends on the distribution characteristic of the ore body and the stability properties of the rock pit wall (Hustrulid W et al., 2013), and the pit walls for the pit with the depth of 100 m is usually inclined maximum 70 degrees (Utili et al., 2022). In the previous simulations, the pit wall slope angle was 50°, and additional models with slope angles of 60° and 70° were conducted to evaluate the effect on tailings consolidation rate when using a permeable envelope (lower slopes were not considered because of operational reasons as it might not be economical when large amount of waste rocks might be generated). Excess PWP dissipation rates tended to slightly increase with the pit wall slope and this effect was more pronounced closer to the permeable envelope (figure 6-6). For instance, the time required to dissipate 90% of excess PWP 2 m from the permeable envelope at the bottom of the pit (z = 0 m) after the placement of the 5th layer was around 44 days for a model with a slope angle of 50° (base case), 37 days for a slope of 60°, and 31 days for a slope angle of 70° (i.e., around 25% faster) (figure 6-6a). This difference decreased as the distance to the permeable envelope increased and become insignificant (< 5%) after around 20 m (figure 6-6a). A similar trend was observed after the placement of the 8th layer (figure 6-6b) and for the rest of the model. The radius of influence of the permeable envelope was also estimated and results indicated that slope angle essentially had no effect on the radius of influence. In conclusion, the slope angle could slightly affect the rate of consolidation close to the permeable envelope, but this effect was limited and decreases with the distance to the envelope.

It is also noted that the slope of the pit in this study had only one bench, while the pit slope was usually composed of several bench levels in practice. However, these benches would be eventually covered by the construction of the permeable envelope along the perimeter of the pit, and they would essentially have no effect on the drainage of tailings materials. More details on the bench effect will also be discussed later.

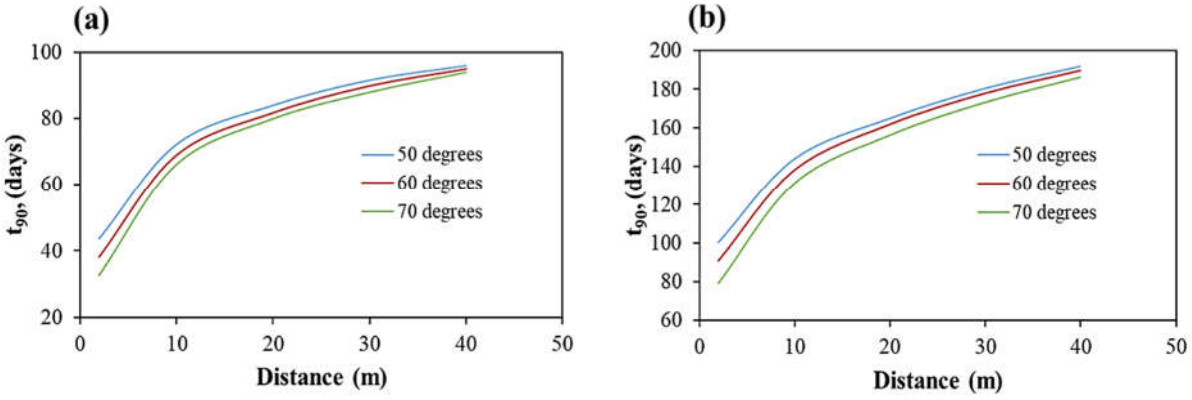

Figure 6-6: Time t_{90} at the bottom of the pit (z = 0 m) for models with various slope angles after the placement of the (a) 5th layer and (b) 8th layer. Distance is measured from the permeable envelope.

6.4.3 Effect of decreasing filling rate with time

The increase of the surface area of the pit as tailings backfilling progresses could lead to the decrease of the filling rate if the production rate remains constant. Simulations of models with layer thickness of the first two layers being 7.5 and 10 m respectively (thickness of other succeeding layers were still 5 m) were thus carried out to model these changes in the filling rate. Greater thickness of tailings layers close to the pit bottom led to the increase of the time for excess PWP to dissipate (figure 6-7). For example, the time required to dissipate 90% of excess PWP at the bottom (z = 0 m) after the placement of the 2nd layer 2 m from the permeable envelope was around 9 days for 5 m thick layers, 18 days for 7.5 m thick layers and 31 days for 10 m thick layers, respectively (figure 6-7a). The effect of the thickness layer was similar father away from the envelope. For example, t_{90} 22 m from the envelope was around 21 days for the 5 m thick layer and 65 days (i.e., around 3 times longer) for the 10 m thick layer (figure 6-7a). The increase in the t_{90} can be attributed to the increase of the excess PWP and the length of drainage paths when tailings layer became thicker due to the increase of the filling rate. A similar trend was also observed after the placement of the next layers, but the effect of the filling rate tended to decrease with the increase of the tailings thickness. t_{90} 22 m from the envelope after the placement of the 5th layer, for example, was 80 days for 5 m thick layers, and 130 days for 10 m thick layers (i.e., around 1.6 times longer) (figure 6-7b). The change in the filling rate, thus, influences on the consolidation rate of tailings.

The corresponding ratio of t_{90} value between models with tailings only and with the permeable envelope, R_{t90}, after the filling of the 2nd layer was somewhat higher for model with larger filling rate (i.e., 3.3 for the 10 m thick layer compared to 2.6 for the 5 m thick layer models at the position of 2 m at pit bottom) (figure 6-7c). These differences tended to decrease and become essentially identical for various filling rate as distance to the permeable envelope increased (figure 6-7c) and as tailings thickness increased (e.g., after the filling of the 5th layer) (figure 6-7d). Results thus indicated that filing rates of tailings somewhat had an effect on the performance of the permeable envelope at locations close to the permeable envelope, and permeable envelope performance then became independent to the filling rates at locations far away from the permeable envelope and as the tailings thickness increased.

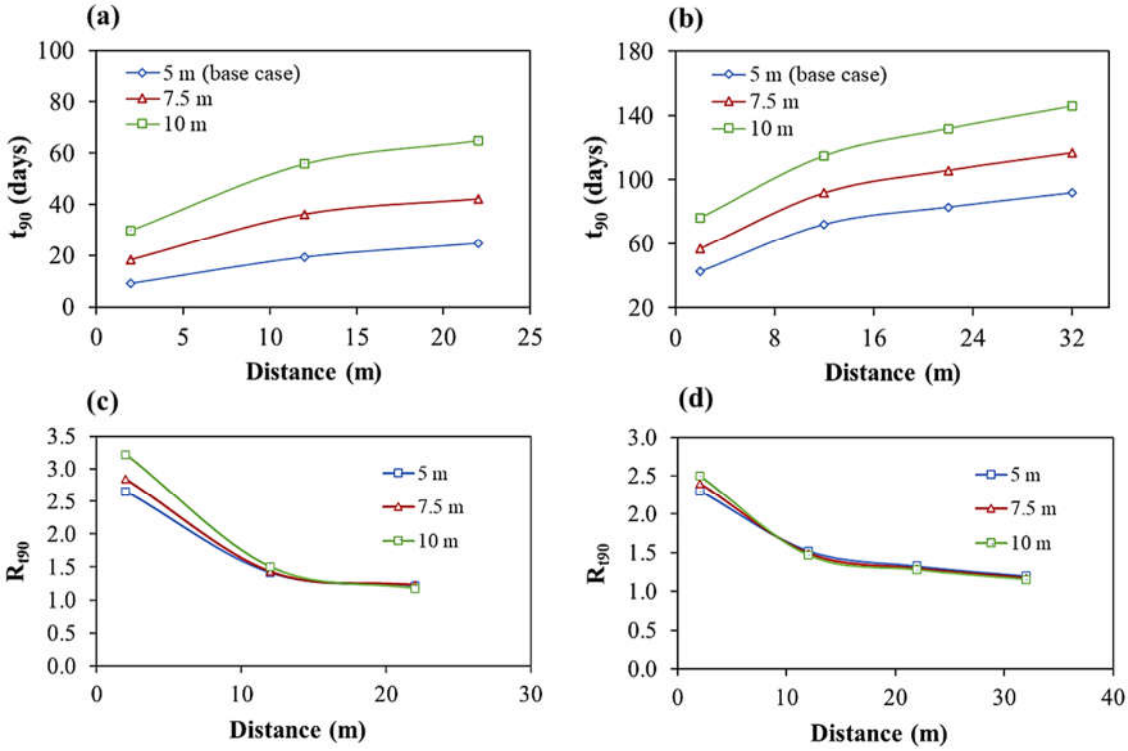

Figure 6-7: Evolution of excess PWP at the pit bottom (z = 0 m) as a function of the filling rate (tailings layer thickness) and distance to the permeable envelope after the placement of the (a) 2nd layer and (b) 5th layer, corresponding ratio of rate of t_{90} between models with tailings only and with the permeable envelope, R_{t90}, for various filling rates after the placement of the (c) 2nd layer, and (d) 5th layer. Distance is measured from the permeable envelope.

6.4.4 Effect of hydraulic conductivity of the permeable envelop

A permeable envelope is often made of coarse waste rocks (MEND, 2015), which hydraulic conductivity typically ranges from 10^{-5} to 10^{-3} m/s (James & Aubertin, 2009). The natural rock mass might also be damaged by the blasting operations during the production, sometimes leading to an increase of their hydraulic conductivity up to 10^{-2} m/s (Rousseau & Pabst, 2020). The hydraulic conductivity of the permeable envelope in this study was around 2 x 10^{-6} m/s which was not representative of actual waste rocks but was necessary to reduce the computational time. The effect of this choice was evaluated by conducting some models where the conductivity of the of permeable envelope was increased to 4 x 10^{-6} m/s and 6 x 10^{-6} m/s.

Simulations indicated that using a reduced value of hydraulic conductivity for the permeable envelope had only a limited influence on the results, and mostly close to the drainage paths. The effect of the hydraulic conductivity of the waste rocks was, however, negligible further than 22 m from the envelope. For example, the time needed to dissipate 90% of the excess PWP in the first layer (z = 0 m) after the placement of the 3rd layer 2 m from the permeable envelope was around 12 days when the waste rock hydraulic conductivity was 6 x 10^{-6} m/s and around 18 days when it was 2 x 10^{-6} m/s (figure 6-8). This (small) difference of t_{90} tended to decrease with the distance from the permeable envelope, and was less than 5% 22 m from the envelope. This effect can be attributed to the fact that farther from the permeable envelope, the drainage of water is mostly controlled by the tailings hydraulic conductivity and not so much by that of drainage path. The same trend was observed for WRI (Case 3) and bottom drain (Case 4). A similar effect was also observed in surface TSF with WRI (Bolduc & Aubertin, 2014).

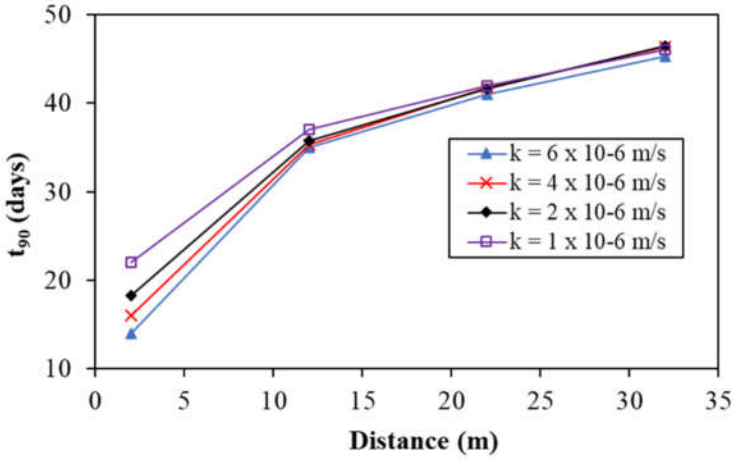

Figure 6-8: Time t_{90} as a function of the distance to the permeable envelope and waste rock hydraulic conductivity in the 1st layer (z = 0 m) after the addition of the 3rd layer. Distance is expressed from the permeable envelope.

6.4.5 Effect of tailings hydro-geotechnical properties

As observed in the previous section, tailings hydraulic conductivity has a significant effect on excess PWP dissipation rate, especially far from the drainage paths. Therefore, another type of gold tailings was also used in the parametric analysis using a permeable envelope, a WRI and bottom drainage at the same time (Case 5). Properties of Westwood gold tailings were obtained from Lévesque (2019) (table 6-2). Westwood tailings were finer and less permeable than Malartic tailings, which would induce a slower rate of consolidation. For example, t_{90} in the middle of the first layer (z = 7.5 m) of Westwood tailings 90 m from the inclusion was around 113 days after the placement of the 5th layer compared to around 98 days of Malartic tailings (figure 6-9). Similar trends were observed elsewhere in the pit. For example, t_{90} in the same position after the addition of the 10th layer was around 240 days for Westwood tailings and around 215 days (10% faster) for Malartic tailings (figure 6-9). The radius of the influences was also estimated and identical for these 2 types of tailings. These results the consolidation rate of Westwood tailings was somewhat slower than that of Malartic tailings. Accordingly, the application of drainage paths would be more important to dewater finer tailings with low hydraulic conductivity, and more WRI might be needed to enhance the consolidation rate depending on the site-specific operational requirements.

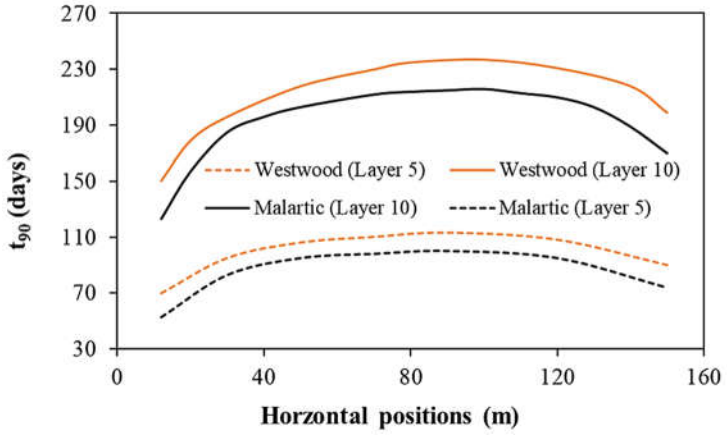

Figure 6-9: Time t_{90} for Westwood and Malartic tailings in the middle of the 1st layer (z = 7.5 m) after the placement of the 5th and 10th layers with both permeable envelope, WRI and bottom drainage. Results for Malartic tailings in the same conditions are shown for comparison.

6.5 Final remarks and discussion

6.5.1 Numerical considerations

An orthogonal corner pit was chosen to simulate pit geometry, which is not necessarily representative of real pit geometries in practice where somewhat circular corner is observed. The practical geometry of a pit was also modelled by Priestley (2011) and Rousseau and Pabst (2022). The geometry of the pit was simplified in this study because of the limitation of the built-in blocks which were used to create the pit geometry. Smaller conceptual models of the pit with orthogonal and circular corners were, therefore, simulated to investigate the potential effect of the geometry on the results. A section near the corner of the pit representing a circular corner with a bottom radius of 40 m and a top radius of 60 m was modelled (figure 6-10a) and compared with a model with an orthogonal corner (figure 6-10b), similar to the geometry used in this study. Tailings were filled in 6 layers of 30 m height over 6 years (i.e., filling rate of 5 m/year). An 8 m wide permeable envelope was simulated along the pit walls.

Materials properties and boundaries were otherwise identical to previous models presented above. Consolidation rate of model for orthogonal corner was faster than that of the circular corner and the difference was insignificant at locations far away from the permeable envelope. For example, t_{90} after the placement of the 6th layer at 5 m from the permeable envelope (section C-C') at the bottom of the pit was around 59 days for the circular corner pit, while that of the orthogonal corner pit was around 47 days (figure 6-11). The difference then decreased as the distance to the permeable envelope increased and become negligible after around 26 m (figure 6-11). Thus, the assumption of an orthogonal corner pit somewhat affected the rate of tailings consolidation, but this effect was limited and only close to the permeable envelope (i.e., 20 m from the permeable envelope).

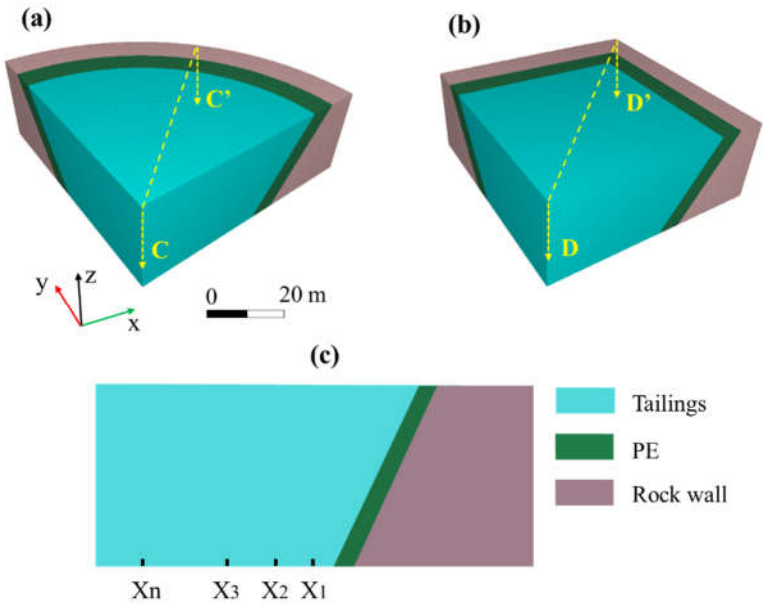

Figure 6-10: Numerical model of (a) a pit with a circular corner and (b) an orthogonal corner and (c) section views C-C' and D-D' at the diagonal of the domain with various monitoring points at the bottom of the pit.

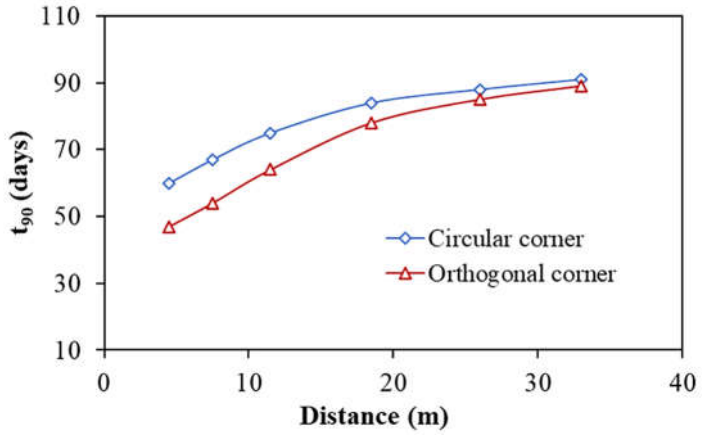

Figure 6-11: Simulated t_{90} at the bottom of the pit 1 year after the placement of the 6th layer for models with circular and orthogonal corner.

The simulations of tailings consolidation using FLAC3D for the case of co-disposal in a pit took around 2 weeks to run. It was also noticed that the contrastive hydraulic conductivity of tailings and waste rocks significantly increased the computational time for the coupled analysis as discussed in the section 4.4. The mesh size in this study was also chosen to ensure a balance of the accuracy of the results and the computational time. Other mesh generation tools might also be used instead of built-in blocks to build more sophisticated geometry of the domain, especially when more waste rocks need to be disposed and complicated configurations of the co-disposal technique might be encountered. Tailings was filled instantaneously in this model instead of progressive placement, yet this assumption has a negligible effect on the calculated results (Nguyen & Pabst, 2022a). The boundary conditions of models needed to be updated after each filling stage, while tailings properties needed to be continuously updated through the whole filling process, all of these aspects required skilled modellers to properly perform these types of analysis.

6.5.2 Discussion

Results presented in this article showed that using drainage paths composed of waste rocks can contribute to accelerate the consolidation of tailings when co-disposal technique was applied in an open pit. However, some limitations and simplifications must be considered before extrapolating these results to other sites and conditions.

First, relations used to update tailings stiffness and hydraulic conductivity derived from column tests (Essayad & Aubertin, 2021; Nguyen & Pabst, 2022b), and were, therefore, valid only for the simulated tailings. In practice, these equations will depend on tailings properties and will vary from one site to another. Experiments and characterization are thus recommended for each application. However, trends and general conclusions regarding pervious envelope and drainage paths are deemed applicable for most hard rock mines.

The elastic-perfectly plastic Mohr-Coulomb model was used in these simulations to simulate tailings behaviour. This model was also used by Boudrias (2018) and Zhou et al. (2019) to study the evolution of tailings consolidation and results were in a reasonable agreement with laboratory experiment and field results. Other models can, however, represent tailings behaviour such as Modified Cam-Clay (MCC) model (Jaouhar, 2012; Boudrias, 2018). The choice of a constitutive model can sometimes have a significant effect on the rate and magnitude of tailings consolidation and should therefore be adapted and calibrated to each case. The approach proposed in this article which consisted in updating tailings stiffness and hydraulic conductivity with void ratio evolution during consolidation could also be applied with MCC model for further study (Zhou et al., 2019).

Simulations have also shown that the corner of the pit could reasonably affect the PWP dissipation rate of tailings. However, this effect is relatively local and becomes negligible above around 20 m from the corners. In other words, 2D models might be sufficient to evaluate co-disposal approaches for large pit with great longitudinal dimensions (e.g., Malartic pit is over 1 km long and 500 m wide). However, 3D simulations are recommended for pit with small dimensions.

Pit slopes might be composed of several benches, yet the construction of the permeable envelope would cover and ease the effect of benches. The construction of permeable envelope might then be related to the repose angle of the waste rocks to ensure the overall stability of the envelope if waste rocks were dumped from the pit crest (Maryam, 2016). The effect of the benches might be more pronounced when the fractured pit wall was used as a natural permeable envelope or when the aim of the mine site is to increase the steepness of the slope, the permeable envelope would then be constructed in a bench by bench manner and was constructed from the bottom of the pit with the same angle as the benches of natural pit slope (Lévesque, 2019). All of the effects of these factors are, however, out of the scope and not simulated in this paper.

Finally, intermediate laboratory tests and/or field-scale tests are recommended to validate these 3-D models and capture potential unknowns that can affect the performances of the technique. Scale effect in particular should also be further studied. The range of loading applied in the compression tests indeed usually vary from around 10 kPa (Bhuiyan et al., 2015) to around 200 kPa (Essayad & Aubertin, 2021; Nguyen & Pabst, 2022b). Loads from the placement of the tailings in a pit could be much higher because of the large depth of the pit. These range of loadings used in the laboratory tests should reasonably reflect the practical conditions (i.e., loads from large tailings thickness) to obtain a better constitutive model for tailings properties.

6.6 Conclusion

In-pit disposal has been demonstrated to be an encouraging mine waste management approach and can offer various environmental and geotechnical advantages compared to the conventional approaches. Unknowns in terms of behaviour of tailings consolidation under the influences of waste rocks either in the form of permeable envelope and/or inclusion, effects of pit morphology and hydro-geotechnical properties of the materials remained challenging. The objective of this article was to address these above uncertainties to ensure a successful mine waste management. 3D models were carried out to evaluate the consolidation behaviour of tailings co-disposed with waste rock in an open pit. Various co-disposal approaches such as a permeable envelope, WRI and bottom drain were evaluated. The effect of filling rate, slope angles, and waste rock properties were also considered.

Based on these results, the following conclusions can be made:

A permeable envelope along the pit walls can contribute to accelerate tailings consolidation, thus reducing faster their hydraulic conductivity, and limiting contacts of tailings with the surrounding environment and regional groundwater. The zone of influence of the permeable envelope appears to be around 2 times the tailings thickness. The use of only a permeable envelope might, therefore, not always be sufficient, especially for wide pits whose radius is greater than 2 times of the tailings depth in case the main objective was to reduce the post-deposition settlement as well as potential differential settlement.

Additional drainage pathways such as a WRI or a bottom drain can contribute to further accelerate the consolidation rate of tailings. Consolidation time in the middle of the pit with the combination of

all drainage paths could be 1.5 times faster compared to the case with permeable envelope only, and over 3 times faster close to the WRI. Steeper slope angles can also result in greater consolidation rates at positions close to the permeable envelope.

The increase in the filling rate somewhat contributed to decrease the tailings consolidation rate, increased the radius of influence of the permeable envelope and this effect was negligible as tailings thickness increased. The decreased hydraulic conductivity of the permeable envelope somewhat affected the rate of consolidation of simulated tailings, yet this effect was insignificant as distances increased. Tailings hydro-geotechnical properties have an important effect on the rate of consolidation of tailings, and more WRI might be required to enhance dissipation rate of fine tailings materials. Finally, the assumption of an orthogonal corner pit used in this model was deemed reasonable and have little effect on the calculated results.

The application of permeable envelope concepts during in-pit disposal with the combination of WRI and bottom drainage drains therefore appears to be beneficial both in terms of reducing contaminant generation and differential settlement. There might be less space for disposing tailings because of the presence of an envelope and WRI but that this could be compensated by other advantages such as the elimination of the need of construction waste rock piles and the prevention of potential contaminants from acid mine drainage when the waste rocks were stored under the water table. These results should be useful for practitioners and contribute to propose efficient codisposal in surface mines. Further research, in particular in the field of complex co-dispose configuration as well as stability analysis of the inclusions could contribute to further optimize in-pit codisposal of tailings and waste rock.

6.7 Acknowledgement

The authors are thankful to the financial support from NSERC, FRQNT and partners of Research Institute on Mines and the Environment (RIME UQAT - Polytechnique; http://rime-irme.ca/en). The authors also gratefully acknowledge Dr. Huy Tran, Dr. Kazim and Itasca technical support team for their valuable support and comments to improve the code in this study.

6.8 References

Abdulnabi, A., Amoako, K., Moran, D., Vanadara, K., Aldaeef, A. A., Esmaeilzadeh, A., . . . Simms, P. (2022). Evaluation of candidate polymers to maximize geotechnical performance of oil sands tailings. *Canadian Geotechnical Journal, 59*(3), 359-371. https://doi.org/10.1139/cgj-2020-0714

Agapito, L. A., & Bareither, C. A. (2018). Application of a one-dimensional large-strain consolidation model to a full-scale tailings storage facility. *Minerals Engineering, 119*, 38-48. https://doi.org/https://doi.org/10.1016/j.mineng.2018.01.013

ASTM D2487-17. (2017). *Standard practice for classification of soils for engineering purposes (Unified Soil Classification System)* (ASTM International.

Aubertin, M. (2013). *Waste rock disposal to improve the geotechnical and geochemical stability of piles.* 23rd World Mining Congress, Montreal, Canada.

Aubertin, M., Bussière, B., Pabst, T., James, M., & Mbonimpa, M. (2016). *Review of reclamation techniques for acid generating mine wastes upon closure of disposal sites.* Geo-Chicago 2016, Chicago, Illinois, USA. https://doi.org/10.1061/9780784480137.034

Benzaazoua, M., Fall, M., & Belem, T. (2004). A contribution to understanding the hardening process of cemented pastefill. *Minerals Engineering, 17*(2), 141-152. https://doi.org/https://doi.org/10.1016/j.mineng.2003.10.022

Bhuiyan, I., Azam, S., & Landine, P. (2015). Consolidation Behavior of a Uranium Tailings Storage Facility in Saskatchewan. *Journal of Hazardous, Toxic, and Radioactive Waste, 19*(4), 040150051-040150057. https://doi.org/doi:10.1061/(ASCE)HZ.2153-5515.0000281

Blight, G. E. (2010). *Geotechnical engineering for mine waste storage facilities*. CRC Press.

Bolduc, F., & Aubertin, M. (2014). Numerical investigation of the influence of waste rock inclusions on tailings consolidation. *Canadian Geotechnical Journal, 51*(9), 1021-1032. https://doi.org/10.1139/cgj-2013-0137

Boudrias, G. (2018). *Évaluation numérique et expérimentale du drainage et de la consolidation de résidus miniers à proximité d'une inclusion de roches stériles* [Mémoire de maîtrise, École Polytechnique de Montréal].

Bussière, B. (2007). Colloquium 2004: Hydrogeotechnical properties of hard rock tailings from metal mines and emerging geoenvironmental disposal approaches. *Canadian Geotechnical Journal, 44*(9), 1019-1052. https://doi.org/10.1139/t07-040

Bussière, B., & Guittonny, M. (2020). *Hard Rock Mine Reclamation From Prediction to Management of Acid Mine Drainage*. CRC Press.

Cameron, H., & Dave, L. (2015). *In-pit Tailings Disposal at Langer Heinrich – Tailings Storage Facilities in a Unique Hydrogeological Setting.* Tailings and Mine Waste Management for the 21st Century Sydney. https://dxi97tvbmhbca.cloudfront.net/upload/user/image/Hore-Luppnow-In-pit_Tailings_Disposal_20152020022721025057 3.pdf

Cui, L., & Fall, M. (2016). An evolutive elasto-plastic model for cemented paste backfill. *Computers and Geotechnics, 71*, 19-29. https://doi.org/https://doi.org/10.1016/j.compgeo.2015.08.013

Essayad, K., & Aubertin, M. (2021). Consolidation of hard rock tailings under positive and negative pore-water pressures: testing procedures and experimental results. *58*(1), 49-65. https://doi.org/10.1139/cgj-2019-0594

Essayad, K., Pabst, T., Chapuis, R. P., & Aubertin, M. (2018). *An experimental study of tailings migration through waste rock inclusions.* 71st Canadian Geotechnical Conference (GeoEdmonton 2018), Edmonton, AB, Canada.

Fahey, M., Helinski, M., & Fourie, A. (2010). Consolidation in accreting sediments: Gibson's solution applied to backfilling of mine stopes. *Géotechnique, 60*(11), 877-882. https://doi.org/10.1680/geot.9.P.078

Ferdosi, B., James, M., & Aubertin, M. (2015). Investigation of the Effect of Waste Rock Inclusions Configuration on the Seismic Performance of a Tailings Impoundment. *Geotechnical and Geological Engineering, 33*(6), 1519-1537. https://doi.org/10.1007/s10706-015-9919-z

Hustrulid W, Kutcha M, & R, M. (2013). *Open pit mine planning and design*. CRC Press.

Itasca. (2021). *FLAC3D 7.0 (Fast Lagrangian Analysis of Continua in 3 Dimensions) User Manual*. Itasca Consulting Group, Inc.

Jahanbakhshzadeh, A., Aubertin, M., Yniesta, S., & Zafarani, A. (2019). *On the seismic response of tailings dikes constructed with the upstream and center-line methods.* 72nd Canadian Geotechnical Conference (GEO 2019), St. John's, Canada.

James, M. (2009). *The use of waste rock inclusions to control the effects of liquefaction in tailings impoundments* [Ph.D. , École Polytechnique de Montréal].

James, M., & Aubertin, M. (2009). *The use of waste rock inclusions in tailings impoundments to improve geotechnical and environmental performance.* Tailings and Mine Waste 2009, Banff, Alberta (pp. 233–245).

Jaouhar, E. M. (2012). *Analyse de l'effet d'inclusions drainantes sur la consolidation de sols fins et de résidus miniers* [Mémoire de maîtrise, École Polytechnique de Montréal].

Jaouhar, E. M., Aubertin, M., & James, M. (2013). *The effect of tailings properties on their consolidation near waste rock inclusions.* 66th Canadian Geotechnical Conference (GeoMontréal 2013), Montréal, Canada.

Larochelle, C. G., Bussière, B., & Pabst, T. (2019). Acid-Generating Waste Rocks as Capillary Break Layers in Covers with Capillary Barrier Effects for Mine Site Reclamation. *Water, Air, & Soil Pollution, 230*(3), 57. https://doi.org/10.1007/s11270-019-4114-0

Lévesque, R. (2019). *Consolidation des résidus miniers dans les fosses en présence d'inclusions de roches stériles* [Mémoire de maîtrise, Ecole Polytechnic Montreal].

Li, L., & Aubertin, M. (2009). Horizontal pressure on barricades for backfilled stopes. Part I: Fully drained conditions. *Canadian Geotechnical Journal, 46*(1), 37-46. https://doi.org/10.1139/T08-104

Maknoon, M., & Aubertin, M. (2021). On the Use of Bench Construction to Improve the Stability of Unsaturated Waste Rock Piles. *Geotechnical and Geological Engineering, 39*(2), 1425-1449. https://doi.org/10.1007/s10706-020-01567-0

Maryam, M. (2016). *Slope stability analysis of waste rock piles under unsaturated conditions following large precipitations* [Ph.D., Polytechnique Montreal].

Mbemba, F., & Aubertin, M. (2021). Physical Model Testing and Analysis of Hard Rock Tailings Consolidation Considering the Effect of a Drainage Inclusion. *Geotechnical and Geological Engineering, 39*(4), 2777-2798. https://doi.org/10.1007/s10706-020-01656-0

McDonald, L., & Lane, J. C. (2010). *Consolidation of in-Pit tailings.* Mine Waste 2010, Perth, Australia (pp. 49-62).

MEND. (2015). MEND Report 2.36.1 In-Pit Disposal of Reactive Mine Wastes: Approaches, Update and Case Study Results.

Morris, P. H. (2002). Analytical Solutions of Linear Finite-Strain One-Dimensional Consolidation. *Journal of Geotechnical and Geoenvironmental Engineering, 128*(4), 319-326. https://doi.org/doi:10.1061/(ASCE)1090-0241(2002)128:4(319)

Nguyen, D., & Pabst, T. (2020). *Comparative experimental study of consolidation properties of hard rock mine tailings.* 73rd Canadian Geotechnical Conference (GeoVirtual 2020), Online.

Nguyen, D., & Pabst, T. (2022a). Consolidation behavior of various types of slurry tailings co-disposed with waste rock inclusions: a numerical study. *Environmental Earth Sciences (Under reviewed)*.

Nguyen, D., & Pabst, T. (2022b). Numerical study of slurry tailings consolidation considering continuous update of material properties. *International Journal of Mining Science and Technology (Under reviewed)*.

Pabst, T., Bussière, B., Aubertin, M., & Molson, J. (2018). Comparative performance of cover systems to prevent acid mine drainage from pre-oxidized tailings: A numerical hydro-geochemical assessment. *Journal of Contaminant Hydrology, 214*, 39-53. https://doi.org/https://doi.org/10.1016/j.jconhyd.2018.05.006

Priestley, D. (2011). *Modeling multidimensional large strain consolidation of tailings* [Master, University of British Columbia].

Rousseau, M. (2021). *Étude numérique de la réduction du transport advectif de contaminants entre les fosses remblayées et l'environnement par l'utilisation de chemins d'écoulements préférentiels* [Ph.D., École polytechnique Montréal].

Rousseau, M., & Pabst, T. (2020). *Blast damaged zone influence on water and solute exchange between backfilled open-pit and the environment.* 73rd Canadian Geotechnical Conference (GeoVirtual 2020), Online.

Rousseau, M., & Pabst, T. (2022). Topology optimization of in-pit codisposal of waste rocks and tailings to reduce advective contaminant transport to the environment. *Structural and Multidisciplinary Optimization, 65*(6), 168. https://doi.org/10.1007/s00158-022-03266-1

Schiffman, R. L. (1982). The consolidation of soft marine sediments. *Geo-Marine Letters, 2*(3-4), 199-203. https://doi.org/10.1007/bf02462763

Somogyi, F. (1980). *Large Strain Consolidation of Fine Grained Slurries.* Presentation at the Canadian Society for Civil Engineering, Winnipeg, Manitoba.

Townsend, & McVay. (1990). SOA: Large Strain Consolidation Predictions. *Journal of Geotechnical Engineering, 116*(2), 222-243. https://doi.org/doi:10.1061/(ASCE)0733-9410(1990)116:2(222)

Utili, S., Agosti, A., Morales, N., Valderrama, C., Pell, R., & Albornoz, G. (2022). Optimal Pitwall Shapes to Increase Financial Return and Decrease Carbon Footprint of Open Pit Mines. *Mining, Metallurgy & Exploration, 39*(2), 335-355. https://doi.org/10.1007/s42461-022-00546-8

Vick, S. G. (1990). *Planning, Design and Analysis of Tailings Dams*. BiTech Publishers Ltd.

Wickland, B. E., Wilson, G. W., Wijewickreme, D., & Klein, B. (2006). Design and evaluation of mixtures of mine waste rock and tailings. *Canadian Geotechnical Journal, 43*(9), 928-945. https://doi.org/10.1139/t06-058

Yang, P. (2016). *Investigation of the geomechanical behavior of mine backfill and its interaction with rock walls and barricades* [Ph.D., École Polytechnique de Montréal].

Zhou, Amodio A, & N., B. (2019). *Informed mine closure by multi-dimensional modelling of tailings deposition and consolidation.* Mine Closure 2019, Perth, Australia.

CHAPTER 7 GENERAL DISCUSSION

7.1 Main results

Tailings disposed in open pits with the presence of a permeable envelope composed of coarse waste rocks and/or combined with WRI inclusions and bottom drains could facilitate both environmental and geotechnical advantages. This concept is also facing several unknowns that can limit its practical applications. Non-linearity of tailings consolidation properties needs to be properly investigated to better capture real consolidation behaviours of tailings. Volume gains or losses of tailings because of the presence of WRIs also need to be explicitly estimated considering operational constraints. Finally, effects of practical constraints including pit depth, pit slope angles, filling rate, mine waste hydraulic properties and the morphology of the pit need also to be comprehensively examined. Modification of tailings properties using advanced numerical analysis was therefore performed and validated by laboratory results. The results were then extrapolated to examine the tailings consolidation behaviours with the presence of various drainage paths co-disposed in an open pit. The main results can be summarized as follows:

- An approach to modify tailings properties under sequential loading was first proposed using advanced numerical tools and was then validated by column tests in chapter 4. Potential discrepancy in tailings consolidation behaviours between models with the assumption of non-linear and fixed properties was quantitatively investigated. Results indicated that the proposed approach could reasonably represent the non-linearity of tailings properties under sequential loadings. Total simulated settlement was in a reasonably good agreement with measured values, while measured settlement could be up to 2 times higher than that of the model using constant stiffness.
- The proposed approach was then applied to study the influences of WRI on consolidation behaviours of four types of tailings filled in a simplified conventional TSF in chapter 5. The volume gains or losses of tailings due to the presence of WRI was also estimated. Results indicated that WRI significantly accelerated PWP dissipation rate in tailings. PWP always reached hydrostatic values at the end of each filling stage for tailings A, B and C, while excess PWP in tailings D (lowest hydraulic conductivity) cannot fully dissipate after

one year. Equivalent constant hydraulic conductivity for tailings A, B and C were also estimated. The zone of influence of WRI was accordingly estimated and was distinctive for each type of tailings. It was decreasing rapidly before remaining relatively stable after the tailings thickness reached 12 m. The use of WRI reduced the available volume for the storage of tailings in the TSF (and/or pit), despite their acceleration effect on the rate of PWP dissipation.

- Results on the approach to consider non-linearity of tailings consolidation properties presented in chapter 4 and the interaction between tailings and WRI in chapter 5 was extrapolated in chapter 6 to unfold uncertainties regarding the consolidation behaviours of tailings disposed in a pit with the presence of various drainage paths composed of waste rocks. 3D numerical models on the tailings co-disposed with waste rocks in an open pit under various disposing scenarios were performed. A permeable envelope constructed along the pit perimeter enhanced the rate tailings consolidation, and thus decreasing their permeability more quickly. The zone of influence of the permeable envelope was around 2 times the tailings height. The application of only a permeable envelope might, therefore, not always be sufficient, especially for the case where the pit radius is greater than 2 times of the tailings depth. Additional drainage pathways such as a WRI or a bottom drain further accelerated the consolidation of tailings, while the combination of all of the drainage paths gave the fastest rate of dissipation. Steeper slope angles resulted in faster consolidation rates. The increase in the filling rate somewhat decreased the rate of tailings consolidation.

7.2 Discussions

In the thesis, advanced numerical simulations were utilized to simulate the consolidation behaviours of slurry tailings considering non-linearity of permeability and stiffness of tailings. Numerical models applying the proposed approach indicated a reasonable agreement between simulated and measured data for compression column tests. This approach was then applied to investigate the consolidation of tailings co-disposed with WRI in a conventional TSF and in an open pit. However, some limitations and hypotheses could affect the results of the simulation, which can be summarized as follows:

- It was challenging to properly correct the values of effective stress applying on the samples, which might have pronounced effects on the input constitutive relations, especially the estimation of Young's modulus and void ratio based on the effective stress (see chapter 3). The maximum ratio between change in PWP and change in the loads applied in this study was around 65%, while that for the tests on the same materials was around 55% (Essayad, 2015) and 80% (Boudrias, 2018) respectively. The overcorrection of effective stress (especially at the few last loading steps) might lead to the underestimation of the values of Young's modulus of tailings which might usually be higher in the field (Bussière, 2007). Apart from friction between the column wall and tailings, the degree of saturation of the sample can also induce uncertainties in the correction of the effective stress. Efforts were made during the sample preparation process to ensure that the sample was fully saturated (e.g., slurry samples were mixed well before being poured into the column to avoid air bubbles in the samples; all the PWP sensors were saturated before being installed to the columns; water flowed from bottom to the top of the columns during the measurement of hydraulic conductivity to further eliminate air bubbles). However, the samples might not be fully saturated despite of all these efforts made. Changes in the stress state of the samples because of the integration of hydraulic conductivity measurement into column tests might also lead to the change in the stress state of the tailings columns. Finally, loading system (level arm) might not be level as the displacement of the sample increased, which might also affect the estimation of the load applied on the samples.
- Tailings columns were simulated without the presence of the rigid column wall as being encountered in practice. Thus, the interaction between tailings and the column wall might not necessarily be reflected in the models in this study. The domain used for the simulation of column tests might also not necessarily represent the true geometry of the tailings columns in the laboratory.
- More loading stages might be needed at a low range of pressures in the column tests for the fine tailings where tailings might exhibit significant non-linear behaviours (Babaoglu & Simms, 2020) to better represent the evolution of tailings properties at a low range of pressures (Fourie et al., 2022).

- The maximum load that can be applied in the column tests was around 200 kPa, which might be sufficient for the conventional ground surface TSFs, but it was much smaller than pressures that might be encountered in pits. Applying constitutive models induced from low loading ranges might thus somewhat underestimate the dissipation rate of PWP in the field as the evolution of tailings hydraulic conductivity might become less non-linear as loads increased. Furthermore, several types of tailings might experience a non-linear relation between void ratio and effective stress at high values of loadings, and a bi-power law function might be required (e.g., oil sand tailings) (Jeeravipoolvarn et al., 2008; Fredlund et al., 2015). This can be avoided by increasing the loads applied, or in case of limitation of the equipment capacity, predictions model can also be used (at least for the preliminary study; see chapter 5).
- The elastic-perfectly plastic Mohr-Coulomb model was utilized with the modification of material properties in this study to represent the tailings behaviour. It is known that there are two methods to deal with volumetric plastic response (Itasca, 2021). The first method is that plastic volumetric strain can be better simulated through the elastoplastic models with cap (e.g., Cap-Yield model, plastic hardening model and Modified Cam-clay model) (Itasca, 2021). On the other hand, there is also a second approach, which is to use the non-linear approach (i.e., Mohr-Coulomb with non-linear elastic with the continuous update of stiffness) (Itasca, 2021). In these non-linear models, if there were no unloading reloading process (i.e., like what was observed in the working conditions of tailings where loadings from the filling process would always remain), we can thus focus on the primary loading, and simulate the volumetric response in tailings. This was the method used in this study, despite the fact that, previous works only used the linear form of Mohr-Coulomb model to simulate the elastic volumetric strain (Jaouhar et al., 2013; Boudrias, 2018). The choice of a constitutive model can play a key role on the rate and magnitude of tailings consolidation and should therefore be adapted and calibrated to each case.
- Young's modulus was derived from the column tests based on the changes in effective stress following a common approach used in the research group (Jaouhar et al., 2013; Essayad, 2015; Boudrias, 2018; Lévesque, 2019), which, in turn, was used as the

constitutive relations for the tailings in the simulations. It was, thus, noted that the Young's modulus in this study was not truly elastic Young's modulus, which was different from that of the conventional Mohr-Coulomb model (see section 2.5). The stiffness was technically non-linear elastic thanks to the updating procedure applied in this study. The evolution of Young's modulus during the column test and a good agreement between simulated and measured displacement (see section 4.3) indicated that the numerical approach to represent changes in stiffness can reasonably capture the non-linear behaviour of the tailings material.

Detailed equations to estimate the values of Young's modulus were presented from equations 3.11 to 3.13, which shown the dependence of Young's modulus to the effective stress. The value of the Young's modulus at the effective stress of 200 kPa was around 5000 kPa. Values obtained for the same effective stress on the same material from previous works was around 6500 (Essayad, 2015) and 7000 kPa (Boudrias, 2018). This can be attributed to the overcorrection of the effective stress in this study, especially at high values of stresses (see above). The maximum correction ratio was around 0.65 in this study, while that used by (Essayad & Aubertin, 2021) was an average value of 0.36.

Relation between Young's modulus and effective stress was derived based on the values of Young's modulus measured at the end of each loading steps. It is however noted that the evolution of the Yong's modulus during each loading steps was also non-linear (section 3.3.3). This thus can add some more uncertainties in the precision of the constitutive equation for the change of the Young's modulus. More loading steps might be added to increase the precision of the equation.

- The constitutive relations between void ratio and effective stress, and hydraulic conductivity and void ratio were first proposed by Gibson et al. (1967) to solve the large strain analysis of materials, These constitutive relations have been widely used and in various studies since then to study the consolidation behaviour of slurry tailings (Somogyi, 1976; Carrier et al., 1983; Schiffman et al., 1984; Townsend & McVay, 1990; Jeeravipoolvarn et al., 2008; Bhuiyan et al., 2015; Fredlund et al., 2015; Agapito & Bareither, 2018; Zhou et al., 2019; Fourie et al., 2022). These relations can be derived from

seepage induced consolidation test (Imai, 1979; Ahmed & Siddiqua, 2014) or from column test (Lévesque, 2019; Essayad & Aubertin, 2021). The application of these relations to model the consolidation of tailing in this study was thus deemed reasonable. On the other hand, with the advance numerical tools, the void ratio that was derived from the volumetric strain of the sample can also be monitored and estimated during the simulation process, and the hydraulic conductivity can also be estimated based on these void ratio values. It should be noted that the "void ratio" variable in the FISH code that was calculated based on the effective stress (Appendix C) was used to calculate the hydraulic conductivity only and was not assigned to the void ratio of tailings materials as the intrinsic values resulting from volumetric strain of the sample.

- Equivalent hydraulic conductivity for several types of tailings can provide partitioners with the brief suggestion on the choice of the hydraulic conductivity of the same type of tailings. It should also be noticed that the application of the equivalent hydraulic conductivity only worked under certain conditions of this study (loading conditions, filling scheme and boundary conditions).

- Top of tailings layers might exhibit desaturation and desiccation, and can locally influence the consolidation rate of tailings (Mbemba & Aubertin, 2021b). These effects were, however, not considered in this project. Negative PWP can be applied at the surface of the tailings samples in column test (Essayad & Aubertin, 2021) to examine the effect of those phenomena on the tailings properties, which, in turn, can be integrated into the model by FISH code.

- Only one row of inclusion was simulated in this study, while there might be several parallel and/or orthogonal inclusions in case the priority of the mine is to manage a large quantity of waste rocks materials (Aubertin et al., 2016). These complex configuration of WRIs can be simulated using advanced mesh generation tools (e.g., Griddle). The optimization of WRIs configuration disposed in the pit to investigate the hydraulic interaction of tailings with WRIs and the local environments was also performed by Rousseau (2021).

- Constitutive relations used to represent the evolutions of tailings stiffness and hydraulic conductivity in this study were obtained from column tests and valid only for the studied

tailings. In reality, these relations will depend on each type of tailings and thus will vary from one site to another. Experimental tests on the characterization of the materials are thus recommended for each type of tailings. Trends and general behaviour regarding the effect of various drainage paths are deemed applicable for most hard rock mines.

- Tailings settlement at locations close to the WRI might be affected by the interface element assigned in the simulations, which might not necessarily represent the real interaction between tailings and WRI. Frictions angles and stiffness of the interface element (in chapter 5) were estimated following the recommendation from the manual. Despite these boundary effects, general behaviours were expected not to be significantly influenced (Li & Aubertin, 2009b; Yang, 2016).
- The shape of the corner of the pit could somewhat affect the evolution of PWP of tailings. This effect was, however, relatively limited and became negligible at a distance higher than 20 m from the corners. As such, 2D simulations might be sufficient to investigate the co-disposal technique for large pits with great longitudinal dimensions (e.g., Malartic pit is over 1 km long for 500 m wide). On the other hand, 3D simulations might be recommended for a small pit.

CHAPTER 8 CONCLUSIONS AND RECOMMENDATIONS

8.1 Conclusions

The consolidation behaviour of tailings co-disposed with waste rocks either in the form of permeable envelopes and/or inclusions in an open pit were evaluated in this study to prove the geotechnical benefits of the drainage paths toward tailings consolidation behaviour. An approach was developed to represent the continuous update of tailings properties and was then validated by results from column tests on the same types of tailings. This technique was then applied to investigate the consolidation behaviours of tailings co-disposed with waste rocks in a simplified conventional TSF and a real scale open pit. The main results from this thesis can be summarized as follows:

- An approach to alter Mohr Coulomb properties was proposed and integrated in FLAC3D to simulate the real evolution of material properties under sequential fillings. The approach was then validated by comparing obtained results with measured values obtained from compression column tests. A parametric study was also carried out to examine the performance of various functions to predict hydraulic conductivity of tailings. The proposed approach can capture reasonably well the non-linear evolutions of tailings properties under compression. Results also indicated that simulations using constant stiffness and hydraulic conductivity could induce a significant discrepancy in terms of both the dissipation rate of excess PWP and the settlement of tailings. KC and KCM models can be used for the prediction of the consolidation rate of tailings, at least, at the preliminary study stage.
- The presence of WRI in a conventional TSF and an open pit could enhance the consolidation rate of tailings. WRI could increase the consolidation rate of tailings by around 3.3 times compared to that of the model without the presence of the WRI. The zone of influence of WRI on dissipation rate of tailings was distinctive for each type of tailings. The construction of WRI in the pit can reduce the volume available for the storage of tailings in open pits, and the volumetric compression resulting from tailings settlement in models with or without WRI could be explicitly computed. Additional height that needs to

be constructed for the TSF to compensate for the presence of the WRI can also be estimated. The assumption of instantaneous filling had a negligible influence on the rate of tailings consolidation.

- The influences of a permeable envelope and various co-disposal scenarios on the consolidation behaviour of tailings in an open pit, as well as the influences of various practical constraints were quantitatively examined using advanced 3-D simulations performed in FLAC3D (Itasca, 2021). A permeable envelope constructed along the perimeter of the pit can accelerate the dissipation rate of PWP and reduce contacts between tailings and the surrounding medium. The zone of influence of the permeable envelope was around 2 times the tailings height. The use of only a permeable envelope might not be sufficient for wide pits with bottom radius being greater than 2 times of the depth of the pit. Additional drainage paths such as a WRI or a bottom drain can further enhance the consolidation rate of tailings. Dissipation rate of PWP in the pit with the combination of all drainage paths can reach over 2.5 times faster compared to that of the model without the presence of drainage paths. Steeper slope angles can bring about a faster dissipation rate at locations close to the permeable envelope. The use of reduced values for the hydraulic conductivity of the WRI might underestimate the rate of dissipation rat of tailings close the WRI. Some post-settlement can be expected at the middle of the pit when the tailings thickness reached 80 m even for the model with the combination of all of the drainage paths. The increase in the filling rate somewhat decreased the consolidation rate of tailings, increased the radius of influence of the permeable envelope and this effect became negligible as tailings thickness increased.

Through this project, the geotechnical benefit of the permeable envelope has been proven. It was however noted that all of the results and conclusions in this study were not meant to be site specific, and only valid for the boundary conditions, loading condition and the state of the tailings (i.e., solid content) applied in this project. The application of permeable envelope concept with the combination of WRI and bottom drains might be beneficial both in terms of the prevention of the generation of contaminants and limitation of the differential settlement. The presence of the pervious surround and WRI might reduce space for the storage of the tailings. This could, however, be compensated by other benefits, which included the elimination of the construction of waste rock

piles in the ground surface and the prevention of potential contaminants released from waste rocks (i.e., when these materials were put under the water table). These results can therefore be useful for practitioners and contribute to a better mine waste management strategy.

8.2 Practical consideration of co-disposal

To be able to apply the co-disposal concept, there should be a second pit that has been mined out or mining has moved underground and exploiting activities in pits have terminated. The application of various drainage paths composed of waste rocks in the pit can accelerate tailings consolidation. The presence of these drainage paths, however, decrease the volume of tailings that can be disposed of in the pit. The difference of volumetric compression (DV) between models with and without drainage paths was around 22% (i.e., volumetric compression of the tailing mass because of the tailings settlement for model without any drainage paths was around 22% higher than that of the model with WRIs). It is however noted that this estimation was based on results derived from chapter 5 for 1 row of inclusion, and it might be a bit different once various drainage paths were applied. The application of waste rock co-disposal, thus, would depend on the mine site-specific objectives. When the primary purpose of the mine is to prevent the contact between tailings and local environment, then the combination of all of these drainage pathways can be beneficial. On the contrary, if the priority was to maximize the volume of tailings that can be placed in the pit, then using only a permeable envelope could be sufficient. Only non-reactive waste rocks were considered in this study; however, reactive waste rocks might also be applied for the co-disposal technique. As such, the placement of reactive waste rocks under the water table might possibly reduce AMD from these materials (Bussière & Guittonny, 2020).

Movement of water from slurry tailings towards the drainage paths composed of coarse waste rocks may cause clogging of the drainage paths and reduce their drainage capacity. Field observations and physical experimental tests indicated, however, that the effect of tailing migrations on the drainage capacity of the WRI was insignificant (Essayad et al., 2018; Mbemba & Aubertin, 2021b). Segregation of materials within the inclusions might be encountered during the placement of waste rocks materials (with a fine layer interbedded within coarser materials), which might be problematic for the stability analysis of the inclusions (especially when the height of the inclusions in the pit was large) (Aubertin et al., 2016; Maknoon & Aubertin, 2021). These

issues were, however, not included in this study and have been examined in another project at RIME.

Blast damage zone (BDZ) resulting from exploiting activities might have a similar effect of permeable envelope and it can, therefore, act as a natural pervious surround (Cameron & Dave, 2015; Rousseau & Pabst, 2020). Transportation of these mine waste down to the bottom of the pit might be expensive, and might increase time and energy costs to build the inclusions.

8.3 Recommendations for prospective works

In addition to the results obtained in this thesis, further recommendation was proposed to further investigate the consolidation behaviour of tailings, especially the interaction with WRIs, which includes:

- A thorough evaluation on the factors affecting the values of the effective stress applied on the tailings samples (i.e., effects of friction between tailings and column wall, loading system, degree of saturation, and the integration of the measurement of hydraulic conductivity in the column test) to improve the precision of the constitutive relations of tailings is recommended.
- Higher loads should be applied in column tests to cover the loading range that might be expected in practice, especially for the case of disposal in a pit. Colum wall can also be simulated to better represent the real conditions in the laboratory.
- Other constitutive models that can capture the plastic volumetric strain of the materials (Cap-Yield model, plastic hardening model and Modified Cam-clay model) with the integration of continuous update of stiffness and hydraulic conductivity can be utilized to investigate consolidation properties of tailings.
- The change in the void ratio induced by the volumetric strain of materials should be captured, which, in turn, can be used to estimate the change of hydraulic conductivity of the tailings. The change of dried density, void ratio should also be monitored to better represent the tailings settlement evolutions. Evolution of hydraulic conductivity along the permeable envelope should also be monitored.

- Different analysis scheme to perform consolidation behaviour of tailings in Flac3D (e.g., fast-flow scheme and uncoupled scheme) might be applied to reduce the computational times, especially for large-scale models.
- Compression column tests were used to validate the developed approach, intermediate laboratory scale or pilot tests in the field with the installation of WRIs are recommended to comprehensively validate the approach and further demonstrate the capability of the approach in examining the consolidation behaviour of tailings deposited in a real pit.
- Interaction between tailings and permeable envelope and the local environment can be evaluated. Flux to the surface, WRI and permeable envelope should be monitored in the simulations. These parameters can be valuable input for the field application (i.e., the capacity of the pumping system for the water management to ensure that they have hydraulic capacity to manage water flowing to the drainage paths).
- Desaturation, desiccation, and creep (if any) (Fourie et al., 2022) should also be considered.

Additional recommendations are provided for a comprehensive application of co-disposal approach in a pit:

- More complex configuration (orthogonal inclusions) of WRIs or in case where several rows of inclusions were installed can be simulated by using advanced mesh generation tools (e.g., Griddle) (Guotao et al., 2020).
- Regarding the reclamation operations, these can also be coupled in the simulations to investigate the influences of tailings post settlement on the cover systems using Flac3D (Zhou et al., 2019).

REFERENCES

Abdulnabi, A., Amoako, K., Moran, D., Vanadara, K., Aldaeef, A. A., Esmaeilzadeh, A., . . . Simms, P. (2022). Evaluation of candidate polymers to maximize geotechnical performance of oil sands tailings. *Canadian Geotechnical Journal, 59*(3), 359-371. https://doi.org/10.1139/cgj-2020-0714

Agapito, L. A. (2015). *Numerical Evaluation of One-Dimensional Large-StrainConsolidation of Mine Tailings* [Master thesis, Colorado State University].

Agapito, L. A., & Bareither, C. A. (2018). Application of a one-dimensional large-strain consolidation model to a full-scale tailings storage facility. *Minerals Engineering, 119*, 38-48. https://doi.org/https://doi.org/10.1016/j.mineng.2018.01.013

Ahmed, S. I., & Siddiqua, S. (2014). A review on consolidation behavior of tailings. *International Journal of Geotechnical Engineering, 8*(1), 102-111. https://doi.org/10.1179/1939787913Y.0000000012

Amos, R. T., Blowes, D. W., Bailey, B. L., Sego, D. C., Smith, L., & Ritchie, A. I. M. (2015). Waste-rock hydrogeology and geochemistry. *Applied Geochemistry, 57*, 140-156. https://doi.org/https://doi.org/10.1016/j.apgeochem.2014.06.020

ASTM D2435/D2435M − 11. *Standard Test Methods for One-Dimensional Consolidation Properties of Soils Using Incremental Loading* (ASTM International.

ASTM D2487-17. (2017). *Standard practice for classification of soils for engineering purposes (Unified Soil Classification System)* (ASTM International.

ASTM D5856. (2015). *Standard test method for measurement of hydraulic conductivity of porous material using a rigid-wall, compaction-mold permeameter: West Conshohocken Philadelphia* (ASTM International.

ASTM D6913/D6913M − 17. (2017). *Standard Test Methods for Particle-Size Distribution (Gradation) of Soils Using Sieve Analysis* (ASTM International.

ASTM D7928 − 17. (2017). *Standard Test Method for Particle-Size Distribution (Gradation) of Fine-Grained Soils Using the Sedimentation (Hydrometer) Analysis* (ASTM International.

Atkinson, M. S., & Eldred, P. J. L. (1981). Consolidation of soil using vertical drains. *Géotechnique, 31*(1), 33-43. https://doi.org/10.1680/geot.1981.31.1.33

Aubertin, M. (2013). *Waste rock disposal to improve the geotechnical and geochemical stability of piles.* 23rd World Mining Congress, Montreal, Canada.

Aubertin, M. (2018). *Waste rock inclusions in tailings impoundment: analysis (and design) based on the Canadian Malartic Mine.* Mines and the environment, Rouyn Noranda, Quebec, Canada.

Aubertin, M., Bussiere, B., & Chapuis, R. P. (1996). Hydraulic conductivity of homogenized tailings from hard rock mines. *Canadian Geotechnical Journal, 33*(3), 470-482. https://doi.org/10.1139/t96-068

Aubertin, M., Bussière, B., Pabst, T., James, M., & Mbonimpa, M. (2016). *Review of reclamation techniques for acid generating mine wastes upon closure of disposal sites.* Geo-Chicago 2016, Chicago, Illinois, USA. https://doi.org/10.1061/9780784480137.034

Aubertin, M., Li, L., Arnold, S., Belem, T., Bussiere, B., Benzaazoua, M., & Simon, R. (2003). *Interaction between backfill and rock mass in narrow stopes.* Soil and Rock America 2003, Cambridge, Mass. (Vol. 1, pp. 1157–1164).

Aubertin, M., Mbonimpa, M., Jolette, D., Bussière, B., Chapuis, R. P., James, M., & Riffon, O. (2002). *Geotechnical stability of tailings impoundments Mining: problems and control methods*. Industrial NSERC Polytechnic Chair - UQAT in Environment and Mine Waste Management.

Awoh, A. S., Mbonimpa, M., Bussière, B., Plante, B., & Bouzahzah, H. (2014). Laboratory Study of Highly Pyritic Tailings Submerged Beneath a Water Cover Under Various Hydrodynamic Conditions. *Mine Water and the Environment, 33*(3), 241-255. https://doi.org/10.1007/s10230-014-0264-x

Azam, S., & Li, Q. (2010). Tailings Dam Failures: A Review of the Last One Hundred Years. *Geotechnical news, 28*, 50-53. https://ksmproject.com/wp-content/uploads/2017/08/Tailings-Dam-Failures-Last-100-years-Azam2010.pdf

Babaoglu, Y., & Simms, P. (2020). Improving Hydraulic Conductivity Estimation for Soft Clayey Soils, Sediments, or Tailings Using Predictors Measured at High-Void Ratio. *Journal of Geotechnical and Geoenvironmental Engineering, 146*(10), 06020016. https://doi.org/doi:10.1061/(ASCE)GT.1943-5606.0002344

Barksdale, R. D. (1987). *Applications of the State of the Art of Stone Columns –Liquefaction, Local Bearing Failure, and Example Calculations*. Washington DC: US Army Corps of Engineers.

Barron, R. A. (1948). Consolidation of fine-grained soils by drain wells. *Transactions of the ASCE, 113*, 718–742.

Bartholomeeusen, G., Sills, G. C., Znidarčić, D., Kesteren, W. V., Merckelbach, L. M., Pyke, R., . . . Chan, D. (2002). Sidere: numerical prediction of large-strain consolidation. *Géotechnique, 52*(9), 639-648. https://doi.org/10.1680/geot.2002.52.9.639

Basack, S., Indraratna, B., Rujikiatkamjorn, C., & Siahaan, F. (2015). Chapter 26 - Theoretical and Numerical Perspectives on Performance of Stone-Column-Improved Soft Ground with Reference to Transport Infrastructure. In B. Indraratna, J. Chu, & C. Rujikiatkamjorn (Eds.), *Ground Improvement Case Histories* (pp. 751-795). Butterworth-Heinemann.

Basack, S., Siahaan, F., Indraratna, B., & Rujikiatkamjorn, C. (2018). Stabilized Soft-Soil Performance Influenced by Clogging and Lateral Deformation: Laboratory and Numerical Evaluation. *International Journal of Geomechanics, 18*(6), 04018058. https://doi.org/doi:10.1061/(ASCE)GM.1943-5622.0001148

Benzaazoua, M., Fall, M., & Belem, T. (2004). A contribution to understanding the hardening process of cemented pastefill. *Minerals Engineering, 17*(2), 141-152. https://doi.org/https://doi.org/10.1016/j.mineng.2003.10.022

Bergado, D. T., Alfaro, M. C., & Balasubramaniam, A. S. (1993). Improvement of soft Bangkok clay using vertical drains. *Geotextiles and Geomembranes, 12*(7), 615-663. https://doi.org/https://doi.org/10.1016/0266-1144(93)90032-J

Bergado, D. T., Balasubramaniam, A. S., Fannin, R. J., & Holtz, R. D. (2002). Prefabricated vertical drains (PVDs) in soft Bangkok clay: a case study of the new Bangkok International

Airport project. *Canadian Geotechnical Journal, 39*(2), 304-315. https://doi.org/10.1139/t01-100

Bhuiyan, I., Azam, S., & Landine, P. (2015). Consolidation Behavior of a Uranium Tailings Storage Facility in Saskatchewan. *Journal of Hazardous, Toxic, and Radioactive Waste, 19*(4), 040150051-040150057. https://doi.org/doi:10.1061/(ASCE)HZ.2153-5515.0000281

Biot, M. A. (1941). General theory of three-dimensional consolidation. *Appl. Physics, 12*(2).

Blight, G. E. (2010). *Geotechnical engineering for mine waste storage facilities*. CRC Press.

Bolduc, F. (2012). *Une étude sur l'utilisation des roches stériles comme inclusions drainantes dans les résidus miniers* [Mémoire de maîtrise, École Polytechnique de Montréal].

Bolduc, F., & Aubertin, M. (2014). Numerical investigation of the influence of waste rock inclusions on tailings consolidation. *Canadian Geotechnical Journal, 51*(9), 1021-1032. https://doi.org/10.1139/cgj-2013-0137

Bonin, M. D., Nuth, M., Dagenais, A.-M., & Cabral, A. R. (2014). Experimental Study and Numerical Reproduction of Self-Weight Consolidation Behavior of Thickened Tailings. *Journal of Geotechnical and Geoenvironmental Engineering, 140*(12), 04014068. https://doi.org/doi:10.1061/(ASCE)GT.1943-5606.0001179

Boudrias, G. (2018). *Évaluation numérique et expérimentale du drainage et de la consolidation de résidus miniers à proximité d'une inclusion de roches stériles* [Mémoire de maîtrise, École Polytechnique de Montréal].

Bussière, B. (2007). Colloquium 2004: Hydrogeotechnical properties of hard rock tailings from metal mines and emerging geoenvironmental disposal approaches. *Canadian Geotechnical Journal, 44*(9), 1019-1052. https://doi.org/10.1139/t07-040

Bussière, B., & Guittonny, M. (2020). *Hard Rock Mine Reclamation From Prediction to Management of Acid Mine Drainage*. CRC Press.

Cameron, H., & Dave, L. (2015). *In-pit Tailings Disposal at Langer Heinrich – Tailings Storage Facilities in a Unique Hydrogeological Setting.* Tailings and Mine Waste Management for

the 21st Century Sydney. https://dxi97tvbmhbca.cloudfront.net/upload/user/image/Hore-Luppnow-In-pit_Tailings_Disposal_20152020022721025057 3.pdf

Cargill, K. W. (1984). Prediction of Consolidation of Very Soft Soil. *Journal of Geotechnical Engineering, 110*(6), 775-795. https://doi.org/doi:10.1061/(ASCE)0733-9410(1984)110:6(775)

Carrier, W. D., Bromwell, L. G., & Somogyi, F. (1983). Design Capacity of Slurried Mineral Waste Ponds. *Journal of Geotechnical Engineering, 109*(5), 699-716. https://doi.org/doi:10.1061/(ASCE)0733-9410(1983)109:5(699)

Carrillo, N. (1942). Simple two- and three-dimensional cases in the theory of consolidation of soils. *Mathematical Physics, 21* (1), 1–5.

Casagrande, L., & Poulos, S. (1969). ON THE EFFECTIVENESS OF SAND DRAINS. *Canadian Geotechnical Journal, 6*(3), 287-326. https://doi.org/10.1139/t69-030

Chapuis, R. P. (2004). Predicting the saturated hydraulic conductivity of sand and gravel using effective diameter and void ratio. *Canadian Geotechnical Journal, 41*(5), 787-795. https://doi.org/10.1139/t04-022

Chapuis, R. P. (2012). Predicting the saturated hydraulic conductivity of soils: a review. *Bulletin of Engineering Geology and the Environment, 71*(3), 401-434. journal article. https://doi.org/10.1007/s10064-012-0418-7

Chapuis, R. P., & Aubertin, M. (2003). On the use of the Kozeny - Carman equation to predict the hydraulic conductivity of soils. *Canadian Geotechnical Journal, 40*(3), 616-628. https://doi.org/10.1139/t03-013

Coffin, J. (2010). *A 3D Model for Slurry Storage Facilities. Boulder, Colorado* [PhD, University of Colorado].

Contreras, C., Yniesta, S., & Aubertin, M. (2020). *Seismic and post-seismic stability of tailings impoundments, considering the effect of reinforcement inclusions.* Paper presented at the 73rd Canadian Geotechnical Conference (GeoVirtual 2020), Online.

Cui, L., & Fall, M. (2016). An evolutive elasto-plastic model for cemented paste backfill. *Computers and Geotechnics, 71*, 19-29. https://doi.org/https://doi.org/10.1016/j.compgeo.2015.08.013

Das, B. (2010). *Principles of Geotechnical engineering*. Cengage Learning.

Davies, M. P. (2002). Tailings Impoundment Failures: Are Geotechnical Engineers Listening? *Geotechnical News*, 31-36. https://miningquiz.com/pdf/Impoundments/Dam_failuresDavies2002.pdf

Dobchuk, B., Nichol, C., Wilson, G. W., & Aubertin, M. (2013). Evaluation of a single-layer desulphurized tailings cover. *Canadian Geotechnical Journal, 50*(7), 777-792. https://doi.org/10.1139/cgj-2012-0119

Dubuc, J., Pabst, T., & Aubertin, M. (2017). *An assessment of the hydrogeological response of the flow control layer installed on the experimental waste rock pile at the lac Tio mine.* 70th Canadian Geotechnical Conference (GeoOttawa 2017), Ottawa, ON, Canada.

Essayad, K. (2015). *Développement de protocoles expérimentaux pour caractériser la consolidation de résidus miniers saturés et non saturés à partir d'essais de compression en colonne* [Mémoire de maîtrise, École Polytechnique de Montréal].

Essayad, K., & Aubertin, M. (2021). Consolidation of hard rock tailings under positive and negative pore-water pressures: testing procedures and experimental results. *Canadian Geotechnical Journal, 58*(1), 49-65. https://doi.org/10.1139/cgj-2019-0594

Essayad, K., Pabst, T., Chapuis, R. P., & Aubertin, M. (2018). *An experimental study of tailings migration through waste rock inclusions.* 71st Canadian Geotechnical Conference (GeoEdmonton 2018), Edmonton, AB, Canada.

Fahey, M., Helinski, M., & Fourie, A. (2010). Consolidation in accreting sediments: Gibson's solution applied to backfilling of mine stopes. *Géotechnique, 60*(11), 877-882. https://doi.org/10.1680/geot.9.P.078

Fala, O., Molson, J., Aubertin, M., & Bussière, B. (2005). Numerical Modelling of Flow and Capillary Barrier Effects in Unsaturated Waste Rock Piles. *Mine Water & the Environment, 24*(4), 172-185. journal article. https://doi.org/10.1007/s10230-005-0093-z

Ferdosi, B., James, M., & Aubertin, M. (2015a). Effect of waste rock inclusions on the seismic stability of an upstream raised tailings impoundment: a numerical investigation. *Canadian Geotechnical Journal, 52*(12), 1930-1944. https://doi.org/10.1139/cgj-2014-0447

Ferdosi, B., James, M., & Aubertin, M. (2015b). Investigation of the Effect of Waste Rock Inclusions Configuration on the Seismic Performance of a Tailings Impoundment. *Geotechnical and Geological Engineering, 33*(6), 1519-1537. https://doi.org/10.1007/s10706-015-9919-z

Fourie, A., Ramon, V., Annika, B., Luis Alberto, T.-C., & Dobroslav, Z. (2022). *Geotechnics of mine tailings: a 2022 State of the Art.* the 20th ICSMGE-State of the Art and Invited Lectures, Sydney, Australia.

Fox, P. J. (1999). Solution Charts for Finite Strain Consolidation of Normally Consolidated Clays. *Journal of Geotechnical and Geoenvironmental Engineering, 125*(10), 847-867. https://doi.org/doi:10.1061/(ASCE)1090-0241(1999)125:10(847)

Fredlund, D. G., & Hasan, J. U. (1979). One-dimensional consolidation theory: unsaturated soils. *Canadian Geotechnical Journal, 16*(3), 521-531. https://doi.org/10.1139/t79-058

Fredlund, M., Donaldson, M., & Chaudhary, K. (2015). *Pseudo 3-D deposition and large-strain consolidation modeling of tailings deep deposits.* Tailings and Mine Waste, Vancouver, BC.

Fredlund, M. D., Donaldson, M., & Gitirana, G. G. (2009). *Large Strain 1D, 2D and 3D consolidation modeling of tailings*. SoilVision Systems Ltd, Saskatoon, SK, Canada. https://communities.bentley.com/products/geotech-analysis/w/wiki/53216/large-strain-1d-2d-and-3d-consolidation-modeling-of-mine-tailings.

FSCONSOL. (1999). *FSCONSOL User's Manual*.

Gibson, R. E. (1958). The Progress of Consolidation in a Clay Layer Increasing in Thickness with Time. *Géotechnique, 8*(4), 171-182. https://doi.org/10.1680/geot.1958.8.4.171

Gibson, R. E., England, G. L., & Hussey, M. J. L. (1967). The Theory of One-Dimensional Consolidation of Saturated Clays. *Géotechnique, 17*(3), 261-273. https://doi.org/10.1680/geot.1967.17.3.261

Gibson, R. E., Schiffman, R. L., & Cargill, K. W. (1981). The theory of one-dimensional consolidation of saturated clays. II. Finite nonlinear consolidation of thick homogeneous layers. *Canadian Geotechnical Journal, 18*(2), 280-293. https://doi.org/10.1139/t81-030

Guerin, F., Wilson, S., & Nicholson, R. (2006). *Optimizing In-Pit Disposal of Problematic Waste Rock using Leaching Tests, Portable XRF, Block and Mass Transport Models.* 13th Annual British Columbia MEND/ML/ARD Workshop, Vancouver, Canada.

Guetif, Z., Bouassida, M., & Debats, J. M. (2007). Improved soft clay characteristics due to stone column installation. *Computers and Geotechnics, 34*(2), 104-111. https://doi.org/https://doi.org/10.1016/j.compgeo.2006.09.008

Guotao, M., Jianrong, X., Anchi, S., & Christine, D. (2020). *Griddle generation of FLAC3D models for the Baihetan Dam project.* Applied Numerical Modeling in Geomechanics, Minneapolis, USA.

Han, J. (2015). *Principles and Practice of Ground Improvement*. Wiley.

Han, J., & Ye, S. L. (2002). A Theoretical Solution for Consolidation Rates of Stone Column‐Reinforced Foundations Accounting for Smear and Well Resistance Effects. *International Journal of Geomechanics, 2*(2), 135-151. https://doi.org/doi:10.1061/(ASCE)1532-3641(2002)2:2(135)

Hansbo, S. (1981). *Consolidation of fine-grained soils by prefabricated drains and lime column installation.* In Proceedings of 10th International Conference on Soil Mechanics and Foundation Engineering, Rotterdam, The Netherlands (Vol. 3, pp. 677–682).

Hansbo, S., Jamiolkowski, M., & Kok, L. (1981). Consolidation by vertical drains. *Géotechnique, 31*(1), 45-66. https://doi.org/10.1680/geot.1981.31.1.45

Hao, S., & Pabst, T. (2022). Experimental Investigation and Prediction of the Permanent Deformation of Crushed Waste Rock Using an Artificial Neural Network Model. *International Journal of Geomechanics, 22*(5), 04022032. https://doi.org/doi:10.1061/(ASCE)GM.1943-5622.0002363

Hawley, M., & Cunning, J. (2017). *Guidelines for Mine Waste Dump and Stockpile Design*. Csiro Publishing.

Holtz, R. D. (1987). Preloading with prefabricated vertical strip drains. *Geotextiles and Geomembranes, 6*(1), 109-131. https://doi.org/https://doi.org/10.1016/0266-1144(87)90061-6

Holtz, R. D., & Kovacs, W. D. (1981). *An Introduction to Geotechnical Engineering*. Englewood Cliffs, N J: Prentice Hall.

Hu, L., Wu, H., Zhang, L., Zhang, P., & Wen, Q. (2017). Geotechnical Properties of Mine Tailings. *Journal of Materials in Civil Engineering, 29*(2), 04016220. https://doi.org/doi:10.1061/(ASCE)MT.1943-5533.0001736

Hustrulid W, Kutcha M, & R, M. (2013). *Open pit mine planning and design*. CRC Press.

Imai, G. (1979). Development of a new consolidation test procedure using seepage *Soils and foundations 19*(3), 45-60. https://doi.org/10.3208/sandf1972.19.3_45

Imai, G. (1981). Experimental studies on sedimentation mechanism and sediment formation of clay materials. *Soils and foundations 21*(1), 7-20. https://doi.org/10.3208/sandf1972.21.7

Indraratna, B. (2015). Chapter 1 - Recent Advances in Soft Soil Consolidation. In B. Indraratna, J. Chu, & C. Rujikiatkamjorn (Eds.), *Ground Improvement Case Histories* (pp. 3-32). Butterworth-Heinemann.

Indraratna, B., Rujikiatkamjorn, C., Balasubramaniam, A. S., & McIntosh, G. (2012). Soft ground improvement via vertical drains and vacuum assisted preloading. *Geotextiles and Geomembranes, 30*, 16-23. https://doi.org/https://doi.org/10.1016/j.geotexmem.2011.01.004

Indraratna, B., Rujikiatkamjorn, C., & Sathananthan, I. (2005). Analytical and numerical solutions for a single vertical drain including the effects of vacuum preloading. *Canadian Geotechnical Journal, 42*(4), 994-1014. https://doi.org/10.1139/t05-029

Itasca. (2021). *FLAC3D 7.0 (Fast Lagrangian Analysis of Continua in 3 Dimensions) User Manual*. Itasca Consulting Group, Inc.

Ito, M., & Azam, S. (2013). Large-strain consolidation modeling of mine waste tailings. *Environmental Systems Research, 2*(1), 7. https://doi.org/10.1186/2193-2697-2-7

Jahanbakhshzadeh, A., Aubertin, M., & Li, L. (2017). Three-dimensional stress state in inclined backfilled stopes obtained from numerical simulations and new closed-form solution. *Canadian Geotechnical Journal, 55*(6), 810-828. https://doi.org/10.1139/cgj-2016-0385

Jahanbakhshzadeh, A., Aubertin, M., Yniesta, S., & Zafarani, A. (2019). *On the seismic response of tailings dikes constructed with the upstream and center-line methods.* 72nd Canadian Geotechnical Conference (GEO 2019), St. John's, Canada.

James, M. (2009). *The use of waste rock inclusions to control the effects of liquefaction in tailings impoundments* [Ph.D. , École Polytechnique de Montréal].

James, M., & Aubertin, M. (2009). *The use of waste rock inclusions in tailings impoundments to improve geotechnical and environmental performance.* Tailings and Mine Waste 2009, Banff, Alberta (pp. 233–245).

James, M., Aubertin, M., & Bussière, B. (2013). *On the use of waste rock inclusions to improve the performance of tailings impoundments.* 18th International Conference on Soil Mechanics and Geotechnical Engineering, Paris, France (pp. 735-738).

Jaouhar, E. M. (2012). *Analyse de l'effet d'inclusions drainantes sur la consolidation de sols fins et de résidus miniers* [Mémoire de maîtrise, École Polytechnique de Montréal].

Jaouhar, E. M., Aubertin, M., & James, M. (2013). *The effect of tailings properties on their consolidation near waste rock inclusions.* 66th Canadian Geotechnical Conference (GeoMontréal 2013), Montréal, Canada.

Jeeravipoolvarn, S. (2010). *Geotechnical Behavior of In-Line Thickened Oil Sands Tailings* [Ph.D., University of Alberta].

Jeeravipoolvarn, S., Chalaturnyk, R. J., & Scott, J. D. (2008). *Consolidation modeling of oil sands fine tailings: history matching.* 61st Canadian Geotechnical Conference, Edmonton, Alberta, Canada (pp. 190 – 197).

Khaled, S. M. (2012). *Geotechnical Investigation of Uranium Tailings* [Master of Applied Science, University of Regina].

Koppula, S. D. (1970). *The consolidation of soil in two dimensions and with moving boundaries* [Ph.D. thesis, University of Alberta].

Lahmira, B., Lefebvre, R., Aubertin, M., & Bussière, B. (2017). Effect of material variability and compacted layers on transfer processes in heterogeneous waste rock piles. *Journal of Contaminant Hydrology, 204*, 66-78. https://doi.org/https://doi.org/10.1016/j.jconhyd.2017.07.004

Larochelle, C. G., Bussière, B., & Pabst, T. (2019). Acid-Generating Waste Rocks as Capillary Break Layers in Covers with Capillary Barrier Effects for Mine Site Reclamation. *Water, Air, & Soil Pollution, 230*(3), 57. https://doi.org/10.1007/s11270-019-4114-0

Lee, K., & Sills, G. C. (1981). The consolidation of a soil stratum, including self-weight effects and large strains. *International Journal for Numerical and Analytical Methods in Geomechanics, 5*(4), 405-428. https://doi.org/https://doi.org/10.1002/nag.1610050406

Leo, C. J. (2004). Equal Strain Consolidation by Vertical Drains. *Journal of Geotechnical and Geoenvironmental Engineering, 130*(3), 316-327. https://doi.org/doi:10.1061/(ASCE)1090-0241(2004)130:3(316)

Lévesque, R. (2019). *Consolidation des résidus miniers dans les fosses en présence d'inclusions de roches stériles* [Mémoire de maîtrise, Ecole Polytechnic Montreal].

Li, L., & Aubertin, M. (2009a). Horizontal pressure on barricades for backfilled stopes. Part I: Fully drained conditions. *Canadian Geotechnical Journal, 46*(1), 37-46. https://doi.org/10.1139/T08-104

Li, L., & Aubertin, M. (2009b). Numerical Investigation of the Stress State in Inclined Backfilled Stopes. *International Journal of Geomechanics, 9*(2), 52-62. https://doi.org/doi:10.1061/(ASCE)1532-3641(2009)9:2(52)

Li, L., & Aubertin, M. (2009c). A Three-Dimensional Analysis of the Total and Effective Stresses in Submerged Backfilled Stopes. *Geotechnical and Geological Engineering, 27*(4), 559-569. https://doi.org/10.1007/s10706-009-9257-0

Li, W., Coop, M. R., Senetakis, K., & Schnaid, F. (2018). The mechanics of a silt-sized gold tailing. *Engineering Geology, 241*, 97-108. https://doi.org/https://doi.org/10.1016/j.enggeo.2018.05.014

Lindsay, M. B. J., Moncur, M. C., Bain, J. G., Jambor, J. L., Ptacek, C. J., & Blowes, D. W. (2015). Geochemical and mineralogical aspects of sulfide mine tailings. *Applied Geochemistry, 57*, 157-177. https://doi.org/https://doi.org/10.1016/j.apgeochem.2015.01.009

Liu, J. C., & Znidarčić, D. (1991). Modeling One Dimensional Compression Characteristics of Soils. *Journal of Geotechnical Engineering, 117*(1), 162-169. https://doi.org/10.1061/(ASCE)0733-9410(1991)117:1(162)

Liu, K. W., & Rowe, R. K. (2015). Numerical modelling of prefabricated vertical drains and surcharge on reinforced floating column-supported embankment behaviour. *Geotextiles and Geomembranes, 43*(6), 493-505. https://doi.org/https://doi.org/10.1016/j.geotexmem.2015.05.006

Lu, M., Wang, S., Sloan, S. W., Sheng, D., & Xie, K. (2015). Nonlinear consolidation of vertical drains with coupled radial–vertical flow considering well resistance. *Geotextiles and Geomembranes, 43*(2), 182-189. https://doi.org/https://doi.org/10.1016/j.geotexmem.2014.12.001

Maknoon, M. (2016). *Slopes stability analyses of waste rock piles under unsaturated conditions following large precipitations* [Ph.D., Ecole Polytechnique de Montreal].

Maknoon, M., & Aubertin, M. (2021). On the Use of Bench Construction to Improve the Stability of Unsaturated Waste Rock Piles. *Geotechnical and Geological Engineering, 39*(2), 1425-1449. https://doi.org/10.1007/s10706-020-01567-0

Martin, V. (2017). *Controlling water infiltration in waste rock piles: design, construction, and monitoring of a large-scale in-situ pilot study.* 70th Canadian Geotechnical Conference (GeoOttawa 2017), Ottawa, ON, Canada.

Maryam, M. (2016). *Slope stability analysis of waste rock piles under unsaturated conditions following large precipitations* [Ph.D., Polytechnique Montreal].

Matt, G. (2015). *Geotechnical Characterization of Bauxite Residue* [Ph.D., The University of Texas at Austin].

Mbemba, F., & Aubertin, M. (2021a). Physical and numerical modelling of drainage and consolidation of tailings near a vertical waste rock inclusion. *Canadian Geotechnical Journal, 0*(0), 1-14. https://doi.org/10.1139/cgj-2020-0372

Mbemba, F., & Aubertin, M. (2021b). Physical Model Testing and Analysis of Hard Rock Tailings Consolidation Considering the Effect of a Drainage Inclusion. *Geotechnical and Geological Engineering, 39*(4), 2777-2798. https://doi.org/10.1007/s10706-020-01656-0

Mbonimpa, M., Aubertin, M., Chapuis, R. P., & Bussière, B. (2002). Practical pedotransfer functions for estimating the saturated hydraulic conductivity. *Geotechnical & Geological Engineering, 20*(3), 235-259. journal article. https://doi.org/10.1023/a:1016046214724

McDonald, L., & Lane, J. C. (2010). *Consolidation of in-Pit tailings.* Mine Waste 2010, Perth, Australia (pp. 49-62).

McLemore, V. T., Fakhimi, A., van Zyl, D., & et al. (2009). *Literature review of other rock piles: Characterization, weathering, and stability*. Report OF–517, Questa Rock Pile Weathering Stability Project. New Mexico Bureau of Geology and Mineral Resources.

MEND. (2015). MEND Report 2.36.1 In-Pit Disposal of Reactive Mine Wastes: Approaches, Update and Case Study Results.

Mittchell, J. K., & Soga, K. (2005). *Fundamentals of Soil Behavior (3rd edition)*. New Jersey : John Wiley et Sons.

Moïse, R., & Thomas, P. (2018). *3D numerical assessment of the permeable envelope concept for inpit disposal of reactive mine wastes.* 71st Canadian Geotechnical Conference (GeoEdmonton 2018), Edmonton, Canada.

Molson, J. W., Fala, O., Aubertin, M., & Bussière, B. (2005). Numerical simulations of pyrite oxidation and acid mine drainage in unsaturated waste rock piles. *Journal of Contaminant Hydrology, 78*(4), 343-371. https://doi.org/https://doi.org/10.1016/j.jconhyd.2005.06.005

Morgenstern, N., Vick, S., Viotti, C., & Watts, B. (2016). *Report on the Immediate Causes of the Failure of the Fundão Dam. Fundão Tailings Dam Review Panel*.

Morris, P. H. (2002). Analytical Solutions of Linear Finite-Strain One-Dimensional Consolidation. *Journal of Geotechnical and Geoenvironmental Engineering, 128*(4), 319-326. https://doi.org/doi:10.1061/(ASCE)1090-0241(2002)128:4(319)

Mudd, Smith. H. D, Kyle. G , & Thompson. A (2011). *In-Pit Tailings – World's Best Practice for Long-Term Management of Tailings.* Metallurgical Plant Design and Operating Strategies, Perth, Australia.

Newson, T., Dyer, T., Adam, C., & Sharp, S. (2006). Effect of Structure on the Geotechnical Properties of Bauxite Residue. *Journal of Geotechnical and Geoenvironmental Engineering, 132*(2), 143-151. https://doi.org/doi:10.1061/(ASCE)1090-0241(2006)132:2(143)

Nguyen, D., & Pabst, T. (2020). *Comparative experimental study of consolidation properties of hard rock mine tailings.* 73rd Canadian Geotechnical Conference (GeoVirtual 2020), Online.

Nguyen, D., & Pabst, T. (2022a). Consolidation behavior of various types of slurry tailings co-disposed with waste rock inclusions: a numerical study. *Environmental Earth Sciences (Under reviewed)*.

Nguyen, D., & Pabst, T. (2022b). Numerical study of slurry tailings consolidation considering continuous update of material properties. *International Journal of Mining Science and Technology (Under reviewed)*.

Nordstrom, D. K., Blowes, D. W., & Ptacek, C. J. (2015). Hydrogeochemistry and microbiology of mine drainage: An update. *Applied Geochemistry, 57*, 3-16. https://doi.org/https://doi.org/10.1016/j.apgeochem.2015.02.008

Pabst, T., Aubertin, M., Bussière, B., & Molson, J. (2017). Experimental and numerical evaluation of single-layer covers placed on acid-generating tailings. *Geotechnical and Geological Engineering, 35*(4), 1421-1438. journal article. https://doi.org/10.1007/s10706-017-0185-0

Pabst, T., Bussière, B., Aubertin, M., & Molson, J. (2018). Comparative performance of cover systems to prevent acid mine drainage from pre-oxidized tailings: A numerical hydro-geochemical assessment. *Journal of Contaminant Hydrology, 214*, 39-53. https://doi.org/https://doi.org/10.1016/j.jconhyd.2018.05.006

Pépin, N., Aubertin, M., & James, M. (2012). Seismic table investigation of the effect of inclusions on the cyclic behaviour of tailings. *Canadian Geotechnical Journal, 49*(4), 416-426. https://doi.org/10.1139/t2012-009

Peregoedova, A. (2012). *Étude experimentale des propriétés hydrogéologiques des roches stériles à une échelle intermediaire de laboratoire* [Mémoire de maîtrise, École polytechnique Montréal].

Peregoedova, A., Aubertin, M., & Bussière, B. (2013). *Laboratory measurement and prediction of the saturated hydraulic conductivity of mine waste rock.* 66th Canadian Geotechnical Conference (GeoMontreal 2013), Montreal, Quecbec, Canada.

Priestley, D. (2011). *Modeling multidimensional large strain consolidation of tailings* [Master, University of British Columbia].

Pu, H., Song, D., & Fox, P. J. (2018). Benchmark Problem for Large Strain Self-Weight Consolidation. *Journal of Geotechnical and Geoenvironmental Engineering, 144*(5), 06018002. https://doi.org/doi:10.1061/(ASCE)GT.1943-5606.0001872

Qi, S., Simms, P., & Vanapalli, S. (2017). Piecewise-Linear Formulation of Coupled Large-Strain Consolidation and Unsaturated Flow. I: Model Development and Implementation. *Journal*

of Geotechnical and Geoenvironmental Engineering, 143(7), 04017018. https://doi.org/doi:10.1061/(ASCE)GT.1943-5606.0001657

Qin, A., Sun, D. a., Yang, L., & Weng, Y. (2010). A semi-analytical solution to consolidation of unsaturated soils with the free drainage well. *Computers and Geotechnics, 37*(7), 867-875. https://doi.org/https://doi.org/10.1016/j.compgeo.2010.07.006

Qiu, Y. J., & Sego, D. C. (2001). Laboratory properties of mine tailings. *Canadian Geotechnical Journal, 38,*, 183-190. https://doi.org/https://doi.org/10.7939/R3WW7704C

Rana, N. M., Ghahramani, N., Evans, S. G., McDougall, S., Small, A., & Take, W. A. (2021). Catastrophic mass flows resulting from tailings impoundment failures. *Engineering Geology, 292*, 106262. https://doi.org/https://doi.org/10.1016/j.enggeo.2021.106262

Rixner, J. J., Kraemer, S. R., & Smith, A. D. (1986). *Prefabricated vertical drains, Vol. 1 (Eng'g. Guidelines)* (FHWA-RD-86/168). Federal Highway Administration.

Robert, M. (2012). *Evaluation of a Three-Dimensional Model for Slurry Storage Facilities* [Master, University of Colorado].

Robertson, P. K., Lucas de Melo, David J. Williams, & Wilson., G. W. (2019). *Report of the Expert Panel on the Technical Causes of the Failure of Feijão Dam I.*

Rousseau, M. (2021). *Étude numérique de la réduction du transport advectif de contaminants entre les fosses remblayées et l'environnement par l'utilisation de chemins d'écoulements préférentiels* [Ph.D., École polytechnique Montréal].

Rousseau, M., & Pabst, T. (2020). *Blast damaged zone influence on water and solute exchange between backfilled open-pit and the environment.* 73rd Canadian Geotechnical Conference (GeoVirtual 2020), Online.

Rousseau, M., & Pabst, T. (2022). Topology optimization of in-pit codisposal of waste rocks and tailings to reduce advective contaminant transport to the environment. *Structural and Multidisciplinary Optimization, 65*(6), 168. https://doi.org/10.1007/s00158-022-03266-1

Santamarina, J. C., Torres-Cruz, L. A., & Bachus, R. C. (2019). Why coal ash and tailings dam disasters occur. *Science, 364*(6440), 526-528. https://doi.org/doi:10.1126/science.aax1927

Schiffman, R. L. (1982). The consolidation of soft marine sediments. *Geo-Marine Letters, 2*(3-4), 199-203. https://doi.org/10.1007/bf02462763

Schiffman, R. L., Pane, V., & Gibson, R. E. (1984). *The theory of One-Dimensional Consolidation of Saturated Clays IV: An overview of Nonlinear Finite Strain Sedimentation and Consolidation.* ASCE Symposium on Sedimentation/Consolidation Models, San Francisco, USA (pp. 1-29).

Schiffman, R. L., Vick, S. G., & Gibson, R. E. (1988). *Behavior and properties of hydraulic fills.* Hydraulic Fill Structures, New York (pp. 166–202).

Shahsavari, M., & Grabinsky, M. (2014). *Cemented Paste Backfill Consolidation with Deposition-Dependent Boundary Conditions.* 67th Canadian Geotechnical Conference (GeoRegina 2014), Regina, Canada.

Shahsavari, M., & Grabinsky, M. (2015). *Mine backfill porewater pressure dissipation: numerical predictions and field measurements.* 68th Canadian Geotechnical Conference (GeoQuébec 2015), Québec, Canada.

Shan, Z., Ling, D., & Ding, H. (2014). Analytical solution for the 1D consolidation of unsaturated multi-layered soil. *Computers and Geotechnics, 57*, 17-23. https://doi.org/https://doi.org/10.1016/j.compgeo.2013.11.009

Shepherd, R. G. (1989). Correlations of Permeability and Grain Size. *Groundwater, 27*(5), 633-638. https://doi.org/10.1111/j.1745-6584.1989.tb00476.x

Somogyi, F. (1976). *Dewatering And Drainage Of Red Mud Tailings* [Ph.D., University of Michigan].

Somogyi, F. (1980). *Large Strain Consolidation of Fine Grained Slurries.* Presentation at the Canadian Society for Civil Engineering, Winnipeg, Manitoba.

Tan, T. S., Yong, K. Y., Leong, E. C., & Lee, S. L. (1990). Sedimentation of Clayey Slurry. *Journal of Geotechnical Engineering, 116*(6), 885-898. https://doi.org/doi:10.1061/(ASCE)0733-9410(1990)116:6(885)

Taylor, D. W. (1948). *Fundamentals of Soil Mechanics*. John Wiley and Sons Inc.

Townsend, & McVay. (1990). SOA: Large Strain Consolidation Predictions. *Journal of Geotechnical Engineering, 116*(2), 222-243. https://doi.org/doi:10.1061/(ASCE)0733-9410(1990)116:2(222)

Utili, S., Agosti, A., Morales, N., Valderrama, C., Pell, R., & Albornoz, G. (2022). Optimal Pitwall Shapes to Increase Financial Return and Decrease Carbon Footprint of Open Pit Mines. *Mining, Metallurgy & Exploration, 39*(2), 335-355. https://doi.org/10.1007/s42461-022-00546-8

Van Eekelen, S. J. M., Bezuijen, A., & van Tol, A. F. (2013). An analytical model for arching in piled embankments. *Geotextiles and Geomembranes, 39*, 78-102. https://doi.org/https://doi.org/10.1016/j.geotexmem.2013.07.005

Vick, S. G. (1990). *Planning, Design and Analysis of Tailings Dams*. BiTech Publishers Ltd.

Walker, R., & Indraratna, B. (2007). Vertical drain consolidation with overlapping smear zones. *Geotechnique, 57*(5), 463-467. https://doi.org/10.1680/geot.2007.57.5.463

Wang, R., Zeng, F., & Li, L. (2021a). Applicability of Constitutive Models to Describing the Compressibility of Mining Backfill: A Comparative Study. *Processes, 9*(12), 2139. https://www.mdpi.com/2227-9717/9/12/2139

Wang, R., Zeng, F., & Li, L. (2021b). Stability analyses of side-exposed backfill considering mine depth and extraction of adjacent stope. *International Journal of Rock Mechanics and Mining Sciences, 142*, 104735. https://doi.org/https://doi.org/10.1016/j.ijrmms.2021.104735

Wickland, B. E., & Wilson, G. W. (2005). Self-weight consolidation of mixtures of mine waste rock and tailings. *Canadian Geotechnical Journal, 42*(2), 327-339. https://doi.org/10.1139/t04-108

Wickland, B. E., Wilson, G. W., Wijewickreme, D., & Klein, B. (2006). Design and evaluation of mixtures of mine waste rock and tailings. *Canadian Geotechnical Journal, 43*(9), 928-945. https://doi.org/10.1139/t06-058

Wijewickreme, D., Sanin, M. V., & Greenaway, G. R. (2005). Cyclic shear response of fine-grained mine tailings. *Canadian Geotechnical Journal, 42*(5), 1408-1421. https://doi.org/10.1139/t05-058

Wilson, D., Amos, R. T., Blowes, D. W., Langman, J. B., Ptacek, C. J., Smith, L., & Sego, D. C. (2018). Diavik waste rock project: A conceptual model for temperature and sulfide-content dependent geochemical evolution of waste rock – Laboratory scale. *Applied Geochemistry, 89*, 160-172. https://doi.org/https://doi.org/10.1016/j.apgeochem.2017.12.007

Yang, P. (2016). *Investigation of the geomechanical behavior of mine backfill and its interaction with rock walls and barricades* [Ph.D., École Polytechnique de Montréal].

Yang, P., Li, L., & Aubertin, M. (2017). A New Solution to Assess the Required Strength of Mine Backfill with a Vertical Exposure. *International Journal of Geomechanics, 17*(10), 04017084. https://doi.org/doi:10.1061/(ASCE)GM.1943-5622.0000975

Yao, D., & Znidarcic, D. (1997). *User's manual for computer program CONDES0, Report prepared for Florida Institute of Phosphate Research, University of Colorado, Boulder, Colorado*.

Yoshikuni, H., & Nakanodo, H. (1974). Consolidation of soils by vertical drain wells with finite permeability *Soils and foundations 14*(2), 35-46. https://doi.org/10.3208/sandf1972.14.2_35

Zafarani, A., Yniesta, S., & Aubertin, M. (2020). *Effect of Height and Downstream Slope on the Seismic Behavior of Tailings Impoundments Reinforced With Waste Rock Inclusions.* 73rd Canadan Geotechnical Conference (GeoVirtual 2020), Online.

Zhang, J., Yao, Z., Wang, K., Wang, F., Jiang, H., Liang, M., . . . Airey, G. (2021). Sustainable utilization of bauxite residue (Red Mud) as a road material in pavements: A critical review. *Construction and Building Materials, 270*, 121419. https://doi.org/https://doi.org/10.1016/j.conbuildmat.2020.121419

Zhou, Amodio A, & N., B. (2019). *Informed mine closure by multi-dimensional modelling of tailings deposition and consolidation.* Mine Closure 2019, Perth, Australia.

APPENDIX A - VERIFICATION OF COUPLED ANALYSIS OF SOIL CONSOLIDATION IN FLAC3D

The thickness of the saturated soil layer was 10 m resting on the impervious base, large horizontal extent and the water table at the surface of the layer (figure A-1). The 1D consolidation of a soil layer under the application of a surface load of 50 kPa was simulated following a coupled analysis scheme in FLAC3D to verify the capability and reliability of the software in modelling the consolidation analysis (figure A-2). The solution in terms of PWP and displacement at the middle of the layer was then compared with the analytical solution following the Terzaghi's solution (figure A-3, A-4). The model was cycled to a flow time of 5000 seconds. The following properties are assigned for the soil:

Dry bulk modulus, K	5×10^8 Pa
Dry shear modulus, G	2×10^8 Pa
Biot's modulus, M	4×10^9 Pa
Biot's coefficient, α	1.0
Permeability, k	10^{-10} m^2/Pa-sec

Results indicated that the coupled analysis scheme in FLAC3D can produce results on PWP evolution and settlement that were in a very good agreement compared to those obtained from Terzaghi's solution with the differences between numerical and analytical solution always smaller than 2% (figure A-3b, A-4b). It thus indicated that the used of the coupled analysis to investigate the consolidation evolution in FLAC3D is reliable.

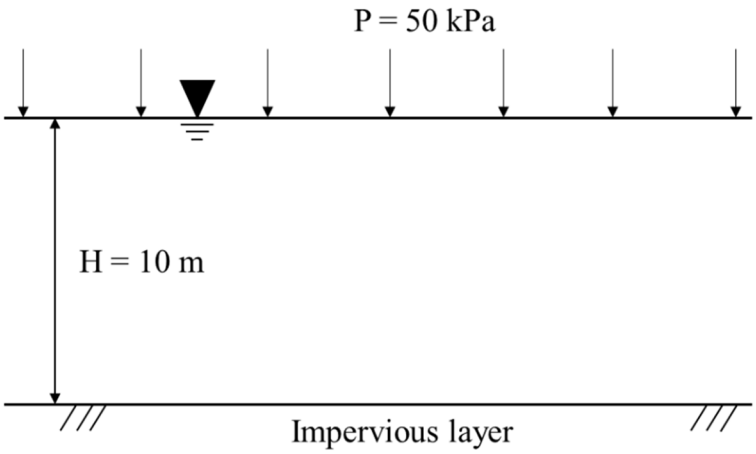

Figure A-1: Soil layer under the application of load.

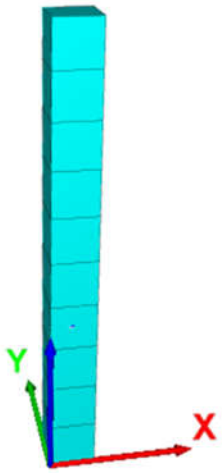

Figure A-2: Simulated domain.

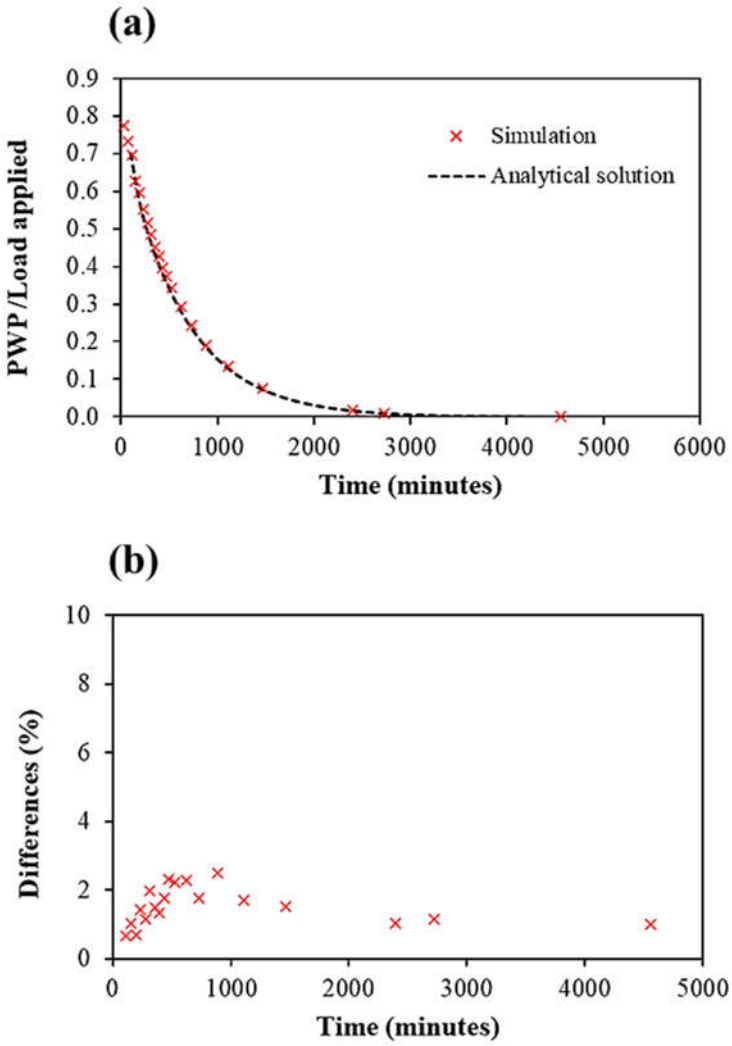

Figure A-3: (a) Comparison of evolution of PWP in 1D consolidation derived from coupled analysis in FLAC3D and analytical solution and (b) Differences between simulated and analytical results.

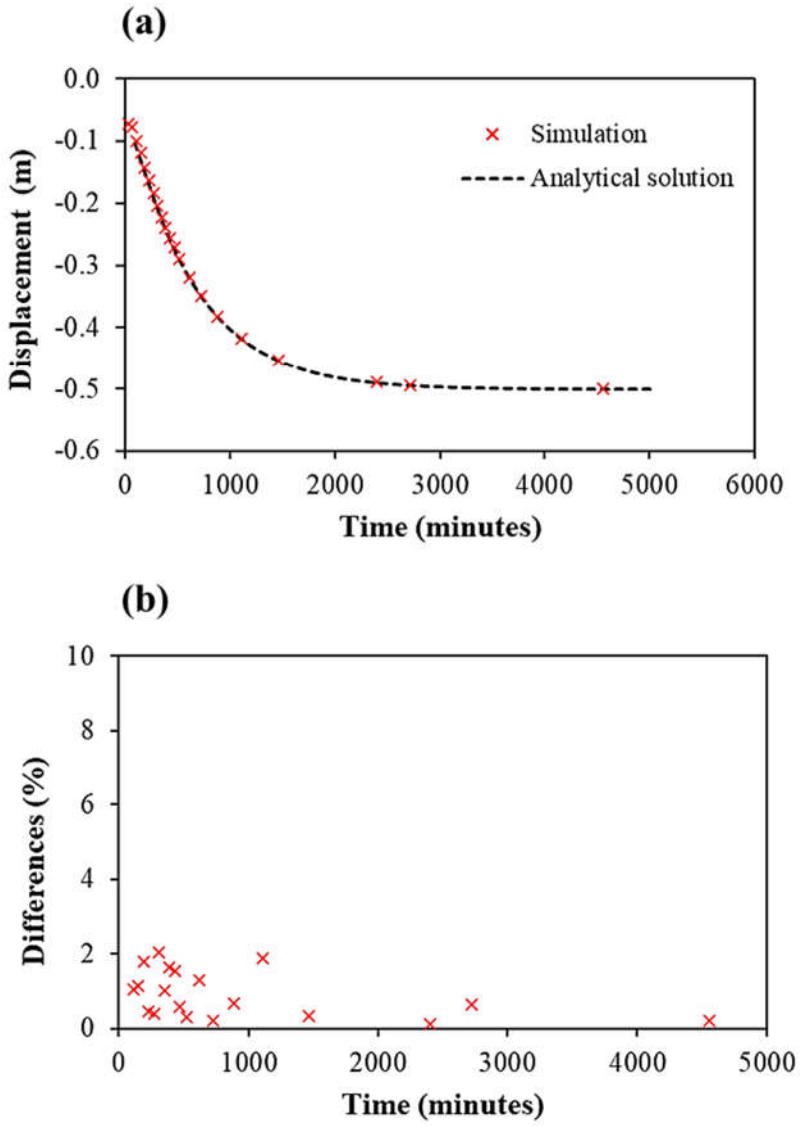

Figure A-4: Comparison of vertical displacement in 1D consolidation derived from coupled analysis in FLAC3D and analytical results.

APPENDIX B - MESH SENSITIVITY ANALYSIS

B1. Influence of the mesh size of the column test models

Since the dissipation of excess PWP in the column test occurred in the vertical direction only, the zone size in the vertical direction was changed to 1, 1.5, 2, 3, 5 and 10 cm respectively to examine the potential effects of the zone size on the dissipation of PWP. Figure B-1 showed the value of time t_{90} at the middle of the column after the apply of the 4th cycle with various mesh sizes of the column. It can be seen that the mesh size had almost no influence on the rate of dissipation of PWP.

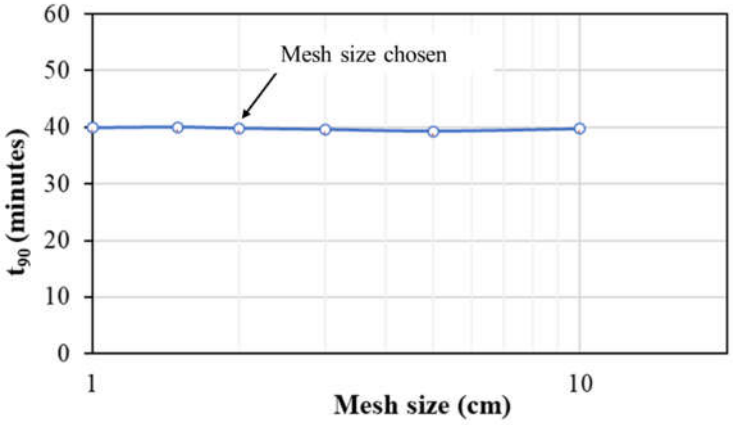

Figure B-1: Time t_{90} at the middle of the column test obtained by numerical models with various mesh sizes.

B2. Influence of the mesh size for models with the presence of WRIs (models of conventional TSF in chapter 5 and of open pit in chapter 6).

Vertical direction:

Since the dissipation of PWP in the vertical direction was not affected by the presence of WRIs, a pseudo 3-D 60 m high model (corresponding to 12 layers) with tailings only was simulated. The mesh size in the vertical direction was changed to 0.5, 1, 2.5 and 5 m respectively. t_{90} was calculated at the elevation of 2.5 m from the bottom of the tailings column after the placement of

layer 5 and layer 7 (figure B-2). The results indicated that the effect of zone size in the vertical direction was insignificant. Thus, the mesh size in the vertical direction for TSF in chapter 5 (1.5 m) and for open pit in chapter 6 (2.5 m) can ensure the stability of the numerical results.

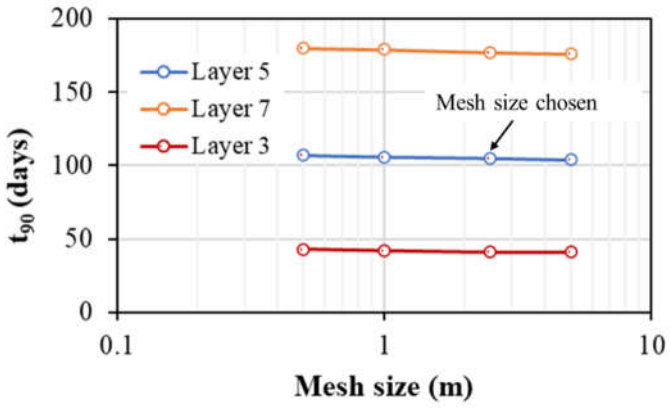

Figure B-2: Time t_{90} at the elevation of 2.5m from the bottom of the model obtained by numerical models with various mesh sizes after the placement of the 3rd, 5th and 7th layers.

Horizontal direction

The dissipation of excess PWP can also occur in the horizontal direction with the presence of the WRIs, models with the tailings co-disposed with WRI was thus run and the horizontal zone size was assigned to various values. The height of the model was 25 m (corresponding to 5 layers), tailings thickness was 16 m, and the thickness of WRI was 2 m (figure B-3). t_{90} was calculated at the elevation of 2.5 m from the bottom of the models after the placement of layer 5 at the horizontal distance of 2 m from the WRI (figure B-4). The result indicated that the horizontal mesh size did have an effect on the stability of the numerical results with the presence of the WRI. It can be seen that the numerical results would be stable if the mesh size was smaller than 2 m, which was also the horizontal mesh size of models in chapter 5. When mesh size was assigned as 4 m (in chapter 6), the dissipation rate could be underestimated by around 17% at locations of 2 m from the WRI, and then decreased to around 13% at 6 m. However, this effect would decrease at locations far away from the WRI.

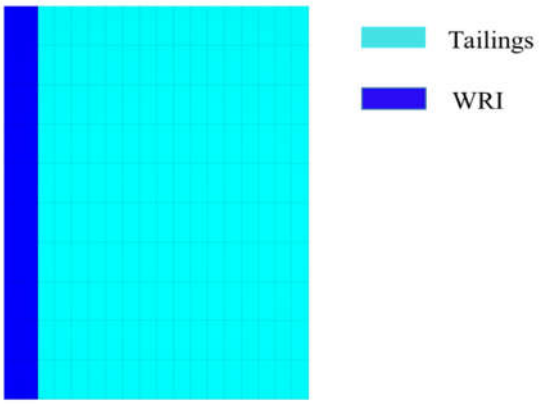

Figure B-3: Simulated domain with the presence of WRI (mesh size = 1 m)

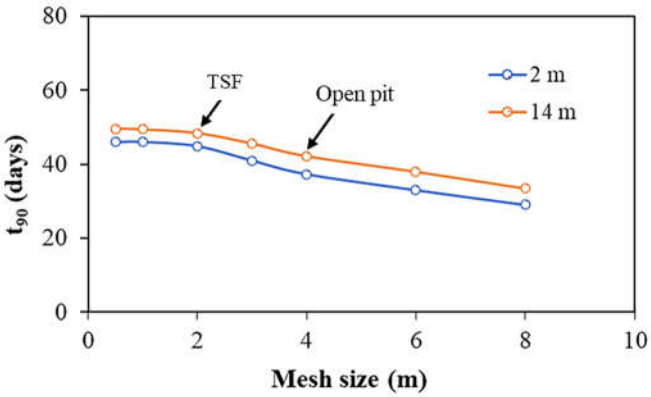

Figure B-4: Time t_{90} at the elevation of 2.5m from bottom of the model and at 2 m and 14 m from the WRI obtained by numerical models with various mesh sizes after the placement of the 5^{th} layer.

APPENDIX C - FISH CODE DEVELOPED TO MODIFY TAILINGS PROPERTIES

```
;input parameters: initial value of Poisson's ratio, dried density, cohesion, friction angle, dilation,
initial porosity, fluid density.
FISH define input
    global p_ratio = 0.28
    global dens = 1.55
    global coh = 0
    global fric = 38
    global dil = 0
    global poros = 0.437
    global f_dens = 1
    ;loading applied
    global load_01 = -3.3
    global load_02 = -26.3
    global load_03 = -55.5
    global load_04 = -80.4
    global load_05 = -95.9
    global load_06 = -116.6
    global load_07 = -139.1
    global load_08 = -158.1
    global load_09 = -178.8
    global load_10 = -198.5
end
@input                                          ;recall the function
=====================================
```

```
; update parameters
FISH define K_update
   Loop foreach local zone zone.list
        ;update of void ratio
      local var_c = 0.814 * (math.abs(zone.stress.effective.zz(zone)))^-0.058
      ;update of permeability
        local perm_01 = 1.24e-6 * (var_c)^4.61
      local perm_02 = Perm_01 * 100
      local perm = (Perm_02 * 1.02e-6)*1000
   End_loop
End
;stiffness update
FISH define E_update
   Loop foreach local zone zone.list
      Local y_mod = 85.6 * math.abs((zone.stress.effective.zz(zone)))^0.74
      local y_min = math.max(180,y_mod)
        ;shear modulus
      local s_mod = y_min / (2.0 * (1.0 + p_ratio))
         ;bulk modulus
      local b_mod = y_min / (3.0 * (1.0 - 2.0 * p_ratio))
   End_loop
end
```

APPENDIX D - EFFECT OF REDUCED BULK MODULUS OF WATER

The water bulk modulus is usually assigned a value of 1-2x10^5 kPa (Itasca, 2021). This value was reduced to 5x10^4 kPa for models in this study to reduce the computation time. Models with the WRI co-disposed with tailings in the simplified TSF (see chapter 5) were run to test the effect of the reduced bulk modulus of water. The evolutions of PWP at the distance of 6 and 14 m from the WRI after the placement of the 3rd layer was calculated (figure D). Results indicated that the effect of reduced value of water bulk modulus on the PWP evolutions was negligible.

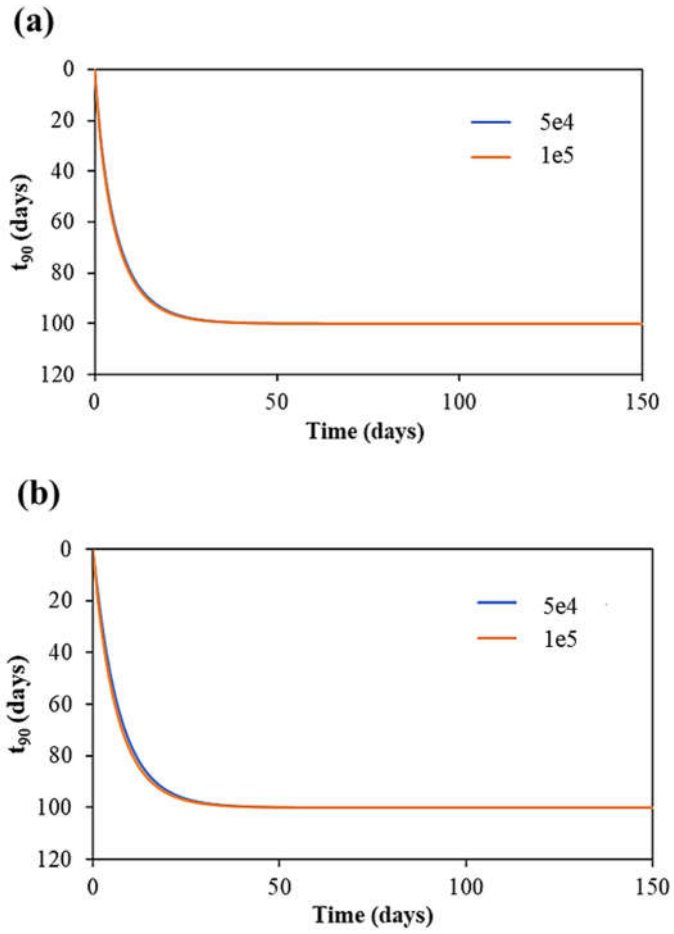

Figure D: PWP evolutions at the horizontal distance of (a) 6 m and (b) 14 m for models with water bulk modulus of 1x10^5 and 5x10^4 after the placement of the 3rd layer.

APPENDIX E - EFFECT OF THE INSTANTANEOUS FILLING ASSUMPTION

Models were also performed to evaluate the potential effect of the filling scheme on the rate of consolidation of tailings co-disposed with WRI in a conventional TSF (see chapter 5). The degree of consolidation at the base of the TSF at the locations of 6 and 19 m from the WRI when the filling height reached 15 m was evaluated for the model with various filling schemes (i.e., after the placement of 5th, 10th and 15th layers for models with filling rate of 3 m/year, 1.5 m/6 months and 1 m/4 months, respectively) (figure E-1). It took almost the same amount of time for models with such filling rates to dissipate 90% of excess PWP, which was around 26 and 37 days at the location of 6 and 19 m from WRI, respectively (figure E-1). The effect of deposition rate on the rate of consolidation of tailings, thus, was negligible.

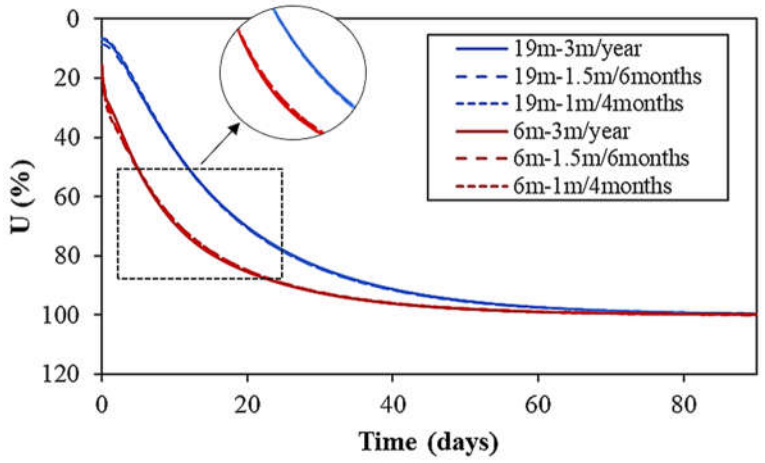

Figure E-1: Rate of consolidation of tailings at the base of the TSF at horizontal distances of 6 and 19 m from the WRI when the filling height reached 15 m for models with various filling rate. t_{90} values were similar for models with various deposition rates.

Finally, models were also performed to investigate the effect of the filling scheme on the consolidation rate of tailings co-disposed with permeable envelope in an open pit (see chapter 6). The degree of consolidation at the elevation of 2.5 m from bottom of the pit at the locations of 5 and 15 m from the permeable envelope when the tailings thickness reached 15 m was examined for models with various filling schemes (i.e., after the placement of 6th and 3rd layers for model

with filling rate of 2.5 m/6 months and 5 m/1 year, respectively) (figure E-2). It can be seen that the effect of the deposition rate on the rate of consolidation of tailings was insignificant.

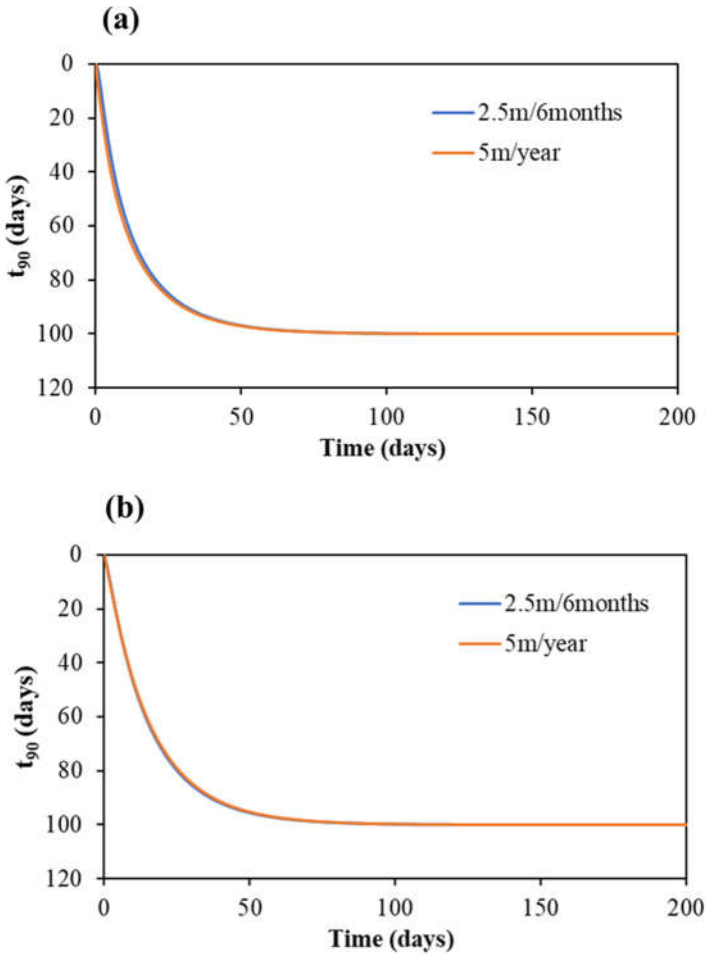

Figure E-2: Rate of consolidation of tailings at z = 2.5 m at horizontal distances of 5 and 15 m from the permeable envelope when the filling height reached 15 m for models with various filling rate. t_{90} values were similar for models with various deposition rates.